

Dynamic Demand for Frequency Response Services in the Great Britain Power System



A thesis submitted to

CARDIFF UNIVERSITY

for the degree of

DOCTOR OF PHILOSOPHY

2014

Meng Cheng

Institute of Energy

Abstract

Dynamic Demand Technology (DDT) developed by Open Energi Ltd. adjusts the power consumption of demand to react rapidly to changes in grid frequency without undermining the inherent control of loads. In this thesis, DDT is used to regulate the power consumption of domestic refrigerators and industrial bitumen tanks for grid frequency control. The feasibility of the loads to participate in frequency response services is studied.

Refrigerators are connected throughout the power system and thus have great potential to be used for frequency control. A frequency controller based on the DDT is applied to refrigerators so that their power consumption varies with frequency deviations autonomously and proportionally. The technique maintains the temperature control of refrigerators and causes little adverse impact on their cold storage of food. A thermodynamic model of refrigerators is developed and validated through field tests on a number of refrigerators at the premises of the Indesit Company. The refrigerator models equipped with frequency control are then integrated into a simplified Great Britain (GB) power system model to investigate their capability for grid frequency control. Results show that the refrigerators change their power consumption in order to reduce deviations of grid frequency. Approximately 500 MW of frequency response is provided by 40 million refrigerators when frequency dropped to below 49.5 Hz. The frequency control is faster than that provided by frequency-sensitive generation.

DDT is also applied to bitumen tanks. Frequency control is developed which is similar to refrigerators. A thermodynamic model of bitumen tanks equipped with the frequency control is developed and validated through field tests. The tank models are then connected to the GB power system model to study the capability of industrial heating loads for grid frequency control. Results show that tanks provide frequency control in a manner similar to and faster than that of frequency-sensitive generation. Approximately 72 MW of frequency response is provided by 5,000 bitumen tanks.

A participant in the Firm Frequency Response (FFR) service is required to deliver a minimum response of 10 MW. Loads with low power consumption need to be aggregated in order to participate. The availability of refrigerators and of tanks for

frequency response varies over a day and is measured through field tests at different times of the day. Based on the measurements of availability, the number of refrigerators and tanks to be aggregated for delivering more than 10 MW of response over a day is calculated. Simulations are carried out with an aggregation of 591 bitumen tank and 622,980 refrigerator models. Results show that more than 10 MW of response is able to be delivered.

For the future GB power system, fast control of frequency is required because of the reduction in system inertia caused by the large-scale use of converter connected generation. A case study is carried out to test the impact of the fast control of loads on the frequency of the future power system. Refrigerator models representing 40 million refrigerators and 500 tank models are connected to the GB power system model with reduced system inertia of 3.1 s. Results show that with the use of DDT, the frequency drop after a sudden loss of 1.8 GW generation is halted quickly and the magnitude of the drop reduced significantly (from 1 Hz to 0.4 Hz).

Declaration

This work has not been submitted in substance for any other degree or award at this or any other university or place of learning, nor is being submitted concurrently in candidature for any degree or other award.

Signed(candidate) Date

STATEMENT 1

This thesis is being submitted in partial fulfillment of the requirements for the degree of(insert MCh, MD, MPhil, PhD etc, as appropriate)

Signed(candidate) Date

STATEMENT 2

This thesis is the result of my own independent work/investigation, except where otherwise stated.

Other sources are acknowledged by explicit references. The views expressed are my own.

Signed(candidate) Date

STATEMENT 3

I hereby give consent for my thesis, if accepted, to be available for photocopying and for inter-library loan, and for the title and summary to be made available to outside organisations.

Signed(candidate) Date

STATEMENT 4: PREVIOUSLY APPROVED BAR ON ACCESS

I hereby give consent for my thesis, if accepted, to be available for photocopying and for inter-library loans after expiry of a bar on access previously approved by the Academic Standards & Quality Committee.

Signed(candidate) Date

Acknowledgement

This research would not have been possible without the guidance and assistance of many kind people.

I would like to show my foremost and sincere gratitude to my brilliant supervisors Prof. Nick Jenkins and Prof. Jianzhong Wu for their continuous support and instructions throughout my PhD study. I also would like to express my appreciation to my industrial supervisor Dr. Stephen Galsworthy from Open Energi and Dr. William Hung for their kind assistance and discussions from the view of industry. Special thanks to Dr. Janaka Ekanayake and Dr. Carlos Ugalde-Loo for their patience, encouragement and guidance on the research. Thanks also to Miss Catherine Roderick for her time and kind assistance on revising the writing of my PhD thesis.

I would like to thank all my friends and colleagues in Cardiff University for their kind assistance and support in all aspects.

Very special thanks to my family especially my great parents for their support and encouragement over the past three years.

The research was funded by Open Energi and Cardiff University through the President's Scholarship. I acknowledge the financial support from both.

Table of Contents

Abstract	i
Declaration	iii
Acknowledgement	iv
List of Figures	ix
List of Tables	xv
Nomenclature	xvii
Chapter 1 Introduction	1
1.1 Anticipated changes in the power system	2
1.2 Potential challenges for the power system	4
1.2.1 Changes in the generation mix	4
1.2.2 Electrification of demand	5
1.3 Role of demand	5
1.4 Research objectives	7
1.5 Thesis structure	8
Chapter 2 State of the Art of Frequency Control and Demand-Side Integration	9
2.1 Frequency control requirements of the GB power system.....	10
2.2 Frequency response services and reserve services in the present GB power system	11
2.2.1 Frequency response services	11
2.2.2 Reserve services	14
2.3 Frequency control from generation units	15
2.3.1 Frequency control of conventional generators	16
2.3.2 Frequency control of wind turbines	23
2.4 Demand-side integration	25
2.4.1 What is demand-side integration?	25
2.4.2 Benefits of demand-side integration	26

2.4.3 Potential provision of response from demand.....	28
2.5 Use of demand for frequency control.....	30
2.5.1 Centralised control of demand	31
2.5.2 Local control of demand	33
2.5.3 Potential value of dynamic demand technology	36
2.6 Conclusion	37
Chapter 3 Domestic Refrigerators for Frequency Control	39
3.1 Introduction.....	40
3.2 Model of refrigerators	41
3.2.1 Thermodynamic model of refrigerators	41
3.2.2 Calibration of the model using test data.....	43
3.2.3 Aggregated model of a population of refrigerators.....	45
3.3 Dynamic control of refrigerators.....	46
3.3.1 Temperature control of a refrigerator.....	47
3.3.2 Grid frequency control of a refrigerator.....	48
3.3.3 Coordinated local frequency control of refrigerators.....	49
3.3.4 Integrated control of a refrigerator	54
3.4 Modelling of GB power system for frequency control	57
3.5 Case study	59
3.5.1 Identification of suitable number of individual refrigerator models.....	59
3.5.2 Sustained low frequency and high frequency events	62
3.5.3 Case study on the GB power system.....	64
3.6 Conclusions.....	76
Chapter 4 Industrial Bitumen Tanks for Frequency Control	78
4.1 Introduction.....	79
4.2 Dynamic control of bitumen tanks.....	79
4.2.1 Temperature control of bitumen tanks	79

4.2.2 Use of bitumen tanks for grid frequency control	79
4.2.3 Integrated control	80
4.2.4 Update of trigger frequencies F_{OFF} and F_{ON}	81
4.3 Modelling of bitumen tanks	85
4.3.1 Thermodynamic model of bitumen tanks	85
4.3.2 Validation of the thermodynamic model.....	90
4.3.3 Curve-fit Model of bitumen tanks.....	92
4.3.4 Comparison of thermodynamic model and curve-fit model	94
4.4 Field tests on bitumen tanks	96
4.4.1 Injection of frequency deviations.....	97
4.4.2 Field tests on tanks during large frequency disturbances	100
4.5 Case studies on the GB power system	103
4.5.1 Simulation of sudden loss in generation	104
4.5.2 Simulation of sudden loss in demand.....	108
4.5.3 Simulation of consecutive loss of two generators.....	111
4.6 Conclusions.....	113
Chapter 5 Demand Aggregation for Frequency Response Service	115
5.1 Introduction.....	116
5.2 Comparison of frequency controller of refrigerators and of bitumen tanks.....	116
5.2.1 Response to a frequency incident.....	117
5.2.2 Recovery from a frequency incident.....	117
5.3 Demand availability at different time of day	118
5.3.1 Analysis of demand availability.....	119
5.3.2 Field investigations on demand availability at different time of day.....	119
5.3.3 Model of demand availability	122
5.4 Demand aggregation for frequency response service	124
5.4.1 Potential response from all refrigerators and bitumen tanks.....	124

5.4.2 Demand aggregation for Firm Frequency Response (FFR) service.....	125
5.4.3 Demand aggregation for FFR service: managing uncertainties.....	127
5.5 Case studies.....	132
5.5.1 Reduce the deviations of grid frequency.....	132
5.5.2 Demand aggregation for Firm Frequency Response service	137
5.5.3 Aggregated demand response in a future power system.....	141
5.6 Conclusions.....	145
Chapter 6 Conclusions.....	147
6.1 Conclusions.....	148
6.1.1 Domestic refrigerators for frequency control.....	148
6.1.2 Industrial bitumen tanks for frequency control.....	149
6.1.3 Demand aggregation for frequency response services.....	150
6.2 Contributions of the thesis	151
6.3 Publications.....	153
6.4 Future work.....	153
References	155
Appendix I	163
Appendix II.....	165
Appendix III	167
Appendix IV.....	170

List of Figures

Fig. 1.1. UK government GHG emission target (1990 base) [6].....	2
Fig. 1.2. Anticipated domestic demand of different loads over a day in 2025 including the increasing connections of heat pumps and electric vehicles [6]	4
Fig. 1.3. Effects of demand-side response on typical UK demand profiles [13]	6
Fig. 2.1. Grid frequency in the GB power system [19].....	10
Fig. 2.2. Frequency control and stability of the GB power system (Modified figure based on [21]).....	11
Fig. 2.3. Timescale of reserve services [30].....	15
Fig. 2.4. Schematic diagram of a generator [34].....	16
Fig. 2.5. Droop characteristics of governor [34].....	19
Fig. 2.6. GB power system primary frequency control model [36].....	19
Fig. 2.7. Modes of frequency control operation [38].....	21
Fig. 2.8. Change of load set-point after primary and secondary frequency control (modified figure based on [39])	22
Fig. 2.9. Minimum frequency response requirement profile for a 0.5 Hz frequency deviation from 50 Hz required by the Grid Code [40].....	23
Fig. 2.10. Supplementary controller for inertial response from VSWT [42].....	24
Fig. 2.11. Present network and C2C network [54].....	27
Fig. 2.12. Electricity demand of GB power system by sectors in 2012 [58]	29
Fig. 2.13. Normal temperature control and frequency control of a refrigerator [73].....	34
Fig. 3.1. Diagram of a refrigerator and its refrigeration cycle (modified figure based on [85]).....	41
Fig. 3.2. Comparison of temperature and compressor state of a cooler in the model and in the real measurements starting at an ambient temperature 22 °C (provided by Open Energi).....	44
Fig. 3.3. Temperature control of a refrigerator	47

Fig. 3.4. Diagram of the frequency control of a refrigerator.....	48
Fig. 3.5. Assignment of trigger frequencies for a population of refrigerators	51
Fig. 3.6. Update of F_{ON} and F_{OFF} during the recovery from frequency events.....	53
Fig. 3.7. Integrated control scheme of refrigerators.....	55
Fig. 3.8. A simplified GB power system model for the study of frequency control.....	58
Fig. 3.9. Relationship of load coincidence factor and the number of customers [92]	60
Fig. 3.10. Effect of number of refrigerator models	61
Fig. 3.11. Power of refrigerators during the sustained periods of low frequency and high frequency.....	62
Fig. 3.12. Variations of T_{Ca} of refrigerators in the frequency events.....	63
Fig. 3.13. Simulation model of refrigerators connected to the GB power system model	64
Fig. 3.14. Variations of grid frequency	65
Fig. 3.15. Power change of generators and power consumption of refrigerators	66
Fig. 3.16. Power consumption of refrigerators 30 minutes after the frequency drop	66
Fig. 3.17. Power change of G1 and G2 30 minutes after the frequency drop.....	66
Fig. 3.18. ON/OFF state of the cooler.....	67
Fig. 3.19. Cavity temperature of the cooler	68
Fig. 3.20. Variations of grid frequency	69
Fig. 3.21. Power change of generators and power consumption of refrigerators	69
Fig. 3.22. Power consumption of refrigerators 30 minutes after the frequency increase	70
Fig. 3.23. ON/OFF state of the cooler.....	71
Fig. 3.24. Cavity temperature of the cooler	71
Fig. 3.25. Variation of grid frequency	72
Fig. 3.26. Power change of generators and power consumption of refrigerators	73
Fig. 3.27. Power consumption of refrigerators and the grid frequency after the frequency incident.....	73

Fig. 3.28. Power change of Generators and power consumption of refrigerators after the frequency incident.....	73
Fig. 3.29. Effect of the diversity in the refrigerator models (<i>div</i>) on the power consumption of refrigerators.....	75
Fig. 3.30. Effect of the diversity in the refrigerator models (<i>div</i>) on the variation of grid frequency.....	75
Fig. 3.31. Effect of the diversity in the refrigerator models (<i>div</i>) on the power change of generators.....	75
Fig. 4.1. Hysteresis temperature control of one tank.....	79
Fig. 4.2. Local control scheme of one tank.....	80
Fig. 4.3. Frequency control of three tanks during a drop of frequency.....	83
Fig. 4.4. Heat transfer process of one bitumen tank.....	86
Fig. 4.5. Internal temperature of a tank and its ON and OFF period.....	87
Fig. 4.6. Tank temperature obtained from the thermodynamic model of 5 bitumen tanks.....	89
Fig. 4.7. Total power consumption of 5 bitumen tanks obtained from the thermodynamic model.....	89
Fig. 4.8. Illustration of t_{rise} and t_{fall} at any temperature of a bitumen tank.....	90
Fig. 4.9. Relationship of t_{rise} and t_{fall} of a bitumen tank (t_{rise} is normalised with t_{ON} and t_{fall} is normalised with t_{OFF}).....	92
Fig. 4.10. t_{rise} and t_{fall} of 5 bitumen tanks.....	93
Fig. 4.11. Total power consumption of 5 bitumen tanks.....	94
Fig. 4.12. Injected grid frequency profile.....	95
Fig. 4.13. Power consumption of tanks.....	96
Fig. 4.14. Setting of field tests by Open Energi.....	97
Fig. 4.15. Field tests with the injection of Frequency Profile 1 in Table 4.6.....	98
Fig. 4.16. Field tests with the injection of Frequency Profile 2 in Table 4.6.....	99
Fig. 4.17. Field tests with the injection of Frequency Profile 3 in Table 4.6.....	100
Fig. 4.18. Response of the 1,140 tanks to the frequency rise.....	101

Fig. 4.19. Response of the 1,140 tanks 30 minutes after the frequency rise.....	101
Fig. 4.20. Response of the 1,140 tanks to the frequency drop	102
Fig. 4.21. Response of the 1,140 tanks 30 minutes after the frequency drop	102
Fig. 4.22. Simplified GB power system model with the connection of 5,000 bitumen tank models	104
Fig. 4.23. Variations of grid frequency	104
Fig. 4.24. Change of power output of generators and power consumption of tanks	105
Fig. 4.25. Power consumption of tanks 30 minutes after the frequency drop.....	105
Fig. 4.26. ON/OFF state of Tank 1	106
Fig. 4.27. Variations of temperature of Tank 1	106
Fig. 4.28. ON/OFF state of Tank 2	107
Fig. 4.29. Variations of temperature of Tank 2.....	107
Fig. 4.30. Variations of grid frequency	108
Fig. 4.31. Change of power output of generators and power consumption of tanks	108
Fig. 4.32. Power consumption of tanks 30 minutes after the frequency drop.....	109
Fig. 4.33. ON/OFF state of Tank 3	110
Fig. 4.34. Variations of temperature of Tank 3.....	110
Fig. 4.35. Variations of grid frequency	111
Fig. 4.36. Change of power output of generators and power consumption of tanks	112
Fig. 4.37. Power consumption of tanks after the drop of frequency	112
Fig. 5.1. ON/OFF cycle and temperature of a refrigerator and a bitumen tank.....	117
Fig. 5.2. HRA and LRA of refrigerators over a winter day.....	120
Fig. 5.3. Seasonal effect on the energy consumption of cold appliances obtained from DECC (modified figure based on [96]).....	121
Fig. 5.4. LRA_r and HRA_r of refrigerators over a summer day	121
Fig. 5.5. HRA_b and LRA_b of bitumen tanks over a day.....	122
Fig. 5.6. Available frequency response from all refrigerators and bitumen tanks over a day.....	124

Fig. 5.7. Scheme of number of tanks and refrigerators to be combined for power reduction of more than 10 MW	126
Fig. 5.8. Standard normal distribution curve.....	131
Fig. 5.9. Scheme of number of tanks and refrigerators to be combined for power reduction of more than 10 MW considering 90% confidence level.....	131
Fig. 5.10. Differences (shaded area) in the number of refrigerators and bitumen tanks with and without the consideration of uncertainties.	132
Fig. 5.11. Power system model with refrigerators and bitumen tanks connected.....	133
Fig. 5.12. Power change (ΔP_{wind}) injected to the power system.....	134
Fig. 5.13. Variation of grid frequency with and without frequency response from loads	134
Fig. 5.14. Power consumption of refrigerators with and without the frequency controller	135
Fig. 5.15. Power consumption of tanks with and without the frequency controller	135
Fig. 5.16. Total power consumption of refrigerators and tanks with and without their type-specific frequency controller.....	136
Fig. 5.17. Injected frequency input	138
Fig. 5.18. Variation of aggregated power consumption of loads at 05:00 – 05:30 during the frequency incident.....	138
Fig. 5.19. Variations of HRA_r and LRA_r of refrigerators.....	139
Fig. 5.20. Variations of HRA_b and LRA_b of bitumen tanks	139
Fig. 5.21. Variations of aggregated power consumption of loads during and after the frequency incident.....	140
Fig. 5.22. Variations of grid frequency	142
Fig. 5.23. Change of power output of generators and power consumption of loads	142
Fig. 5.24. Power consumption of loads after the frequency incident.....	143
Fig. 5.25. Variations of HRA and LRA of refrigerators during and after the frequency incident.....	143

Fig. 5.26. Variations of *HRA* and *LRA* of bitumen tanks during and after the frequency incident..... 144

List of Tables

TABLE 1.1. Capacity of Different Generation Types Connected to the GB Transmission System in the ‘Gone Green scenario’ [8]	3
TABLE 2.1. A Summary of Different Frequency Response Services [27].....	13
TABLE 2.2. Cost of Different Frequency Response Services in January and July 2014 [28]-[29].....	13
TABLE 2.3. Cost of Different Reserve Services in January and July 2014 [28]-[29] ...	15
TABLE 2.4. Inertia Constant of Different Types of Generators [37].....	20
TABLE 2.5. Demand Response Functions of Domestic Loads [39].....	29
TABLE 2.6. Potential Demand Response from Other Non-domestic Sectors [60].....	30
TABLE 2.7. Potential Provision of Response from Demand Estimated in 2011 [8]	30
TABLE 2.8. Comparison of the Use of Demand to Participate in FFR Service through DDT with the Use of Demand for FCDM Service [81].....	37
TABLE 3.1. Parameters of the Cooler Model Calibrated at an Ambient Temperature 22 °C.....	43
TABLE 3.2. Parameters of the Freezer Model Calibrated at an Ambient Temperature 22 °C.....	45
TABLE 3.3. Diversity in the Refrigerators	46
TABLE 3.4. Dynamic Update of Trigger Frequencies F_{ON} and F_{OFF}	54
TABLE 3.5. Truth Table of Logic Gates in Fig. 3.7.....	56
TABLE 3.6. Parameters Used for G1 and G2 (System Base of 33,702 MW).....	59
TABLE 3.7. Aggregated Model of Different Number of Individual Refrigerator Models	59
TABLE 3.8. Simulation Time of each Aggregated Model	61
TABLE 3.9. Parameters of the GB Power System Model (System Base of 41 GW).....	72
TABLE 4.1. Truth Table of Logic Gates of Fig. 4.2.	81
TABLE 4.2. Update of Trigger Frequency F_{OFF}	84

TABLE 4.3. Update of Trigger Frequency F_{ON}	85
TABLE 4.4. Parameters of Each Tank.....	89
TABLE 4.5. t_{ON} and t_{OFF} of the Curve-fit Model.....	92
TABLE 4.6. Computational Speed of the Thermodynamic Model and Curve-fit Model for Simulating the Normal Operating Cycle of 500 Tanks over 10 Hours.....	94
TABLE 4.7. Description of Injected Frequency Profiles during the Field Tests.....	97
TABLE 5.1. LRA_r and LRA_b at Different Time of a Day.....	126
TABLE 5.2. Payment Structure of Firm Frequency Response Service [97].	127
TABLE 5.3. Expectations and Standard Deviations of LRA_r and LRA_b at Different Time of Day.....	129

Nomenclature

List of abbreviation

BM	Balancing Mechanism
C2C	Capacity to Customers
CLNR	Customer-Led Network Revolution
CPP	Critical Peak Clipping
DECC	Department of Energy and Climate Change
DER	Distributed Energy Resources
DFIG	Doubly-Fed Induction Generator
DSI	Demand-Side Integration
DSO	Distribution System Operator
EU	European Union
EV	Electric Vehicle
FCDM	Frequency Control by Demand Management
FFR	Firm Frequency Response
FR	Fast reserve
FSM	Frequency Sensitive Mode
FSWT	Fixed Speed Wind Turbine
GB	Great Britain
GHG	Green House Gas
HVAC	Heating Ventilation and Air Conditioning
ICT	Information and Communications Technology
IG	Induction Generator
ILMC	Intelligent Load Management Controller
LFSM	Limited Frequency Sensitive Mode
MFR	Mandatory Frequency Response
MGCC	Micro Grid Central Controller
NOP	Normal Open Point
RTP	Real-Time Pricing
SG	Synchronous Generator
STOR	Short Term Operating Reserve
ToU	Time-of-Use
TSO	Transmission System Operator
UK	United Kingdom
VPP	Virtual Power Plant
VSWT	Variable Speed Wind Turbine

Chapter 1

Introduction

In this chapter, anticipated changes in the power system are discussed. These changes will give rise to challenges for the operation of the future power system. The role of demand in dealing with these challenges is outlined. The research objectives of using dynamic demand for grid frequency control are specified. Finally, the thesis structure is provided.

1.1 Anticipated changes in the power system

Climate change caused by rising Green House Gas (GHG) emissions threatens the global population. As discussed in [1], more than two thirds of GHG emissions are caused by the ways in which energy is produced and used. For example, the use of fossil fuel is recognised as one of the main reasons for GHG emissions.

The European Union (EU) and the Government of the United Kingdom (UK) are aiming to reduce the use of fossil fuels for energy production [2]-[3]. As the fossil fuel is mainly imported, reliance on their imports is expensive [2] and causes concern for the security of energy supply [3].

As a measure to address climate change and reduce dependency on imported fossil fuels, the EU has set the following ‘20/20/20’ energy and climate targets for the year 2020 [4]:

- A 20% reduction in GHG emissions from 1990 levels
- Raising the share of energy consumption produced from renewable resources to 20%
- A 20% improvement in energy efficiency

Furthermore, the UK government has established a legally binding target [5] to reduce UK GHG emissions by at least 80% in 2050 from the 1990 baseline as depicted in Fig. 1.1.

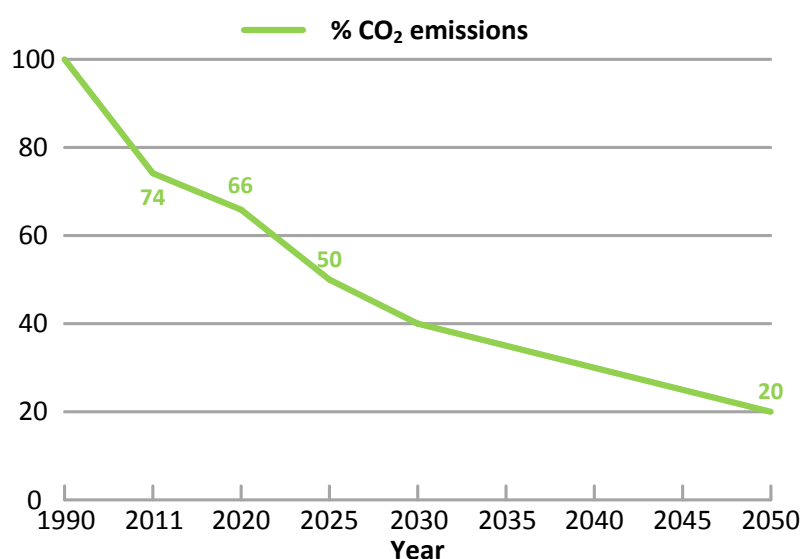


Fig. 1.1. UK government GHG emission target (1990 base) [6]

In order to meet energy and climate targets, the Great Britain (GB) power system operator, National Grid, has proposed significant changes to the generation mix for the future power system. Conventionally, electricity has largely been produced by generators that burn fossil fuels and emit GHG. It is anticipated that in the decarbonised power system of the future, more electricity will be generated from renewable, low-carbon resources such as wind and solar. These will replace the generation capacity of fossil fuels and thus GHG emissions will be reduced.

National Grid considers the *Gone Green Scenario* [7] as one plausible means to meet the UK energy and climate targets. The generation capacity of different resources was estimated for the year 2020/21 and was compared with the year 2010/11 [8] as shown in Table 1.1. A significant increase in wind generation is expected by 2020/21: it is forecast to reach approximately 27% of the total generation capacity. Generation from coal and oil is expected to decrease.

TABLE 1.1. Capacity of Different Generation Types Connected to the GB Transmission System in the 'Gone Green scenario' [8]

Generation Type	Capacity (GW)	
	Year 2010/11	Year 2020/21
Coal	28.2	14.5
Coal(CCS)	0	0.6
Nuclear	10.8	11.2
Gas	31.9	34.7
Oil	3.4	0
Pumped Storage	2.7	2.7
Wind	3.8	26.8
Interconnectors	3.3	5.8
Hydro	1.1	1.1
Biomass	0	1.6
Marine	0	1.4
Total	85.2	100.4

In addition to the changes in electricity generation, anticipated changes in electricity demand that include the electrification of heating (for example the use of heat pumps) and transport (for example the use of electric vehicles) [9] will also contribute to the reduction of GHG emissions. Fig. 1.2 shows the expected domestic demand of different loads over a day in 2025 [6]. An increase in demand of heat pumps and electric vehicles is forecast (their demand is negligible at present). These changes reduce the GHG emissions from the heating and transport sectors.

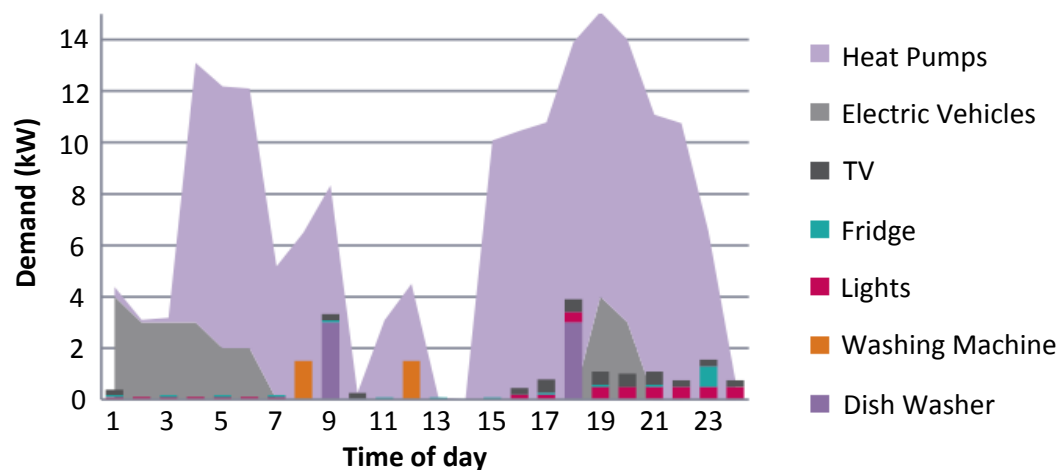


Fig. 1.2. Anticipated domestic demand of different loads over a day in 2025 including the increasing connections of heat pumps and electric vehicles [6]

In summary, changes in the generation mix and electrification of demand are expected to be two of the key characteristics of measures taken to meet energy and climate targets. However, changes in these two areas will create challenges for the operation of the future power system.

1.2 Potential challenges for the power system

1.2.1 Changes in the generation mix

Changes in the generation mix will give rise to three significant challenges in balancing generation and demand.

The first challenge is that some renewable resources provide a variable supply of energy. For instance, wind power generation relies on the wind blowing. The increasing use of intermittent renewable energy causes uncertainties to electricity generation dispatch.

The second challenge is that the largest generating unit considered in the GB power system in 2014 is 1,800 MW compared to 1,320 MW in previous years [10]. As a result, the maximum generation in-feed loss increased from 1,320 MW to 1,800 MW.

The above two challenges demand more generation reserve from the part loaded, fossil fuel generators to meet demand when generation is insufficient and to deliver extra power after a sudden loss of generation.

The third challenge presented by changes in the generation mix is that renewable energy resources are mainly connected through power electronic converters. The replacement of conventional generation by generation from renewable energy will lead to the reduction of power system inertia [11]. As a result, when there are imbalances between generation and demand, changes in grid frequency will be more rapid. Therefore, faster frequency control will be expected.

1.2.2 Electrification of demand

The power system will need to meet an increasing demand for electricity due to the increase numbers of heat pumps and electrical vehicles. The increasing demand may lead to higher peak demand and to network congestion during the period of peak demand. Therefore, the present electricity network needs to be reinforced. It is estimated that for the North West network of the UK alone [12], network expansion will cost £9 billion by 2025. Furthermore, network reinforcements can be intrusive for local communities and involve extensive excavations and disruptions [12].

1.3 Role of demand

In order to confront the challenges that are anticipated in the future power system, demand needs to be flexible and play an active role. As depicted in Fig. 1.3, the flexibility of demand can be categorised into two aspects. One is to change power consumption of demand following the generation and hence to reduce the imbalances between supply and demand. The other is to reduce peak demand by load shifting and hence to defer network reinforcements.

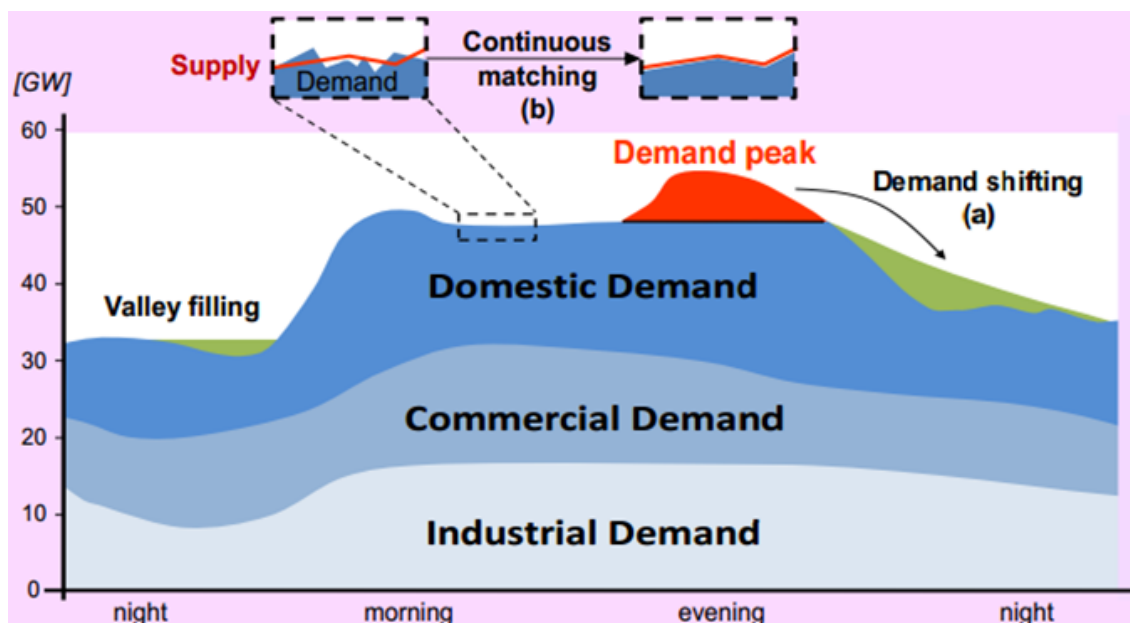


Fig. 1.3. Effects of demand-side response on typical UK demand profiles [13]

It is expected that the flexibility of demand will be enhanced by rolling out smart meters across the UK. All homes and small businesses will have them installed by 2020 [14].

Smart meters display real-time information on energy use and cost for the user. Time varying price schemes such as Time-of-Use (ToU) pricing [15] will be offered to customers. It is therefore expected that customers will change their patterns of electricity use as a direct result of the data made available to them by smart meters and of the financial savings offered by the time varying price schemes. This will contribute to reduction of peak demand and of network congestion allowing the system operator to defer making substantial investments in network reinforcements.

The possibility of using smart meters for the reduction of imbalances between generation and demand was investigated in [16]. A direct load control scheme used a smart meter and a smart load controller to switch OFF domestic appliances if there was a drop of grid frequency. The control scheme made demand flexible for grid frequency control. However, the communication delay of the control scheme reduced the capability of frequency control from flexible demand. Frequency control can be obtained if the delay is less than 200 ms [16]. As frequency measurement was removed from the functional specifications of the UK smart meters in 2010 [17], the time taken by smart meter to read frequency through a Home Area Network (HAN) may be as high as 3.3 s [16]. Hence, it is currently not feasible to use a smart meter for frequency control under the UK smart meter specifications.

To avoid the use of communication infrastructure, demand is able to reduce imbalances between generation and demand in response to local measurements of grid frequency. Some non-critical loads are able to be switched ON/OFF rapidly so as to arrest deviations in grid frequency. Furthermore, such immediate frequency response from flexible demand gives a partial solution to the reduction of system inertia. This thesis will investigate the use of flexible demand in response to locally measured frequency deviations.

1.4 Research objectives

This thesis focuses on the investigation of using demand for frequency control in the power system. The research objectives are:

- To investigate the use of domestic refrigerators for grid frequency control:
Decentralised frequency control for refrigerators is developed, enabling their total power consumption to be controlled by deviations of grid frequency. Frequency control does not undermine the temperature control ability of a refrigerator and hence will have little adverse impact on its performance. The capability of refrigerators to provide grid frequency control is studied by connecting refrigerator models to a GB power system model.
- To investigate the use of industrial bitumen tanks for grid frequency control:
Decentralised frequency control for bitumen tanks is developed, allowing their total power consumption to be controlled by deviations of grid frequency. The temperature control ability of a bitumen tank heater is not undermined. Bitumen tanks with grid frequency control capability are modelled and connected to the GB power system model. Their capability to respond to grid frequency deviations is then studied.
- To investigate the technical feasibility of the participation of loads in the Firm Frequency Response service:
The GB system operator requires a participant in the Firm Frequency Response service to deliver a minimum of 10 MW of frequency response. Refrigerator and bitumen tank loads available for grid frequency control vary over a day. To deliver at least 10 MW of frequency response, the number of loads to be frequency-responsive and aggregated is calculated taking into account their availability for grid frequency control at different times of day.

1.5 Thesis structure

The structure of the thesis is as follows:

In chapter 2, grid frequency control requirements and the present frequency response services in the GB power system are reviewed. Frequency control provided by generators is discussed. A study of demand-side integration leads to a review of grid frequency control provided by demand.

Chapter 3 presents the use of refrigerators for grid frequency control. It describes the development of a thermodynamic model of refrigerators. It also illustrates a simplified GB power system model that was developed for the study of grid frequency control. Case studies undertaken to verify the capability of refrigerators to provide grid frequency control are presented.

Chapter 4 focuses on the use of bitumen tanks for grid frequency control. It describes the development of a thermodynamic model of bitumen tanks and the development of a simplified model of bitumen tanks based on field measurements. The accuracy and computational time of the two models are compared. The chapter then describes field tests on a number of tanks which were undertaken to verify their frequency control capability. Case studies carried out to show the capability of bitumen tanks to provide grid frequency control are given.

In chapter 5, the number of refrigerator and bitumen tank loads to be aggregated to deliver the 10 MW of frequency response required by the system operator is determined. The availability of loads for frequency control at different time over a day is considered. Availability was measured through field investigations and modelled. Case studies undertaken to verify the technical feasibility of the participation of loads in the Firm Frequency Response service are presented.

Chapter 6 concludes and summarises the thesis. Contributions of the thesis, suggestions for future work and publications are listed.

Chapter 2

State of the Art of Frequency Control and Demand-Side Integration

This chapter reviews frequency control in the power system. Frequency control requirements and frequency response services of the present GB power system are illustrated. Frequency control provided by generating units is discussed. Following a study of demand-side integration, an alternative means of using demand to provide grid frequency control is investigated.

2.1 Frequency control requirements of the GB power system

Frequency in the power system is a continuously changing variable which indicates the balance of total generation and system demand on a second-by-second basis [18]. In the GB power system, nominal grid frequency is 50 Hz as shown in Fig. 2.1. The steady-state limit of grid frequency is required to be $50 \pm 1\%$ (Hz) [18]. If generation is greater than demand, frequency rises. If generation is less than demand, frequency drops.

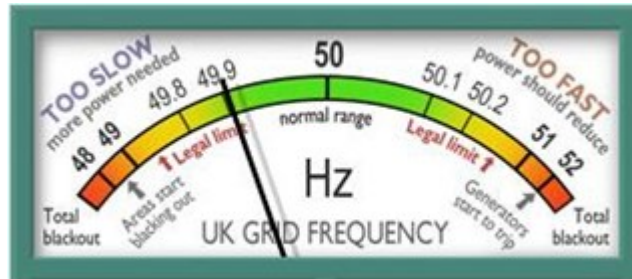


Fig. 2.1. Grid frequency in the GB power system [19]

The operational policy to meet the frequency control requirement is listed below [20].

- *Grid frequency under normal conditions is maintained within operational limits of ± 0.2 Hz.*
- *For sudden loss of generation or demand up to 300 MW, the maximum frequency change is limited to ± 0.2 Hz.*
- *For sudden loss of generation or demand greater than 300 MW but less than or equal to 1,320 MW, the maximum frequency change is limited to ± 0.5 Hz.*
- *For sudden loss of generation greater than 1,320 MW and less than or equal to 1,800 MW, the frequency change is limited to -0.8 Hz with frequency restored to 49.5 Hz within 1 minute.*

Fig. 2.2 illustrates the frequency control and stability of the GB power system [21]. Under normal operating conditions, frequency control is continuously provided by frequency-sensitive generators which maintain the frequency at 50 Hz. For occasional sudden loss of generation which causes a severe drop in frequency, for instance a drop to below 48.8 Hz, frequency control is provided both by generation and by load reduction from public distribution networks [22] in stages to avoid shutdown of the entire power system [23].

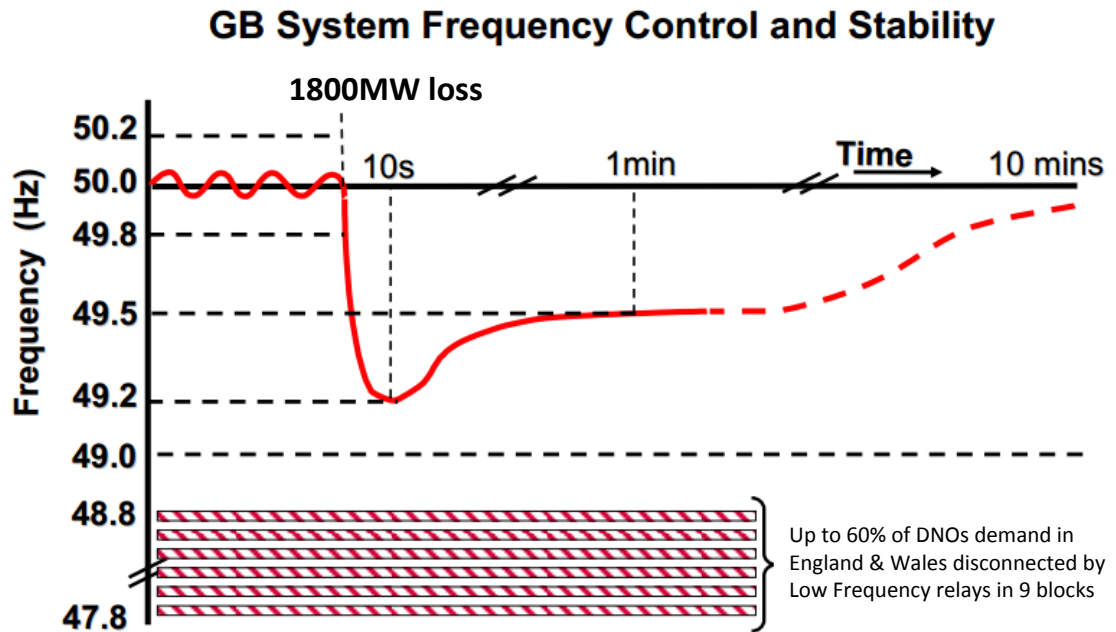


Fig. 2.2. Frequency control and stability of the GB power system (Modified figure based on [21])

2.2 Frequency response services and reserve services in the present GB power system

The GB system operator maintains the balance between demand and generation through a variety of balancing services including frequency response services and reserve services. These two balancing services aim to maintain grid frequency within its steady-state limits and to restore frequency after any sudden changes in demand or generation. Both generation and demand are able to participate in these services.

2.2.1 Frequency response services

Frequency response services can be categorised into two types [18]: dynamic frequency response and non-dynamic frequency response (i.e. static response).

- Dynamic response: a service provided continuously in order to manage the normal second-by-second power imbalances in the power system.
- Non-dynamic response: a discrete service only triggered at a pre-defined deviation of grid frequency.

Frequency response services [18] include Mandatory Frequency Response (MFR), Firm Frequency Response (FFR) and Frequency Control by Demand Management (FCDM):

- *Mandatory Frequency Response (MFR)* [24]

MFR is an automatic change in active power output of generating units in response to frequency changes. All large generators (over 100 MW) connected to the GB transmission system are mandated to have the capability to provide this service.

MFR is achieved through one of three response services:

Primary Response – provision of additional active power within 10 s after an event and that can be sustained for another 20 s

Secondary Response – provision of additional active power within 30 s after an event and that can be sustained for another 30 min

High Frequency Response – reduction of active power within 10 s after an event and that can be sustained indefinitely

- *Firm Frequency Response (FFR)* [25]

FFR is the firm provision of dynamic or non-dynamic response to changes in frequency.

National Grid procures FFR service through a competitive tender process. Tenders can be for low frequency events, for high frequency events or for both.

- *Frequency Control by Demand Management (FCDM)* [26]

FCDM provides frequency response by the interruption of demand. Electricity demand is automatically interrupted when the frequency crosses the low frequency relay setting (typically at 49.7 Hz). Such interruptions are likely to occur between approximately 10 to 30 times per annum [26].

FCDM is required to manage large deviations in frequency which may be caused by, for instance, a sudden and significant loss of generation.

Table 2.1 gives a summary of the characteristics of the three frequency response services currently available in the GB power system that are listed above.

TABLE 2.1. A Summary of Different Frequency Response Services [27]

Services	MFR	FFR	FCDM
Dynamic?	Yes	Yes/No	No
Participants	Generation	Generation/Demand	Demand
Minimum threshold for participation	Have a 3-5% governor droop characteristics	Deliver a minimum of 10 MW of response	-Provide the service within 2 seconds of instruction -Deliver for minimum 30 minutes -Deliver minimum 3 MW, which may be achieved through aggregation
How to participate	Mandatory for large generators connecting to the GB Transmission System	Monthly tender	Bilateral negotiation

At present, frequency response services are provided mainly by frequency-sensitive generators. These generators are inefficient and expensive to operate as they are part loaded and consume significant amounts of fuel. The GB system operator therefore incurs significant costs in maintaining frequency response services as they are required to be available continuously and provided within seconds. As an example, the cost of each frequency response service in January 2014 and July 2014 are given in Table 2.2. The data came from the Monthly Balancing Services Summary provided by National Grid [28]-[29].

TABLE 2.2. Cost of Different Frequency Response Services in January and July 2014 [28]-[29]

Services	January 2014	July 2014
MFR (mandatory response)	£3.46 million	£4.06 million
FFR & FCDM (commercial response)	£9.64 million	£10.21 million
Total cost	£13.1 million	£14.27 million

2.2.2 Reserve services

Reserve services are despatched after the frequency response services are called upon in order to reduce frequency deviations and to complement the frequency response services.

At certain times of day, the system operator needs to have access to sources of extra power. This is referred to as reserve. Reserve can be in the form of either increase in generation or reduction in demand and serves to manage uncertainties in demand or generation [30].

Different reserve services are ready to deliver services on different time scales as listed below:

- *Fast Reserve (FR)* [31]

FR provides rapid and reliable delivery of active power by increasing generation or reducing demand. It is activated within 2 minutes following receipt of instructions from the system operator. The service is delivered at a rate in excess of 25 MW/minute. The minimum delivery is 50 MW. The reserve energy is sustainable for a minimum of 15 minutes.

An FR service provider has to be available over a pre-agreed period so that it can offer the required volume of reserve on the instruction of the system operator.

FR contributes to reducing frequency changes by taking over from the frequency response services. Once despatched, it restores the capability of primary and secondary response.

- *Short Term Operating Reserve (STOR)* [32]

STOR is provided by means of standby generation or demand reduction. It is fully delivered within 240 minutes on the instruction of the system operator. The minimum delivery is 3 MW. The fully delivered capacity is sustained for at least 2 hours.

- *Balancing Mechanism (BM) start-up* [33]

This service gives the system operator access to additional unscheduled generation. It contains two elements: BM start-up and hot standby. Upon request, BM start-up brings generating units to a state that it can synchronise in the power system within 89 minutes. Hot standby maintains the BM unit in a state of readiness to synchronise to the power system for an agreed period of time.

Reserve Services are summarised in Fig. 2.3. The timescale of a reserve service is depicted starting from instructions by the system operator to the time that the service is fully delivered. For example, at peak demand period of a day, National Grid instructs certain amount of providers to deliver the STOR service. Once the instruction is despatched for the peak demand period, the STOR provider should fully deliver the service within 240 min.

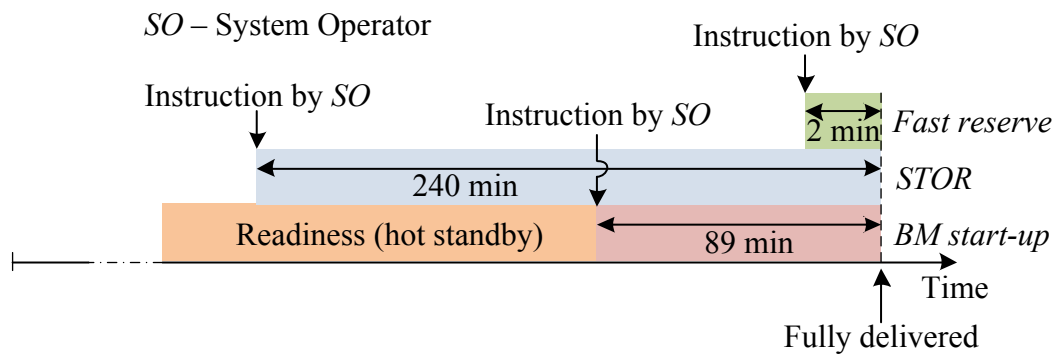


Fig. 2.3. Timescale of reserve services [30]

The cost of each reserve service for January 2014 and July 2014 is listed in Table 2.3. The data comes from the Monthly Balancing Services Summary provided by National Grid [28]-[29]. It is observed that the system operator incurred significant costs on reserve services.

TABLE 2.3. Cost of Different Reserve Services in January and July 2014 [28]-[29]

Services	January 2014	July 2014
Fast reserve	£5.83 million	£5.02 million
STOR	£8.42 million	£4.69 million
BM Start-Up	£0	£0
Total cost	£14.25 million	£9.71 million

2.3 Frequency control from generation units

Conventionally, frequency control in the power system mainly relies on synchronous power plants. They are operated part loaded in order to provide additional power output in the event of drops in grid frequency. Frequency response services from generators are performed by their frequency control capabilities.

2.3.1 Frequency control of conventional generators

Grid frequency is related to the speed of rotation of generators all over the grid which is defined as shown in (2.1). In a large interconnected system, synchronous generators are directly connected and hence all have the same frequency [23] (50 Hz in the GB power system). A change in active power demand at one location is reflected in the system by a change in frequency [34]. Therefore, frequency control of a power system can be illustrated as the frequency control of one lumped generator.

$$\omega = \frac{d\theta}{dt} \quad (2.1)$$

where ω (rad/s) is the angular velocity and θ (rad) is the angular displacement. A simplified schematic of a generator is shown in Fig. 2.4. A generator consists of a control valve, a rotating mass and a governor unit.

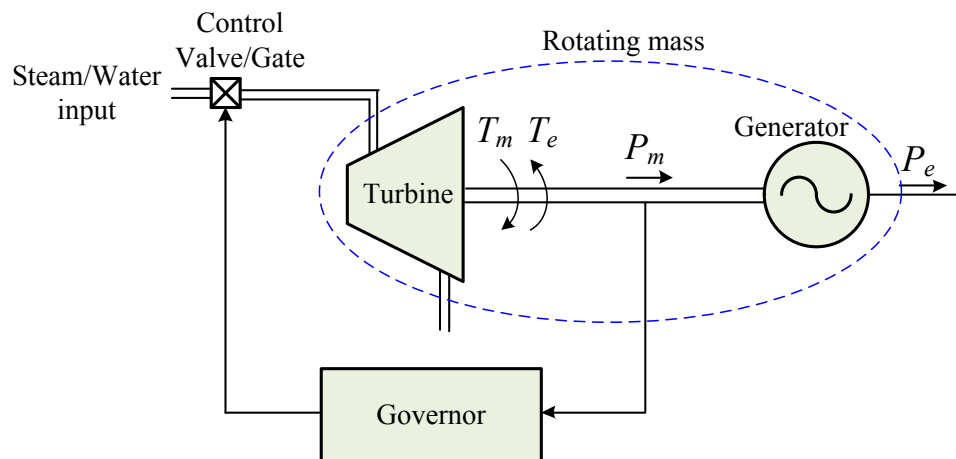


Fig. 2.4. Schematic diagram of a generator [34]

T_m (Nm) is the mechanical torque which is applied by the turbine to the shaft. T_e (Nm) is the electrical torque which is applied by the generator to the shaft. When there is an unbalance between the mechanical torque T_m (Nm) and the electrical torque T_e (Nm), a net torque causes acceleration or deceleration. The moment of inertia of generator and turbine J (kg m^2) is then accelerated or decelerated. The equation of motion is described by (2.1) [35]:

$$J \frac{d\omega_r}{dt} = T_m - T_e \quad (2.1)$$

where ω_r (rad/s) is angular velocity of the rotating mass and t (s) is time. In order to normalise equation (2.1), a per unit inertia constant H was used. H is defined as the

kinetic energy at synchronous speed ω_s (rad/s) divided by generator rating S_B (VA) as shown in (2.2):

$$H = \frac{\frac{1}{2}J(\omega_s)^2}{S_B} \quad (2.2)$$

Therefore, J is represented by $2HS_B/\omega_s^2$ according to (2.2) and substituted into (2.1):

$$2H \frac{d \frac{\omega_r}{\omega_s}}{dt} = \frac{T_m - T_e}{\frac{S_B}{\omega_s}} \quad (2.3)$$

As the base torque is $T_B = S_B/\omega_s$, equation (2.3) can be represented in terms of per unit quantities as:

$$2H \frac{d\omega_r}{dt} = T_m - T_e \quad (2.4)$$

For the active power-frequency control, according to [34], equation (2.4) is expressed in terms of power rather than torque by using the relationship $P = T\omega_r$. Applying a small deviation (Δ) of each term of the relationship from their initial value:

$$\begin{cases} P = P_0 + \Delta P \\ T = T_0 + \Delta T \\ \omega_r = \omega_0 + \Delta\omega_r \end{cases} \quad (2.5)$$

By substituting (2.5) into the relationship between power and torque, and then neglecting the higher order terms [34], equation (2.6) is obtained.

$$\Delta P_m - \Delta P_e = \Delta T_m - \Delta T_e \quad (2.6)$$

where P_m is the mechanical power transferred from the turbine to the shaft and P_e is the electrical power output of the generator.

Based on (2.4) and (2.6), the rotating speed of the generator and the power is written as:

$$2H \frac{d(\Delta\omega_r)}{dt} = \Delta P_m - \Delta P_e \quad (2.7)$$

For balanced conditions, $P_m = P_e$ and $\omega_r = \omega_s$. For imbalanced conditions, the difference in power $P_m - P_e$ is supplied by the energy stored in the rotating mass.

In the power system, loads such as pumps or fans are sensitive to frequency. The overall frequency-sensitive loads are lumped into the damping constant D (pu) and expressed by (2.8) [34]:

$$\Delta P_e = \Delta P_L + D\Delta\omega_r \quad (2.8)$$

where ΔP_L represents frequency-insensitive loads and $D\Delta\omega_r$ represents frequency-sensitive loads.

Therefore, equation (2.7) is re-written as (2.9).

$$\Delta P_m - \Delta P_L = 2H \frac{d(\Delta\omega_r)}{dt} + D\Delta\omega_r \quad (2.9)$$

Equation (2.9) gives the response of rotating mass and frequency-sensitive loads in the power system to any power imbalances.

Hence, changes in ΔP_m and ΔP_L will lead to changes in the rotating speed of turbine. For any deviations of the rotating speed from the synchronous speed (in relation to grid frequency), the governor unit is used to return the rotating speed to the synchronous speed by regulating the valve/gate position of the turbine as shown in Fig. 2.4. The valve/gate position determines the power output. A droop control is set in the governor.

The droop is characterised by parameter R , which is defined as the ratio of frequency change to change of generator power output as shown in (2.10). This is illustrated by Fig. 2.5.

$$R = \frac{\Delta f}{\Delta P} \times 100\% = \frac{\omega_{NL} - \omega_{FL}}{\omega_s} \times 100\% \text{ (pu)} \quad (2.10)$$

where ω_{NL} is the steady-state speed at no load, ω_{FL} is the steady-state speed at full load and ω_s is the rated speed.

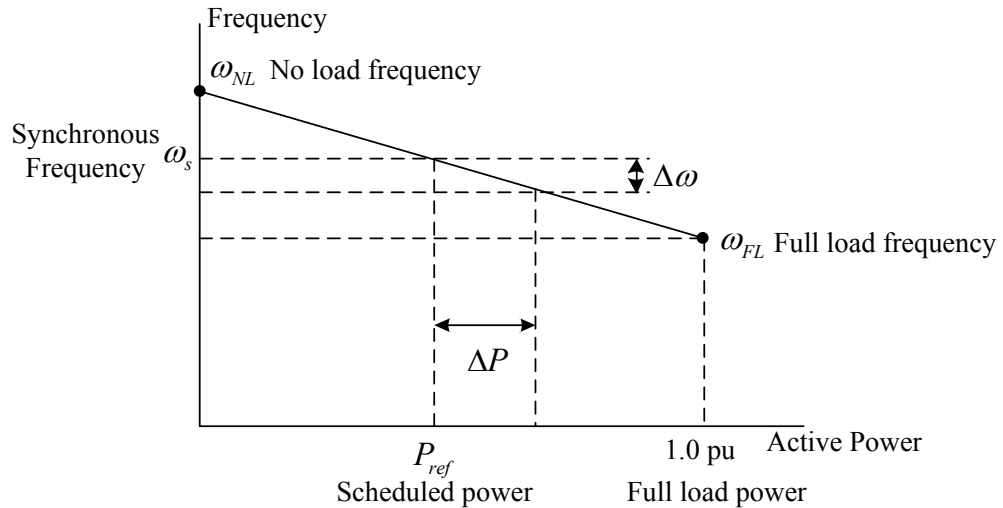


Fig. 2.5. Droop characteristics of governor [34]

Therefore, for any deviations of grid frequency, generators change their power output according to the droop control. This is referred to as primary frequency control. For any increase in demand or loss in generation (causing a drop in frequency), primary response service is provided automatically by governors. For any loss in demand or increase in generation (causing a rise in frequency), high frequency response service is provided automatically by governors.

A model of primary frequency control was developed in [36], as shown in Fig. 2.6. The model consists of the diagrams that are shown in Fig. 2.4.

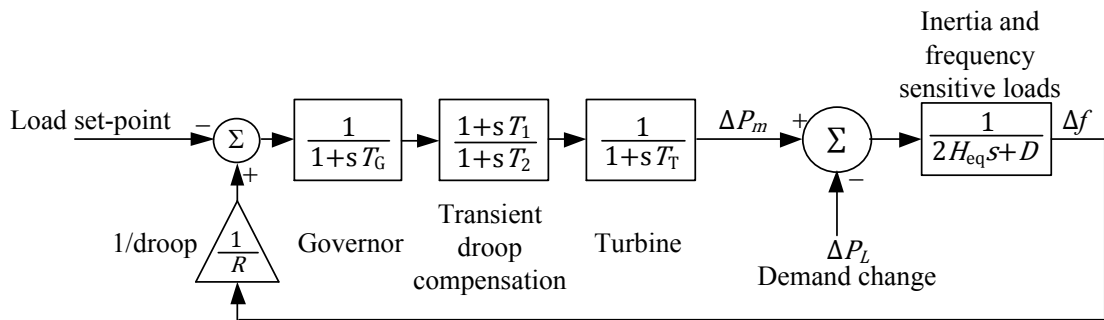


Fig. 2.6. GB power system primary frequency control model [36]

As illustrated in Fig. 2.6, when system demand (P_L) and power output of generators (P_m) are imbalanced, frequency (f) will deviate from its nominal value. The initial rate of frequency change is determined by the equivalent inertia of generators (H_{eq}) in the power system.

Different types of generating units have different values of inertia constant. Typical inertia constants are listed in Table 2.4 [36]. The equivalent system inertia is calculated

as the weighted sum of inertia constants of different types of generation in relation to system base [37]. The weight of one type of generation is calculated using (2.11). The equivalent system inertia is determined by (2.12).

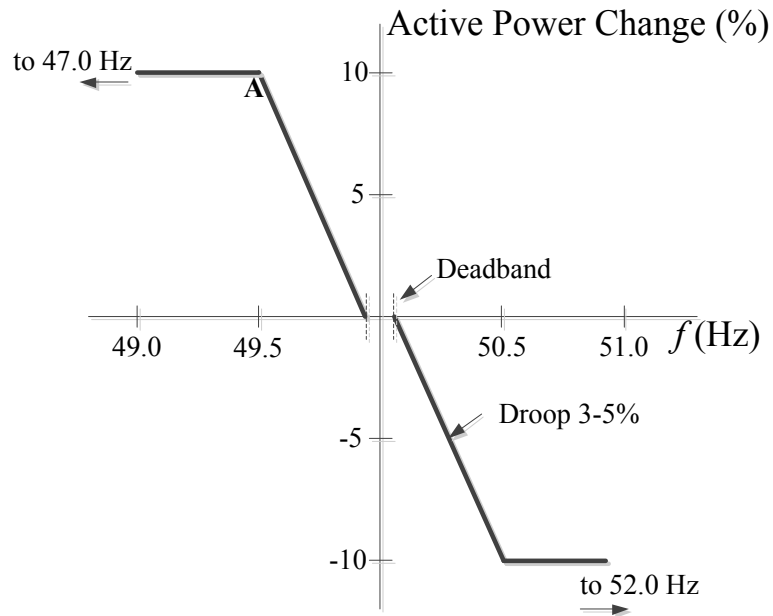
TABLE 2.4. Inertia Constant of Different Types of Generators [37]

$H_{interconnector}$	$H_{coal\ plant}$	H_{CCGT}	$H_{nuclear\ plant}$	H_{wind}
0 s	4-5 s	9 s	3 s	0-4 s

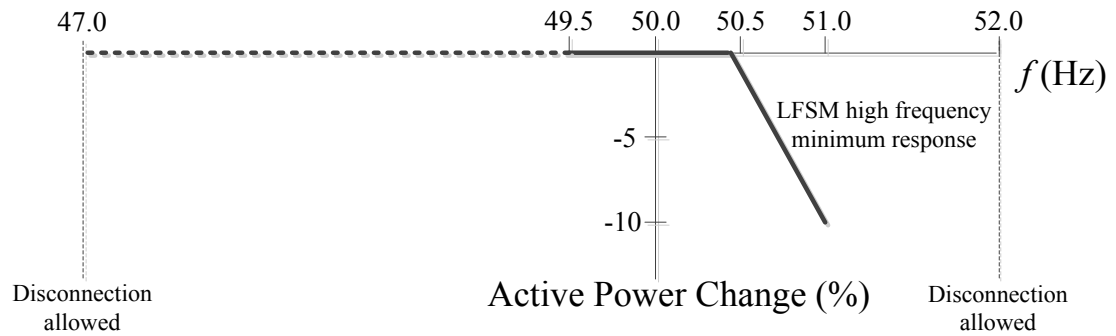
$$H_{system} = H_{machine} \times \frac{S_{B,machine}}{S_{B,system}} \quad (2.11)$$

$$H_{eq} = H_1 \frac{S_{B,1}}{S_{B,eq}} + H_2 \frac{S_{B,2}}{S_{B,eq}} + \dots + H_n \frac{S_{B,n}}{S_{B,eq}} \quad (2.12)$$

As illustrated by Fig. 2.6, governors use droop control to regulate power output of generators in response to frequency deviations. However, taking into account the level of system demand, the system operator will schedule generators to operate in one of two modes [38] as shown in Fig. 2.7: Frequency Sensitive Mode (FSM) and Limited Frequency Sensitive Mode (LFSM).



(a) Frequency sensitive mode



(b) Limited frequency sensitive mode

Fig. 2.7. Modes of frequency control operation [38]

In FSM, generators provide active power change to maintain frequency within the range 49.5 – 50.5 Hz using droop control as shown in Fig. 2.7(a).

In LFSM, as shown in Fig. 2.7(b), only high frequency response capability is required when frequency rises higher than 50.4 Hz. A 2% reduction in generator power output is required for a frequency rise of 0.1 Hz. This is equivalent to a droop of 10% ($R = (\Delta f / \Delta P) \times 100\% = (\frac{0.1\text{Hz}}{50\text{Hz}} / 2\%) \times 100\% = 10\%$). If frequency is within 49.5 – 50.4 Hz, generators maintain their output unchanged [38].

As shown in Fig. 2.8, the original operating point of a generator is O . Following a sudden load change (ΔP_L), generators provide primary frequency control by changing their output to P'_o . Grid frequency will reach a steady state (f'_o) which deviates from the nominal value (f_0). Some generators will then be scheduled to change their power output further (to P''_o) in order to return frequency to its nominal value [39]. This process, which changes the load set-point of a generator, is defined as secondary frequency control and delivers secondary response service.

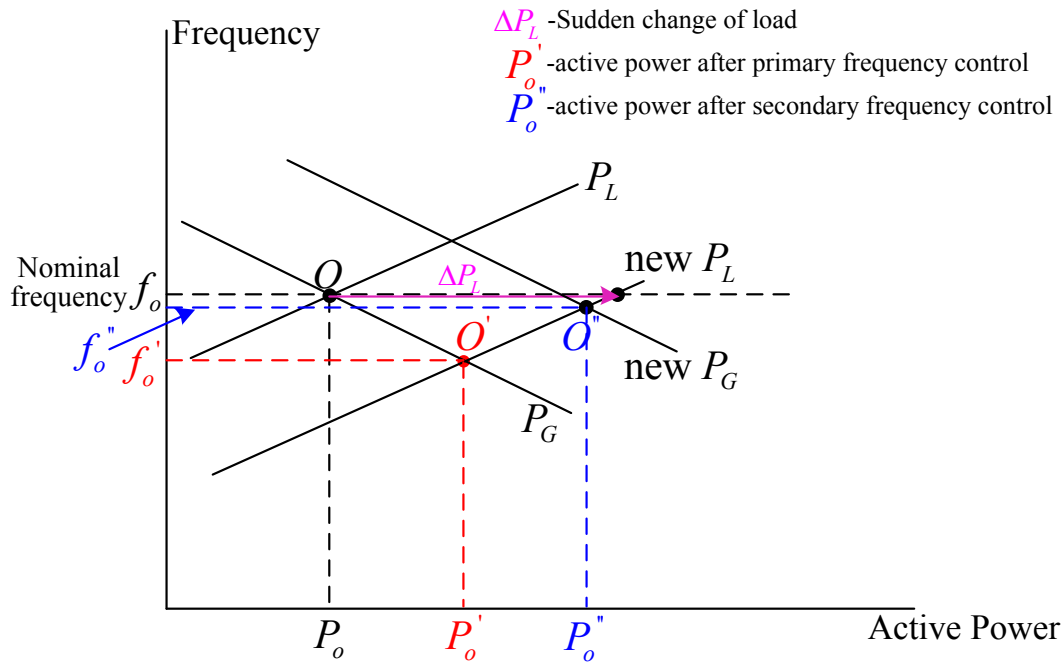


Fig. 2.8. Change of load set-point after primary and secondary frequency control (modified figure based on [39])

The Grid Code specifies the minimum frequency response that a generating unit should provide as shown in Fig. 2.9 [40]. The percentage of frequency response levels and loading levels are defined based on the Registered Capacity (RC) of a generating unit. For frequency deviations of up to 0.5 Hz from 50 Hz, generating units at different loading levels are required to provide frequency response of at least the levels indicated by the lines 'Minimum Primary/Secondary Response' and 'Minimum High Frequency Response' (Fig. 2.9). Generating units operating at 95% - 100% of their registered capacity should provide some response in accordance with the dotted lines 'Plant Dependent Primary/Secondary Response' and 'Plant Dependent High Frequency Response' (Fig. 2.9).

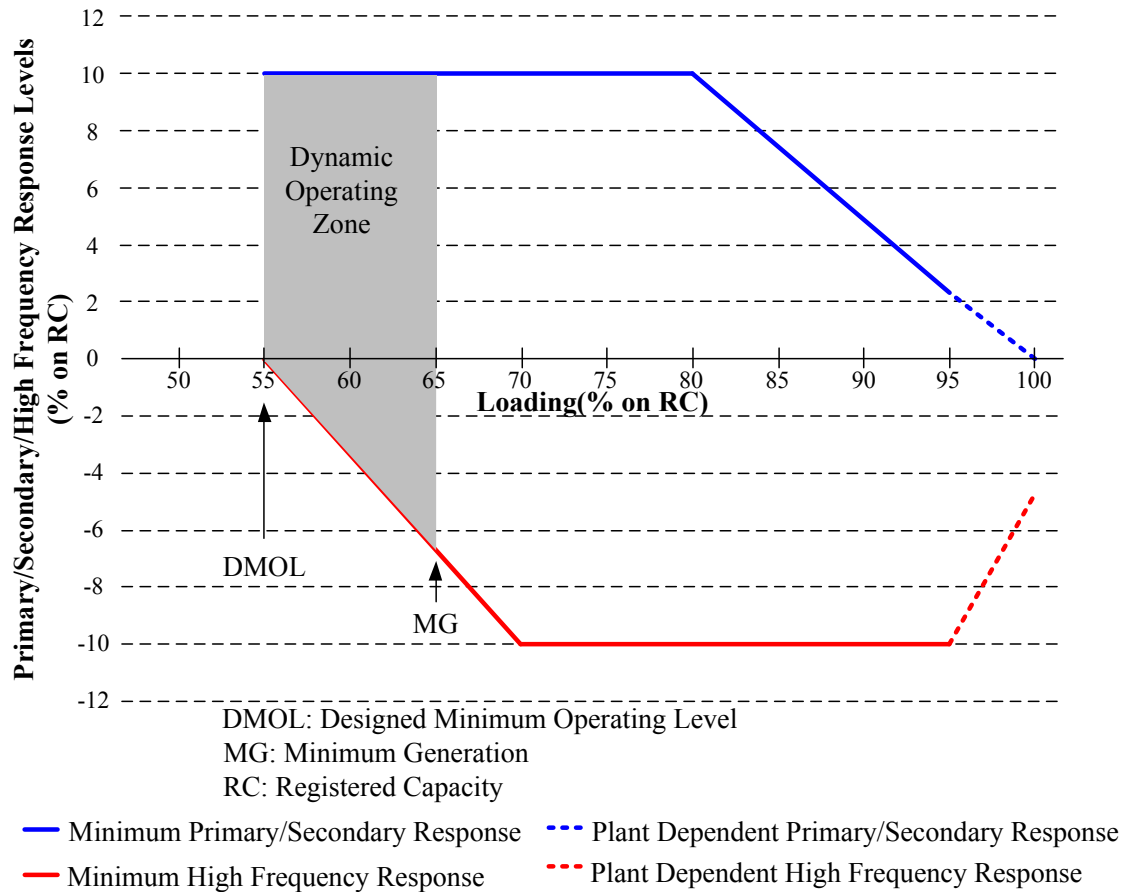


Fig. 2.9. Minimum frequency response requirement profile for a 0.5 Hz frequency deviation from 50 Hz required by the Grid Code [40]

In summary, even though it is costly and inefficient to operate part loaded, fossil fuel generators, frequency control in the present power system still relies on these generators to maintain grid frequency within its steady-state limits.

2.3.2 Frequency control of wind turbines

Integration of renewable energy resources through power electronics will lead to a reduction of system inertia and may cause unacceptable excursions of grid frequency. To address this issue, research has been carried out to obtain synthetic inertia response from both fixed speed and variable speed wind turbines.

Fixed speed wind turbine (FSWT) operates with a squirrel cage induction generator. The stator of the generator is directly connected to the grid. Therefore, the stator field rotates at the grid frequency (ω_s). The difference of the rotor speed (ω_r) and ω_s is referred to as the slip s which is given in (2.12) [41]. When frequency falls, s increases. Electromagnetic torque of the generator increases proportionally with s [42]. Hence, the output power of the wind turbine increases.

$$s = \frac{\omega_s - \omega_r}{\omega_s} \tag{2.12}$$

Variable speed wind turbines (VSWTs) are more widely used than FSWTs because they offer efficient power generation over a wide range of wind speeds and are able to regulate power factor [42].

A VSWT can be a Full Rated Converter-based (FRC) using a synchronous or induction generator or a Doubly Fed Induction Generator (DFIG) [41]. For example, the stator of an FRC synchronous generator is connected to the grid through converters which decouples the stator rotating speed from the grid frequency. Therefore, unlike conventional synchronous generators, no inertial response is provided automatically when grid frequency changes. As a result, if a VSWT replaces conventional power generation, the system inertia will be reduced.

Frequency support from VSWT was discussed in [37], [41]-[45]. Supplementary controllers were added to extract the kinetic energy from the turbine and even the energy stored in the DC link capacitor as shown in Fig. 2.10 [42]. The use of such supplementary controllers enables a VSWT to provide synthetic inertia of approximately 4 s.

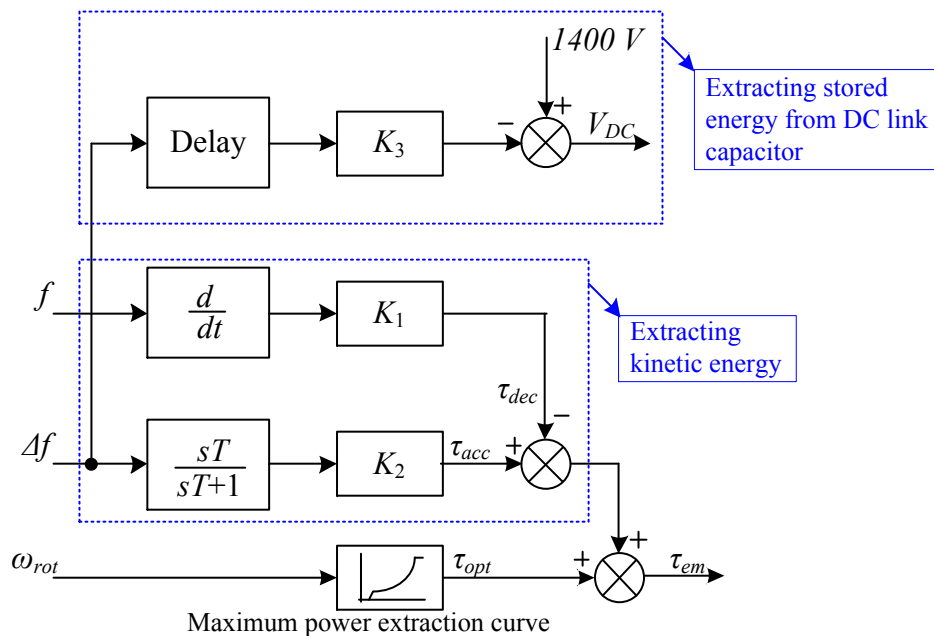


Fig. 2.10. Supplementary controller for inertial response from VSWT [42]

2.4 Demand-side integration

As described in Section 2.3, generation can be regulated in order to meet demand and hence maintain grid frequency at 50 Hz. However, demand is also able to play an active role.

2.4.1 What is demand-side integration?

According to [46], Demand-Side Integration (DSI) is a set of measures that uses loads, local generation and storage in order to support network operations and also to enhance the quality of power supply. It includes activities that encourage customers to change the patterns of their electricity consumption. It also includes mechanisms that manage demand in response to supply conditions.

Firstly, to change patterns of electricity consumption, DSI is able to provide services such as peak clipping, valley filling and load shifting. Peak clipping reduces power consumption of loads during periods of peak demand. Valley filling increases demand during off-peak periods through the use of energy storage. Load shifting moves loads from peak demand periods to off-peak periods using appliances that operate with duty cycles such as washing machines [47]. Total energy consumption of loads is not affected.

DSI may be implemented through price-based schemes which change patterns of electricity use. These schemes include time of use tariff (ToU), real-time pricing (RTP) and critical peak pricing (CPP). A ToU tariff indicates that for different time blocks, a different unit price is used. For example in the UK, with the ‘Economy 7’ tariff, electricity is cheaper at night than during the day [48]. RTP means that the price of electricity fluctuates with time to reflect changes of the wholesale electricity price [46]. CPP is a combination of ToU and RTP with its basic structure similar to that of ToU. The normal peak price is replaced by a much higher CPP price if the supply price is high or if the system frequency or voltage is outside the operational limits [46]. Hence, if use patterns of customers are changed as a result of these price-based schemes, it is expected that the difference in demand between the peak demand period and off-peak demand period will be reduced. In addition, due to the shift of demand from peak to off-peak period, customers may benefit from reduced electricity bills. For example, ref [49]

developed a control algorithm on domestic appliances in response to the RTP tariff so that the cost of running smart appliances was minimised.

DSI also helps to manage demand in response to drop of frequency when system emergencies occur. An example of this is load shedding. As discussed in Section 2.2, if frequency drops to below 49.7 Hz, some contracted large loads, such as steelworks, will be switched OFF. If frequency continues to drop to 48.8 Hz, loads on public distribution networks will be shed in stages so as to avoid shutdown of the entire power system.

2.4.2 Benefits of demand-side integration

Previous research has investigated the benefits of demand-side integration. These benefits can be summarised into technical benefits, economic benefits and environmental benefits.

A. Technical benefits for network operation

A1: DSI reduces demand during peak demand periods by peak clipping and load shifting. This reduces the required generation at peak demand periods.

A2: flexibility in power consumption of demand is able to react to variances in power generation from renewable energy sources. For example, flexible demand can be controlled to use the excess wind generation [50]. Hence, wind curtailment is reduced.

A3: DSI helps reduce the impact of congestion in the power system. With the increasing connection of new demand, such as electric vehicles, present network capacity becomes insufficient. This may cause congestion in the power system especially during peak demand periods. As a result, network reinforcement or expansion is required.

As discussed in the project Customer Led Network Revolution (CLNR) [51], reinforcement of the transmission network can be deferred if DSI contributes to decreasing national or regional network congestion. Reinforcement of the distribution network is also deferred as demand can be shifted to off-peak time or to times when distributed generation such as PV is generating power.

The project ‘Capacity to Customers (C2C)’ [52] is trying to find a method to defer network reinforcement through DSI. The present network, as shown in Fig. 2.11(a), uses only half of the circuit capacity. The spare capacity of the circuits is used to improve the reliability of supply to loads. As proposed by the C2C

project, Electricity North West Limited (ENWL) offers contracts to customers who are willing to participate in a DSI scheme in which their supply will not be restored for a fixed period (e.g. 8 hours) after a fault, as pre-agreed in the contract [53]. Then the Normal Open Point (NOP) of the network is closed as shown in Fig. 2.11(b) in order to take up the spare capacity and connect more loads [54]. When a fault occurs on one of lines, supply to all customers on the faulted circuit will be interrupted. Supply to the majority of customers will be restored within minutes. The manageable demand may not be restored before the end of the pre-agreed period. Therefore, DSI can reduce the network congestion that results from the connection of new demand.

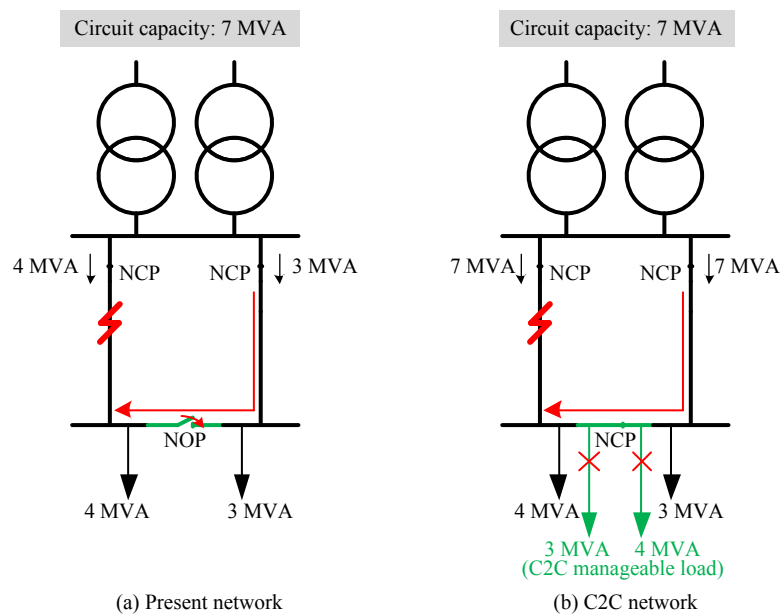


Fig. 2.11. Present network and C2C network [54]

Furthermore, response from DSI is geographically distributed across the country. This also contributes to the reduction of congestion on transmission and distribution networks [55].

A4: demand is able to provide frequency response or reserve services in the power system. When grid frequency drops, demand can be interrupted within 2 s as required by the Frequency Control by Demand Management (FCDM) service. The spinning reserve capacity of part loaded generators for frequency control is therefore reduced. Demand also provides reserve such as the Short-Term Operating Reserve (STOR) service [56].

B. Economic benefits for network investment

The technical benefits that are listed above will offer economic benefits as follows.

B1: peak demand is usually supplied by expensive power plants such as the Open Cycle Gas Turbine units [55]. The reduction in peak demand by DSI helps reduce the overall cost of generating electricity during that period.

B2: successful integration of renewable energy sources requires both spinning and standing reserve to be available so as to allow the system to cope with their intermittent power generation. This leads to increased operating costs. If DSI is able to replace some reserve capacity, operating costs of the power system will be reduced [57].

B3: DSI defers network reinforcement, which reduces the significant cost of investment in new capacity and also reduces customer bills. An Ofgem consultation document presented in 2009 estimates that investment in the entire UK network between 2009 and 2025 will amount to £53.4 billion [12].

B4: balancing services provided by DSI can reduce the spinning reserve capacity of frequency-sensitive generation. These generators are part-loaded, which is inefficient and gives rise to high fuel costs [55]. It is estimated by National Grid that, by the year 2020, the additional cost of retaining more reserve without contributions from DSI is expected to increase by £55 million from the level of the year 2009 [22].

C. Environmental benefits

C1: GHG emissions will be reduced as DSI facilitates penetration of renewable energy resources. The capacity of conventional generation which burns coal or oil will be reduced.

C2: DSI is able to replace the spinning reserve capacity of frequency-sensitive generators which emits GHG.

C3: DSI is able to reduce peak demand and network congestions. This facilitates the increasing connection of electric vehicles and therefore reduces GHG emissions from the transport sector.

2.4.3 Potential provision of response from demand

The domestic sector represents the single largest consumer of electricity in the GB power system, as shown in Fig. 2.12. The potential demand response from the domestic

sector is therefore significant. Table 2.5 lists the domestic loads that may have demand response functions.

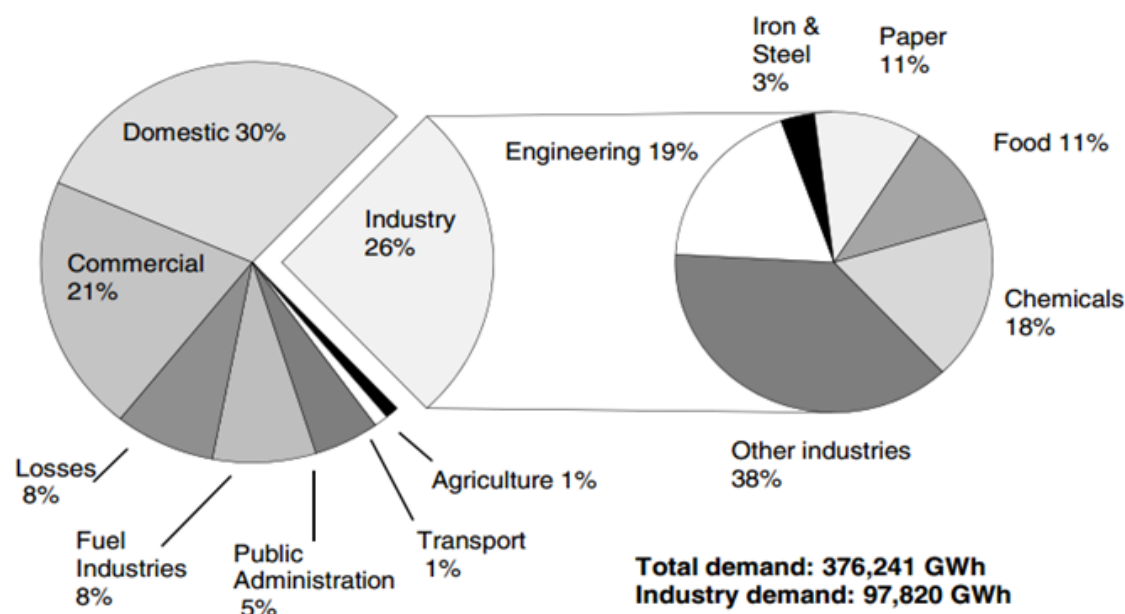


Fig. 2.12. Electricity demand of GB power system by sectors in 2012 [58]

TABLE 2.5. Demand Response Functions of Domestic Loads [39]

Appliances	Demand response functions
Refrigerators	-Delay defrost process -Modify running time at power system peak -Energy saving via change of temperature set-points
Wet appliances (i.e. dish washers and washing machine)	-Delay wash and dry -Modify cycling time -Energy saving washing cycles
Cooker	-Cook with reduced power
Water heater	-Reduce power at power system peak

The use of industrial demand for demand response is well established in the GB power system. Industrial loads such as steelworks and cement works [59] are able to provide frequency response service through FCDM as discussed in Section 2.2.1.

According to [60], demand response during peak periods from other non-domestic sectors, including commercial and public, can also be expected as shown in Table 2.6.

TABLE 2.6. Potential Demand Response from Other Non-domestic Sectors [60]

Commercial or public sector	Estimated load flexibility during peak hour of winter week day (GW)
Retail	0.4
Education	0.2
Commercial offices	0.1
Others	0.6
Total	1.2

According to an estimate by National Grid, a total of 2 GW of demand response could be feasible during peak hours by 2020 [8]. The contribution from different load types is given in Table 2.7. It is mentioned in [8] that the National Grid estimate was a little lower than other similar estimates as efficiency savings of future appliances was taken into consideration.

TABLE 2.7. Potential Provision of Response from Demand Estimated in 2011 [8]

Load type	Potential amount of services (MW)
Commercial loads (e.g. Air conditioning)	840
Industrial refrigeration	260
Domestic wet and refrigeration appliances	200
Heat pumps	570
Electric vehicles	100
Total	1970

2.5 Use of demand for frequency control

Demand is an efficient means to provide frequency control in a power system. At present, large industrial loads [59] that are under contract with National Grid are able to offer frequency response services through FCDM as discussed in Section 2.2.1. However, such load shedding is activated only for severe drops in frequency and the loads require manual reconnection after the recovery of frequency.

Different control strategies using demand, in particular small-size domestic demand for frequency control, have been studied which will be discussed in the following sections.

A Smart Grid integrated with a two-way communication network encourages the control of power consumption of loads in response to grid frequency in a centralised mode.

In the research reported in this thesis, the control of power consumption of loads in response to local measurements of grid frequency was investigated. Use of ICT infrastructure is avoided.

As background to the research that has been carried out, both centralised frequency control and local frequency control of demand are summarised below.

2.5.1 Centralised control of demand

Centralised control of demand relies on an Information and Communications Technology (ICT) infrastructure enabling communications between manipulated demand and its upper layer such as an aggregator, DNO or TSO. Four centralised control methods are now described.

The first method is a direct load control scheme for frequency regulation as discussed in [61]. Within each control period, appliances predicted their power level and energy consumption for the next sample time while sending their present power level and energy consumption to the DNO. The DNO created histograms of the capacity of available load change using the received information and then sent them to the TSO. The TSO summarised the histograms and determined the switching thresholds for each appliance based on frequency deviations. These thresholds are then sent to appliances via the DNO. An appliance compared its predicted power level and energy consumption with the received threshold and then switched ON/OFF accordingly. However, the control required a considerable amount of communications between appliances, the DNO and the TSO. The communication is required to be relatively fast so as to ensure that control actions are triggered promptly once a frequency deviation is detected.

The second method in ref. [62] and the third method in ref. [63] proposed load control algorithms used for non-critical loads in a Micro Grid (MG) in order to regulate frequency.

The load control algorithm proposed by [62] measured grid frequency at the point of common coupling of a MG. When frequency deviated out of its steady-state limits, the percentage of loads to be switched in order to reduce the frequency deviation was

calculated. When frequency recovered, interrupted loads started to be reconnected by 5% for each time-step. The latency of communication between the control centre and non-critical loads was simulated. The control remained stable with latency up to 300 ms.

In [63], a Micro Grid Central Controller (MGCC) communicated with the Intelligent Load Management Controller (ILMC) of each non-critical load in order to use the loads for frequency control. The ILMC sent a record of lost energy (E) caused by previous shedding of a load and power consumption (P) of a load to the MGCC. The MGCC then determined the highest P and E and the lowest P and E amongst loads, and sent the values back to each ILMC.

The loads to be shed first were selected by identifying those with the lowest E and, from that group, those with the highest P.

- Identification of the lowest E ensures equity of switching amongst loads because, if a load has been shed for a long period, it is therefore less likely to be shed again.
- Identification of the highest P ensures that load shedding starts with the load with the largest power consumption. This reduces the number of loads to be interrupted.

The ILMC then worked out at which frequency a load was shed or reconnected. By taking into account previous lost energy and power consumption of loads, the load control minimised the impact of frequency control on the performance of loads.

The fourth method is another form of centralised control of demand. It was the use of time-flexible loads to assist or even replace spinning reserves. This was first published by [64] in 1980. For such demand, it is not critical when electrical energy is consumed [65]. Hence, its power consumption is able to be time-shifted without noticeable impacts on load owners. Therefore, time-flexible demand is considered to be an appropriate choice for grid frequency control.

Thermal loads are considered time-flexible and appropriate for frequency control. Their power consumption can be shifted in time as long as their temperature constraints are satisfied. Water heaters and Heating Ventilation and Air Conditioning (HVAC) loads were investigated to provide regulating services using a direct load control as discussed

in [66]-[67]. Power consumption of these thermal loads was controlled to follow the regulation signals sent by the system operator.

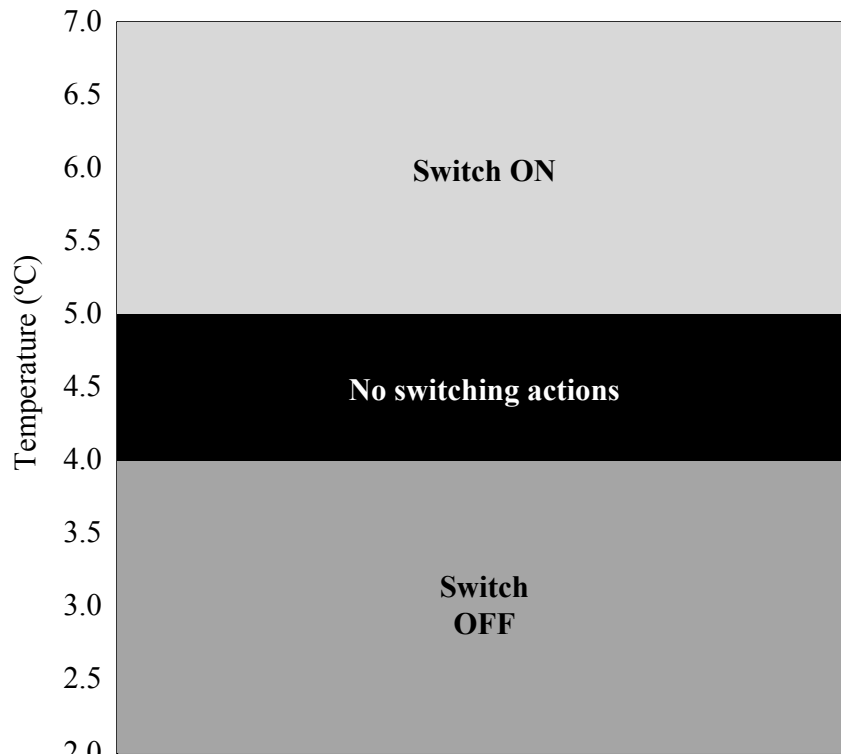
Another form of centralised control of thermal household appliances was described in [68]-[69]. The control enabled a large group of loads to act as distributed energy storage. By defining a droop characteristic according to frequency deviations, the central controller specified the amount of active power reserve required from demand. Ref [68] coordinated a large group of loads in order to track the active power reserve by their aggregated power consumption. The individual temperature limitations of loads were not breached. Ref [69] constructed a portfolio of loads for a load aggregator. Before each delivery period, loads sent their state information (such as the temperature status) to the aggregator. An optimisation problem to minimise the cost of an aggregator delivering a certain volume of primary frequency reserve was also formulated. After solving the optimisation problem, the aggregator sent activation commands to loads.

2.5.2 Local control of demand

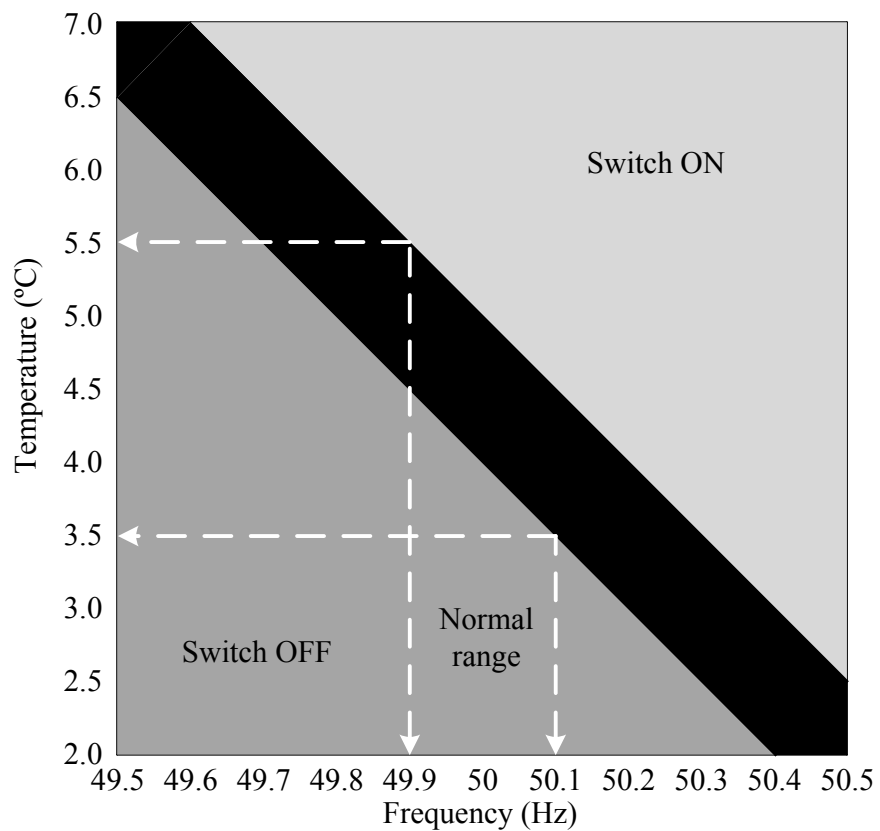
The centralised frequency control from demand requires communications between large numbers of units. Communication latency makes it difficult to achieve a second-by-second management of grid frequency. Furthermore, the complexity and cost of ICT infrastructures are significant hurdles. Therefore, local control was developed in order for demand to respond to locally measured frequency deviations.

One method of local load control to regulate grid frequency was presented in [16], [70]-[72]. When frequency dropped to lower than a pre-defined set-point, a load was switched OFF and the time stamp was recorded. A random time lag was given to each load before they were reconnected. This avoided the simultaneous reconnections of loads. It was shown that the aggregated behaviour of these loads was able to provide frequency control. However in [16], smart meters were used to read grid frequency and to execute the load control. In [70]-[72], a frequency sensor was connected to the wall outlet of a load for measurement of grid frequency [70]. The load control algorithm was integrated to the load.

Another method of local frequency control of demand was Dynamic Demand Technology (DDT), which is mainly used for thermal loads at present. For these loads, their inherent control is to compare their present temperature with temperature set-points and then determine their ON/OFF state and power consumption. DDT controlled



(a) Normal temperature control of a refrigerator



(b) Defined temperature and frequency relationship of a refrigerator

Fig. 2.13. Normal temperature control and frequency control of a refrigerator [73]

the temperature set-points of a load to vary in line with frequency deviations [73]-[78]. This is illustrated by Fig. 2.13, in which a refrigerator is controlled in order to respond to frequency deviations [73].

Normal temperature control of a refrigerator is depicted in Fig. 2.13(a). The refrigerator has a low temperature set-point of 4 °C, below which it will be switched OFF. The refrigerator has a high temperature set-point of 5 °C, above which it will be switched ON.

Frequency control of a refrigerator is shown in Fig. 2.13(b). Temperature set-points of a refrigerator are controlled to vary with frequency. When the frequency is 50 Hz, temperature set-points are the same as those shown in Fig. 2.13(a). When the frequency drops to 49.9 Hz, low and high temperature set-points change to 4.5 °C and 5.5 °C respectively. The refrigerator will be switched OFF when the temperature drops to 4.5 °C rather than to 4 °C. Alternatively, when frequency rises to 50.1 Hz, low and high temperature set-points change to 3.5 °C and 4.5 °C respectively. The refrigerator is switched ON when the temperature rises to 4.5 °C rather than to 5 °C.

The collective behaviour of a number of refrigerators with such frequency control is illustrated in Fig. 2.14 [75], where 10 units were assumed to be in an ON state, 6 units were assumed to be in an OFF state and the frequency was at 50 Hz in Fig. 2.14(a). If the frequency drops as shown in Fig. 2.14(b), temperature set-points increase. Hence, the number of refrigerators in an ON state was reduced to 7.

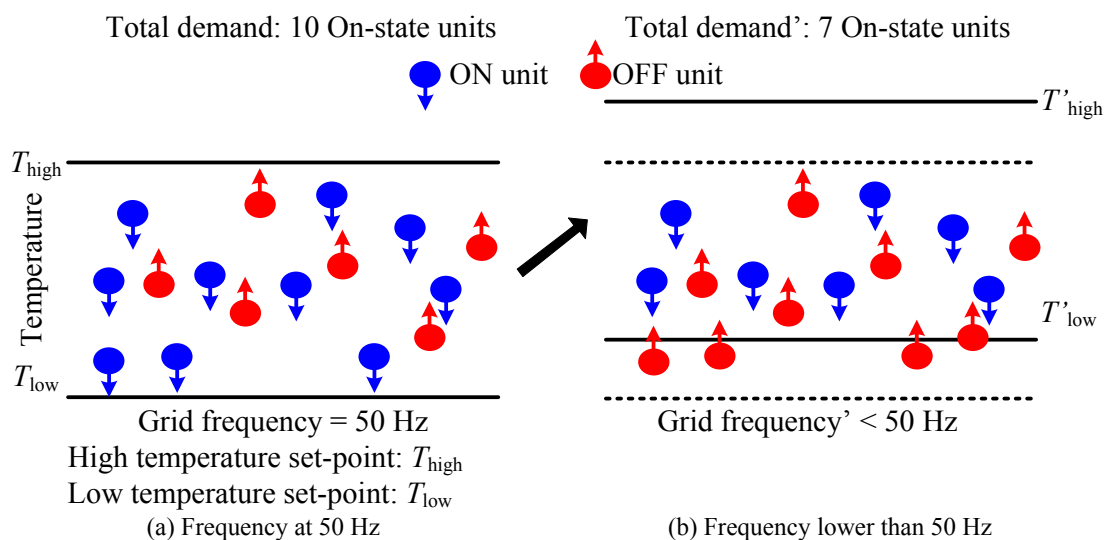


Fig. 2.14. Collective behaviour of refrigerators with control of temperature set-points by frequency
(Modified figure based on [75])

An aggregated model of 1,000 refrigerators was developed and connected to a power system model in [73]. Simulation results showed that the control offered by refrigerators reduced the drop of frequency. However, it is proposed in [73] that the control may cause refrigerators to be synchronised in temperature states following a severe frequency incident. This will lead to another frequency drop as refrigerators are reconnected to the grid simultaneously.

DDT was also applied to dishwashers in [79]. The switching frequency of a dishwasher was set to be inversely proportional to its internal temperature. The length of time before a dishwasher was reconnected was also inversely proportional to its internal temperature. Simulation results showed that an aggregated number of dishwashers was able to change load in response to deviations of frequency.

Therefore, localised control is feasible for frequency regulations by demand. It avoids the need for ICT infrastructure and provides fast response to frequency deviations by switching ON/OFF loads within seconds. Furthermore, DDT considers temperature status of a load to determine when a load is switched ON/OFF in response to frequency. As a result, the impact of frequency control on the performance of loads is minimised.

The potential and benefits of DDT are now examined more closely in the following Section 2.5.3.

2.5.3 Potential value of dynamic demand technology

DECC published a document [80] which estimated the potential of Dynamic Demand Technology (DDT) in the provision of frequency response services. It was assumed that 40 million refrigerators were connected in the GB power system. With DDT applied to these refrigerators, their maximum frequency response was estimated to be between 728 to 1,174 MW. Furthermore, the report suggested that these refrigerators will be able partially to replace the spinning reserve capacity of part loaded, fossil-fuel generation, resulting in a reduction of fuel costs of £28.8m - £222m per annual and a total CO₂ saving of 0.68 – 1.74 Mton per annum.

Benefits of the use of demand to participate in Firm Frequency Response (FFR) service through DDT were compared with the use of demand to participate in the Frequency Control by Demand Management (FCDM) service as shown in Table 2.8 [81]. DDT allows demand to provide response to bi-directional frequency deviations without

undermining operational parameters of loads. An FFR service provider has greater revenue than an FCDM service provider. Hence, for a service provider, it is more beneficial to use demand for the FFR service than to use it for the FCDM service.

TABLE 2.8. Comparison of the Use of Demand to Participate in FFR Service through DDT with the Use of Demand for FCDM Service [81]

Key factors	Demand use DDT for dynamic frequency response (FFR ¹)	Demand for FCDM ²
Revenue for frequency drop (£/MW/Year)	45,000	15,000 – 25,000
Revenue for frequency rise (£/MW/Year)	55,000	No
Keep assets within operational parameters	Yes	No

FFR¹: Firm Frequency Response

FCDM²: Frequency Control by Demand Management

Therefore, DDT is an effective means of frequency control in the power system. It contributes to system operations and meanwhile provides significant benefits to service participants.

2.6 Conclusion

The review of literature indicates that the present GB power system mainly relies on the frequency control capabilities of frequency-sensitive generators to provide frequency response services. However, these part loaded, fossil fuel generators make the power system less efficient and cause GHG emissions. Demand-side integration allows demand to play an active role in the future power system. Frequency control from demand reduces the reliance on frequency-sensitive generators. Centralised frequency control from demand is able to regulate grid frequency but it requires a well-established ICT infrastructure. Therefore, local frequency control from demand is potentially more attractive. In the following chapters, DDT is used for domestic refrigerators and industrial bitumen tanks to provide grid frequency control locally. This frequency control does not undermine the inherent temperature control of loads. It is fully

automatic and invisible to users. The feasibility of the participation of these loads in frequency response services is presented.

Chapter 3

Domestic Refrigerators for Frequency Control

This chapter investigates the use of domestic refrigerators for grid frequency control. A thermodynamic model of a refrigerator is developed and calibrated using data from tests on a number of refrigerators. An aggregated model of a population of refrigerators with diversified individual thermal behaviour is also developed. An autonomous and decentralised frequency controller is developed enabling refrigerators to change their power consumption in proportion to deviations of grid frequency. The frequency control will not interfere with refrigerators' primary function of cold storage. The aggregated model of refrigerators equipped with frequency control is then connected to a simplified GB power system model. Simulation results show that refrigerators help reduce frequency deviations in a way similar to that of frequency-sensitive generators. Refrigerators provide a faster response to frequency deviations than frequency-sensitive generators.

3.1 Introduction

The domestic sector accounts for a significant proportion of the total electrical energy consumption in the UK. In year 2012, domestic electrical energy consumption was 114,698 GWh, which was 36.1% of the total consumption in that year [82]. Hence, there is significant potential for the domestic sector to be utilised for demand response in the power system.

Domestic refrigerators were studied for the provision of frequency control in the power system. A domestic refrigerator is able to be connected to the grid at all times and consumes electricity with an ON/OFF cycle. It is available for frequency control because its power consumption is time-flexible. Power consumption of a refrigerator is able to be shifted in response to frequency deviations with little disruption to its cold storage performance.

In the GB power system, there are approximately 40 million domestic refrigerators [83] connected to the grid. Their average load as estimated in [84] for the year 2030 will be approximately 1,300 MW in summer and 1,000 MW in winter.

A diagram of a refrigerator is shown in Fig. 3.1. The cavity is the place for cold storage of food. It has thermal contact with the room. Heat is therefore transferred from the room to the cavity through the thermal contact. This leads to a temperature rise inside the cavity. The temperature of the cavity controls the ON/OFF state of the compressor. If the temperature rises higher than its high set-point T_{high} , the compressor is switched ON and starts cooling the cavity. If the temperature is lower than its low set-point T_{low} , the compressor is switched OFF.

When the compressor is switched ON, the refrigeration cycle starts and causes the refrigerant material inside the pipe to flow. During the flow of refrigerant, the evaporator absorbs heat from the cavity through the thermal contact between the evaporator and the cavity. Heat is then dissipated to the outside through the condenser. The temperature inside the refrigerator drops.

The operating principle of the cooler and freezer of a refrigerator is similar. In this study, it was assumed that the cooler and the freezer work independently. They were modelled using the same mechanism but were different in their temperature set-points. Refrigerator is the term used in this thesis to mean either a cooler or a freezer.

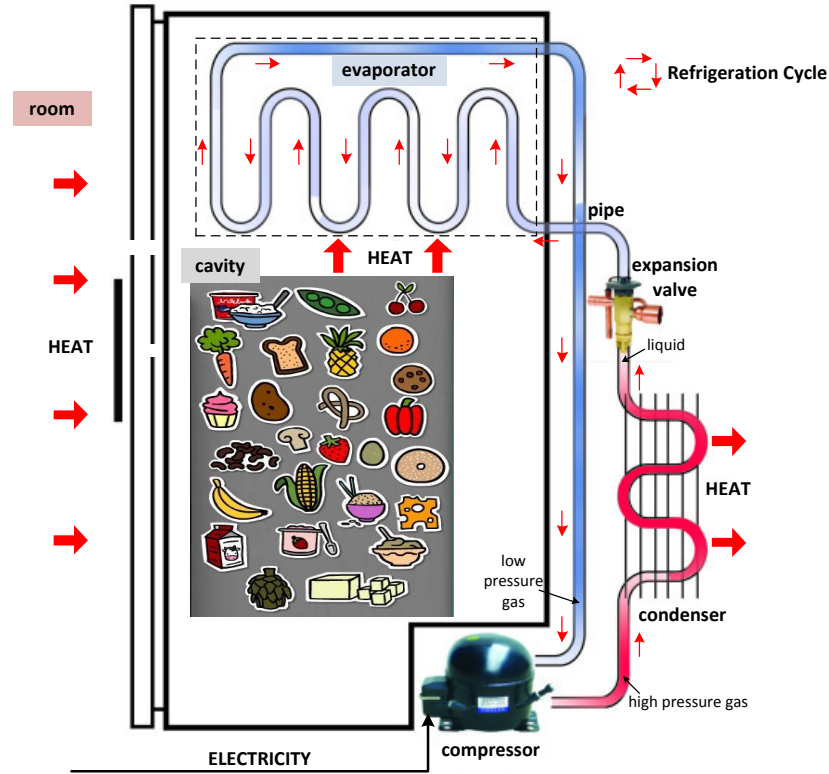


Fig. 3.1. Diagram of a refrigerator and its refrigeration cycle (modified figure based on [85])

3.2 Model of refrigerators

3.2.1 Thermodynamic model of refrigerators

To reflect the temperature variation of a refrigerator, a thermodynamic model was developed.

As depicted in Fig. 3.1, the evaporator absorbs heat from the cavity. The rate of heat absorbed [86] P_{absorb}^{Ev} (W) is:

$$P_{absorb}^{Ev}(t) = U^{CaEv} A^{CaEv} (T_{Ca}(t) - T_{Ev}(t)) \quad (3.1)$$

where Ca represents the cavity, Ev represents the evaporator and $CaEv$ represents the thermal contact between cavity and evaporator. U^{CaEv} ($\text{Wm}^{-2}\text{K}^{-1}$) is the heat transfer coefficient of the thermal contact, A^{CaEv} (m^2) is the area of the thermal contact, T_{Ca} (K) is the cavity temperature and T_{Ev} (K) is the evaporator temperature.

Heat in the evaporator is released by the work done by the compressor. The rate of heat released $P_{release}^{Ev}$ (W) is:

$$P_{release}^{Ev}(t) = P_r s_c(t) \quad (3.2)$$

where P_r (W) is power consumption of the compressor and s_c is the compressor state. s_c is 1 if it is ON and s_c is 0 if it is OFF. s_c is determined by the comparison of T_{Ca} with its temperature set-points T_{high} and T_{low} :

$$s_c(t) = \begin{cases} 1, & \text{if } T_{Ca}(t) > T_{high} \\ 0, & \text{if } T_{Ca}(t) < T_{low} \end{cases} \quad (3.3)$$

Therefore, the net rate of heat transfer in the evaporator P_{net}^{Ev} (W) is:

$$P_{net}^{Ev}(t) = P_{absorb}^{Ev}(t) - P_{release}^{Ev}(t) \quad (3.4)$$

The net rate of heat transfer causes variation of T_{Ev} . The relationship between the net rate of heat transfer and variation of T_{Ev} [87] is:

$$P_{net}^{Ev}(t) = c_v^{Ev} m^{Ev} \frac{dT_{Ev}(t)}{dt} \quad (3.5)$$

where c_v ($\text{Jkg}^{-1}\text{K}^{-1}$) is the specific heat capacity and m (kg) is the mass of the evaporator.

By combining (3.1)-(3.5), a first order differential equation of T_{Ev} was obtained:

$$\frac{dT_{Ev}(t)}{dt} = \frac{U^{CaEv} A^{CaEv}}{c_v^{Ev} m^{Ev}} (T_{Ca}(t) - T_{Ev}(t)) - \frac{P_r s_c(t)}{c_v^{Ev} m^{Ev}} \quad (3.6)$$

For the cavity, a similar analysis was carried out. The cavity has heat absorbed from the ambient room. The rate of heat absorbed P_{absorb}^{Ca} (W) is:

$$P_{absorb}^{Ca}(t) = U^{CaAmb} A^{CaAmb} (T_{Amb} - T_{Ca}(t)) \quad (3.7)$$

where Amb represents the ambient room and CaAmb represents thermal contact between the cavity and the ambient room. U^{CaAmb} ($\text{Wm}^{-2}\text{K}^{-1}$) is the heat transfer coefficient of the thermal contact, A^{CaAmb} (m^2) is the area of the thermal contact and T_{Amb} (K) is the ambient room temperature.

Heat in the cavity is released to the evaporator. The rate of heat released $P_{release}^{Ca}$ (W) is:

$$P_{release}^{Ca}(t) = U^{CaEv} A^{CaEv} (T_{Ca}(t) - T_{Ev}(t)) \quad (3.8)$$

Therefore, the net rate of heat transfer in the cavity P_{net}^{Ca} (W) is:

$$P_{net}^{Ca}(t) = P_{absorb}^{Ca}(t) - P_{release}^{Ca}(t) \quad (3.9)$$

The net rate of heat transfer causes the variation of T_{Ca} . The relationship is given by:

$$P_{net}^{Ca}(t) = c_v^{Ca} m^{Ca} \frac{dT_{Ca}(T)}{dt} \quad (3.10)$$

By combining (3.7)-(3.10), a first order differential equation of T_{Ca} was obtained:

$$\frac{dT_{Ca}(t)}{dt} = \frac{U^{CaAmb} A^{CaAmb}}{c_v^{Ca} m^{Ca}} (T_{Amb} - T_{Ca}(t)) - \frac{U^{CaEv} A^{CaEv}}{c_v^{Ca} m^{Ca}} (T_{Ca}(t) - T_{Ev}(t)) \quad (3.11)$$

A thermodynamic model of a refrigerator is developed in *DIGSILENT PowerFactory* by solving the differential equations (3.6) and (3.11).

3.2.2 Calibration of the model using test data

For a refrigerator, physical parameters such as U , A , c_v and m are known. The parameters used in the model were provided by Open Energi. The company obtained the parameters through tests on refrigerators at the premises of Indesit¹ at an ambient temperature of around 22 °C. Table 3.1 shows the parameters of a cooler. The temperature and compressor state of the model were compared with real measurements as shown in Fig. 3.2.

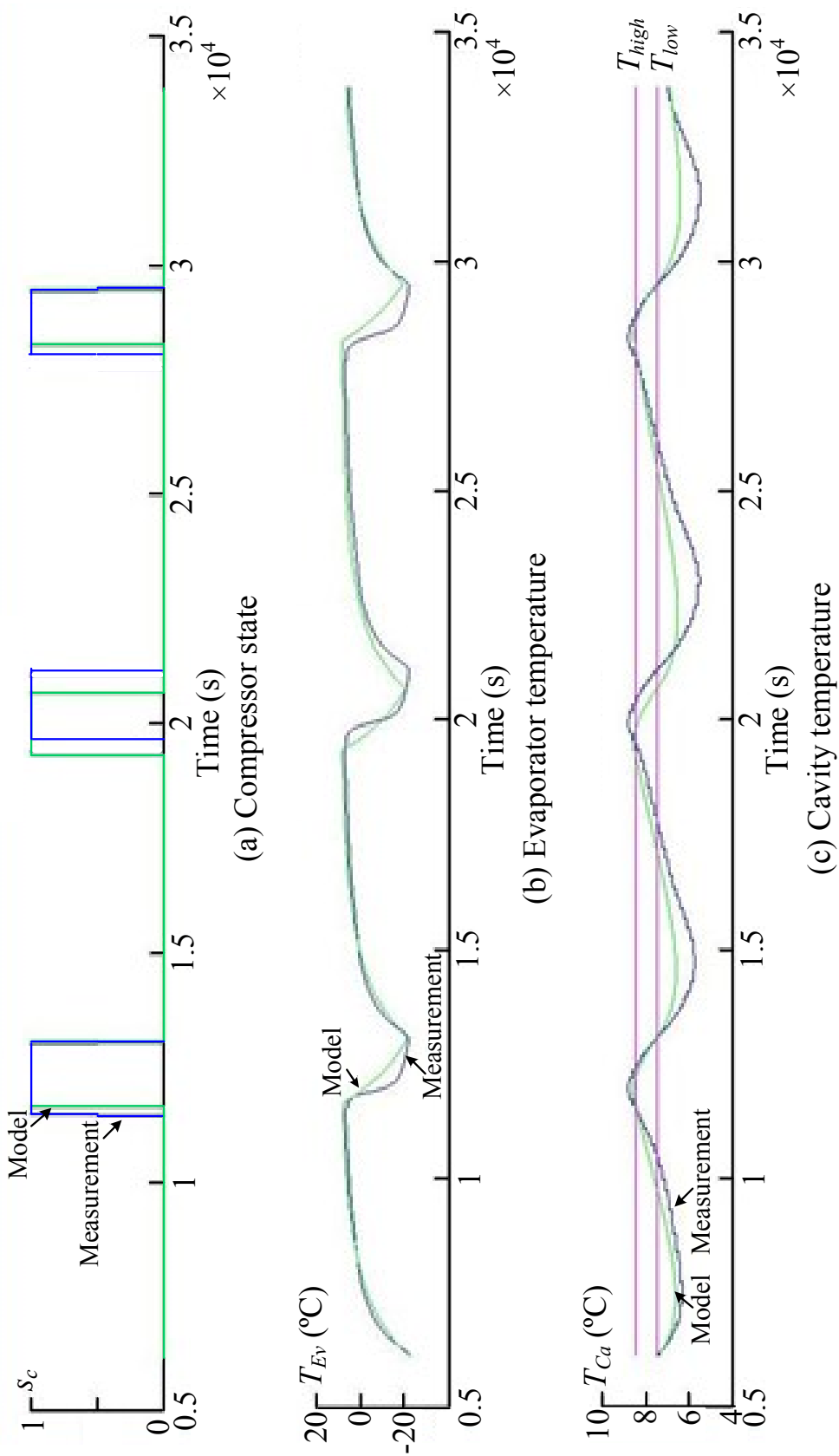
TABLE 3.1. Parameters of the Cooler Model Calibrated at an Ambient Temperature 22 °C.

m^{Ev}	m^{Ca}	A^{CaEv}	A^{CaAmb}	U^{CaEv}	c_v^{Ev}	U^{CaAmb}	c_v^{Ca}	P_r	T_{high}	T_{low}
(kg)	(kg)	(m ²)	(m ²)	(Wm ⁻² K ⁻¹)	(Jkg ⁻¹ K ⁻¹)	(Wm ⁻² K ⁻¹)	(Jkg ⁻¹ K ⁻¹)	(W)	(°C)	(°C)
0.5	1.0	0.81	3.24	1.2	3436	0.2	12196	50	8.5	7.5

¹ Indesit is a company in Italy whose legal name is 'Indesit Company SpA'

Fig. 3.2. Comparison of temperature and compressor state of a cooler in the model and in the real measurements starting at an ambient temperature 22 °C (provided by

Open Energy)



The difference between the model and the real measurements in Fig. 3.2 was caused by the varying ambient temperature. The model assumed a constant ambient temperature of 22 °C while, during the real measurements over approximately 8 hours, the ambient temperature varied constantly. The influence of ambient temperature on the thermodynamics of refrigerators is further discussed in Appendix I. Simulation results show that ambient temperature has significant impact on the temperature variations and ON/OFF cycle of a refrigerator.

Similarly, the parameters of a freezer provided by Open Energi are shown in Table 3.2.

TABLE 3.2. Parameters of the Freezer Model Calibrated at an Ambient Temperature 22 °C.

m^{Ev}	m^{Ca}	A^{CaEv}	A^{CaAmb}	U^{CaEv}	c_v^{Ev}	U^{CaAmb}	c_v^{Ca}	P_r	T_{high}	T_{low}
(kg)	(kg)	(m ²)	(m ²)	(Wm ⁻² K ⁻¹)	(Jkg ⁻¹ K ⁻¹)	(Wm ⁻² K ⁻¹)	(Jkg ⁻¹ K ⁻¹)	(W)	(°C)	(°C)
0.5	1	0.81	3.24	0.9	3779	0.2	9147	50	-15	-16

3.2.3 Aggregated model of a population of refrigerators

An aggregated model of a population of refrigerators was also developed. Diversity amongst refrigerators was considered. This diversity refers to the differences in the physical parameters such as the size of refrigerators and mass of food stored.

The four physical parameter terms, $\frac{U^{CaEv}A^{CaEv}}{c_v^{Ev}m^{Ev}}$, $\frac{P_r}{c_v^{Ev}m^{Ev}}$, $\frac{U^{CaEv}A^{CaEv}}{c_v^{Ca}m^{Ca}}$, $\frac{U^{CaAmb}A^{CaAmb}}{c_v^{Ca}m^{Ca}}$, shown in equations (3.6) and (3.11), indicates the refrigerator size and mass of food stored and were obtained from Table 3.1 and Table 3.2 for one refrigerator. For a population of refrigerators, each of the four physical parameter terms of a refrigerator was multiplied by a random number r . For each individual refrigerator, r was selected uniformly in the range calculated in (3.12).

$$r \sim \text{Uniform}([1 - div], [1 + div]), div \in [0, 1] \quad (3.12)$$

where div is defined as a diversity factor which indicates the difference amongst refrigerators. div is in the range between 0 and 1. Table 3.3 gives the range of r values corresponding to each div value.

TABLE 3.3. Diversity in the Refrigerators

<i>div</i>	<i>r</i>
0	Uniform(1,1)
0.1	Uniform(0.9,1.1)
0.2	Uniform(0.8,1.2)
0.3	Uniform(0.7,1.3)
0.4	Uniform(0.6,1.4)
0.5	Uniform(0.5,1.5)
0.6	Uniform(0.4,1.6)
0.7	Uniform(0.3,1.7)
0.8	Uniform(0.2,1.8)
0.9	Uniform(0.1,1.9)
1	Uniform(0,2)

- If *div* is 0, *r* is 1 and each of the four physical terms $\left(\frac{U^{CaEv}A^{CaEv}}{c_v^{Ev}m^{Ev}}, \frac{P_r}{c_v^{Ev}m^{Ev}}, \frac{U^{CaEv}A^{CaEv}}{c_v^{Ca}m^{Ca}}, \frac{U^{CaAmb}A^{CaAmb}}{c_v^{Ca}m^{Ca}}\right)$ of refrigerators amongst the population is multiplied by 1. Therefore, there will be no differences amongst the refrigerators.
- If *div* is 0.5, *r* is distributed uniformly in the range of 0.5 to 1.5. By multiplying each of the four terms of a refrigerator by *r*, the parameters will be $\pm 50\%$ different from the parameters shown in Table 3.1 and Table 3.2 over the refrigerator population.
- The refrigerator models are more diversified with a *div* closer to 1.

Tests carried out by Open Energi on 100 empty refrigerators determined a *div* of 0.2. This was used for initial simulation studies. However, as described in Section 3.5, sensitivity analysis by varying the value of *div* was carried out. It was determined that a higher *div* value would be more realistic for the modelling of refrigerators in UK homes in order to reflect the level of diversity of refrigerator size and amount of food stored.

3.3 Dynamic control of refrigerators

The inherent controller of a refrigerator is a temperature controller which controls the cavity temperature T_{Ca} to be within its set-points (T_{high} and T_{low}). A decentralised and autonomous frequency control for refrigerators was developed enabling refrigerators to vary their power consumption with frequency deviations dynamically. Although in real

life, a significant proportion of refrigerators have only one compressor that controls both the cooler and freezer, in this thesis, the model was simplified and assumed that the cooler and freezer work independently as a result of their similarities in thermodynamics and operating principles. In addition [88], combined refrigerators with two compressors provide separate operation of the fridge and freezer compartment while enabling precise temperature settings for refrigeration and freezing. Food is stored in optimum conditions while a considerable amount of power is saved. Therefore, each fridge and freezer has an independent frequency controller. The frequency controller changes the ON/OFF state of refrigerators in response to frequency deviations without undermining the cold storage of a refrigerator.

3.3.1 Temperature control of a refrigerator

The ON/OFF state of a refrigerator is controlled by comparing T_{Ca} with T_{high} and T_{low} as shown in Fig. 3.3.

If T_{Ca} reaches T_{high} at A, the refrigerator is switched ON. Then T_{Ev} starts dropping immediately. However, due to the process of heat transfer through the thermal contact between the evaporator and cavity, there is a delay before T_{Ca} starts to drop.

When T_{Ca} reaches T_{low} at C, the refrigerator is switched OFF. Then T_{Ev} starts increasing almost immediately. There is a delay before T_{Ca} starts to rise. Refrigerator remains OFF until T_{Ca} again reaches T_{high} .

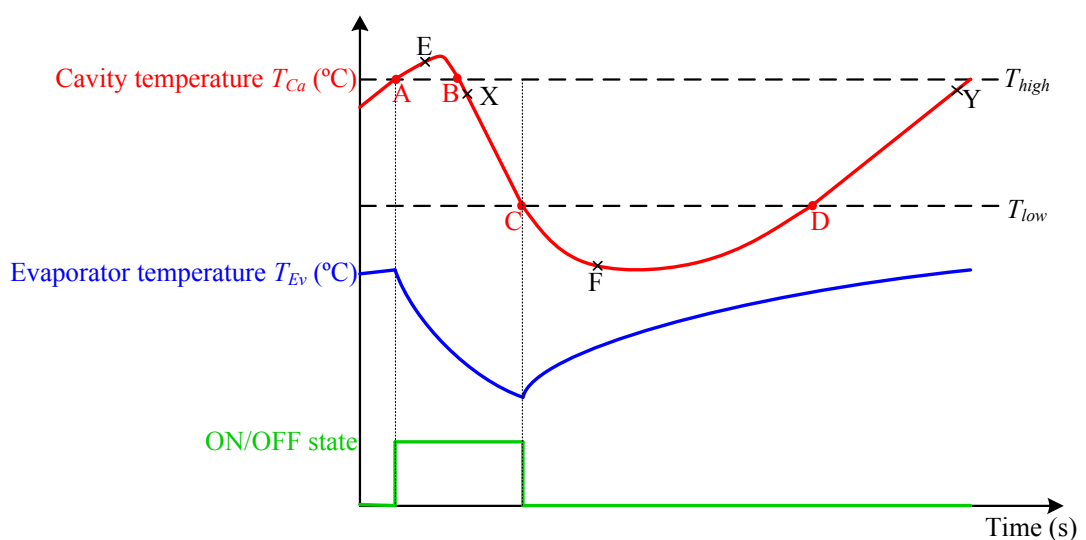


Fig. 3.3. Temperature control of a refrigerator

3.3.2 Grid frequency control of a refrigerator

A diagram of the frequency control of a refrigerator is shown in Fig. 3.4. The grid frequency f is measured and compared with two trigger frequencies F_{ON} and F_{OFF} . F_{ON} is in the range of 50-50.5 Hz and F_{OFF} is in the range of 49.5-50 Hz. The output of the frequency control is then determined by continuously comparing f with F_{ON} and F_{OFF} .

- If f is higher than F_{ON} , then the output S_{HF} is 1, indicating that the refrigerator will be switched ON as a result of a frequency rise.
- If f is lower than F_{OFF} , then the output S_{LF} is 1, indicating that the refrigerator will be switched OFF in response to a frequency drop.

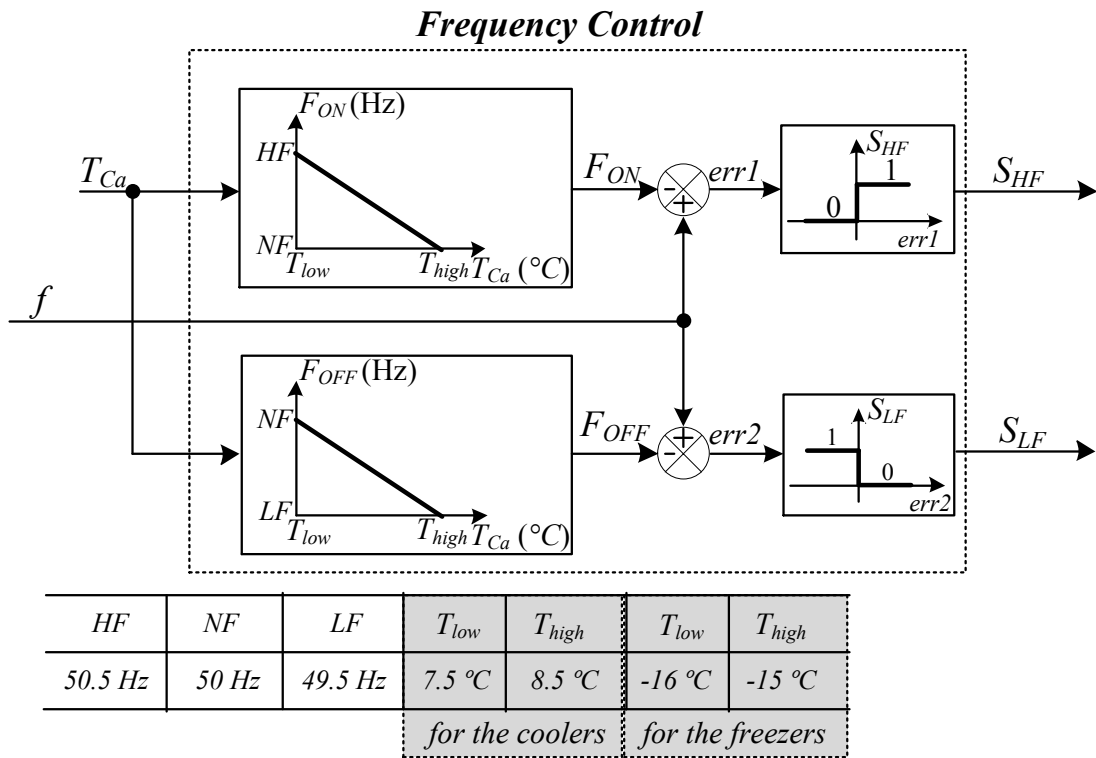


Fig. 3.4. Diagram of the frequency control of a refrigerator

F_{ON} and F_{OFF} are defined to vary with T_{Ca} linearly within the band between T_{low} and T_{high} as shown in Fig. 3.4. Therefore, T_{Ca} is also an input to the frequency controller. If T_{Ca} is outside the band between T_{low} and T_{high} , frequency control will not be triggered because it will cause the temperature in the cavity to be too high/low and hence undermines the cold storage of a refrigerator. For example, as illustrated in Fig. 3.3, T_{Ca} is higher than T_{high} within the period AB. The refrigerator has switched ON at A. If this refrigerator is switched OFF at E in response to a frequency drop, its T_{Ca} will rise further and may cause the food stored to be spoiled. Similarly, within section CD, the

refrigerator will not be switched ON in response to a frequency rise as this will cause T_{Ca} to drop even further below T_{low} .

In Fig. 3.4, the values of temperature set-points of refrigerators are determined by the user. The impact of the differences between temperature set-points are further discussed in Appendix II. In this study, quite a small difference between T_{high} and T_{low} , i.e. 1 °C difference, was used to represent a minimum capability for refrigerators to provide frequency response.

As shown in Fig. 3.4, the linear relationship between F_{ON} and T_{Ca} and the linear relationship between F_{OFF} and T_{Ca} are given by (3.13) and (3.14).

$$F_{ON}(t) = \frac{NF - HF}{T_{high} - T_{low}}(T_{Ca}(t) - T_{low}) + HF, T_{Ca}(t) \in [T_{low}, T_{high}] \quad (3.13)$$

$$F_{OFF}(t) = \frac{LF - NF}{T_{high} - T_{low}}(T_{Ca}(t) - T_{high}) + LF, T_{Ca}(t) \in [T_{low}, T_{high}] \quad (3.14)$$

where HF is the high limit of F_{ON} , LF is the low limit of F_{OFF} . HF and LF were set to be 50.5 Hz and 49.5 Hz which are consistent with the required steady-state limits of grid frequency in the GB power system. NF represents the nominal frequency which is 50 Hz.

In summary, for one refrigerator, if it is in ON-state with a temperature slightly lower than T_{high} (Point X in Fig. 3.3), it is less likely to be switched OFF. As the linear relationship between F_{OFF} and T_{Ca} shown in Fig. 3.4, the refrigerator will be given an F_{OFF} close to LF (at 49.5 Hz). Therefore, this refrigerator which is less likely to be switched OFF, i.e. at high temperature, will not be switched OFF unless frequency has severely dropped to 49.5 Hz.

If one refrigerator is in OFF-state with a temperature slightly lower than T_{high} (point Y in Fig. 3.3), according to the linear relationship between F_{ON} and T_{Ca} , this refrigerator will be switched ON if f rises slightly higher than NF (50 Hz shown in Fig. 3.4).

3.3.3 Coordinated local frequency control of refrigerators

For a population of refrigerators, at a given time, their T_{Ca} are different according to their inherent diversity. Therefore, they are given different F_{ON} and F_{OFF} as calculated by (3.13) and (3.14). As a result, following a deviation in frequency, refrigerators will

be triggered in sequence instead of switching ON/OFF simultaneously. The greater the deviation of frequency, the higher the number of refrigerators responds to the frequency deviation.

A refrigerator with the highest T_{Ca} is given an F_{ON} closest to 50 Hz while a refrigerator with the lowest T_{Ca} is given an F_{ON} farthest from 50 Hz as indicated by Fig. 3.4. Therefore, following a rise in frequency, refrigerators are switched ON starting from the one with the highest T_{Ca} .

Similarly, a refrigerator with the lowest T_{Ca} is given an F_{OFF} closest to 50 Hz while a refrigerator with the highest T_{Ca} is given an F_{OFF} farthest from 50 Hz as shown in Fig. 3.4. Therefore, following a drop in frequency, refrigerators are switched OFF starting from the one with the lowest T_{Ca} .

However, if there is a sudden and severe drop in frequency, a large number of refrigerators will be switched OFF almost simultaneously.

- It is necessary to switch OFF refrigerators with a similar temperature at different times and at different frequencies. This will ensure that temperature of refrigerators amongst a number of refrigerators maintains to be different.
- It is also necessary to try to minimise the number of refrigerators that will be re-connected to the grid at the same time after the refrigerators were switched OFF in response to the frequency drop.

Methods to address the above two concerns are now explained.

3.3.3.1 To minimise the number of refrigerators with the same T_{Ca} to be switched simultaneously for frequency response

In addition to T_{low} and T_{high} of each refrigerator, a mid-temperature, T_{mid} , defined by (3.15) is also pre-set. As shown in Fig. 3.5(a), the linear relationship between F_{ON} and T_{Ca} are sectioned at T_{mid} . This is achieved by incorporating a random number, HD , at T_{mid} to calculate F_{ON} of a refrigerator at T_{mid} as shown in (3.16). HD is uniformly distributed between 0 and 1 and is randomly assigned to each refrigerator.

$$T_{mid} = T_{low} + 0.5 \times (T_{high} - T_{low}) \quad (3.15)$$

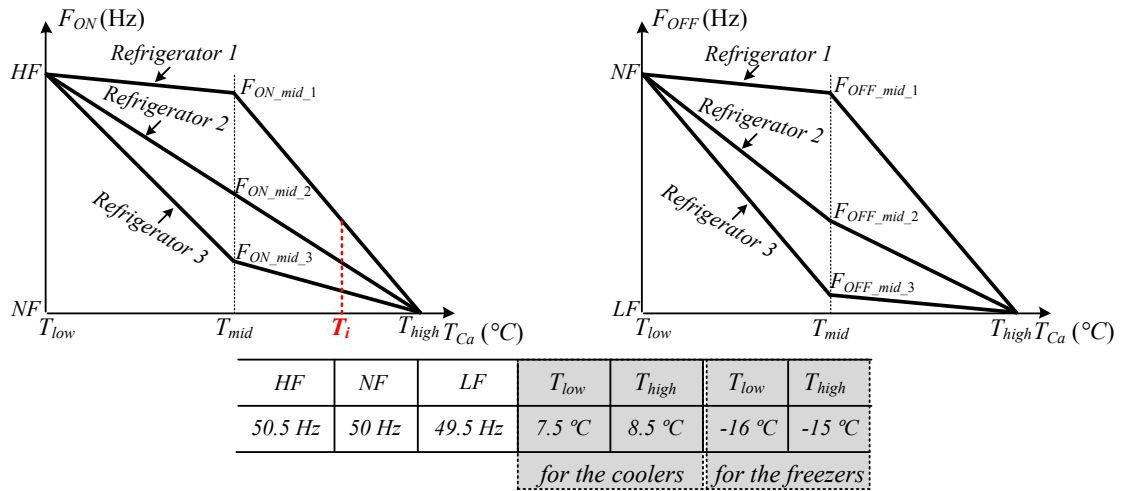
$$F_{ON_mid_n} = NF + HD \times (HF - NF), n = 1, 2, \dots \quad (3.16)$$

where n is the refrigerator ID number (*Refrigerator 1*, *Refrigerator 2* shown in Fig. 3.5(a)).

The calculation of F_{ON} at T_{mid} generates the different curves of F_{ON} against T_{Ca} for different refrigerators as depicted by the two-sectional linear relationship shown in Fig. 3.5(a). The relationship between F_{ON} and T_{Ca} is written by (3.17).

$$F_{ON}(t) = \begin{cases} \frac{F_{ON_{mid}} - HF}{T_{mid} - T_{low}} (T_{Ca}(t) - T_{low}) + HF, & T_{Ca}(t) < T_{mid} \\ \frac{NF - F_{ON_{mid}}}{T_{high} - T_{mid}} (T_{Ca}(t) - T_{mid}) + F_{ON_{mid}}, & T_{Ca}(t) \geq T_{mid} \end{cases} \quad (3.17)$$

As HD follows a uniform distribution, it ensures that the linear relationship between F_{ON} and T_{Ca} in Fig. 3.4 is still maintained over the population. For the three refrigerators shown in Fig. 3.4(a), if they are with the same T_{Ca} , for instance T_i at a given time, their F_{ON} is different and hence they will be triggered ON for different levels of frequency rise. As a result, temperature and the ON/OFF state of refrigerators are more different amongst the refrigerator population.



(a) F_{ON} of a population of refrigerators

(b) F_{OFF} of a population of refrigerators

Fig. 3.5. Assignment of trigger frequencies for a population of refrigerators

Similarly as shown in Fig. 3.5(b), F_{OFF} at T_{mid} is written by:

$$F_{OFF_{mid_n}} = LF + LD \times (NF - LF), n = 1, 2, \dots \quad (3.18)$$

where n is the refrigerator ID number. LD is also the incorporated random number following the uniform distribution between 0 and 1 for the calculation of F_{OFF} of each refrigerator at T_{mid} ($F_{OFF_{mid_n}}$). The calculation of $F_{OFF_{mid_n}}$ gives different curves of

F_{OFF} against T_{Ca} for different refrigerators as the two-sectional linear relationship shown in Fig. 3.5(b). The relationship between F_{OFF} and T_{Ca} is depicted by (3.19).

$$F_{OFF}(t) = \begin{cases} \frac{F_{OFF_{mid}} - NF}{T_{mid} - T_{low}} (T_{Ca}(t) - T_{low}) + NF, & T_{Ca}(t) < T_{mid} \\ \frac{LF - F_{OFF_{mid}}}{T_{high} - T_{mid}} (T_{Ca}(t) - T_{mid}) + F_{OFF_{mid}}, & T_{Ca}(t) \geq T_{mid} \end{cases} \quad (3.19)$$

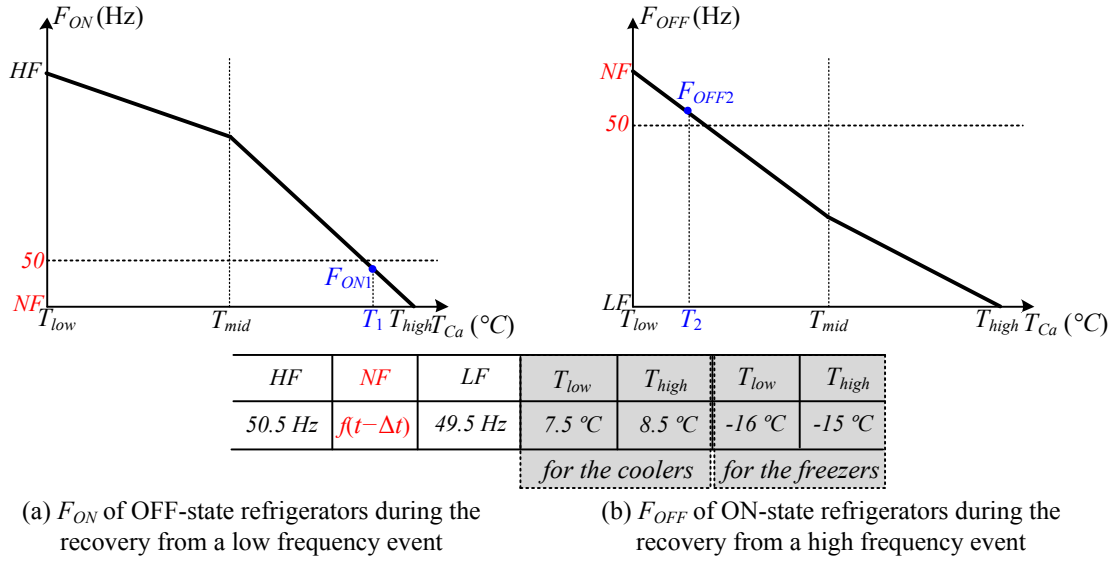
3.3.3.2 To minimise the number of refrigerators to revert back simultaneously after the provision of frequency response

To avoid simultaneous connection of refrigerators after a sudden and severe frequency drop, when frequency starts to recover, some of the OFF-state refrigerators are controlled to be switched ON before their T_{Ca} reach T_{high} . This is referred to as early switching action in this thesis.

When frequency is below 50 Hz, F_{ON} is autonomously re-calculated using (3.17) by assigning NF the value of $f(t-\Delta t)$ rather than the 50 Hz that was used in Fig. 3.5(a). Δt is the sampling time of the grid frequency measurements which was 200 ms. The re-calculation and update of F_{ON} is shown in (3.20). As a result, F_{ON} of some refrigerators is shifted to be lower than 50 Hz as shown in Fig. 3.6(a).

$$F_{ON}(t) = \begin{cases} \frac{F_{ON_{mid}} - HF}{T_{mid} - T_{low}} (T_{Ca}(t) - T_{low}) + HF, & T_{Ca}(t) < T_{mid} \\ \frac{f(t - \Delta t) - F_{ON_{mid}}}{T_{high} - T_{mid}} (T_{Ca}(t) - T_{mid}) + F_{ON_{mid}}, & T_{Ca}(t) \geq T_{mid} \end{cases} \quad (3.20)$$

Fig. 3.6(a) shows an example of one refrigerator with a temperature T_1 and a trigger frequency F_{ON1} which is updated to be lower than 50 Hz. Before f recovers to reach 50 Hz, the refrigerator will be switched ON if f becomes higher than F_{ON1} . Therefore, when frequency starts to recover, some of the OFF-state refrigerators are switched ON early before their T_{Ca} reach T_{high} . As the relationship shown in Fig. 3.6(a), f will recover to be higher than F_{ON} of a refrigerator with a temperature closest to T_{high} first. Hence, following the frequency recovery, power consumption of refrigerators will start to recover gradually. This reduces the number of refrigerators that will be connected to the grid at the same time.


 Fig. 3.6. Update of F_{ON} and F_{OFF} during the recovery from frequency events

Similar rules apply to the ON-state refrigerators after a frequency rise event. Some of them are controlled to be switched OFF earlier than they otherwise would be following the frequency recovery from the frequency rise. As shown in Fig. 3.6(b), when frequency is above 50 Hz, F_{OFF} is re-calculated using (3.19) by assigning NF the value of $f(t-\Delta t)$ instead of 50 Hz. This is written by (3.21). Therefore, the ON-state refrigerators start to be switched OFF earlier before their T_{Ca} reach T_{low} such as the refrigerator shown in Fig. 3.6(b) which will be switched OFF at T_2 rather than at T_{low} when f recovers to be lower than F_{OFF2} . The refrigerator with the lowest T_{Ca} will be switched OFF first because f will recover to fall below F_{OFF} of this refrigerator first.

$$F_{OFF}(t) = \begin{cases} \frac{F_{OFF_{mid}} - f(t - \Delta t)}{T_{mid} - T_{low}} (T_{Ca}(t) - T_{low}) + f(t - \Delta t), & T_{Ca}(t) < T_{mid} \\ \frac{LF - F_{OFF_{mid}}}{T_{high} - T_{mid}} (T_{Ca}(t) - T_{mid}) + F_{OFF_{mid}}, & T_{Ca}(t) \geq T_{mid} \end{cases} \quad (3.21)$$

In the frequency control of a refrigerator, when calculating F_{ON} and F_{OFF} , the value of NF in Fig. 3.5 and Fig. 3.6 are combined to cover both the frequency response behaviour and the frequency recovery behaviour. Hence, equation (3.22) and (3.23) are obtained.

NF for calculating F_{ON} :

$$NF = \min(50, f(t - \Delta t)) \quad (3.22)$$

NF for calculating F_{OFF} :

$$NF = \max(50, f(t - \Delta t)) \quad (3.23)$$

The calculation and update of F_{ON} and F_{OFF} are summarised in Table 3.4.

TABLE 3.4. Dynamic Update of Trigger Frequencies F_{ON} and F_{OFF}

f measurement: $f(t)$	NF of calculating $F_{ON}(t)$ in (3.17)	NF of calculating $F_{OFF}(t)$ in (3.19)
$f(t) \geq 50$ Hz	NF=50 Hz for frequency rise	NF= $f(t-\Delta t)$ for frequency recovery
$f(t) < 50$ Hz	NF= $f(t-\Delta t)$ for frequency recovery	NF=50 Hz for frequency drop

3.3.4 Integrated control of a refrigerator

Based on the principles described in Section 3.3.1-3.3.3, an integrated control scheme for both frequency and temperature control of a refrigerator was developed. It is shown in Fig. 3.7.

The frequency control measures the grid frequency f and generates the state signals S_{HF} and S_{LF} . As discussed in Section 3.3.2, if f is higher than F_{ON} , the output S_{HF} is 1. If f is lower than F_{OFF} , the output S_{LF} is 1.

The temperature control measures the cavity temperature T_{Ca} and generates the state signals S_T , S_{LT} and S_{HT} . S_T is the ON/OFF state determined by the inherent hysteresis temperature control discussed in Section 3.3.1. S_{LT} is 1 if T_{Ca} is lower than T_{low} . This assures that the refrigerator will stay in OFF state even though there is a rise in frequency. Therefore, the frequency control will not undermine the cold storage performance of a refrigerator. Similarly, S_{HT} is set to 1 if T_{Ca} is higher than T_{high} . This assures that the refrigerator will stay in ON state even though there is a drop in frequency.

The final switching signal S_{final} is then determined by the state signals S_{HF} , S_{LF} , S_T , S_{LT} and S_{HT} according to Table 3.4. '0' represents OFF state and '1' represents ON state.

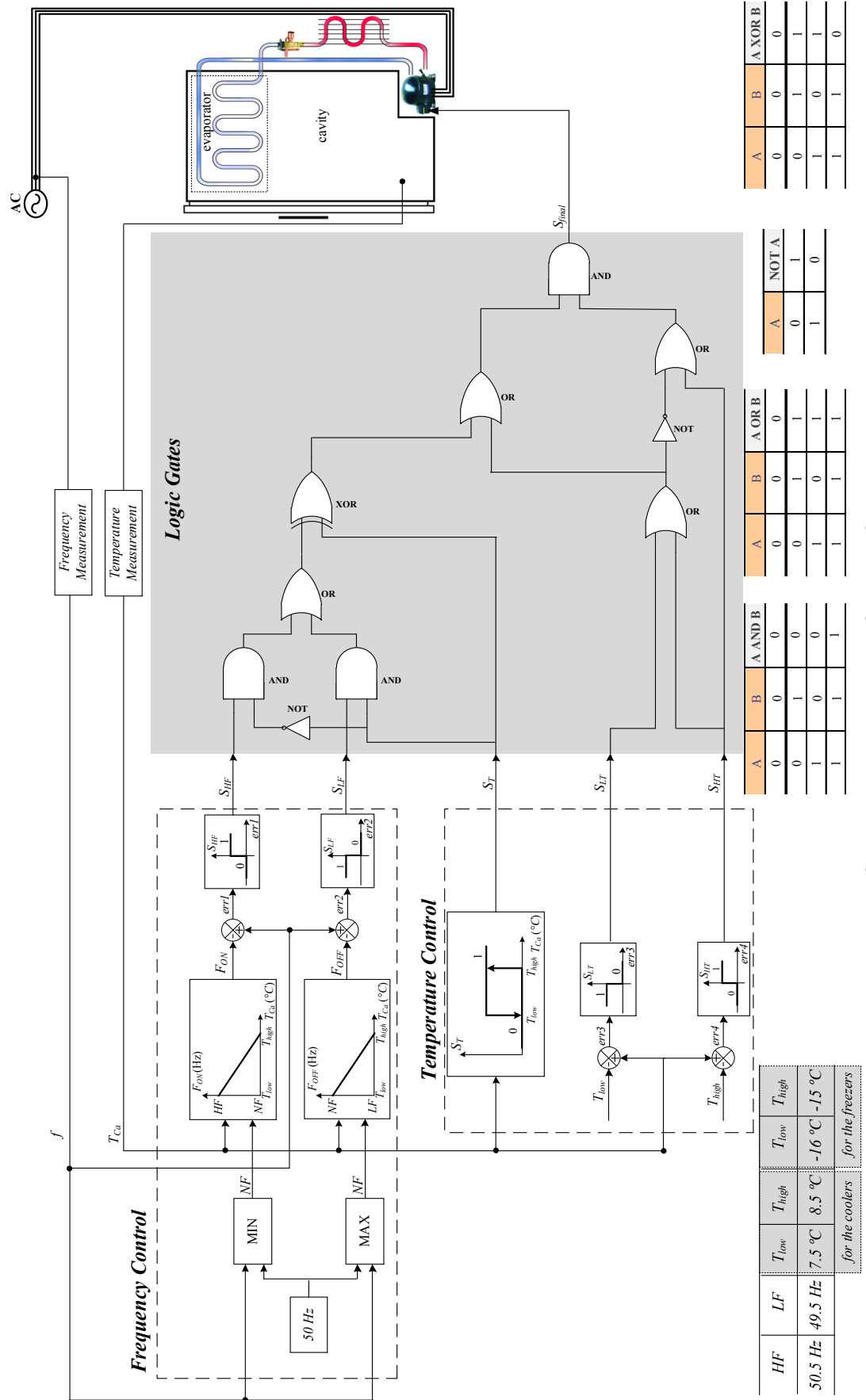


Fig. 3.7. Integrated control scheme of refrigerators

TABLE 3.5. Truth Table of Logic Gates in Fig. 3.7.

Row Number	S_T	S_{LT}	S_{HT}	S_{LF}	S_{HF}	S_{final}	Conditions
1	0	0	0	0	0	0	$S_{final} = S_T, ^*NFE$
2	1	0	0	0	0	1	$S_{final} = S_T, ^*NFE$
3	0	0	0	0	1	1	$S_{final} = 1, ^*HFE$
4	1	0	0	0	1	1	$S_{final} = 1, ^*HFE$
5	0	0	0	1	0	0	$S_{final} = 0, ^*LFE$
6	1	0	0	1	0	0	$S_{final} = 0, ^*LFE$
7	0	0	0	1	1	1	Error: f cannot be higher than F_{ON} and lower than F_{OFF} simultaneously
8	1	0	0	1	1	0	
9	0	0	1	0	0	1	Error: S_T must be 1 because $T_{Ca} > T_{high}$
10	1	0	1	0	0	1	$S_{final} = 1, ^*HT$ regardless of *HFE or *LFE
11	0	0	1	0	1	1	Error: S_T must be 1 because $T_{Ca} > T_{high}$
12	1	0	1	0	1	1	$S_{final} = 1, ^*HT$ regardless of *HFE or *LFE
13	0	0	1	1	0	1	Error: S_T must be 1 because $T_{Ca} > T_{high}$
14	1	0	1	1	0	1	$S_{final} = 1, ^*HT$ regardless of *HFE or *LFE
15	0	0	1	1	1	1	Error: S_T must be 1 because $T_{Ca} > T_{high}$
16	1	0	1	1	1	1	$S_{final} = 1, ^*HT$ regardless of *HFE or *LFE
17	0	1	0	0	0	0	$S_{final} = 0, ^*LT$ regardless of *HFE or *LFE
18	1	1	0	0	0	0	Error: S_T must be 0 because $T_{Ca} < T_{low}$
19	0	1	0	0	1	0	$S_{final} = 0, ^*LT$ regardless of *HFE or *LFE
20	1	1	0	0	1	0	Error: S_T must be 0 because $T_{Ca} < T_{low}$
21	0	1	0	1	0	0	$S_{final} = 0, ^*LT$ regardless of *HFE or *LFE
22	1	1	0	1	0	0	Error: S_T must be 0 because $T_{Ca} < T_{low}$
23	0	1	0	1	1	0	$S_{final} = 0, ^*LT$ regardless of *HFE or *LFE
24	1	1	0	1	1	0	Error: S_T must be 0 because $T_{Ca} < T_{low}$
25	0	1	1	0	0	1	Error: T_{Ca} cannot be higher than T_{high} and lower than T_{low} simultaneously
26	1	1	1	0	0	1	
27	0	1	1	0	1	1	
28	1	1	1	0	1	1	
29	0	1	1	1	0	1	
30	1	1	1	1	0	1	
31	0	1	1	1	1	1	
32	1	1	1	1	1	1	

*NFE: No Frequency Event

*HFE: High Frequency Event

*LFE: Low Frequency Event

*HT: High Temperature, i.e. the refrigerator is at a high temperature above its T_{high} .

*LT: Low Temperature, i.e. the refrigerator is at a low temperature below its T_{low} .

Table 3.5 is illustrated as follows:

- ✓ In Rows 1-8, S_{LT} and S_{HT} are 0 indicating that T_{Ca} is between T_{low} and T_{high} . Frequency control is able to be provided by these refrigerators.
 - Rows 1-2 are cases of ‘No Frequency Event’ because S_{LF} and S_{HF} are 0. The final state (S_{final}) of the compressor follows the temperature control ($S_{final} = S_T$).
 - Rows 3-4 are cases of ‘High Frequency Event’ because S_{HF} is 1. An OFF-state refrigerator ($S_T = 0$) will be switched ON ($S_{final} = 1$) to provide high frequency response.
 - Rows 5-6 are cases of ‘Low Frequency Event’ because S_{LF} is 1. An ON-state refrigerator ($S_T = 1$) will be switched OFF ($S_{final} = 0$) to provide low frequency response.
 - Rows 7-8 are not feasible cases because f cannot be lower than F_{OFF} and higher than F_{ON} simultaneously, i.e. $S_{HF} = 1$ and $S_{LF} = 1$.
- ✓ Rows 9-16 are cases of T_{Ca} being higher than T_{high} because S_{HT} is 1. The refrigerator must be in ON state regardless of any frequency events.
- ✓ Rows 17-24 are the cases of T_{Ca} being lower than T_{low} because S_{LT} is 1. The refrigerator must be in OFF state regardless of any frequency events.
- ✓ Rows 25-32 are not feasible cases because the T_{Ca} cannot be lower than T_{low} and higher than T_{high} simultaneously, i.e. $S_{HT} = 1$ and $S_{LT} = 1$.

3.4 Modelling of GB power system for frequency control

A simplified GB power system model for the study of grid frequency control was developed based on [36] and [89]. The model is shown in Fig. 3.8.

The inertia constant H_{eq} of the GB power system is 6.5 s. This was estimated based on a frequency incident of September 30th 2012 [90] in the GB power system. It was caused by the failure of an interconnector which led to a loss of generation of approximately 1,000 MW. The average rate of change of frequency measured by the Phase Measurement Units was 0.113 Hz/s. System demand at the time of the incident was 33,702 MW [91]. H_{eq} was then estimated using (3.21). The effect of frequency dependent loads in the power system is lumped into a damping constant D which was set to be 1 pu [89].

$$\frac{df}{dt} = \frac{P_{loss}}{2H_{eq}} \text{ (p.u.)} \quad (3.21)$$

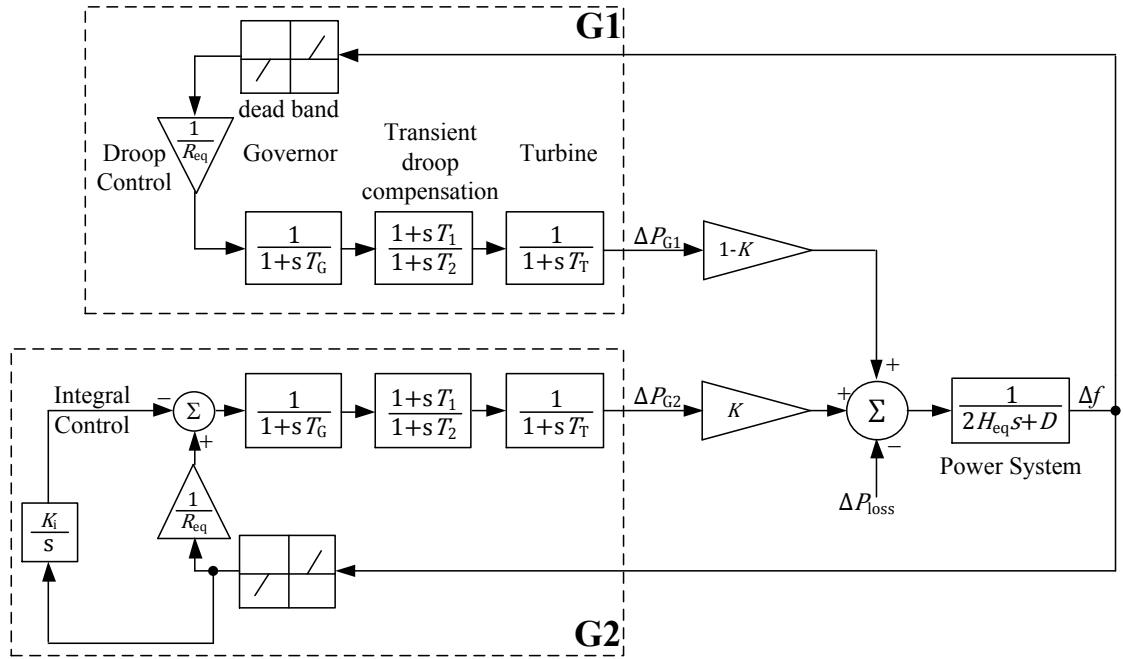


Fig. 3.8. A simplified GB power system model for the study of frequency control

The GB Grid Code [40] requires that all large generators should have a governor droop characteristic of 3-5% for the provision of primary frequency control. Considering different demand levels, some generators may be required also to provide secondary frequency control. Therefore, the generation system was represented by two lumped generators as shown in Fig. 3.8. G1 represents the generators that provide only primary response. G2 represents the generators that provide both primary and secondary frequency control. K was set at 0.8 assuming that 80% of generators were scheduled for secondary frequency control.

The model of G1 includes the governor dead band of ± 15 mHz [40]. The governor droop characteristic is represented by the gain $1/R_{eq}$. The governor time constant is T_G . A transient droop compensator is used to ensure the stable performance of the frequency control [89]. Its time constants are T_1 and T_2 . The mechanical power is then generated from the turbine with a time constant of T_T .

The model of G2 is similar to that of G1. To model its provision of secondary frequency control, an integral control loop with the parameter K_i was added in order to restore the grid frequency to 50 Hz. Parameters for G1 and G2 are shown in Table 3.6.

TABLE 3.6. Parameters Used for G1 and G2 (System Base of 33,702 MW).

Dead Band (pu)	R_{eq} (pu)	T_G (s)	T_1 (s)	T_2 (s)	T_T (s)	K_i (pu)
± 0.0003	0.05	0.2 s	2 s	20 s	0.3 s	0.05

3.5 Case study

To investigate the capability of refrigerators for grid frequency control and their impacts on the power system, three case studies were carried out.

3.5.1 Identification of suitable number of individual refrigerator models

It is infeasible and unnecessary to have 40 million independent refrigerator models presented in Section 3.2 to represent all refrigerators connecting to the GB power system. Instead, an aggregated model with a smaller number of individual refrigerator models was developed and then scaled up by multiplying the number of individual refrigerators by a number in order to represent the 40 million. The number of individual refrigerator models to be aggregated and scaled to represent the total 40 million is shown in Table 3.7.

TABLE 3.7. Aggregated Model of Different Number of Individual Refrigerator Models

Aggregated Model	Number of individual refrigerator models	Multiplied number
1	100	400,000
2	500	80,000
3	1,000	40,000
4	5,000	8,000
5	10,000	4,000
6	50,000	800
7	100,000	400

When Aggregated Model 1 is used, it is an aggregation of 100 individual refrigerator models with different states in their temperature, ON/OFF state, size and amount of food stored. By multiplying 400,000 to represent the entire refrigerator population in the UK, this assumes that 400,000 refrigerators were in similar states. When Aggregated

Model 7 is used, it is an aggregation of 100,000 individual refrigerator models with different states. By multiplying 400 to represent the entire refrigerator population in the UK, this assumes that 400 refrigerators were in similar states.

According to Ref [92], the coincidence factor of loads becomes constant if the number of customers is greater than 10,000, as depicted in Fig. 3.9. This means that even if there will be more loads, the loads that are in similar states remains at the level of 10,000 loads. It is therefore unnecessary to increase the number of individual refrigerator models used for an aggregated model to be beyond 10,000.

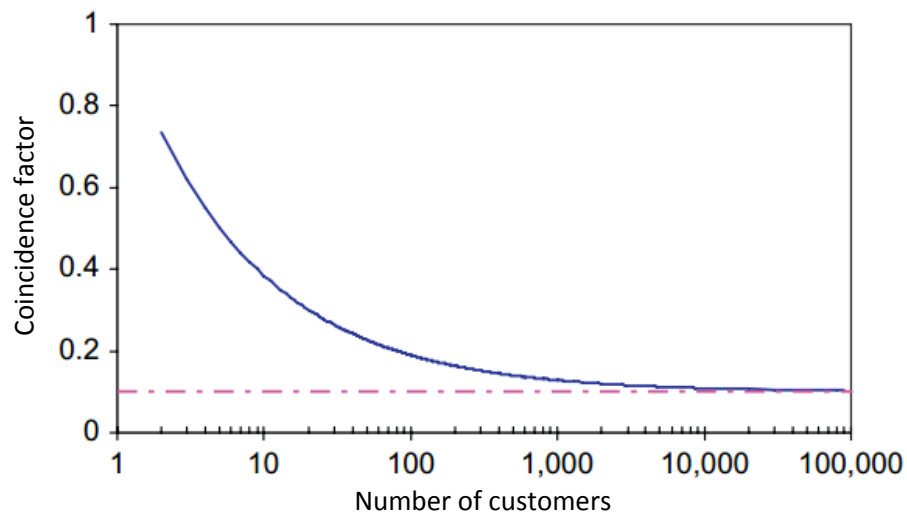
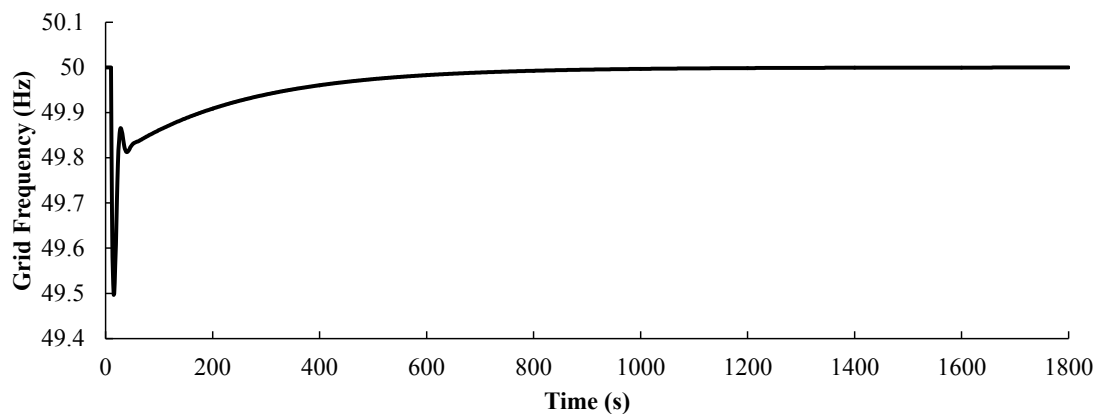
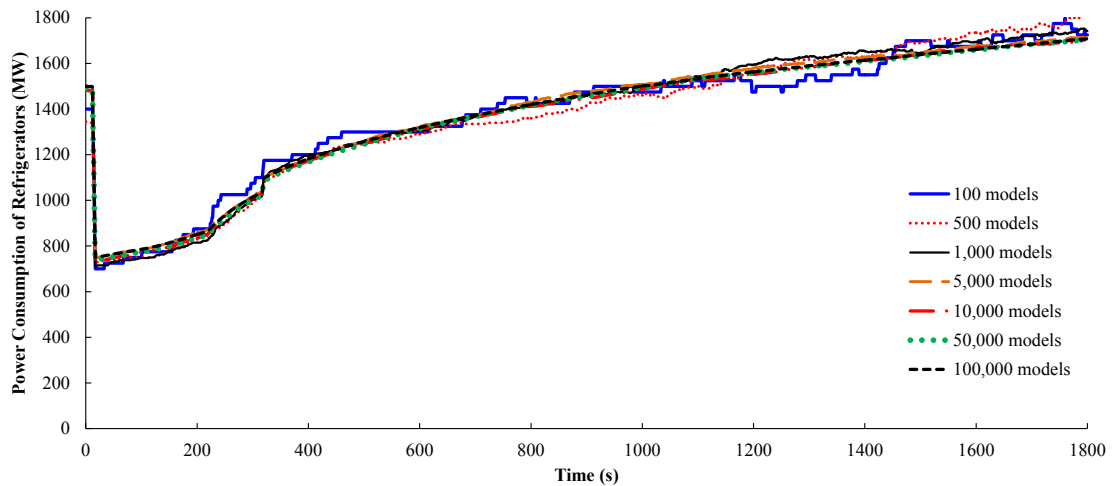


Fig. 3.9. Relationship of load coincidence factor and the number of customers [92]

The frequency profile shown in Fig. 3.10(a) was injected to each of the five aggregated models that are listed in Table 3.6. Each individual refrigerator model was equipped with the dynamic controller presented in Section 3.3. It was assumed that each refrigerator has a power rating of 0.1 kW. Fig. 3.10(b) shows the simulation results.



(a) Input frequency profile



(b) Power consumption of refrigerators

Fig. 3.10. Effect of number of refrigerator models

It can be seen that the total power consumption of the refrigerators in all seven aggregated models decreased following the frequency drop. The aggregated models with 10,000, 50,000 and 100,000 individual refrigerator models showed a gradual and similar power change. The simulation time for each aggregated model is compared in Table 3.8. Considering the accuracy and efficiency of the model, the Aggregated Model 5 with 10,000 individual refrigerator models was used for the following studies.

TABLE 3.8. Simulation Time of each Aggregated Model

Aggregated Model	Number of individual refrigerator models	Multiplied number	Simulation time
1	100	400,000	3.56 s
2	500	80,000	4.76 s
3	1,000	40,000	5.48 s
4	5,000	8,000	11.23 s
5	10,000	4,000	19.15 s
6	50,000	800	80.89 s
7	100,000	400	160.25 s

However, for the aggregated models with 100 and 500 individual refrigerator models (Aggregated Model 1 and 2 in Table 3.7), the power change of the refrigerators was less gradual than the other aggregated models. This indicates that the number of individual refrigerators in Aggregated Model 1 and 2 were too small to represent the load diversity of 40 million refrigerators.

3.5.2 Sustained low frequency and high frequency events

A case study was undertaken using four thousand aggregated models each with 10,000 individual refrigerator models to represent 40 million refrigerators. The individual refrigerator model is described in Section 3.2. Each refrigerator model was equipped with the dynamic controller illustrated in Section 3.3. Power consumption of each refrigerator (a combined cooler and freezer) was 100 W.

A step change in frequency from 50 to 49.5 Hz was injected to the aggregated refrigerator models at 90 s to investigate the capability of the dynamic controller during a sustained depression of frequency. Similarly, a step change in frequency from 50 to 50.5 Hz was also injected at 90 s so as to represent a sustained period of high frequency. The power consumption of refrigerators during the sustained low frequency and high frequency events are shown in Fig. 3.11.

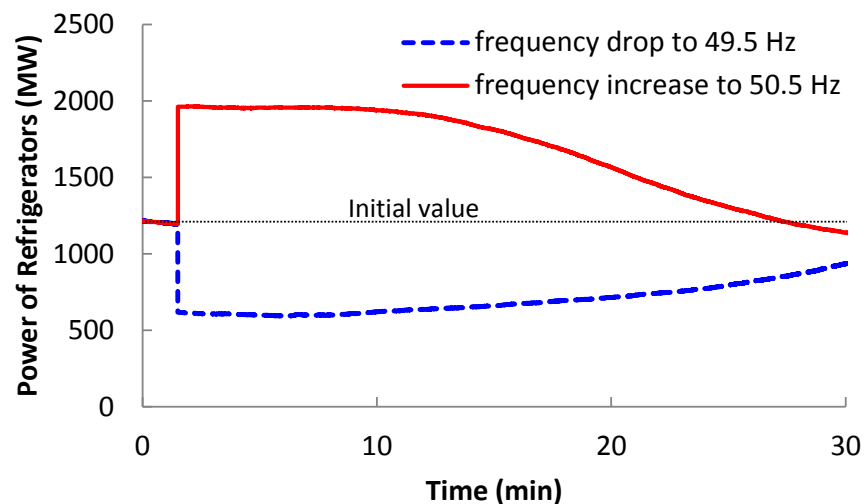


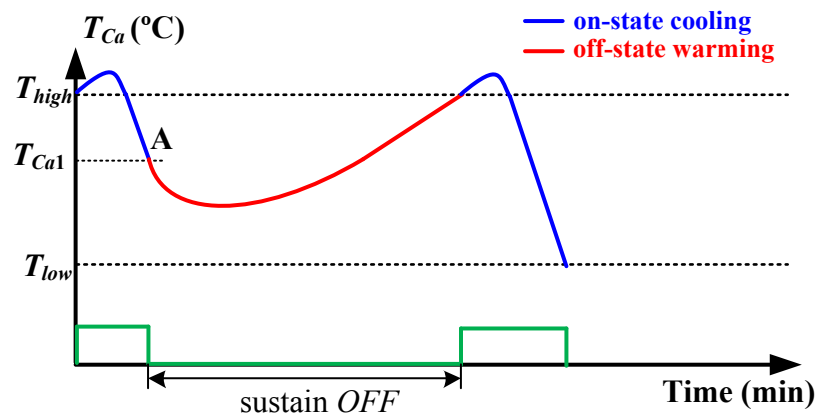
Fig. 3.11. Power of refrigerators during the sustained periods of low frequency and high frequency

The power consumption of refrigerators is reduced when frequency drops to 49.5 Hz and remains low for nearly 10 minutes. After 10 minutes, the response from refrigerators is exhausted and they start to be reconnected because their T_{Ca} reach T_{high} . As a result, the power consumption of refrigerators increases gradually.

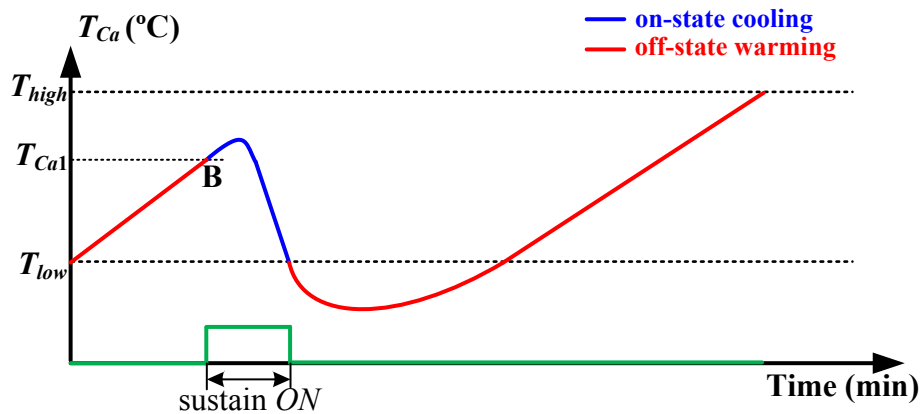
The power consumption of refrigerators increases when frequency rises to 50.5 Hz and remains high for nearly 10 minutes. After 10 minutes, the high frequency response from refrigerators is exhausted and they switch OFF as their T_{Ca} reach T_{low} . The power consumption of refrigerators reduces gradually.

As indicated in Fig. 3.11, the sustained high frequency response from refrigerators (curve ‘frequency increase to 50.5 Hz’) exhausts faster than the sustained low frequency response (curve ‘frequency drop to 49.5 Hz’) after 10 minute. This is because the OFF-state period of a refrigerator is usually longer than the ON-state period. Fig. 3.12(a) and Fig. 3.12(b) illustrate the reason that the depletion of high frequency response is faster than that of the low frequency response.

Fig. 3.12(a) represents the case that a frequency drop occurred at A when the refrigerator was in ON-state and was at a temperature of T_{Ca1} . Fig. 3.12(b) represents the occurrence of a frequency rise at B when the same refrigerator was in OFF-state but was also at the same temperature of T_{Ca1} .



(a) T_{Ca} during a sustained period of low frequency



(b) T_{Ca} during a sustained period of high frequency

Fig. 3.12. Variations of T_{Ca} of refrigerators in the frequency events

The refrigerator in Fig. 3.12(a) is in ON-state until point A. The temperature of the refrigerator reaches T_{Ca1} . It is switched OFF at A as a result of the frequency drop. The refrigerator is OFF until its T_{Ca} reaches T_{high} .

The refrigerator in Fig. 3.12(b) is in OFF-state until point B and the temperature of the refrigerator is T_{Ca1} . It is switched ON at B as a result of the frequency rise. The refrigerator remains ON until its T_{Ca} reaches T_{low} .

It can be seen that, the sustained ON-period in Fig. 3.12(b) is much shorter than the sustained OFF-period in Fig. 3.12(a). Hence, the capability of a refrigerator to provide a sustained low frequency response is higher than to provide a sustained high frequency response.

3.5.3 Case study on the GB power system

This case study shows an investigation of the impacts of the refrigerators with dynamic controller on the GB power system. The simulation model is shown in Fig. 3.13. The GB power system model presented in Section 3.4 with inertia H_{eq} of 6.5 s was used for this study. Four thousand aggregated models each with 10,000 individual refrigerator models were connected to the GB power system model in order to represent the 40 million refrigerators that are connected in the GB power system. Power consumption of each refrigerator was 0.1 kW.

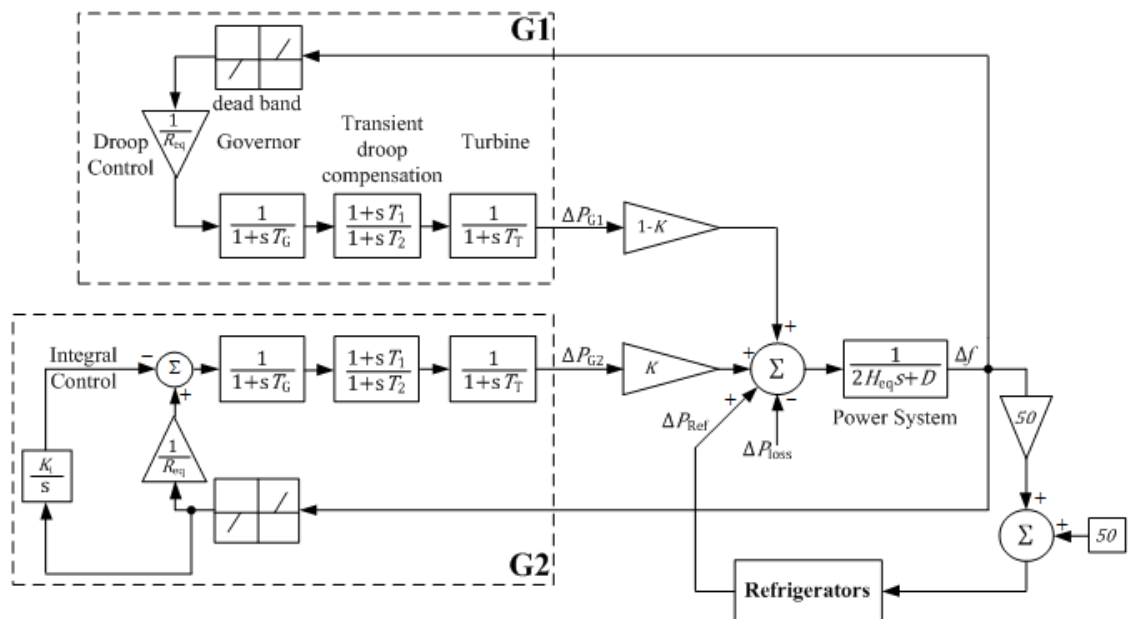


Fig. 3.13. Simulation model of refrigerators connected to the GB power system model

Case 1: Simulation of sudden loss in generation

Simulations were carried out to investigate the capability of refrigerators to provide response to a frequency drop. The case was set assuming a low system demand of 20 GW on a summer night. A loss of generation of 1,320 MW ($\Delta P_{loss} = 1,320/20,000 = 0.066 p.u.$) was used to create a frequency event.

Two sets of simulation results, one with the refrigerators' response and one without the refrigerators' response, are compared in Fig. 3.14-3.17. In these figures, f represents the grid frequency, Pr represents the power consumption of refrigerators, ΔPr represents the change of power consumption of refrigerators, ΔPg is the total power change of generators with $\Delta Pg1$ representing the power change of G1 and $\Delta Pg2$ representing the power change of G2.

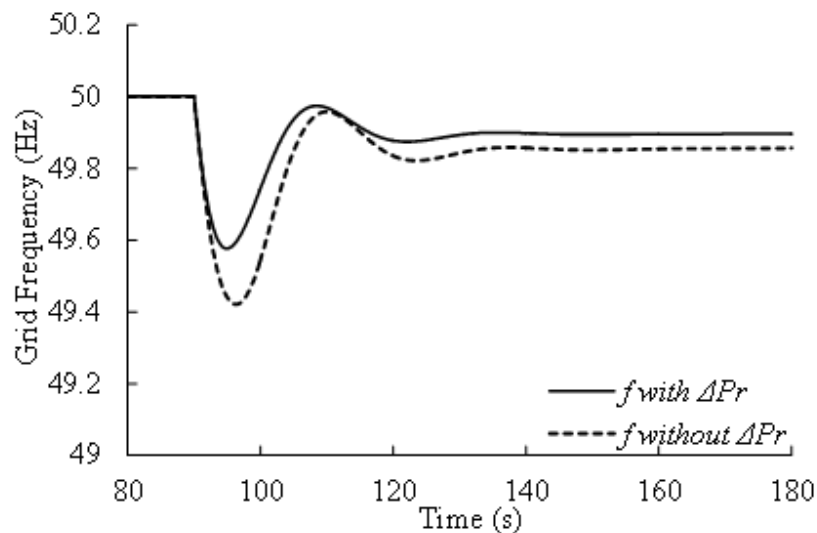


Fig. 3.14. Variations of grid frequency

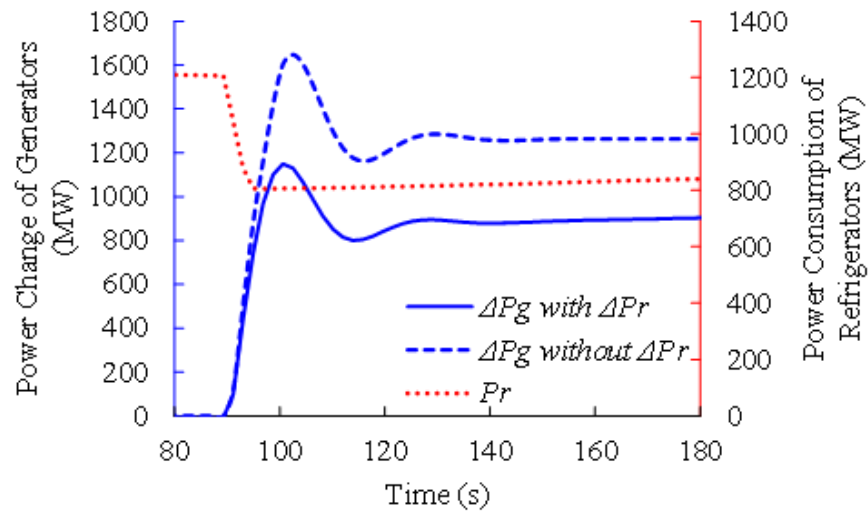


Fig. 3.15. Power change of generators and power consumption of refrigerators

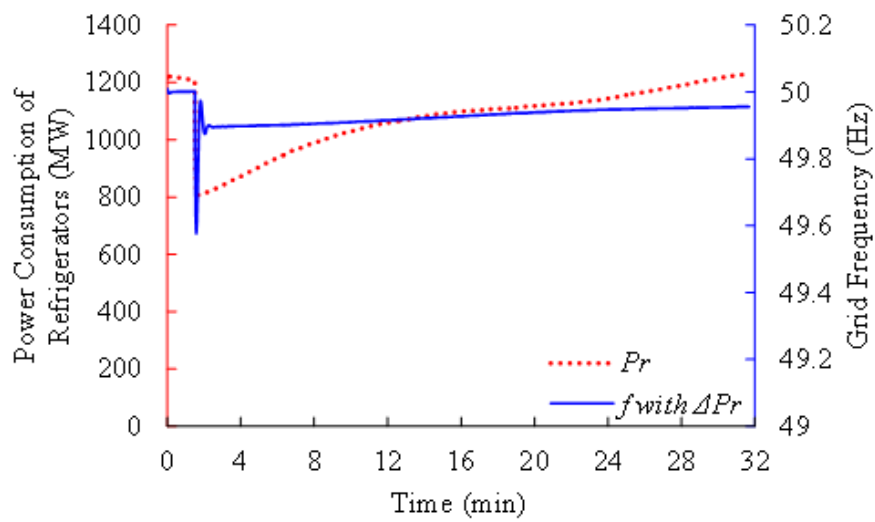


Fig. 3.16. Power consumption of refrigerators 30 minutes after the frequency drop

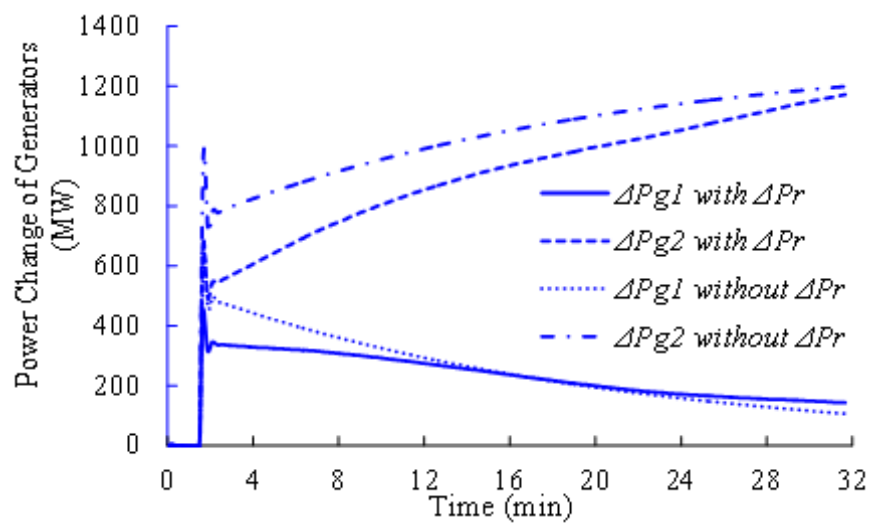


Fig. 3.17. Power change of G1 and G2 30 minutes after the frequency drop

Fig. 3.14 shows the drop of frequency after the sudden loss of generation. Fig. 3.15 shows the changes of power output of generators (see the left axis) and of the power consumption of refrigerators (see the right axis). The power consumption of refrigerators reduced almost immediately following the frequency drop. With this load reduction of approximately 400 MW, the drop of frequency was halted at 49.58 Hz. Without the load reduction of refrigerators, the frequency dropped to 49.42 Hz. The increase of power output of frequency-sensitive generators was also reduced with the power reduction of refrigerators.

Fig. 3.16 shows that, following the recovery of frequency (see the right axis), power consumption of refrigerators (see the left axis) increased according to the early switching actions illustrated in Section 3.3.3. Fig. 3.17 shows the change of power output of generators during the recovery of frequency. G1 provided only primary response for at least 30 s and then its power output started to decline. G2 provided both primary and secondary response for at least 30 minutes after the frequency drop. It restored the grid frequency and also the lost thermal energy of refrigerators which switched OFF early in response to the frequency drop.

Without applying the loss of generation, the original ON/OFF state and T_{Ca} of a cooler are shown in Figs. 3.18-3.19 ('without f drop'). This original ON/OFF state and T_{Ca} were compared with that of the same cooler to which simulation of the loss of generation was applied ('with f drop'). Fig. 3.18 compares ON/OFF cycle of the cooler and Fig. 3.19 compares T_{Ca} of the cooler.

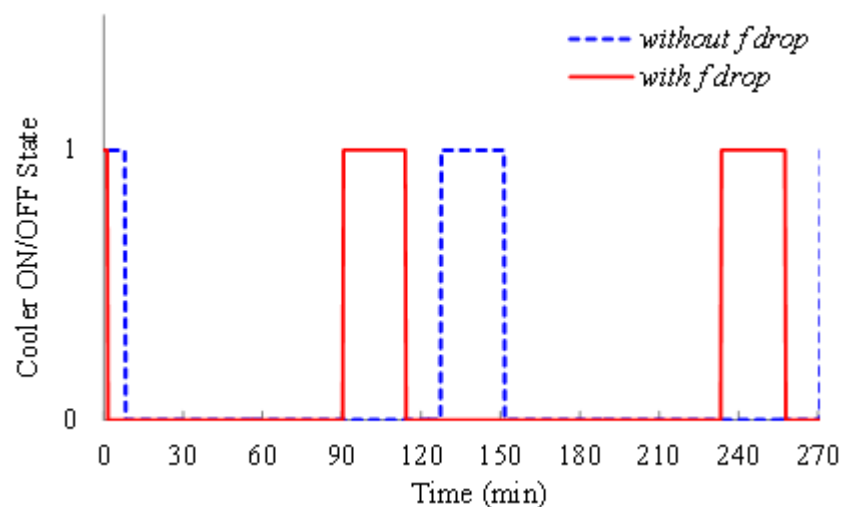


Fig. 3.18. ON/OFF state of the cooler

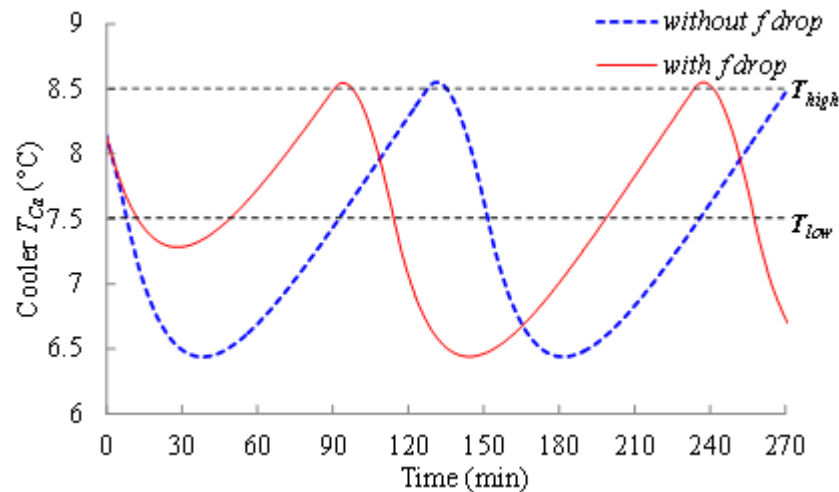


Fig. 3.19. Cavity temperature of the cooler

As shown in Fig. 3.18, the cooler was switched OFF earlier at 1.5 min (or 90 s) for the frequency drop compared to the case ‘without *f drop*’ in which the refrigerator was switched OFF at 8 min. Fig. 3.19 shows that the T_{Ca} of the cooler stayed within its original range even though it was switched OFF earlier. This confirms that the shift of duty cycle does not have an adverse impact on the cold storage performance of a refrigerator. Similar behaviours occurred in the freezer.

Case 2: Simulation of sudden loss in demand

Simulations were carried out to investigate the capability of refrigerators to provide response to a frequency rise. System demand of 20 GW on a summer night was assumed. A loss in demand of 1,000 MW ($\Delta P_{loss} = -0.05 pu$) was applied to the simulation model, as shown in Fig. 3.13. The simulation results without and with the frequency response from refrigerators are compared in Fig. 3.20-3.22.

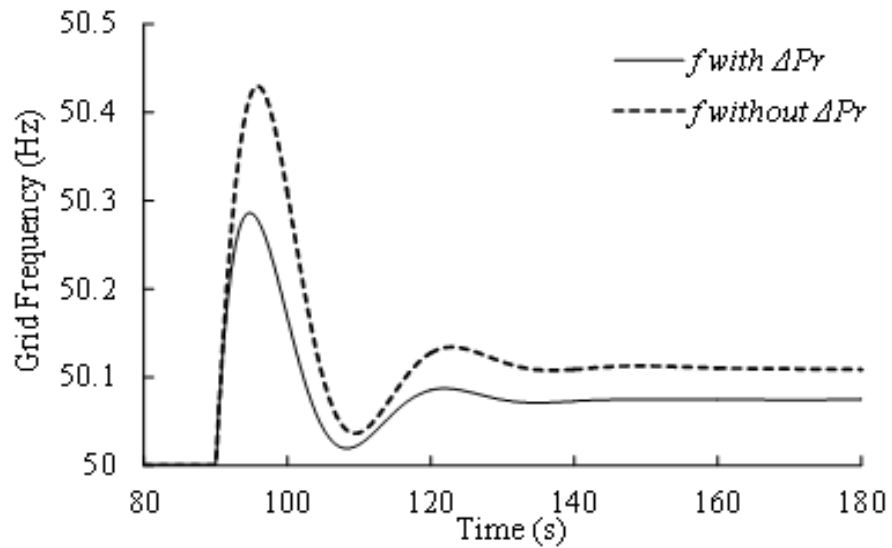


Fig. 3.20. Variations of grid frequency

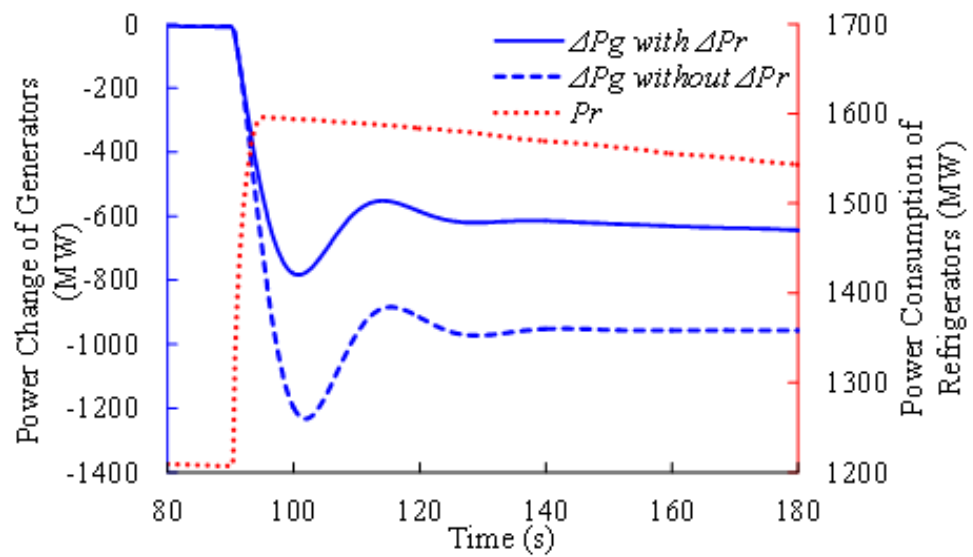


Fig. 3.21. Power change of generators and power consumption of refrigerators

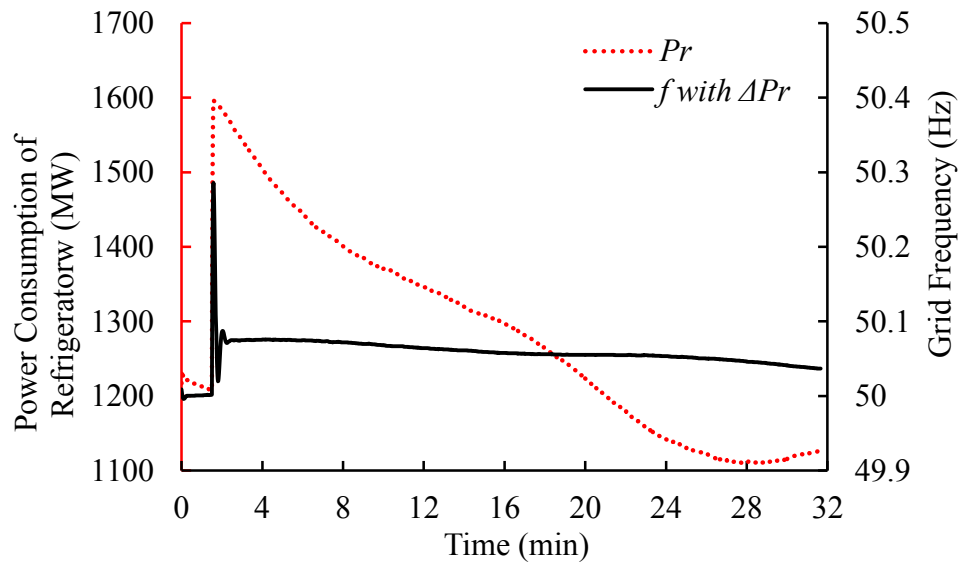


Fig. 3.22. Power consumption of refrigerators 30 minutes after the frequency increase

Fig. 3.20 shows the frequency increase after the sudden loss of demand. Fig. 3.21 shows the changes of power output of generators (see the left axis) and of the power consumption of refrigerators (see the right axis). Power consumption of refrigerators increased almost immediately following the frequency increase. With the 400 MW increase in load, frequency increased to a maximum of 50.29 Hz, compared to the 50.42 Hz that it reached without any frequency response from refrigerators. Reduction in power output of frequency-sensitive generators was also reduced with the frequency response from refrigerators.

Fig. 3.22 shows that following the recovery of frequency (see the right axis), the power consumption of refrigerators reduced (see the left axis) indicating that refrigerators started to recover from the frequency rise event.

The ON/OFF state and T_{Ca} of a cooler during and after the frequency increase is given in Figs. 3.23-3.24 (*'with f increase'*). The ON/OFF state and T_{Ca} of the same cooler without applying the loss of demand is also shown (*'without f increase'*). The ON/OFF state and T_{Ca} are compared to show the influence of the frequency increase on the behaviour of a cooler.

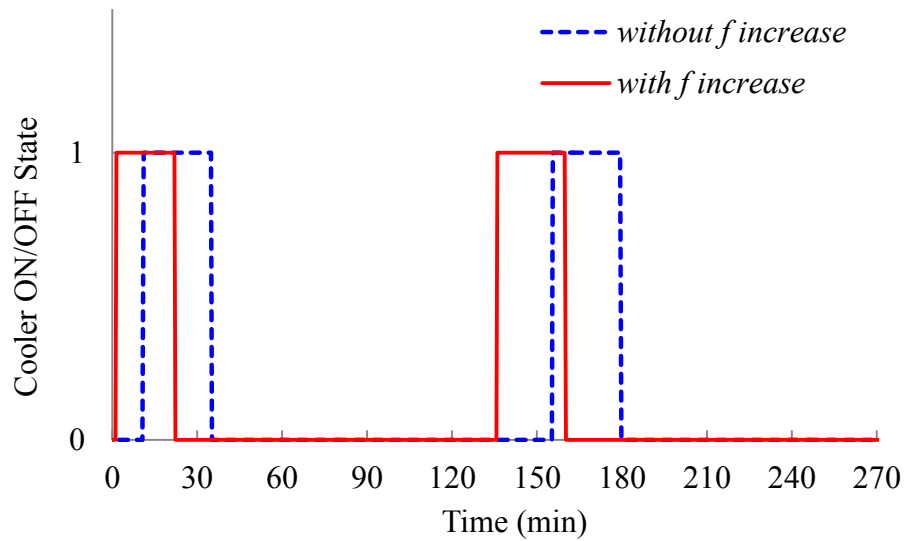


Fig. 3.23. ON/OFF state of the cooler

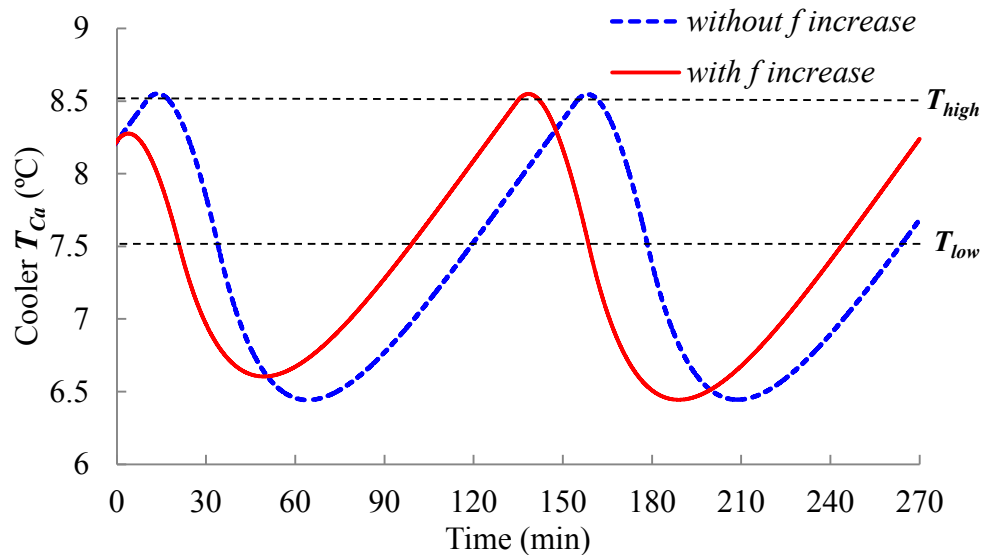


Fig. 3.24. Cavity temperature of the cooler

As shown in Fig. 3.23, the cooler was switched ON earlier at 1.5 min (90 s) in response to the frequency increase compared to the case ‘*without f increase*’ in which the refrigerator was switched ON at 10 min. Fig. 3.24 shows that T_{Ca} of the cooler stayed within its original range even though it was switched ON earlier because of the frequency increase. Similar behaviours occurred for the freezer.

Case 3: Simulation of consecutive loss of two generators

A case study was undertaken considering a multiple loss of generators. The case was designed based on the severe frequency incident that occurred on 28 May 2008 in the GB power system [22]. It was mainly caused by an unrelated consecutive loss of two generators (345 MW and 1,237 MW). System demand was 41 GW.

To obtain a frequency profile similar to the loss of the two generators in the incident, the parameters of the GB power system model in Fig. 3.13 were set as shown in Table 3.9.

TABLE 3.9. Parameters of the GB Power System Model (System Base of 41 GW).

Dead Band (pu)	R_{eq} (pu)	T_G (s)	T_1 (s)	T_2 (s)	T_T (s)	K (pu)	K_i (pu)	H_{eq} (s)	D (pu)
± 0.0003	0.5	0.2 s	8 s	20 s	0.3 s	0.8	0.006	6.5	1

The loss of the first generator of 345 MW at 90 s and the loss of the second generator of 1,237 MW at 185 s were applied to the model. Two sets of simulation results during the frequency incident, one with the refrigerators' response and one without the refrigerators' response, are compared in Figs. 3.25 and 3.26. Figs. 3.27 and 3.28 show the grid frequency, power consumption of refrigerators and power change of generators after the recovery of frequency.

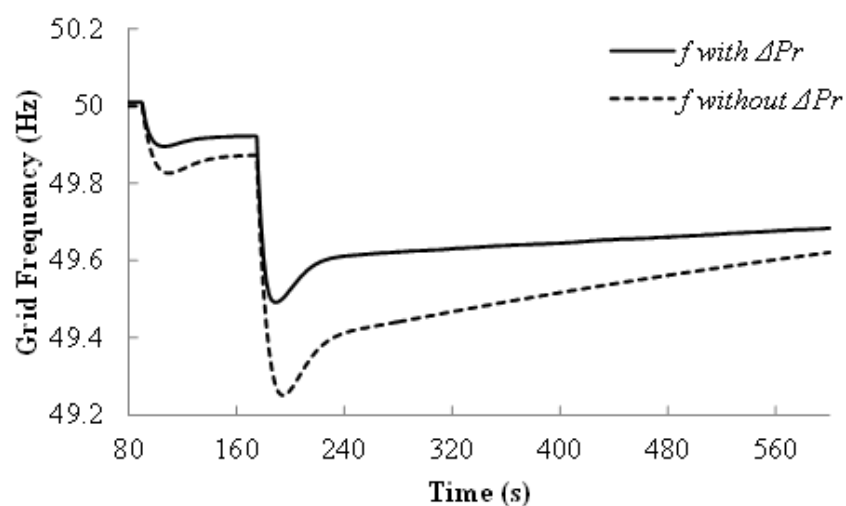


Fig. 3.25. Variation of grid frequency

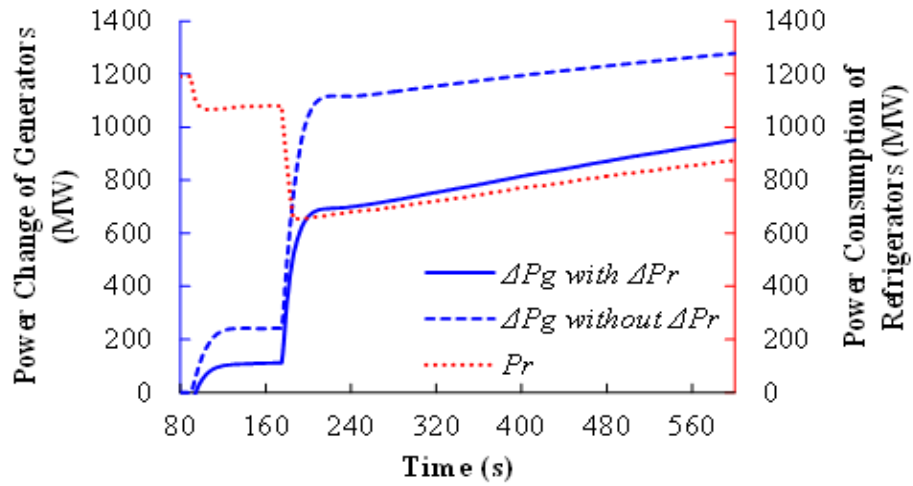


Fig. 3.26. Power change of generators and power consumption of refrigerators

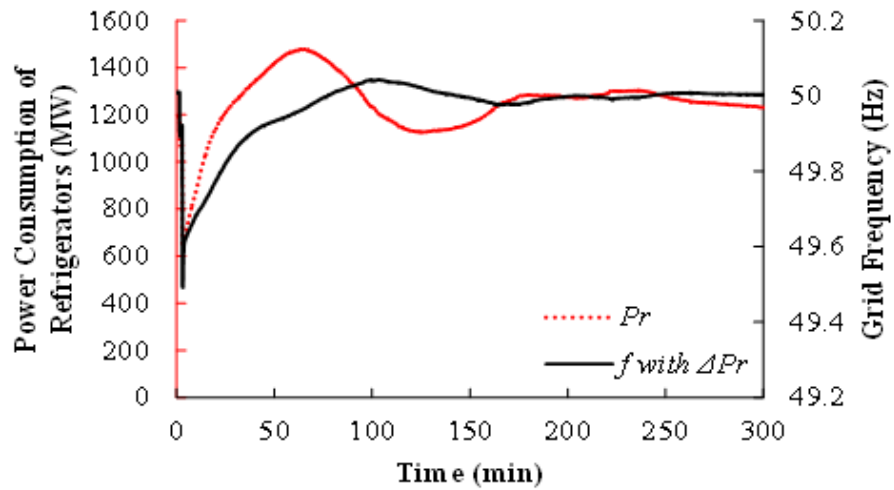


Fig. 3.27. Power consumption of refrigerators and the grid frequency after the frequency incident

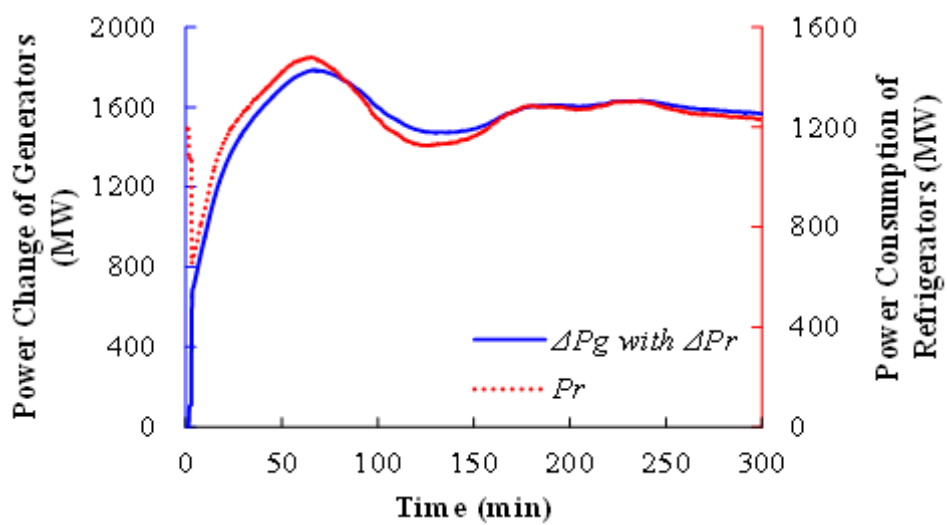


Fig. 3.28. Power change of Generators and power consumption of refrigerators after the frequency incident

Fig. 3.25 shows the variations of grid frequency and Fig. 3.26 shows the change of power output of generators (see the left axis) and the power consumption of refrigerators (see the right axis). After the loss of 345 MW generator, with the load change of refrigerators of approximately 100 MW, the frequency dropped to 49.9 Hz. Without the load change from refrigerators, the frequency dropped to 49.82 Hz. Following the loss of 1,237 MW generator, refrigerators provided further 430 MW of load reduction. The frequency only dropped to 49.5 Hz. This is a significant improvement on the frequency drop when compared to 49.24 Hz which occurred without the load change of refrigerators. The power consumption of the refrigerators varied in proportion to the drops of frequency. Approximately 530 MW of load change from 40 million refrigerators helped to reduce the frequency drop significantly during large frequency disturbances. The change of power output of frequency-sensitive generators was also decreased substantially with the load change.

Fig. 3.27 shows the power consumption of refrigerators (see the left axis) and the grid frequency (see the right axis) after the frequency incident. The lost thermal energy of refrigerators, caused by the sustained period of low frequency, was restored gradually. This restored energy was obtained from the change of power output of back-up generation in the power system as depicted by Fig. 3.28.

An increase in the power consumption of refrigerators occurred after the frequency incident (30-90 min) as shown in Fig. 3.27. This resulted from the simultaneous switching OFF of refrigerators following the severe frequency drop which led to the reduction of load diversity. As presented in Section 3.2, in the aggregated model of refrigerators, the diversity amongst the refrigerators (*div*) was indicated by the incorporation of the parameter *div*. In the previous simulations, a *div* of 0.2 determined by tests on 100 empty refrigerators was used. However, for the modelling of refrigerators in UK homes, a higher *div* was expected to be more realistic because of the greater level of diversity of refrigerator size and amount of food stored.

A sensitivity analysis was then carried out to show the effect of *div*. The values *div* of 0.2, 0.5 and 0.8 were used. Simulations were carried out using a similar GB power system model to that depicted in *Case 3.3*. Results of the sensitivity analysis are shown in Figs. 3.29-3.31.

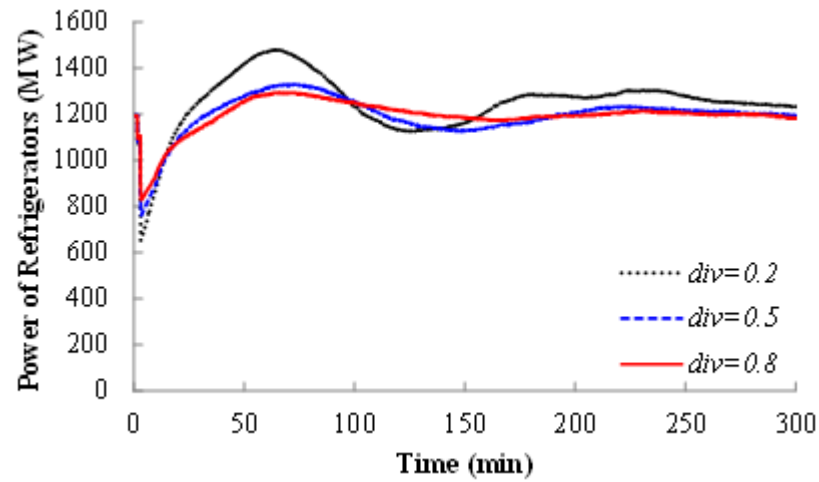


Fig. 3.29. Effect of the diversity in the refrigerator models (div) on the power consumption of refrigerators

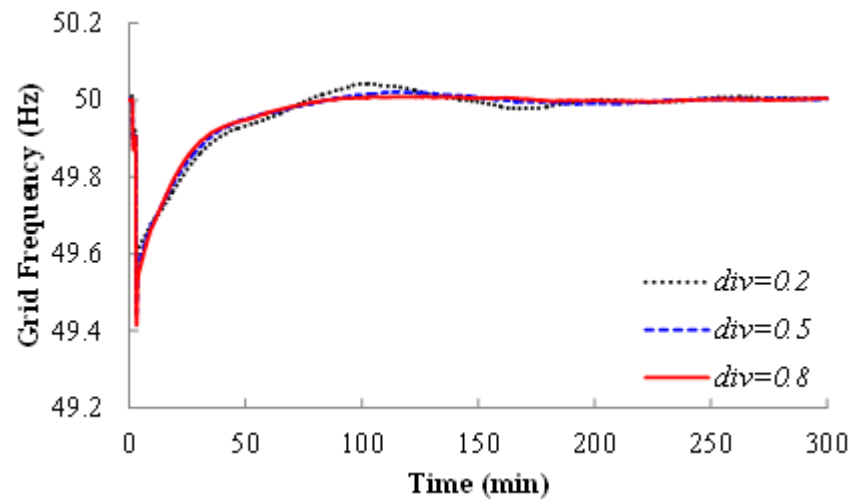


Fig. 3.30. Effect of the diversity in the refrigerator models (div) on the variation of grid frequency

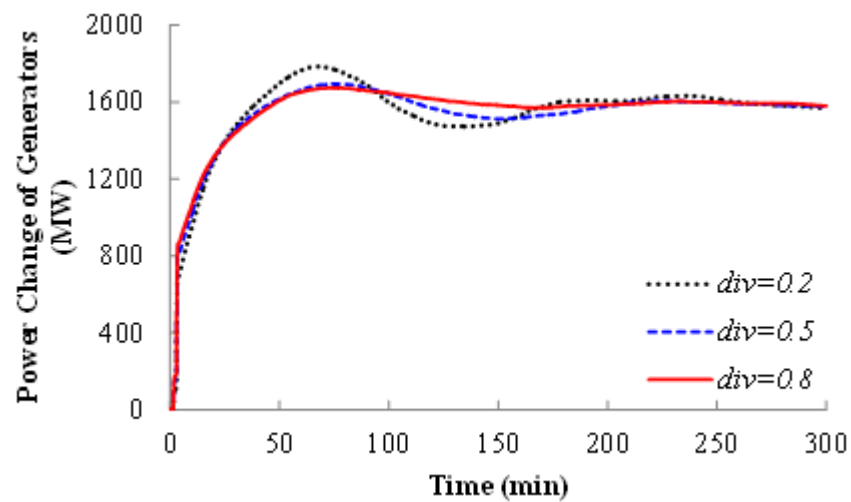


Fig. 3.31. Effect of the diversity in the refrigerator models (div) on the power change of generators

With an increasing *div*, increase in the power consumption of refrigerators after the severe frequency incident reduced significantly, as shown in Fig. 3.29. The fluctuations in grid frequency as a result of the re-connection of refrigerators also reduced, as shown in Fig. 3.30. The power change of generators became less frequent as given by Fig. 3.31.

A *div* of 0.8 was used for the modelling of UK homes. However, as shown in Fig. 3.29, the amount of load change at the second drop of frequency (185 s) reduced briefly with a *div* of 0.8 compared to a *div* of 0.2. The amount of load change from refrigerators was quantified through field investigations and will be presented in Chapter 5.

3.6 Conclusions

An autonomous and decentralised frequency controller allows refrigerators to change their power consumption dynamically in proportion to frequency deviations. The frequency control does not undermine the inherent temperature control of a refrigerator and therefore has little adverse impact on its cold storage performance.

A thermodynamic model of a refrigerator was developed. The model was calibrated with data from tests undertaken by Open Energi on a number of refrigerators at the premises of Indesit. An aggregated model of a population of refrigerators was developed by incorporating a diversity factor to represent the inherent diversity amongst the population.

Sensitivity analysis was firstly carried out to find the suitable number of refrigerator models to be aggregated and scaled up in order to represent the power level of 40 million refrigerators in the GB power system.

Case studies on the injection of a sustained low grid frequency signal and a sustained high grid frequency signal were undertaken. During the period of sustained high grid frequency, refrigerators were able to be ON for at least 10 minutes. During the period of sustained low grid frequency, refrigerators were able to be OFF for at least 10 minutes. After 10 minutes, the response of refrigerators exhausted and the power consumption of refrigerators started to recover gradually.

A simplified GB power system model was developed for the study of frequency control. Case studies were also undertaken by connecting the aggregated model of refrigerators to the GB power system model. Results showed that refrigerators were able to change

their power consumption almost immediately following the frequency deviations. A power reduction of 530 MW was provided by refrigerators when frequency dropped to approximately 49.5 Hz. With the power change of refrigerators, deviations of grid frequency were reduced. The amount of power change of frequency-sensitive generators was also decreased.

Refrigerators with the dynamic controller are able to help reduce the frequency deviations proportionally and dynamically in a way similar to that of frequency-sensitive generators. If deployed at scale, they have the potential to replace the spinning reserve capacity of frequency-sensitive generators.

Chapter 4

Industrial Bitumen Tanks for Frequency Control

An autonomous and decentralised frequency control was developed enabling bitumen tanks to change their power consumption in proportion to deviations of grid frequency. The frequency control of a tank will not interfere with its primary function of storing hot bitumen. A thermodynamic model of bitumen tanks was developed and validated with data from field tests on a number of bitumen tanks. An aggregated model of bitumen tanks, each equipped with the frequency control, was then developed. Field tests on 76 tanks equipped with the frequency control were undertaken. The variations of power consumption of tanks in simulations and in field tests were compared during large deviations of frequency. The aggregated model was then connected to the GB power system model. Simulation results showed that the load change of tanks contributed to the reduction of frequency deviations in a way similar to frequency-sensitive generators. Tanks provided a faster response to frequency deviations than that provided by frequency-sensitive generators.

4.1 Introduction

Bitumen is mainly used for road construction and needs to be stored in the liquid form [93]. Large, well-insulated bitumen tanks are used for the storage of hot bitumen. A heater is installed in each tank to heat bitumen prior to use.

The heater of a bitumen tank is connected to the grid at all times. It consumes power with an ON/OFF cycle. Therefore, its power consumption is time-flexible and can be shifted in order to provide frequency response. The typical power consumption of a tank is 40 kW when its heater is ON. According to investigations by Open Energi, there are approximately 500 bitumen tanks in the GB power system.

4.2 Dynamic control of bitumen tanks

4.2.1 Temperature control of bitumen tanks

The heater in a bitumen tank follows a hysteresis temperature control as shown in Fig. 4.1. The tank temperature controls the ON/OFF state of a heater. When tank temperature reaches its high set-point T_{high} , the heater will be switched OFF. When tank temperature reaches its low set-point T_{low} , the heater will be switched ON. The typical ON/OFF cycle of a well-insulated tank is 2 hours ON and 4.5 hours OFF.

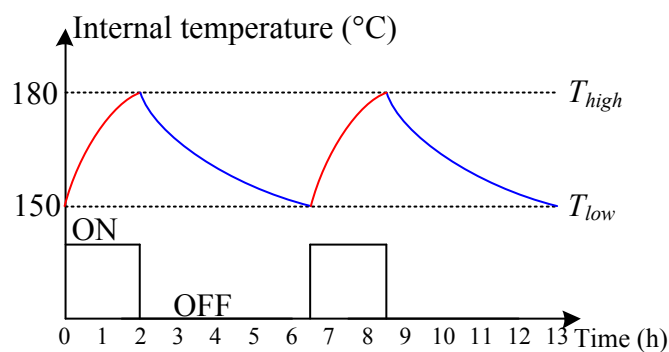


Fig. 4.1. Hysteresis temperature control of one tank

4.2.2 Use of bitumen tanks for grid frequency control

A frequency control was developed for bitumen tanks as shown in Fig. 4.2 (*'Frequency control'*). The input of the frequency controller is the grid frequency f and it is constantly compared with two trigger frequencies F_{ON} and F_{OFF} . The outputs of the

frequency controller are the state signals S_{LF} and S_{HF} , which are determined by the comparison.

- If f is greater than F_{ON} , S_{HF} is 1, indicating the tank will be triggered ON as a result of a rise in frequency.
- If f is lower than F_{OFF} , S_{LF} is 0, indicating the tank will be triggered OFF as a result of a drop in frequency.

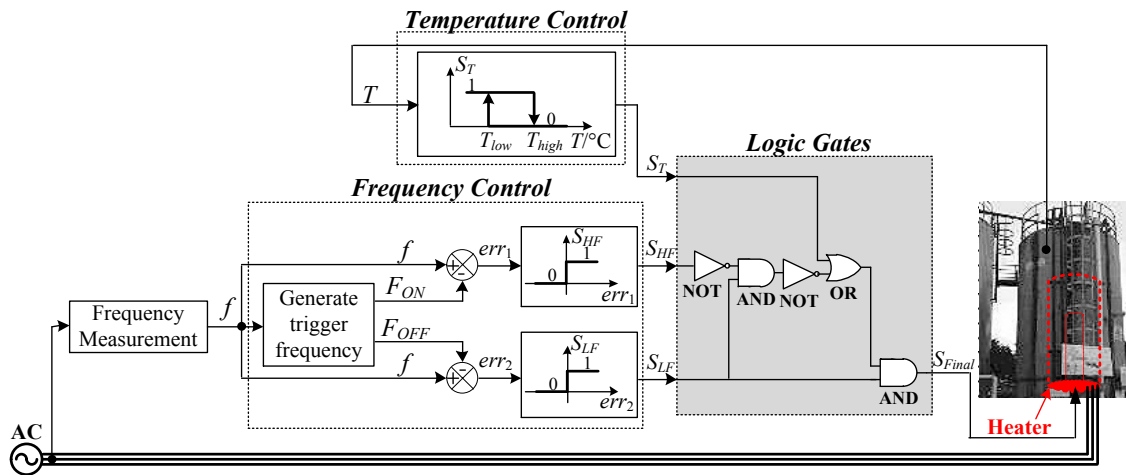


Fig. 4.2. Local control scheme of one tank

Initially, F_{ON} and F_{OFF} are generated randomly using a uniform distribution within their ranges. F_{ON} is in the range of 50-50.5 Hz and F_{OFF} is in the range of 49.5-50 Hz. Trigger frequencies determine the sequence of tanks to be switched. Following a rise in frequency, tanks are switched ON starting from the one with the lowest F_{ON} in its range. Following a drop in frequency, tanks are switched OFF starting from the one with the highest F_{OFF} in its range. Therefore, the larger the frequency deviates from 50 Hz, the higher the number of tanks that will be switched.

4.2.3 Integrated control

The integrated control of a tank including both temperature and grid frequency control is also shown in Fig. 4.2. The temperature control measures the temperature (T) in the tank and generates the state signal (S_T). The frequency control measures the grid frequency (f) and generates the state signals (S_{LF} and S_{HF}). The final switching signal (S_{Final}) to the heater is then determined by the state signals S_T , S_{LF} and S_{HF} as shown in Table 4.1. ‘1’ indicates ‘ON-state’ and ‘0’ indicates ‘OFF-state’.

In the event of a rise in frequency, if f becomes higher than F_{ON} , then S_{HF} is 1 and S_{LF} is 1 as shown in rows 1-2. The tank is switched ON ($S_{Final} = 1$).

In the event of a drop in frequency, if f becomes lower than F_{OFF} , then S_{LF} is 0 as shown in rows 3-4. The tank is switched OFF ($S_{Final} = 0$).

If f varies between F_{ON} and F_{OFF} of a tank, the tank follows its temperature control as shown in rows 5-6 ($S_{Final} = S_T$).

Rows 7-8 are not feasible states because f cannot be lower than F_{OFF} but higher than F_{ON} simultaneously.

TABLE 4.1. Truth Table of Logic Gates of Fig. 4.2.

Row	S_T	S_{HF}	S_{LF}	S_{Final}
1	0	1	1	1
2	1	1	1	1
3	0	0	0	0
4	1	0	0	0
5	0	0	1	0
6	1	0	1	1
7	0	1	0	0
8	1	1	0	0

The control also has the following considerations:

- To avoid frequent switching actions which may damage the heater, a minimum ON/OFF time of at least 25 s is applied to each tank.
- A maximum number of switches per hour was set to be 8. This is also to avoid too many switching actions.

4.2.4 Update of trigger frequencies F_{OFF} and F_{ON}

In the frequency control of a bitumen tank, its trigger frequencies F_{OFF} and F_{ON} are updated autonomously based on measurements of the present sample of the frequency $f(t)$ and the previous frequency sample $f(t-\Delta t)$. The sampling time, Δt , of the grid frequency measurements was selected as 200 ms. This is to be consistent with the frequency meter that Open Energi used to measure the grid frequency. The frequency meter uses a fixed window of 200 ms over which it takes an average reading of frequency.

Three tanks were selected as examples to illustrate the reasons for which it is beneficial to update F_{OFF} . Fig. 4.3(a) shows the case for F_{OFF} unchanged and Fig. 4.3(b) shows the case in which F_{OFF} was updated with f .

Conventional direct control of a load in response to drops in frequency is shown in Fig. 4.3(a). Tanks 1, 2 and 3 have F_{OFF} of 49.9 Hz (F_{OFF1}), 49.8 Hz (F_{OFF2}) and 49.6 Hz (F_{OFF3}). Following a drop of frequency, Tank 1 is switched OFF followed by Tank 2. When f starts to recover and rises towards 50 Hz, Tank 2 reverts back ON at t_2 followed by Tank 1 at t_1 . This implies that Tank 1, which was switched OFF first, is reconnected last. Moreover, Tank 3 is not switched OFF at all since F_{OFF3} remains lower than f . Tank 1 is without energy for a long time while Tank 3 provides no response to the frequency drop. In this case the frequency response from the three tanks is uneven and tanks with a lower F_{OFF} provide reduced frequency response.

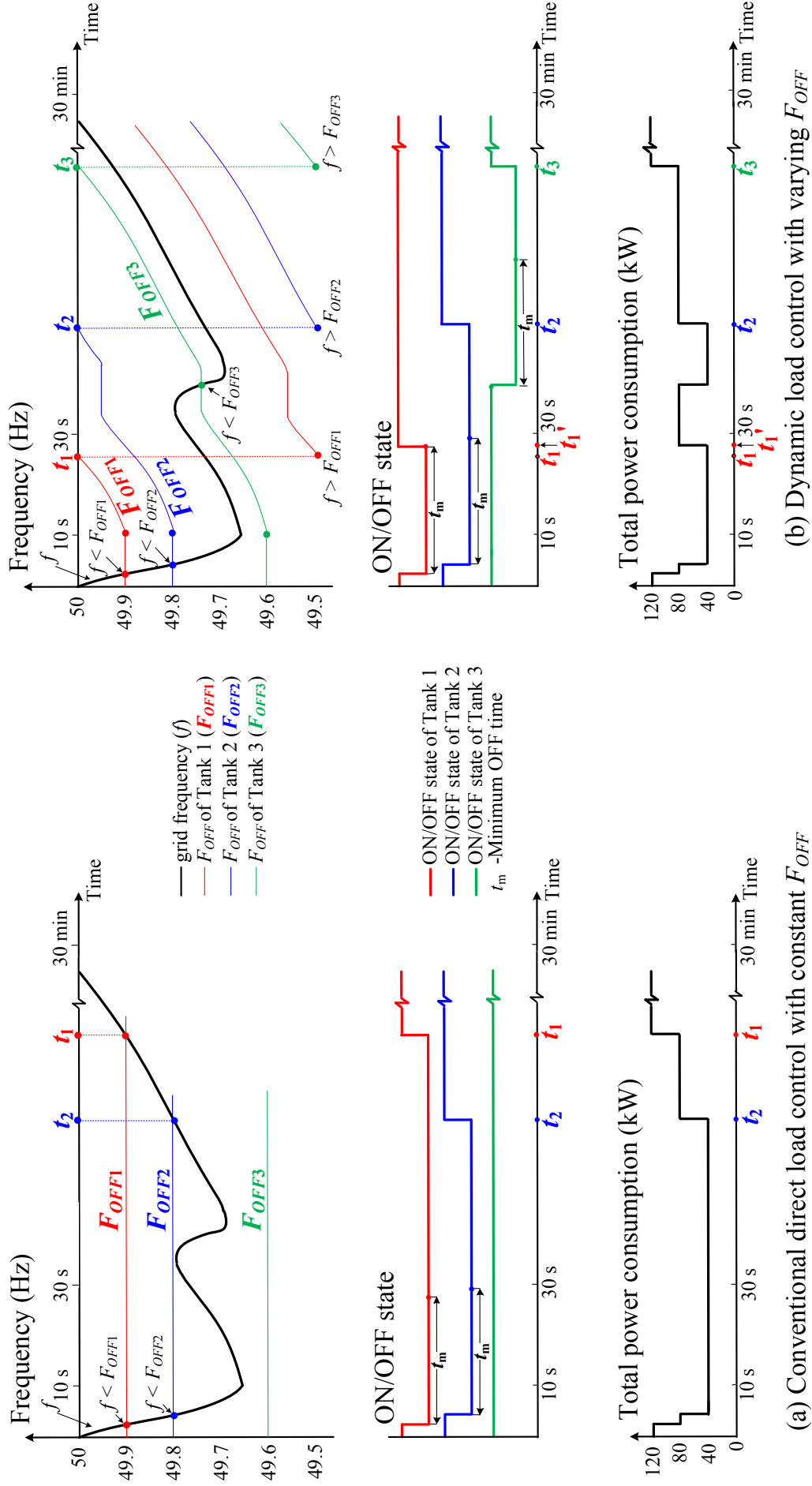


Fig. 4.3. Frequency control of three tanks during a drop of frequency

A dynamic load control, which updates F_{OFF} and F_{ON} dynamically, is shown in Fig. 4.3(b). It was implemented in order to maintain an even distribution of switching requests amongst tanks. F_{OFF} is updated following the rules that are listed in Table 4.2.

TABLE 4.2. Update of Trigger Frequency F_{OFF} .

Variation of frequency f		Update of F_{OFF}
$f \geq 50 \text{ Hz}$		$F_{OFF}(t) = F_{OFF}(t - \Delta t)$ (4.1)
$f < 50 \text{ Hz}$	If f is dropping or remains constant: $f(t) \leq f(t - \Delta t)$	$F_{OFF}(t) = F_{OFF}(t - \Delta t)$ (4.2)
	If f is rising: $f(t) > f(t - \Delta t)$	$F_{OFF}(t) = F_{OFF}(t - \Delta t) + f(t) - f(t - \Delta t)$ (4.3) If $F_{OFF}(t)$ reaches 50 Hz: $F_{OFF}(t) = F_{OFF}(t) - 0.5 \text{ Hz}$ (4.4)

- When f is above 50 Hz, F_{OFF} remains unchanged (4.1).
- When f is below 50 Hz:
 - if f is dropping or remains constant below 50 Hz, then F_{OFF} remains unchanged (4.2).
 - if f is rising but is below 50 Hz, then F_{OFF} is updated by adding the variations of f as illustrated in (4.3). If F_{OFF} reaches 50 Hz, F_{OFF} is then re-set to 49.5 Hz by subtracting 0.5 Hz (4.4). This makes F_{OFF} to be the lowest trigger frequency. f is then greater than F_{OFF} which triggers the tank to revert back ON.

The effect of updating F_{OFF} is shown in Fig. 4.3(b). Tank 1 is switched ON first following the recovery of f because F_{OFF1} reaches 50 Hz first and is re-set to 49.5 Hz at t_1 . Tank 1 is switched ON at t'_1 instead of t_1 because of the minimum OFF-time t_m of 25 s. Comparing the OFF-time of Tank 1 to that in Fig. 4.3(a), the loss of energy to Tank 1 is reduced significantly.

Tank 2 is switched ON at t_2 following the recovery of f . Its OFF-time is also shorter than that in Fig. 4.3(a).

Tank 3 has a low initial F_{OFF} (F_{OFF3}) and it was not switched OFF at the first drop of f . However, when the second drop of f occurs, Tank 3 is switched OFF as F_{OFF3} has been updated to be greater than f . Tank 3 is then reconnected at t_3 . Compared to Fig. 4.3(a), Tank 3 provides additional frequency response.

By dynamically updating F_{OFF} , the response of tanks is made more sensitive and proportional to variations of grid frequency. This can be seen by comparing the total power consumption in Fig. 4.3(b) to that in Fig. 4.3(a). Tanks are controlled to recover starting from the one that was the first to be disconnected. All tanks have an equal opportunity to provide frequency response and the shift of their heating cycle is minimised.

The trigger frequency F_{ON} is also updated using a similar method which follows the rules listed in Table 4.3.

TABLE 4.3. Update of Trigger Frequency F_{ON} .

Variation of frequency f		Update of F_{ON}
$f \leq 50 \text{ Hz}$		$F_{ON}(t) = F_{ON}(t - \Delta t)$ (4.5)
$f > 50 \text{ Hz}$	If f is rising or remains constant: $f(t) \geq f(t - \Delta t)$	$F_{ON}(t) = F_{ON}(t - \Delta t)$ (4.6)
	If f is dropping: $f(t) < f(t - \Delta t)$	$F_{ON}(t) = F_{ON}(t - \Delta t) + f(t) - f(t - \Delta t)$ (4.7) If $F_{ON}(t)$ reaches 50 Hz: $F_{ON}(t) = F_{ON}(t) + 0.5 \text{ Hz}$ (4.8)

4.3 Modelling of bitumen tanks

4.3.1 Thermodynamic model of bitumen tanks

The heat transfer process of a bitumen tank is shown in Fig. 4.4. The rate of its heat supply P_{supply} (W) is:

$$P_{supply}(t) = P \times s_h(t) \quad (4.9)$$

where P is the power consumption of the heater and s_h is the heater state. s_h is 1 if the heater is ON and s_h is 0 if the heater is OFF. s_h is determined by constantly comparing the internal temperature of a tank (T) with its temperature set-points T_{high} and T_{low} as shown in (4.10). T_{high} is typically 180 °C and T_{low} is typically 150 °C:

$$s_h(t) = \begin{cases} 1, & \text{if } T(t) < T_{low} \\ 0, & \text{if } T(t) > T_{high} \end{cases} \quad (4.10)$$

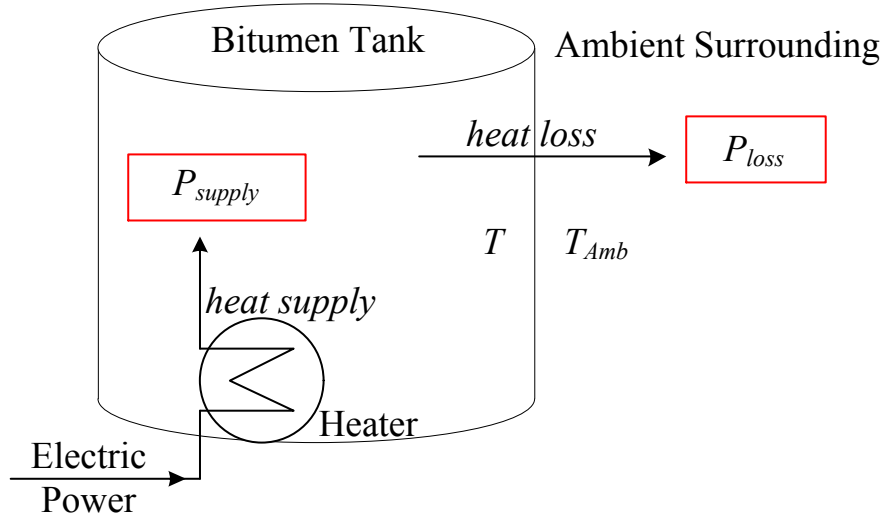


Fig. 4.4. Heat transfer process of one bitumen tank

The rate of heat loss P_{loss} (W) in a bitumen tank is [86]:

$$P_{loss}(t) = UA(T(t) - T_{Amb}) \quad (4.11)$$

where U ($\text{Wm}^{-2}\text{K}^{-1}$) is the overall heat transfer coefficient, A (m^2) is the area of the tank, T (K) is the internal temperature of the tank, T_{Amb} (K) is the ambient temperature.

The net rate of heat transfer is:

$$P_{net}(t) = P_{supply}(t) - P_{loss}(t) \quad (4.12)$$

The net rate of heat transfer results in the variations of internal temperature T (K) of the tank [87]:

$$P_{net}(t) = c_v m \frac{dT(t)}{dt} \quad (4.13)$$

where c_v ($\text{Jkg}^{-1}\text{K}^{-1}$) is the specific heat capacity, m (kg) is the mass of a bitumen tank.

By combining (4.9)-(4.13), a first order differential equation for T was obtained:

$$\frac{dT(t)}{dt} = \frac{P_{sh}(t)}{c_v m} - \frac{UA(T(t) - T_{Amb})}{c_v m} \quad (4.14)$$

Equation (4.14) has two possible solutions depending on the heater state s_h . Variations of T follow the exponential increase and decay [94]-[95]. Therefore, it was assumed the solution to (4.14) as:

- When heater is ON $s_h(t) = 1$:

$$T(t) = a_1 + b_1 e^{-t/\tau_{ON}} \quad (4.15)$$

where τ_{ON} is the time constant of the ON-period of a tank.

- When heater is OFF $s_h(t) = 0$:

$$T(t) = a_2 + b_2 e^{-t/\tau_{OFF}} \quad (4.16)$$

where τ_{OFF} is the time constant of the OFF-period of a tank.

The typical ON and OFF period (t_{ON} and t_{OFF}) and temperature variations of a bitumen tank are shown in Fig. 4.5.

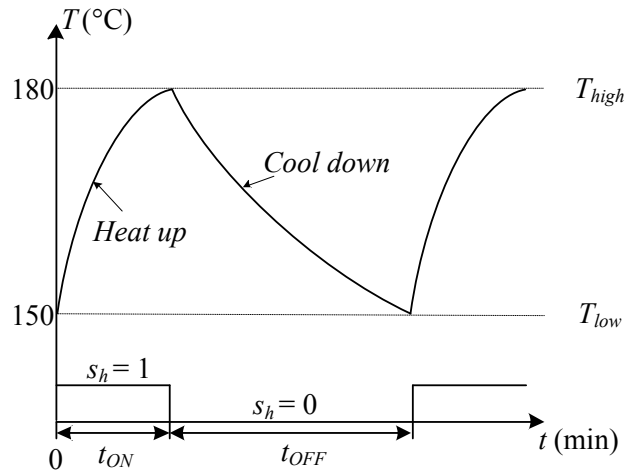


Fig. 4.5. Internal temperature of a tank and its ON and OFF period

It was assumed that when $s_h(t) = 1$, the exponential increase of T reaches T_{high} (180 °C) at $t_{ON} = 2\tau_{ON}$. It is to be noted that, for an exponential function, the final value will not be reached until $t \rightarrow \infty$ [95] and therefore the above assumption was made. Using (4.15), equations (4.17) and (4.18) are obtained:

- When $t = 0$ min, $T(t) = T_{low}$ (150 °C in Fig. 4.5):

$$T_{low} = a_1 + b_1 \quad (4.17)$$

- When $t = t_{ON} = 2\tau_{ON}$, $T(t) = T_{high}$ (180 °C in Fig. 4.5):

$$T_{high} = a_1 + b_1 e^{-2} \quad (4.18)$$

Solving the above two equations, a generic equation of the tank temperature for the ON-period is obtained:

$$T(t) = \frac{T_{low}e^{-2} - T_{high}}{e^{-2} - 1} + \frac{T_{high} - T_{low}}{e^{-2} - 1} e^{-t/\tau_{ON}}, 0 \leq t < t_{ON} \quad (4.19)$$

Similarly for the OFF period shown in Fig. 4.5, it was also assumed that when $s_h(t) = 0$, the exponential growth of T reaches T_{low} (150 °C) at $2\tau_{OFF}$. Equation (4.16) is rewritten by (4.20) as the OFF-period starts at $t = t_{ON}$.

$$T(t) = a_2 + b_2 e^{-(t-t_{ON})/\tau_{OFF}} \quad (4.20)$$

Hence, it is obtained that:

- When $t - t_{ON} = 0$ min, $T(t) = T_{high}$ (180 °C in Fig. 4.5):

$$T_{high} = a_2 + b_2 \quad (4.21)$$

- When $t - t_{ON} = t_{OFF} = 2\tau_{OFF}$, $T(t) = T_{low}$ (150 °C in Fig. 4.5):

$$T_{low} = a_2 + b_2 e^{-2} \quad (4.22)$$

Solving the above two equations, a generic equation of tank temperature for the OFF-period is obtained:

$$T(t) = \frac{T_{high}e^{-2} - T_{low}}{e^{-2} - 1} + \frac{T_{low} - T_{high}}{e^{-2} - 1} e^{-(t-t_{ON})/\tau_{OFF}}, t_{ON} \leq t < t_{OFF} \quad (4.23)$$

A thermodynamic model of bitumen tanks was therefore developed by deriving equations (4.19) and (4.23) for different tanks that have different ON/OFF period and time constants.

A simulation was then carried out on the thermodynamic model of five different bitumen tanks over 10 hours in Matlab/Simulink. The power rating of each tank was 40 kW. The ON/OFF period and time constants of tanks are shown in Table 4.4. In order to reflect the diversity amongst tanks, the five tanks were assigned a different initial ON/OFF state and different initial temperature by randomising the starting time t in (4.19) and (4.23). The temperature curves of each tank are shown in Fig. 4.6. The total power consumption of five tanks is shown in Fig. 4.7.

TABLE 4.4. Parameters of Each Tank.

Tanks	1	2	3	4	5
On period	124 min	165 min	167 min	157 min	47 min
Off period	351 min	221 min	277 min	336 min	143 min
τ_{ON}	62 min	82 min	83 min	79 min	24 min
τ_{OFF}	176 min	111 min	138 min	168 min	72 min

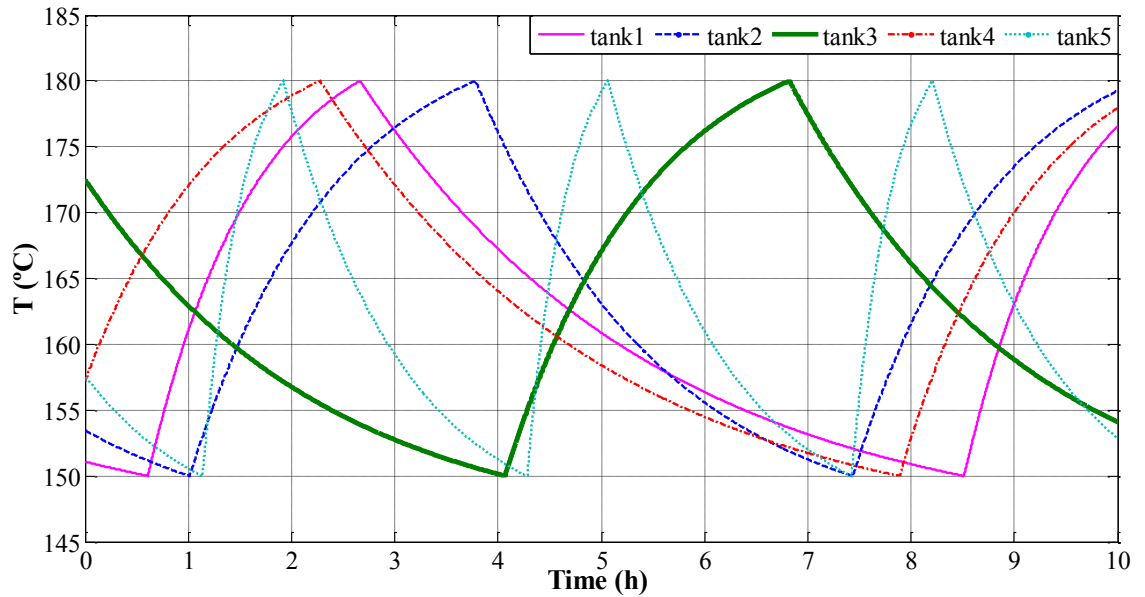


Fig. 4.6. Tank temperature obtained from the thermodynamic model of 5 bitumen tanks

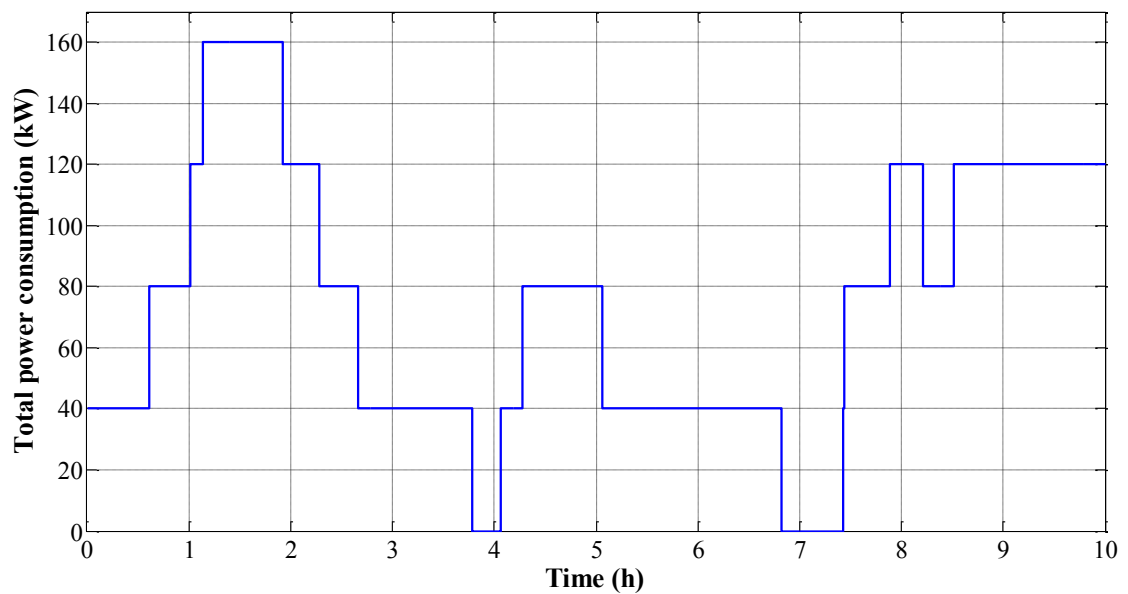


Fig. 4.7. Total power consumption of 5 bitumen tanks obtained from the thermodynamic model

4.3.2 Validation of the thermodynamic model

Heating and cooling of a tank is shown in Fig. 4.8(a). The tank is switched ON at T_{low} (point A) and the tank temperature follows curve AB. Conversely, the tank is switched OFF at T_{high} (point B) and the tank temperature follows curve BC. However, when a tank is used for frequency control, it may be switched ON/OFF at an intermediate temperature. In Fig. 4.8(a), the tank is ON at D. If the heater remains ON, temperature will follow the curve DB for a time t_{rise} until T_{high} is reached at B. If the heater is switched OFF at D, temperature will follow the curve DE for a time t_{fall} until T_{low} is reached at E. A similar process occurs as shown in Fig. 4.8 (b) where a tank is initially OFF at point M.

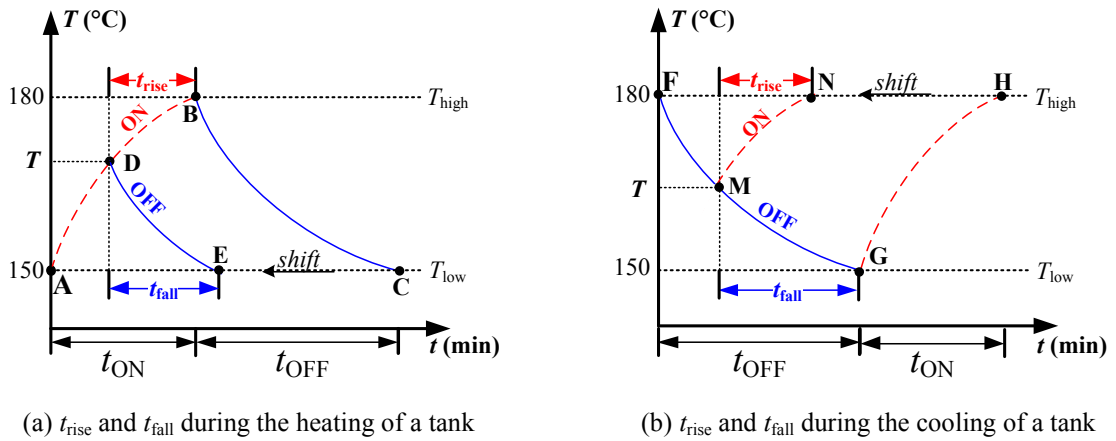


Fig. 4.8. Illustration of t_{rise} and t_{fall} at any temperature of a bitumen tank

The minimum possible value of t_{rise} is zero and occurs when temperature reaches T_{high} . The maximum possible value of t_{rise} is the total ON-period t_{ON} when temperature is at T_{low} . Similarly, the range of t_{fall} is from zero to t_{OFF} .

As illustrated in Fig. 4.8, for a tank with known ON and OFF period, a pair of t_{rise} and t_{fall} are calculated for different temperatures T using the inverse functions of (4.19) and (4.23). For each T , the calculated pair of t_{rise} and t_{fall} is plotted by a cross in Fig. 4.9(a). Using the curve fitting function ‘cftool’ in Matlab, a semi-circle relationship between t_{rise} and t_{fall} is obtained. The analytical expression is shown by (4.24) and (4.25).

$$t_{rise} = t_{ON} \sqrt{1 - \left(\frac{t_{fall}}{t_{OFF}}\right)^2} \quad (4.24)$$

$$t_{\text{fall}} = t_{\text{OFF}} \sqrt{1 - \left(\frac{t_{\text{rise}}}{t_{\text{ON}}}\right)^2} \quad (4.25)$$

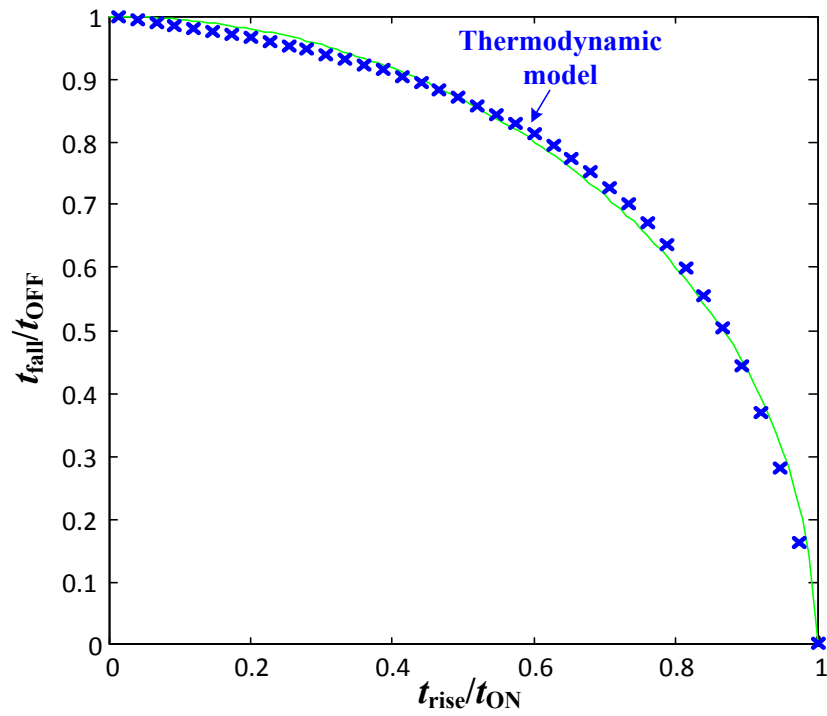
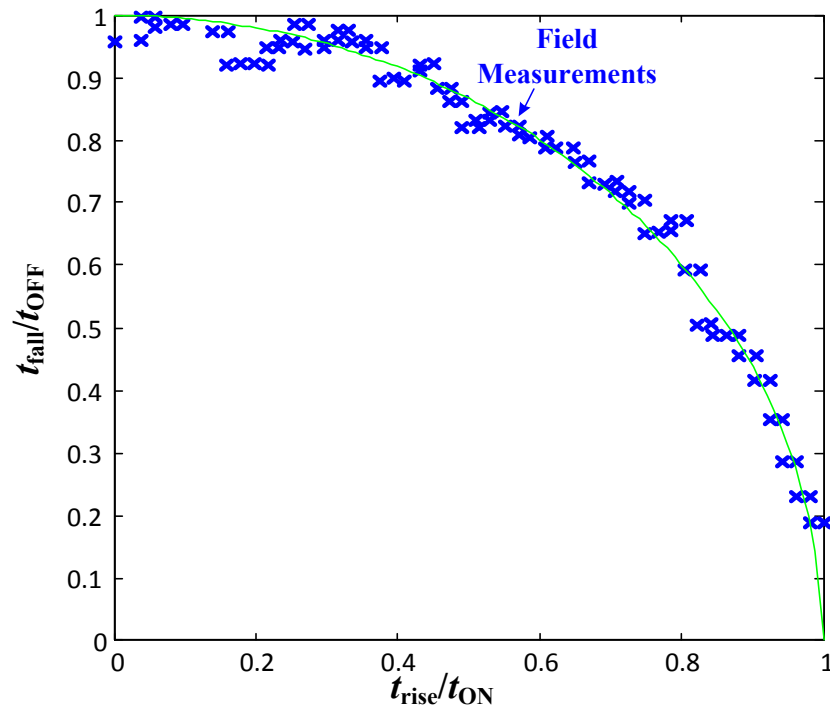
(a) t_{rise} and t_{fall} calculated using the thermodynamic model(b) t_{rise} and t_{fall} of field measurements

Fig. 4.9. Relationship of t_{rise} and t_{fall} of a bitumen tank (t_{rise} is normalised with t_{ON} and t_{fall} is normalised with t_{OFF})

t_{rise} and t_{fall} were also measured on two 25 kW and two 40 kW real bitumen tanks at different times of day. The test results were used to validate the thermodynamic model. Fig. 4.9(b) shows the field measurements of t_{rise} and t_{fall} at different temperatures of a 40 kW tank (indicated by the crosses). Other tanks show similar results. It can be seen that the relationships in (4.24) and (4.25) which were obtained from the thermodynamic model were validated by the field measurements in Fig. 4.9(b).

4.3.3 Curve-fit Model of bitumen tanks

A simplified curve-fit model was also developed in Matlab/Simulink. Variations of the tank temperature over time were modelled using variations of t_{rise} and t_{fall} over time.

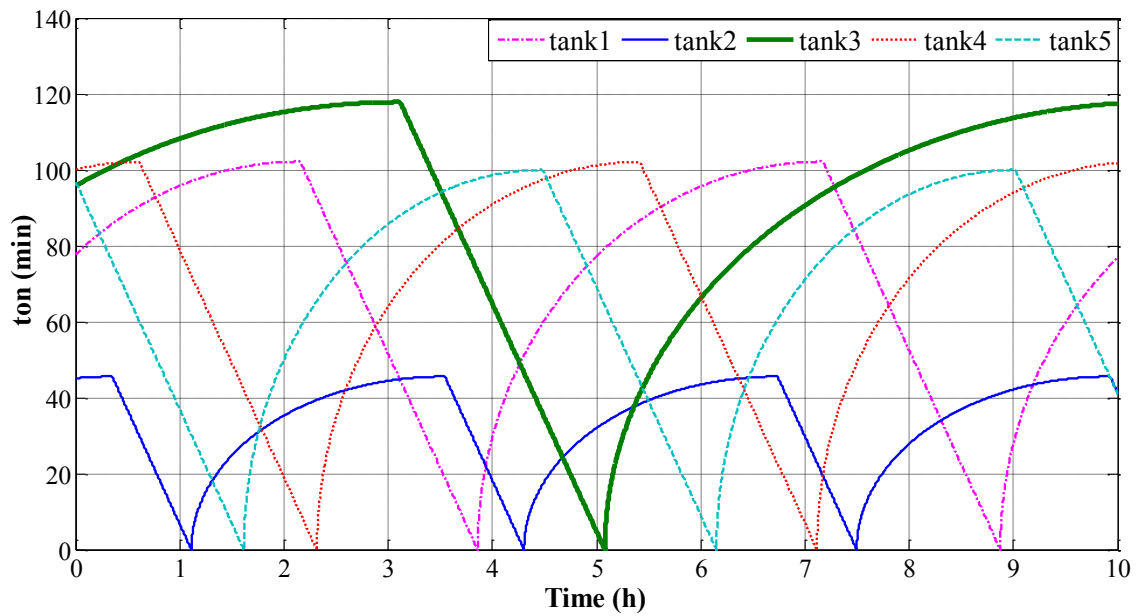
Based on Fig. 4.8, Table 4.5 was used to model the variations of t_{rise} and t_{fall} for all the possible thermal states. Δt is the time step. Equation (4.27) was based on (4.25) and equation (4.28) was based on (4.24).

TABLE 4.5. t_{ON} and t_{OFF} of the Curve-fit Model

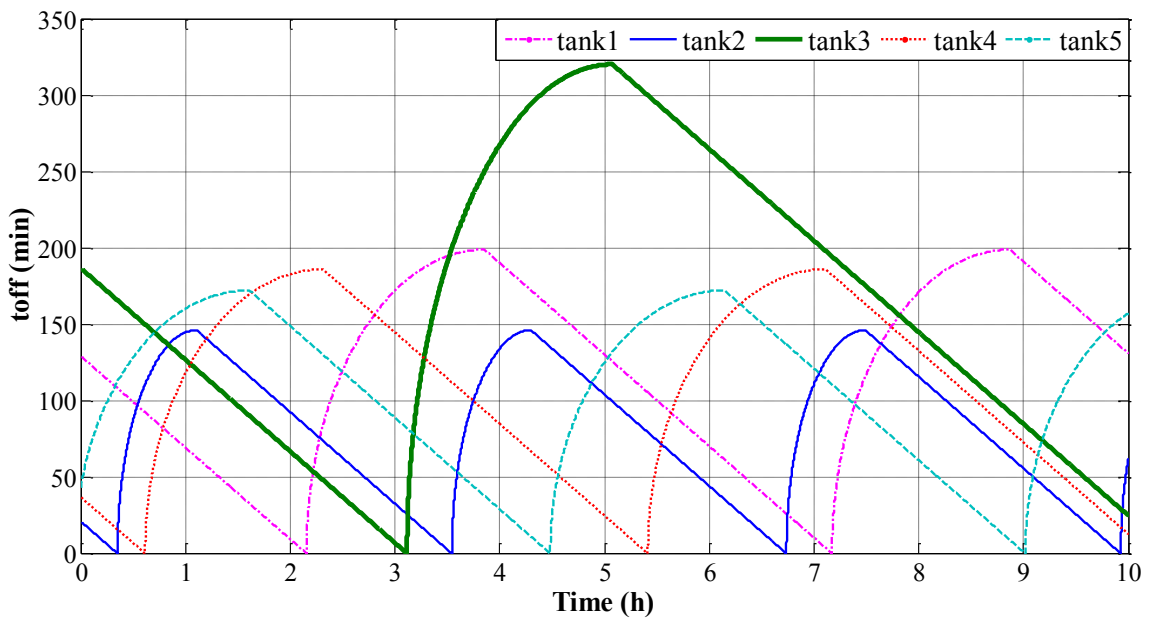
Heater State	Corresponding Curve in Fig. 4.8	Variations of t_{ON} and t_{OFF}
Remain ON at t	DB	$t_{\text{rise}}(t + \Delta t) = t_{\text{rise}}(t) - \Delta t$ (4.26)
Switched ON at t	MN	$t_{\text{fall}}(t + \Delta t) = t_{OFF} \times \sqrt{1 - \left[\frac{t_{\text{rise}}(t) - \Delta t}{t_{ON}} \right]^2}$ (4.27)
Remain OFF at t	MG	$t_{\text{rise}}(t + \Delta t) = t_{ON} \times \sqrt{1 - \left[\frac{t_{\text{fall}}(t) - \Delta t}{t_{OFF}} \right]^2}$ (4.28)
Switched OFF at t	DE	$t_{\text{fall}}(t + \Delta t) = t_{\text{fall}}(t) - \Delta t$ (4.29)

A simulation was carried out using the curve-fit model of five bitumen tanks with a power rating of 40 kW over 10 hours. The five tanks were assigned different initial t_{rise} and t_{fall} in order to reflect the diversity amongst tanks. t_{rise} was assigned randomly in the range of 0 to t_{ON} . t_{fall} was assigned randomly in the range of 0 to t_{OFF} . The value of t_{ON} was distributed randomly within the range of 42 to 180 min, which was measured on different tanks in the field tests. Similarly, t_{OFF} was distributed randomly within the

range of 60 to 480 min. t_{rise} and t_{fall} of the five tanks are shown in Fig. 4.10 and their total power consumption is shown in Fig. 4.11.



(a) t_{rise} of 5 bitumen tanks.



(b) t_{fall} of 5 bitumen tanks.

Fig. 4.10. t_{rise} and t_{fall} of 5 bitumen tanks

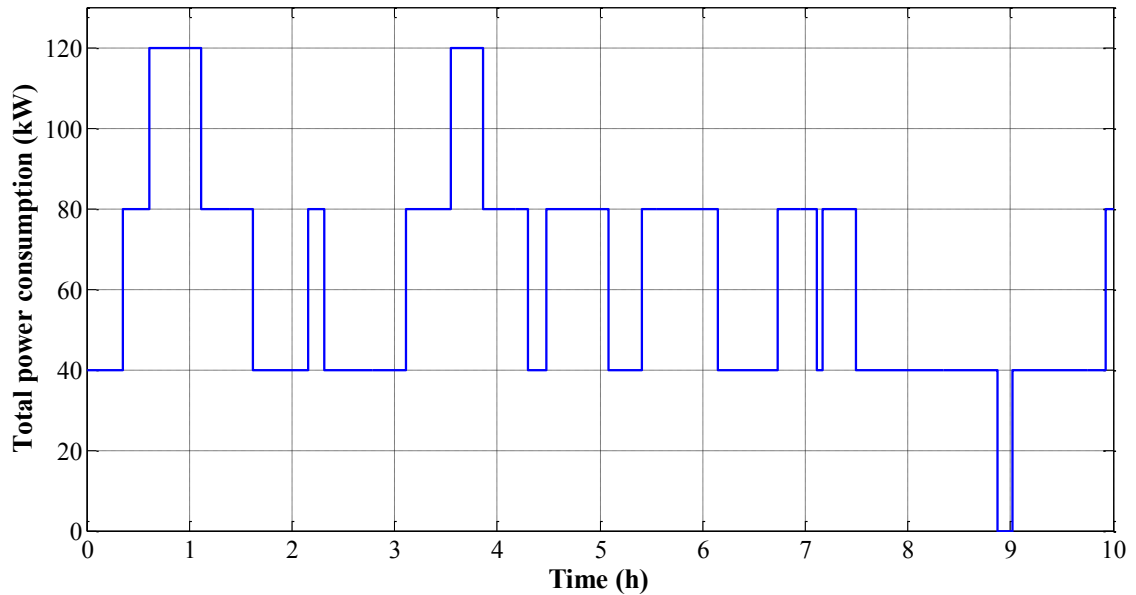


Fig. 4.11. Total power consumption of 5 bitumen tanks

It can be seen that t_{rise} in Fig. 4.10(a) decreases linearly according to (4.26) if the heater is ON and increases according to (4.28) if the heater is OFF. T_{fall} in Fig. 4.10(b) decreases linearly according to (4.29) if the heater is OFF and increases according to (4.27) if the heater is ON.

4.3.4 Comparison of thermodynamic model and curve-fit model

Simulations using the thermodynamic model developed by (4.19) and (4.23) and using the curve-fit model based on the equations in Table 4.5 were undertaken. Simulation results and performance of the two models were compared.

The first simulation was carried out on both models to simulate the normal operating cycle of 500 tanks over 10 h with a simulation time step of 1 s. Table 4.6 shows a comparison of the actual time it takes to run the simulation with each model ('Computer Running Time'). The results showed that the curve-fit model has a faster computational speed than the thermodynamic model.

TABLE 4.6. Computational Speed of the Thermodynamic Model and Curve-fit Model for Simulating the Normal Operating Cycle of 500 Tanks over 10 Hours.

Model	Number of Tanks	Simulation Time	Time Step	Computer Running Time
Thermodynamic Model	500	10 h	1 s	5.5 min
Curve-fit Model	500	10 h	1 s	3.6 min

The second simulation was carried out on both models with each tank equipped with the frequency controller. 500 tanks were simulated and each tank had a power consumption of 40 kW. A frequency profile shown in Fig. 4.12 was injected into the two models. In order to compare the two models, the initial states of the two models were set to be consistent. Simulation results are shown in Fig. 4.13.

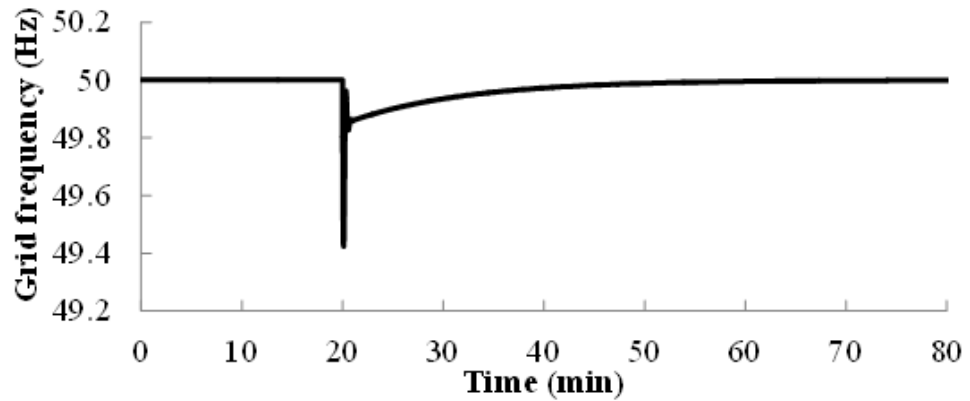
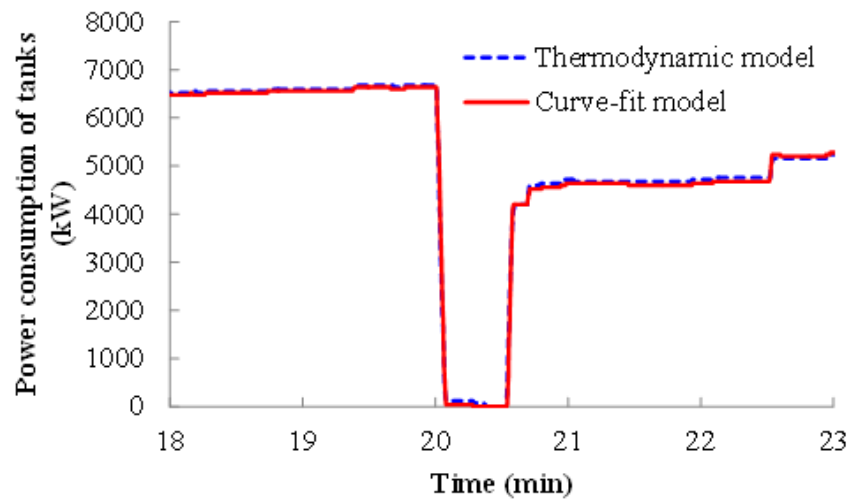
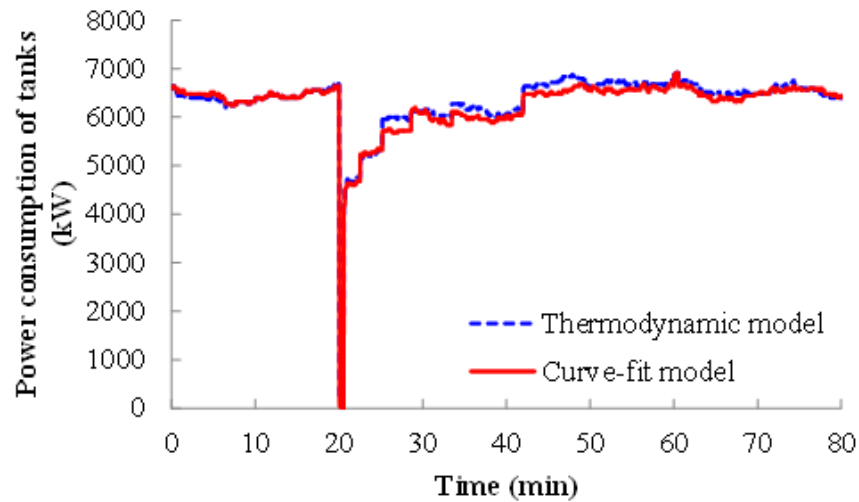


Fig. 4.12. Injected grid frequency profile



(a) Power consumption of tanks at the drop of frequency



(b) Power consumption of tanks 1 hour after the drop of frequency

Fig. 4.13. Power consumption of tanks

It can be seen that the power consumption of tanks in the thermodynamic model was similar to that of the tanks in the curve-fit model. Tanks in both models were switched OFF when frequency dropped and were reconnected following the frequency recovery.

The simplified curve-fit model of tanks is able to reflect the thermodynamics of a tank accurately. The modelling method avoids the acquisition of physical parameters such as the heat coefficient, thermal mass and size of tanks. The only information required is the ON/OFF period of the tanks which is easily obtained through field measurements. The method can be applied to the modelling of other load types for which thermodynamic models are otherwise essential [96]. Therefore, the curve-fit model was used for the following studies in this thesis.

4.4 Field tests on bitumen tanks

Two groups of field tests were carried out on bitumen tanks by Open Energi. Fig. 4.14 describes the setting of the field tests. Grid frequency is measured and sent to the device ('Jace630') of Open Energi Panel. The frequency is then sent to the controller of each tank ('Mitsubishi QX PLC' in Fig. 4.14). The power consumption of the tank is measured and sent back to Open Energi Panel for monitoring.

For field tests, the Open Energi Panel is able to switch off the sending of grid frequency measurement and inject frequency profiles to the controller of each tank instead.

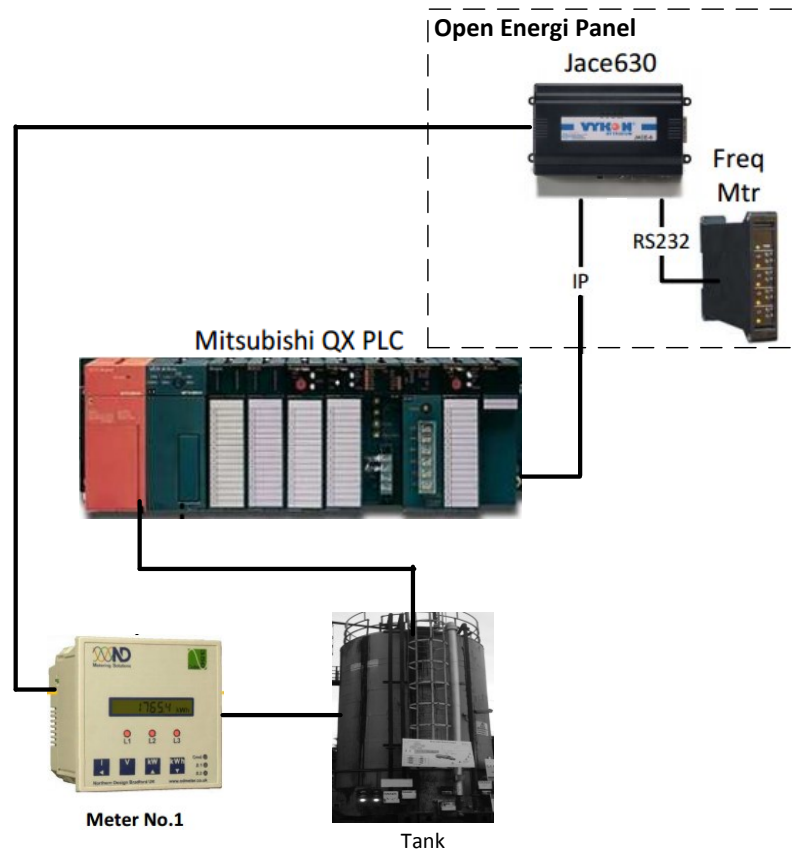


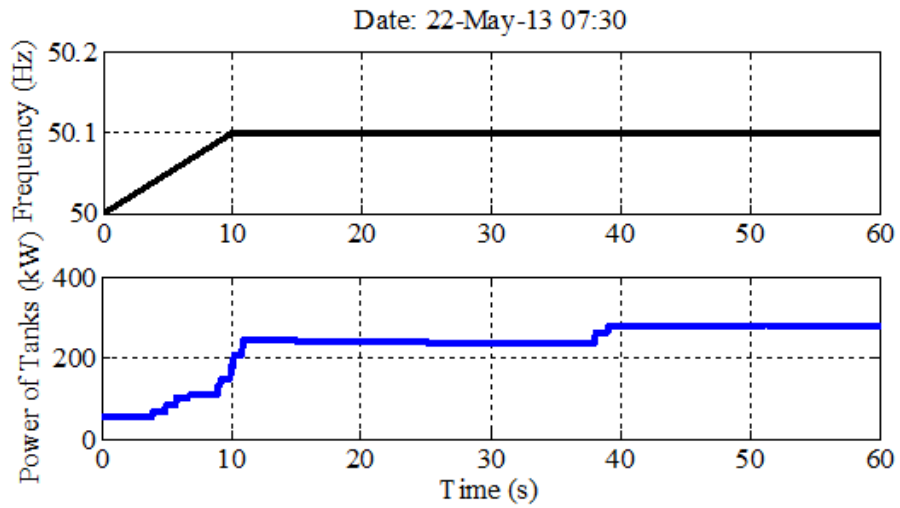
Fig. 4.14. Setting of field tests by Open Energi

4.4.1 Injection of frequency deviations

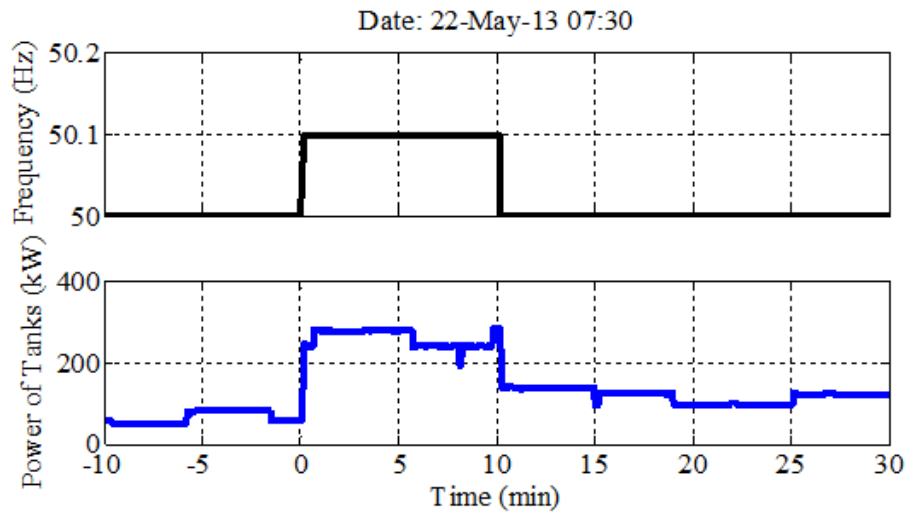
A series of field tests were undertaken at different times of day on 22 May 2013. The tests were carried out on 42 tanks with power ratings from 17 to 75 kW. Each tank was equipped with a frequency controller. The grid frequency input to these frequency controllers was replaced by an external frequency signal as described in Table 4.7. Power consumption of the 42 tanks was measured during the frequency injections and then aggregated to obtain the power consumption of a population of 42 tanks. Results of the tests are shown in Figs. 4.15-4.17.

TABLE 4.7. Description of Injected Frequency Profiles during the Field Tests.

Frequency Profile	Description
1	Ramp to 50.1 Hz in 10 s and stay at 50.1 Hz for 10 min
2	Ramp to 50.2 Hz in 10 s and stay at 50.2 Hz for 30 min
3	Ramp to 50.5 Hz in 10 s and stay at 50.5 Hz for 30 min

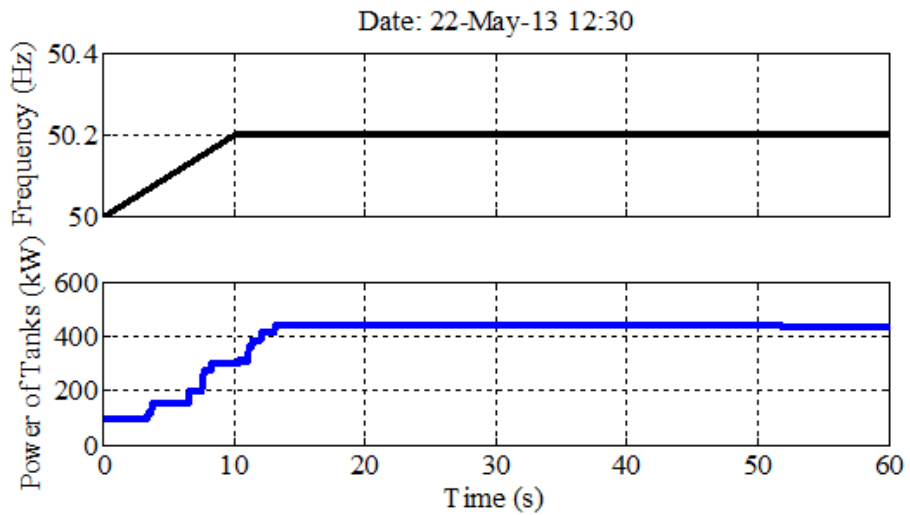


(a) Power consumption of tanks at the rise of frequency to 50.1 Hz

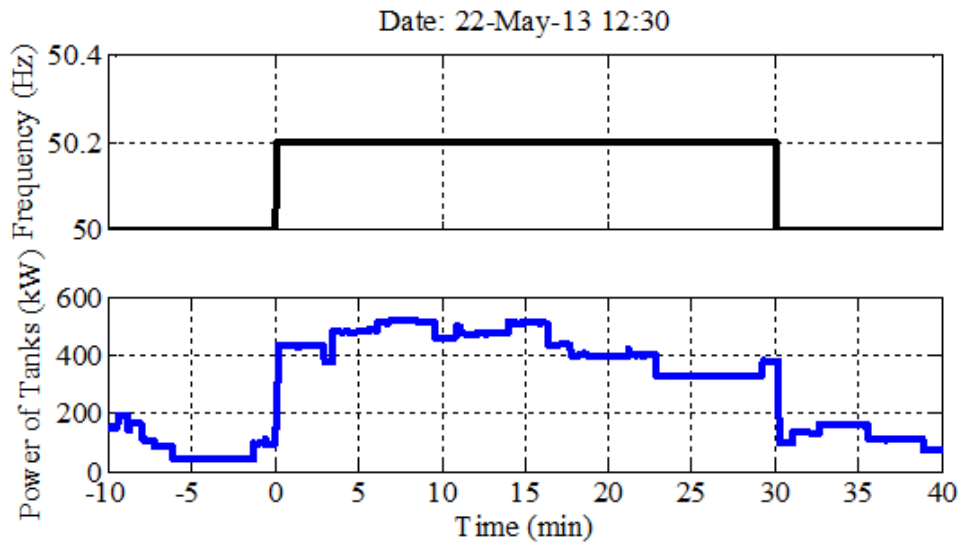


(b) Power consumption of tanks with frequency at 50.1 Hz for 10 min

Fig. 4.15. Field tests with the injection of Frequency Profile 1 in Table 4.6

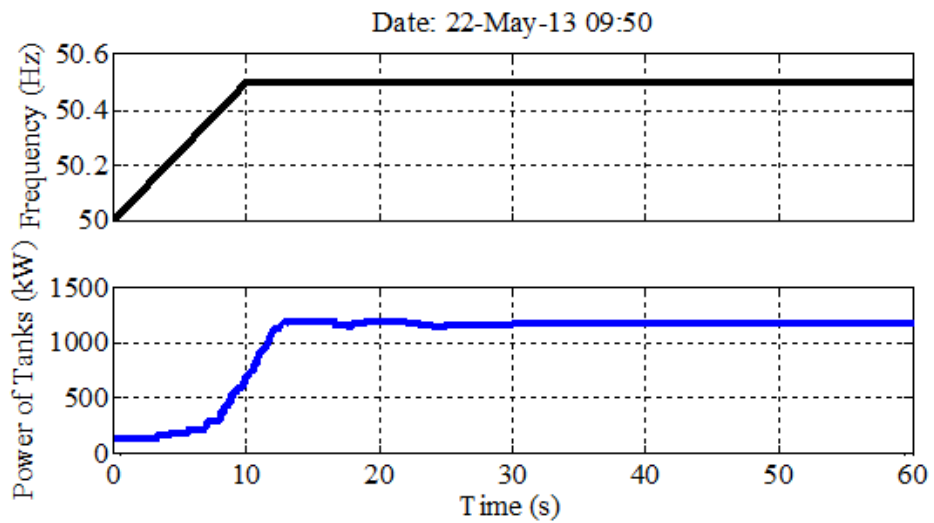


(a) Power consumption of tanks at the rise of frequency to 50.2 Hz

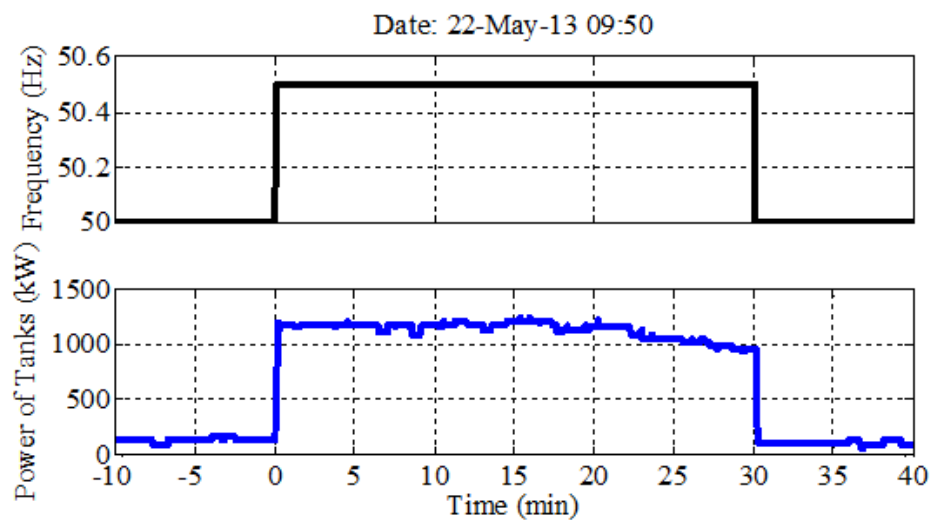


(b) Power consumption of tanks with frequency at 50.2 Hz for 30 min

Fig. 4.16. Field tests with the injection of Frequency Profile 2 in Table 4.6



(a) Power consumption of tanks at the rise of frequency to 50.5 Hz



(b) Power consumption of tanks with frequency at 50.5 Hz for 30 min

Fig. 4.17. Field tests with the injection of Frequency Profile 3 in Table 4.6

As can be seen, following the ramp up of frequency, the power consumption of tanks increased. When frequency was kept at a higher value, the power consumption of tanks also stayed at a higher level. Tanks were able to sustain a frequency response for at least 30 min.

Comparing the power consumption of tanks in Figs. 4.15-4.17, the greater the frequency rises, the higher their power consumption will be. Therefore, tanks were able to provide a level of frequency response which was in proportion to the deviations of frequency.

4.4.2 Field tests on tanks during large frequency disturbances

A series of field tests were carried out by Open Energi in July 2013 on 76 tanks with power ratings from 17 to 75 kW. Two frequency profiles were injected to the frequency controller of all the tanks simultaneously. One profile included a frequency rise to 50.5 Hz and the other included a frequency drop to 49.2 Hz. The profiles were applied 15 times at different time of day. Power consumption of the 76 tanks was measured during the 15 frequency injections. The power consumption of all 76 tanks obtained from the 15 frequency injections was aggregated to obtain the power consumption of an equivalent tank population of 1,140 tanks (76×15). The results are shown in Fig. 4.18 and Fig. 4.19 for the frequency increase and in Fig. 4.20 and Fig. 4.21 for the frequency drop.

The curve-fit tank model presented in section 4.3 was used to simulate the field tests. The two frequency profiles were applied to an aggregation of 1,140 tank models. The aggregated power consumption of modelled tanks was compared to that of the field tests as shown in Figs. 4.18-4.21.

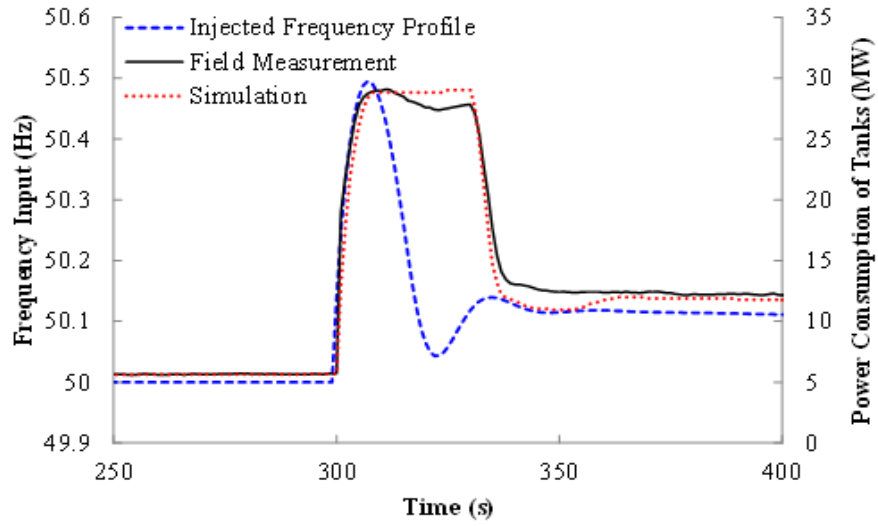


Fig. 4.18. Response of the 1,140 tanks to the frequency rise

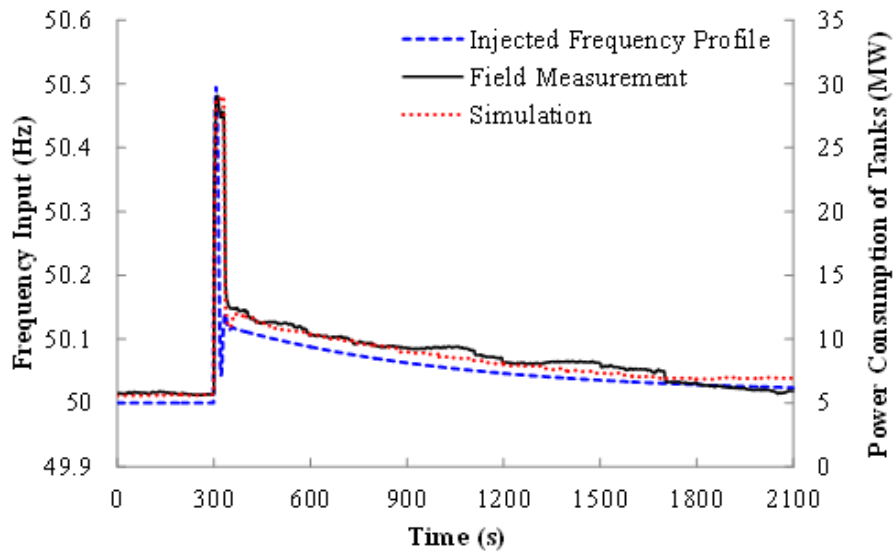


Fig. 4.19. Response of the 1,140 tanks 30 minutes after the frequency rise

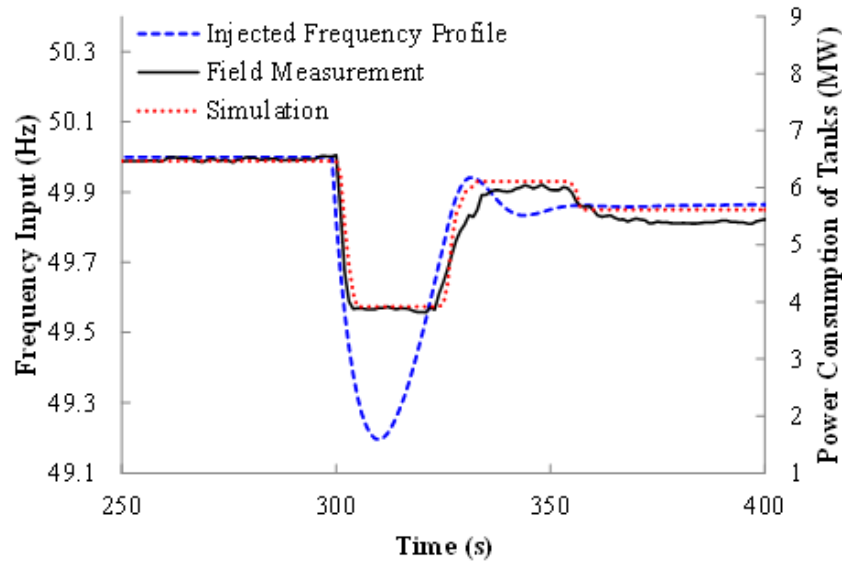


Fig. 4.20. Response of the 1,140 tanks to the frequency drop

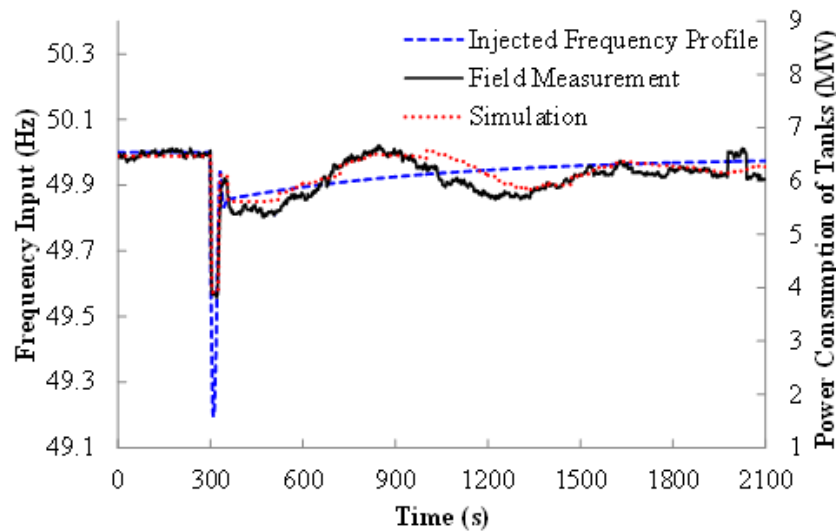


Fig. 4.21. Response of the 1,140 tanks 30 minutes after the frequency drop

As shown in Figs. 4.18-4.21, the results obtained from the field tests and simulation show similar power consumption of tanks upon frequency disturbances. The slight differences in power consumption were caused by different initial states of the tested and modelled tanks and also the randomisation of F_{ON} and F_{OFF} in their frequency controller.

Fig. 4.18 shows that, when frequency rose, some tanks in OFF state were switched ON. After the frequency rise, the tanks reverted back to their previous OFF state following frequency recovery, as shown by Fig. 4.19.

Fig. 4.20 shows that, when frequency dropped, some tanks in ON state were switched OFF. After the frequency drop, the tanks reverted back to their previous ON state following frequency recovery, as shown in Fig. 4.21.

In both cases, the delay in tanks being switched in response to frequency deviations was measured in the field tests as 0.7 s. This is much faster than the governor response of generators (fully delivered in 5-10 s).

When frequency was below 50 Hz, the power consumption of tanks was lower than its pre-event level at all times. At around 800 s in Fig. 4.21, power consumption of tanks returned to the pre-event level. This was because most low frequency tests were undertaken in the early morning (2 am). At this time of day, many tanks were close to the minimum temperature limit and were ready to be switched ON to take advantage of the lower electricity price overnight (e.g. British Summer Time 1:30 am – 8:30 am). Hence, after the drop in frequency, these tanks were switched ON while the price of electricity was low.

4.5 Case studies on the GB power system

Case studies were carried out in order to assess a number of scenarios where bitumen tanks are connected to the GB power system. The tank model used was that presented in Section 4.3.3. An aggregated model of 5,000 tanks was connected to the GB power system model as illustrated in Section 3.4. The power rating of each tank was 40 kW. The integrated model is shown in Fig. 4.22.

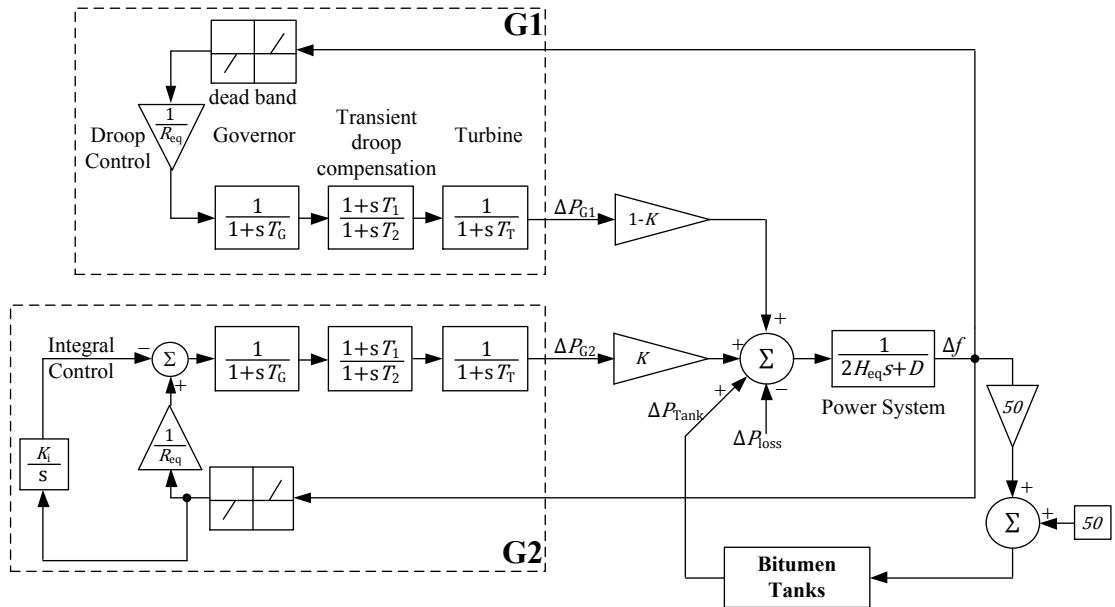


Fig. 4.22. Simplified GB power system model with the connection of 5,000 bitumen tank models

4.5.1 Simulation of sudden loss in generation

A case study was carried out for a low system demand of 20 GW on a summer night. A generation loss of 1,320 MW ($\Delta P_{loss} = 0.066$ pu in Fig. 4.22) was applied to the model in Fig. 4.22 at 90 s.

Two sets of simulation results, one with tank response and one without tank response, are compared in Figs. 4.23-4.25. In these figures f represents the grid frequency, Pt is the power consumption of tanks, ΔPt is the change in power consumption of tanks, i.e. the tanks' response, and ΔPg represents the total power change of generators.

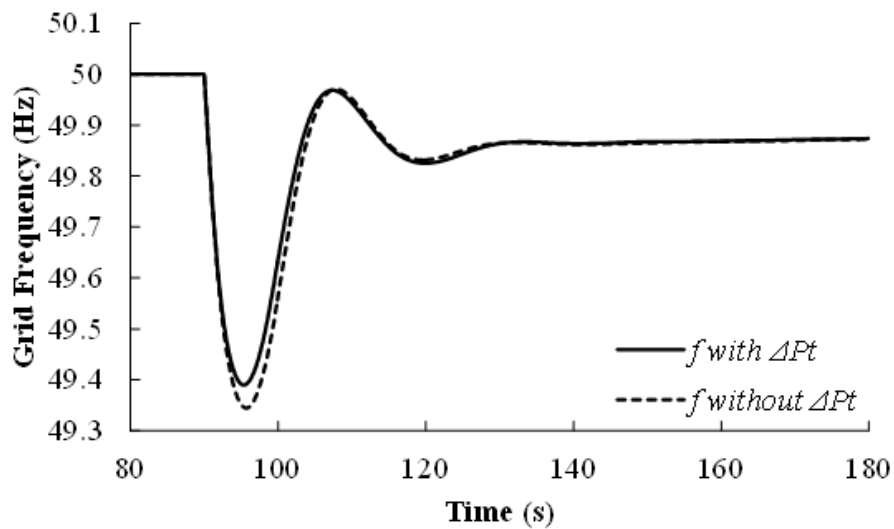


Fig. 4.23. Variations of grid frequency

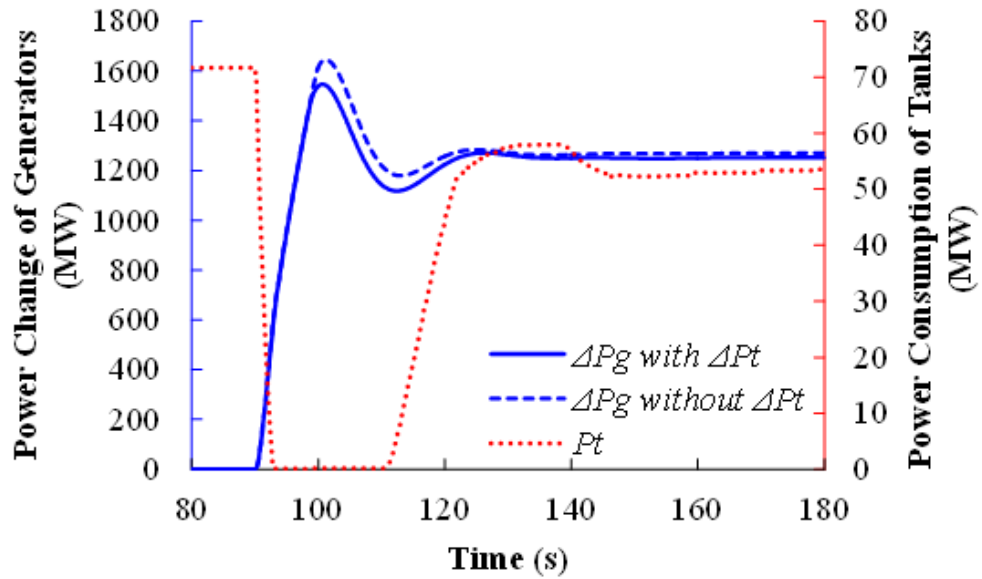


Fig. 4.24. Change of power output of generators and power consumption of tanks

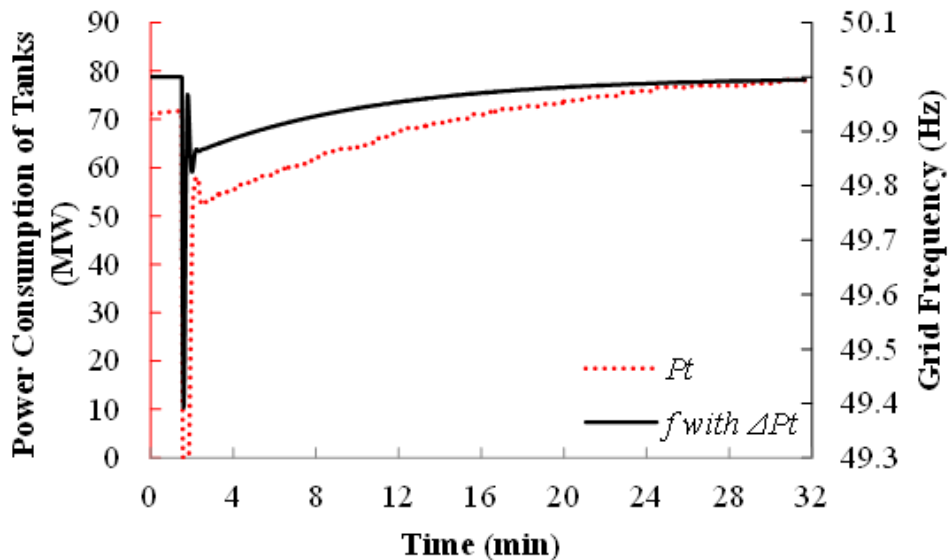


Fig. 4.25. Power consumption of tanks 30 minutes after the frequency drop

Fig. 4.23 shows the frequency after the loss of generation. Fig. 4.24 shows the change of power of generators (see the left axis) and the power consumption of tanks (see the right axis). The power consumption of tanks reduced almost immediately following the drop of frequency at 90 s. With the 72 MW of load change from 5,000 tanks, the maximum drop in frequency reduced by 0.05 Hz (from 49.34 to 49.39 Hz). The change of generator output was also reduced.

When frequency started to recover, tanks that had been disconnected were not reconnected immediately. These tanks remained OFF for at least the minimum OFF-time of 25 s before they were reconnected. Fig. 4.25 shows the increase of the power

consumption of tanks (see the left axis) following the recovery of frequency (see the right axis).

Using bitumen tanks to respond to frequency drops causes a shift of their ON/OFF cycles because tanks are switched OFF earlier than they otherwise would be. This leads to unconventional variations of their heating process. However, if the tank temperature T stays within the range set by the tank operator, then the shift of ON/OFF cycle will have little adverse impact for the user.

The original ON/OFF state and T of two tanks (Tank 1 and Tank 2) (without a loss of generation applied) are shown in Figs. 4.26-4.29. The original ON/OFF states and T were compared with those of the same tanks when a loss of generation was applied in simulation. The comparison of ON/OFF cycles is shown in Fig. 4.26 and Fig. 4.28. The comparison of T is shown in Fig. 4.27 and Fig. 4.29.

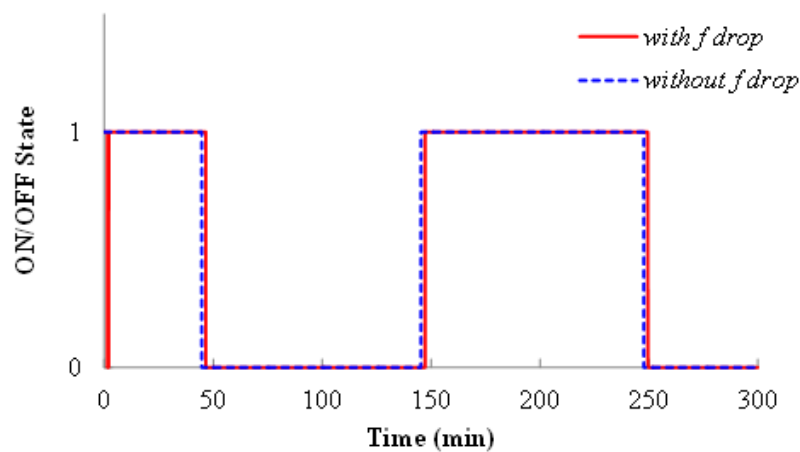


Fig. 4.26. ON/OFF state of Tank 1

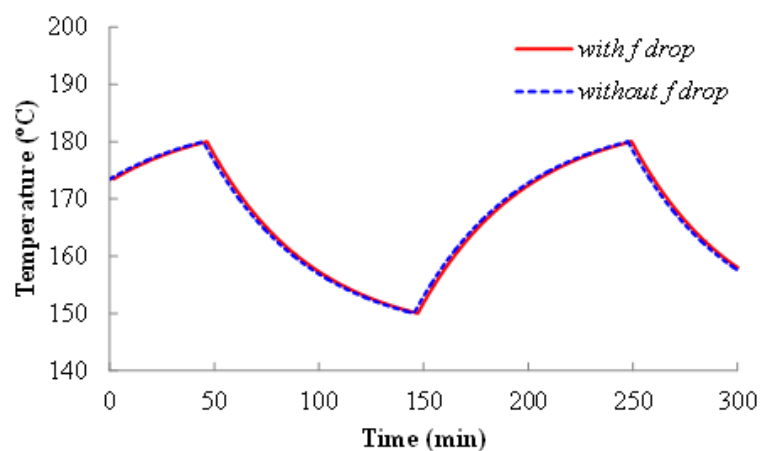


Fig. 4.27. Variations of temperature of Tank 1

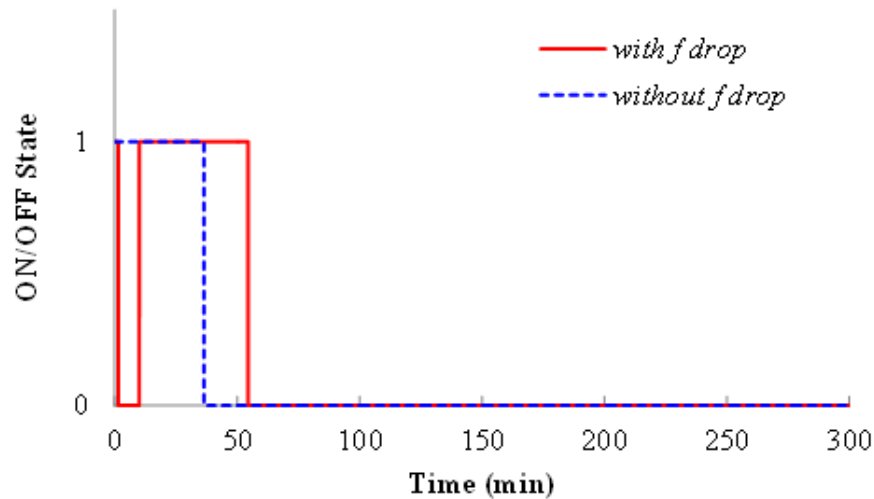


Fig. 4.28. ON/OFF state of Tank 2

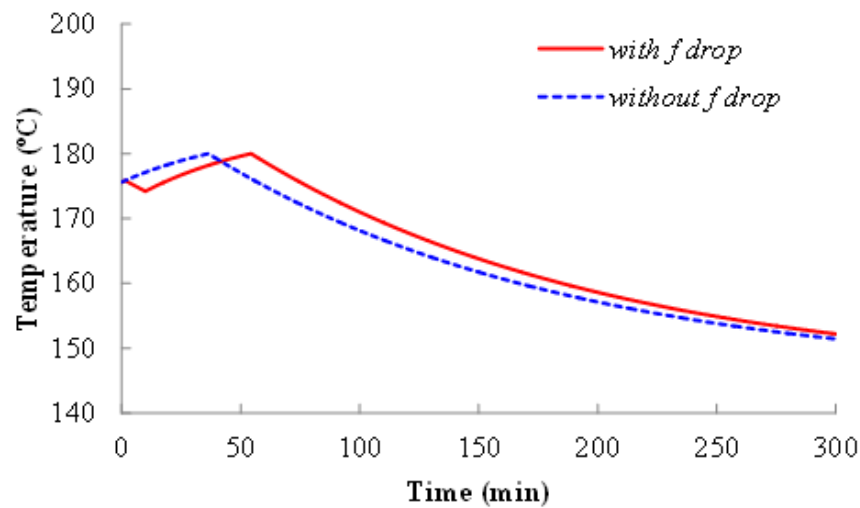


Fig. 4.29. Variations of temperature of Tank 2

Fig. 4.26 and Fig. 4.27 show the ON/OFF state and temperature of Tank 1. With the drop of frequency, at 1.51 min, Tank 1 was switched OFF earlier than that it would have been in its standard cycle. With the recovery of frequency, Tank 1 reverted quickly back to ON state at 2.1 min. The shift of the ON/OFF cycle caused by the simulated frequency drop was slight. Therefore, the temperature of Tank 1 stayed within its pre-set range.

Fig. 4.28 and Fig. 4.29 show the ON/OFF state and temperature of Tank 2. It can be seen Tank 2 was switched OFF at 1.53 min and did not revert back to ON until 10 min. The temperature of Tank 2 also stayed within its range. The ON/OFF cycle was shifted as it was switched OFF earlier. However, such a shift of ON/OFF cycle may also occur during the normal operation of tanks, e.g. when adding bitumen to the tanks.

By comparing the normal operation of the two tanks ('without f drop') with those in a case of frequency drop ('with f drop') in Fig. 4.26 and Fig. 4.28, it is also shown that, following the recovery of frequency, tanks were reverted back to ON state gradually rather than simultaneously.

4.5.2 Simulation of sudden loss in demand

A case study was carried out by applying a sudden demand loss of 1,000 MW ($\Delta P_{\text{loss}} = -0.05$ pu) to the model in Fig. 4.22 at 90 s. A low system demand of 20 GW for a summer night was used. Simulation results are shown in Figs. 4.30-4.32.

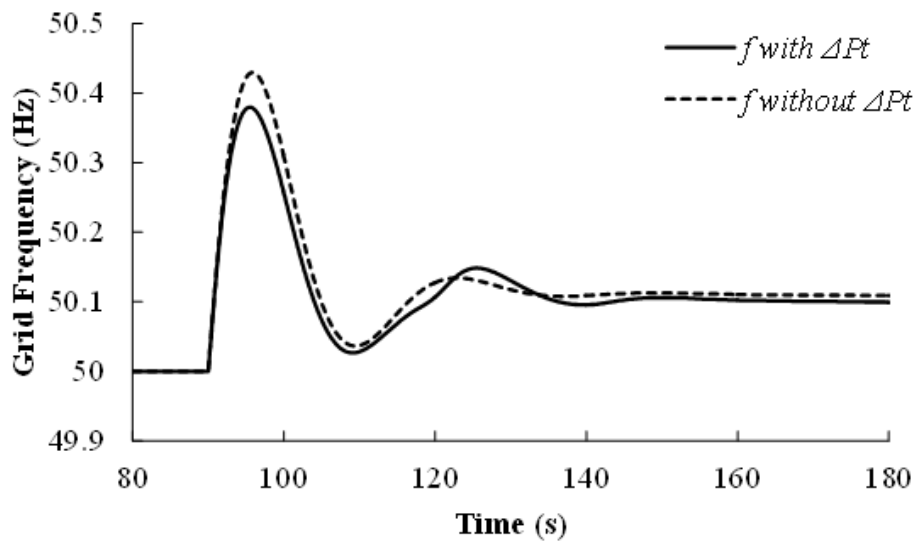


Fig. 4.30. Variations of grid frequency

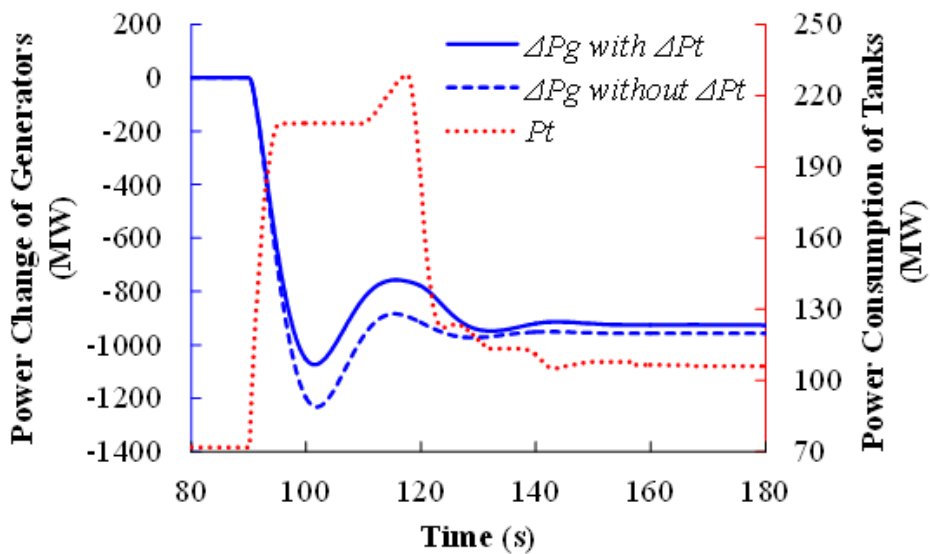


Fig. 4.31. Change of power output of generators and power consumption of tanks

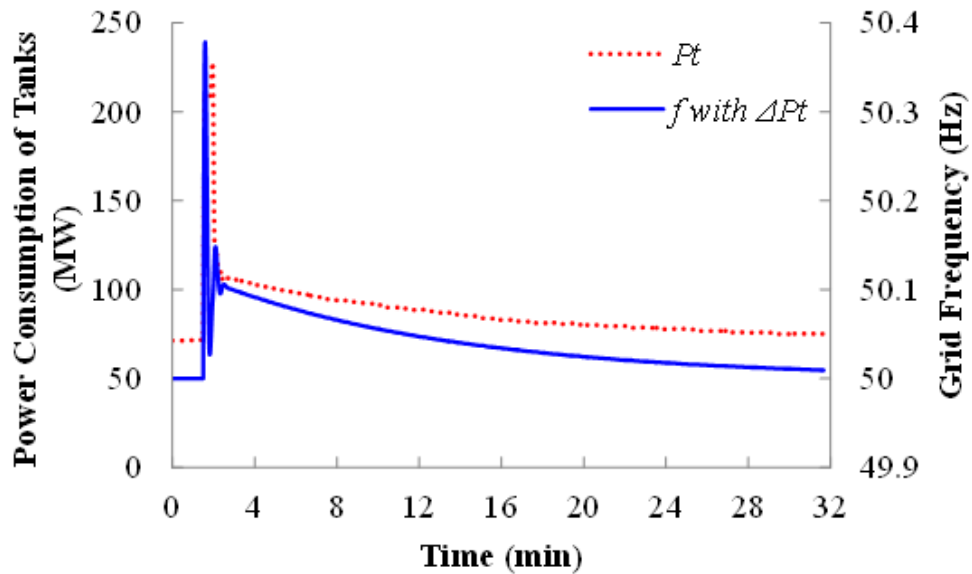


Fig. 4.32. Power consumption of tanks 30 minutes after the frequency drop

Fig. 4.30 shows the rise of frequency after the sudden loss in demand. Fig. 4.31 shows the change of power output of generators (see the left axis) and the power consumption of tanks (see the right axis). The power consumption of tanks increased almost immediately following the frequency increase. The total increase in the power consumption of 5,000 tanks was 138 MW when frequency increased to 50.39 Hz. Without the load increase, frequency reached a maximum value of 50.42 Hz. Frequency deviations were reduced with the load change of tanks. Variations of the power output of frequency-sensitive generators also reduced.

When frequency started to recover, tanks that had been switched ON did not revert back to OFF state immediately. These tanks remained ON for at least the minimum ON-time of 25 s.

As shown in Fig. 4.31, there was an increase in the power consumption of tanks at 110 s. When generators provide response to sudden variations of frequency, there may be an overshoot of power output before the steady state is reached. Such overshoots lead to fluctuations in grid frequency. Therefore, tanks increased their loads at 110 s so as to follow the increase in frequency at 110 s.

Fig. 4.32 shows the power consumption of tanks (see the left axis) during the recovery of grid frequency (see the right axis). Power consumption of tanks reduced gradually following the frequency recovery.

The influence of frequency rise on the primary functions of tanks is shown in Figs. 4.33-4.34. The original ON/OFF state and T of a tank (Tank 3) (without a loss of demand applied) were compared with those of the same tank when a loss of demand was applied in simulation. The comparison of ON/OFF cycle is shown in Fig. 4.33 and the comparison of T is shown in Fig. 4.34.

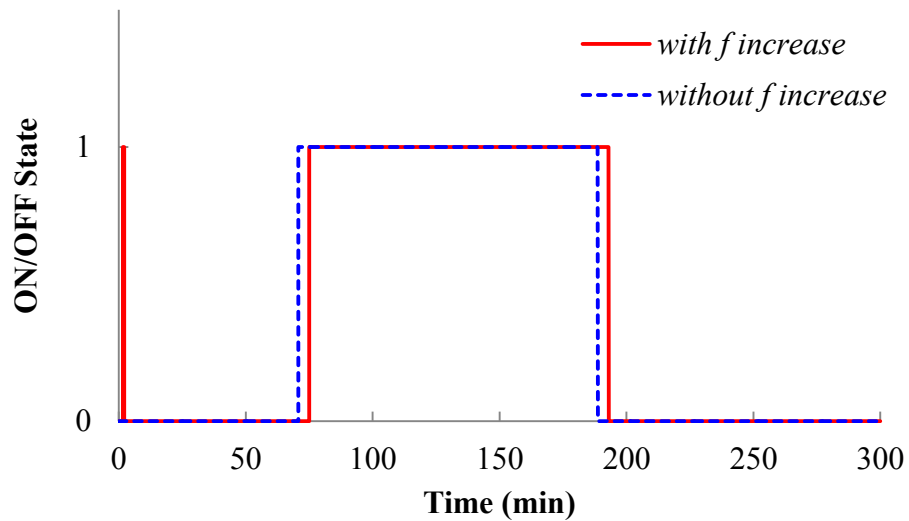


Fig. 4.33. ON/OFF state of Tank 3

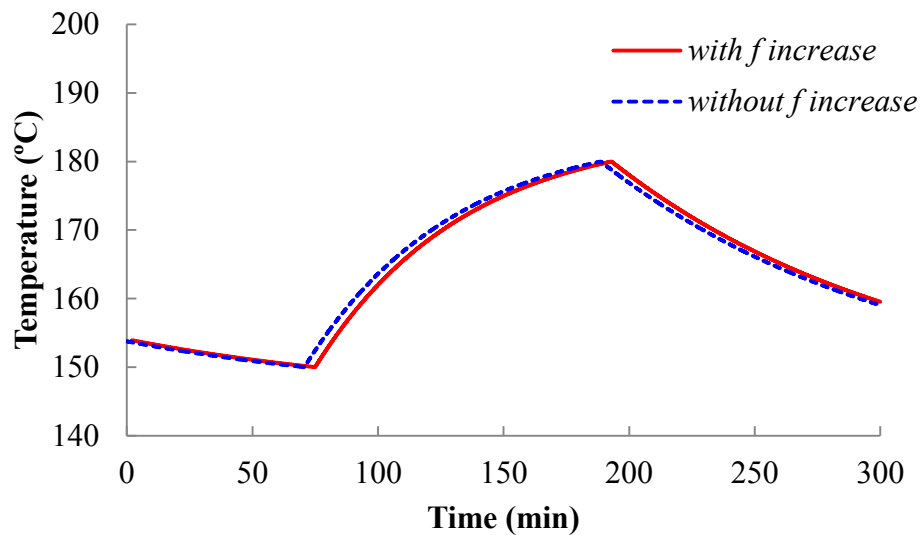


Fig. 4.34. Variations of temperature of Tank 3

As can be seen, tank 3 was switched ON at the time of the frequency rise (1.53 min) and reverted back OFF at 2 min (120 s). The shift of its ON/OFF cycle was barely perceptible, as shown in Fig. 4.33. The tank temperature stayed within its pre-set range.

4.5.3 Simulation of consecutive loss of two generators

A case study was undertaken for a multiple loss of generators. The case was based on the severe frequency incident of 28 May 2008 as presented in Case 3.3 of Section 3.5.3.

The GB power system model was similar to that used in Case 3.3 of Section 3.5. 5,000 tank models (as illustrated in Section 4.3.3), each with a power rating of 40 kW, were connected to the GB power system model. The loss of the first generator of 345 MW at 90 s and the loss of the second generator of 1,237 MW at 185 s were applied to the model. Simulation results, one with tank response and one without tank response are compared in Figs. 4.35 and 4.36. Fig. 4.37 gives the power consumption of tanks following the frequency recovery.

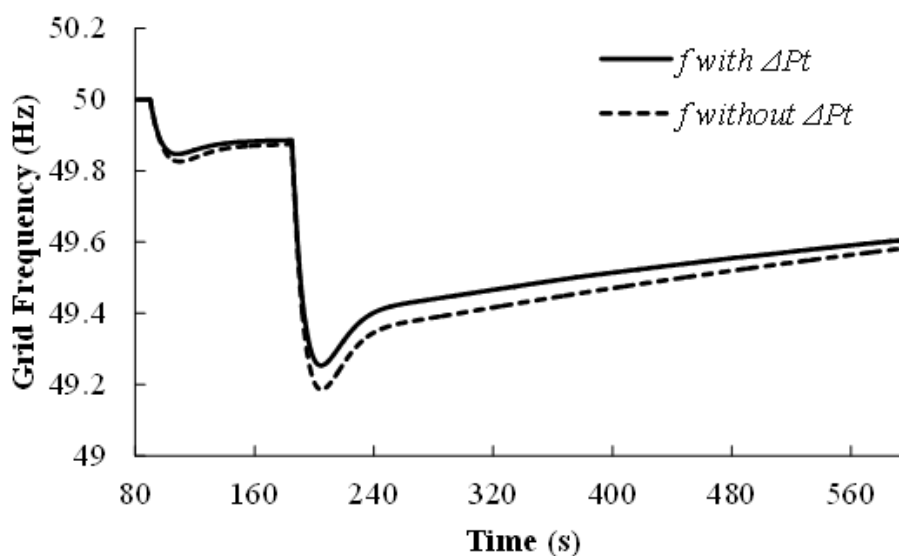


Fig. 4.35. Variations of grid frequency

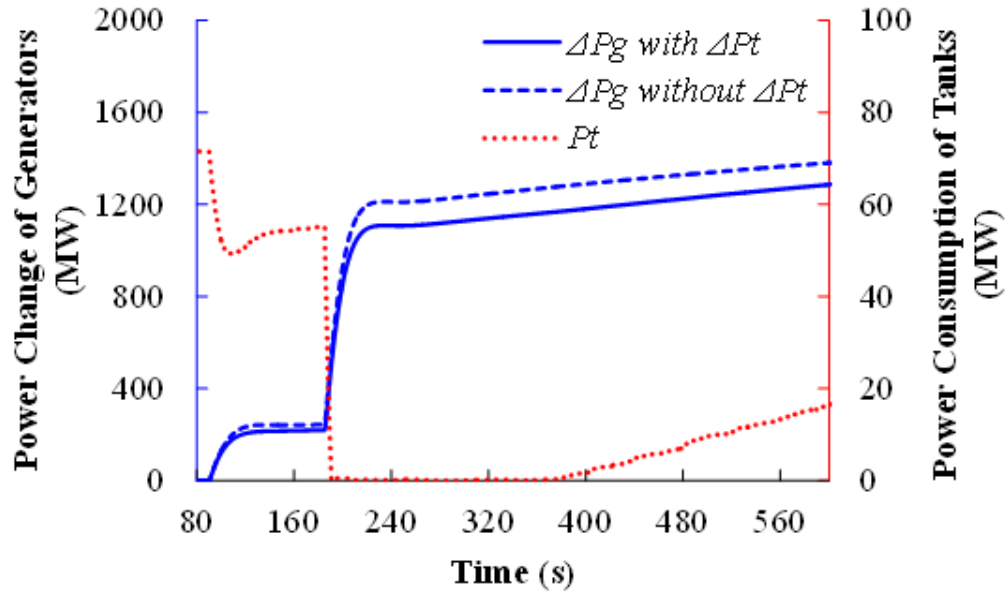


Fig. 4.36. Change of power output of generators and power consumption of tanks

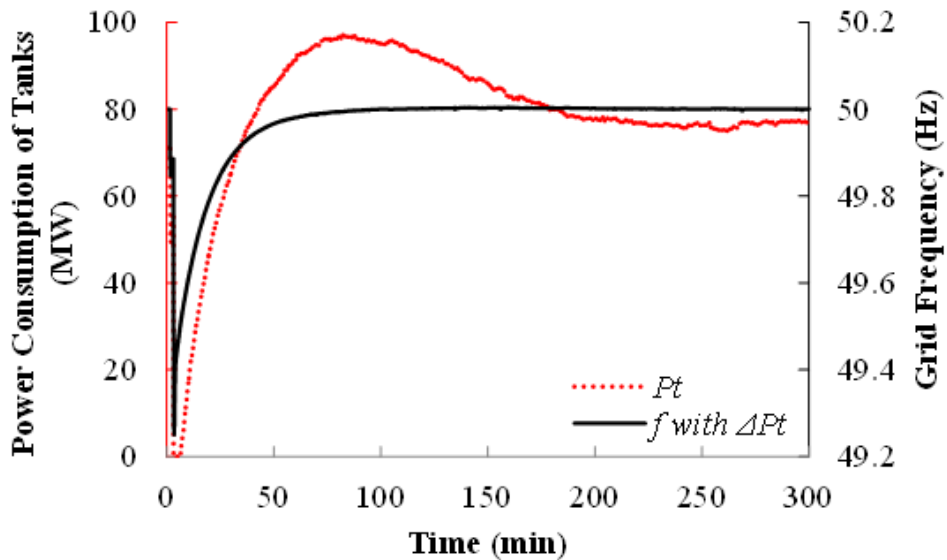


Fig. 4.37. Power consumption of tanks after the drop of frequency

Fig. 4.35 shows the variations of grid frequency. Fig. 4.36 shows the change of power output of generators (see the left axis) and the power consumption of tanks (see the right axis). After the loss of the 314 MW generator, power consumption of tanks reduced by 20 MW. Following the loss of 1,237 MW generator, power consumption of tanks reduced by a further 60 MW. The frequency dropped to 49.23 Hz. Without response of tanks, the frequency dropped to 49.19 Hz. The change of power output of frequency-sensitive generators also decreased.

As frequency started to recover, tanks were not reconnected until frequency returned to above 49.5 Hz at 380 s. This was because the trigger frequency F_{OFF} of tanks, as illustrated in Section 4.2, was set in the range of 49.5-50 Hz. Therefore, when frequency returned to above 49.5 Hz, tanks started to be reconnected in sequence.

Fig. 4.37 shows the power consumption of tanks (see the left axis) and the grid frequency (see the right axis). The lost thermal energy of tanks caused by the periods of sustained low frequency (90 s-30 min) was restored gradually after the incident (30-200 min).

4.6 Conclusions

A decentralised frequency controller allows bitumen tanks to change their power consumption in proportion to deviations of grid frequency. Each tank has an equal possibility of responding to frequency deviations. The frequency control does not interfere with the primary function of a tank for the storage of hot bitumen.

Field tests were undertaken on a population of bitumen tanks in order to validate the frequency control of tanks. Different deviations of grid frequency were injected to the frequency controller of tanks and the deviations in frequency were sustained for 30 minutes. Test results showed that tanks were able to sustain a frequency response for at least 30 minutes. The higher the deviations of frequency, the higher number of tanks responds.

A simplified thermodynamic model of a tank was developed and validated through field measurements. A simplified curve-fit model of a tank was also developed based on the field measurements. The performance of the two models was compared. The curve-fit model was then used for simulations because it has faster computational speed than the other. An aggregated model of tanks equipped with frequency control was developed and verified against the field tests. The tank model behaved similarly to the tanks in the field tests.

The aggregated model of tanks was then integrated into the simplified GB power system model. Case studies showed that deviations of grid frequency were reduced with the immediate load change of tanks. The power change of frequency-sensitive generators also decreased.

The load change of 72 MW from 5,000 tanks was small in the context of the GB power system. However, if such frequency control is applied to other types of loads, their contribution to reducing frequency deviations will be considerable. This type of frequency control of loads will provide an effective alternative to the frequency response service currently provided mainly by frequency-sensitive generators.

Chapter 5

Demand Aggregation for Frequency Response Service

The differences in the frequency controller of refrigerators and of bitumen tanks are discussed. The availability of the two types of loads to provide frequency control without undermining their primary functions was analysed. Field investigations were then carried out by Open Energi to measure the availability of refrigerators and of bitumen tanks at different time of day. Using the measured availability, the number of refrigerators and bitumen tanks to be aggregated in order to provide a certain amount of frequency response service to the system operator was calculated. The availability of refrigerators and of bitumen tanks for grid frequency control was then modelled. Variations of the availability during and after frequency incidents were simulated. Results showed that the aggregated loads were available to provide frequency control dynamically and hence to participate in the Firm Frequency Response service of the GB power system.

5.1 Introduction

Previous chapters have verified that domestic refrigerators and industrial bitumen tanks are able to provide frequency control in the power system. However, the frequency response from each load is invisible to the system operator. The power consumption of each unit is usually quite small and hence the frequency response from each unit. To allow the frequency response from loads to be visible and adopted by the system operator, loads need to be aggregated in order to provide certain amount of frequency response.

The number of domestic refrigerators and industrial bitumen tanks to be aggregated for the provision of a certain amount of frequency response was evaluated. These frequency-responsive loads will then be able to participate in the frequency response service of the GB power system.

5.2 Comparison of frequency controller of refrigerators and of bitumen tanks

In order to clarify the capability of refrigerators and bitumen tanks to provide grid frequency control, the frequency controller for refrigerators in Chapter 3 and for bitumen tanks in Chapter 4 were compared before aggregation.

The difference in the following two inherent characteristics of refrigerators and of bitumen tanks led to the different design of their frequency controllers.

Firstly, bitumen tanks have much longer ON/OFF cycles than those of refrigerators. This is depicted in Fig. 5.1. Depending on the stored contents, size and insulating materials, the typical ON/OFF cycle of a refrigerator is 15 min/ 45 min [73] while the ON/OFF cycle of a bitumen tank can be quite long. Based on the measurements of ON/OFF cycle carried out by Open Energi, depending on the user, the ON cycle of bitumen tanks can be within 30 min to 3 h and the OFF cycle can be 1 h to 9 h.

Secondly, the temperature difference between set-points (T_{high} and T_{low}) of a tank (typically within 30 °C) is much higher than that of a refrigerator (typically 1-2 °C) as shown in Fig. 5.1. The variation of internal temperature (T) of a bitumen tank has a wider range than the variation of cavity temperature (T_{Ca}) of a refrigerator.

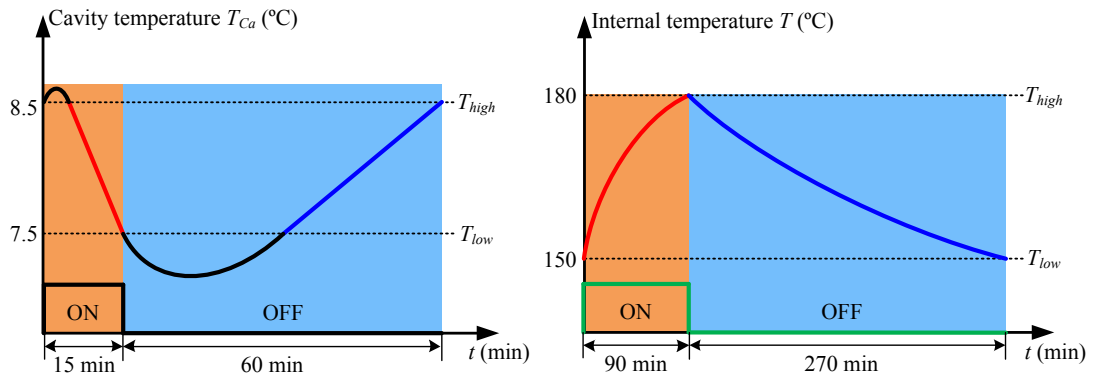


Fig. 5.1. ON/OFF cycle and temperature of a refrigerator and a bitumen tank

5.2.1 Response to a frequency incident

The required timescale of frequency response in the GB power system is within 10 s and can be as long as 30 min. Hence, a load will be switched OFF for a drop in frequency and may have to remain OFF for 30 min. For refrigerators, the 30-min interruption will cause T_{Ca} of a number of refrigerators to reach their T_{high} . These refrigerators have to be reconnected and other refrigerators then have to be switched OFF for further frequency response. For bitumen tanks, which have a much longer OFF cycle, the 30-min interruption is not expected to cause large variations in tank temperature T . A tank is usually capable of sustaining a 30-min interruption.

Therefore for refrigerators, the cavity temperature T_{Ca} is used to determine which refrigerator is switched ON/OFF first in response to frequency deviations. As illustrated in Section 3.3, following a drop in frequency, refrigerators are switched OFF starting from the one that has the lowest T_{Ca} . Following a rise in frequency, refrigerators are switched ON starting from the one that has the highest T_{Ca} . Hence, the number of refrigerators to be switched ON/OFF in response to frequency deviations is reduced.

For bitumen tanks, the internal temperature T is not considered to determine the order of switching the tanks. As presented in Section 4.2, following frequency deviations, tanks are triggered sequentially from the one having a trigger frequency closest to 50 Hz.

5.2.2 Recovery from a frequency incident

After a frequency drop incident, following the recovery of frequency, T_{Ca} of some refrigerators may have reached their T_{high} and reconnected. If frequency recovers fast, refrigerators will be triggered ON starting from the one with the highest T_{Ca} (early switching action illustrated in Section 3.3). This allows refrigerators to complement

their lost thermal energy for frequency response. Also, the recovery of power consumption of refrigerators following the recovery of frequency ensures the linear relationship between the frequency deviations and load change. Similar rules apply to the recovery of power consumption of refrigerators from a frequency rise incident.

As the ON/OFF cycle of tanks is much longer, following the frequency recovery from a frequency drop incident, temperature of most tanks is not expected to reach their temperature set-point and reconnect. If frequency recovers, tanks need to be switched ON to ensure the linear relationship between the frequency deviations and load change. Therefore, as presented in Section 4.2, the tank which switched OFF first is controlled to revert back ON first. This also maintains equal opportunities for each tank to be switched. The interruption of power supply of each tank is minimised. Similar rules apply to the recovery of power consumption of tanks from a frequency rise incident.

Domestic refrigerators are a load type with a short ON/OFF cycle while industrial bitumen tanks are a load type with a long ON/OFF cycle. Using type-specific frequency controllers, both types of loads provide frequency response similar to that is provided by droop control of frequency-sensitive generators. Therefore, the higher the number of refrigerators and tanks that are aggregated, the larger the spinning reserve capacity of frequency-sensitive generators they can replace.

5.3 Demand availability at different time of day

At a given time, only a fraction of loads are in ON-state and consuming power, and therefore are available to be switched OFF for drops in frequency and vice versa for rises in frequency. The system operator needs to be notified of the availability of demand to provide frequency response as it varies with time. Then the system operator is able to estimate and despatch the amount of frequency response that demand can deliver.

Ref [16] used domestic appliances to provide frequency response. To maintain frequency within its steady-state limits, the amount of frequency response that is required from domestic appliances at different time of day was estimated. Ref. [95] used Electric Vehicles (EVs) to provide frequency response in the power system. The amount of frequency response from EVs showed a temporal distribution over a day.

5.3.1 Analysis of demand availability

Demand availability in this chapter is defined as the percentage of loads that is available for frequency response without compromising their primary functions. Demand availability was divided into low response availability (*LRA*) and high response availability (*HRA*). It was assumed that each refrigerator and bitumen tank in the UK is equipped with a frequency controller. *LRA* is the percentage of loads that is available to be switched OFF at a given time for drops in frequency. Similarly, *HRA* is the percentage of loads that is available to be switched ON for rises in frequency.

In order not to undermine the conventional control of loads, at any time, only loads with a temperature within their high and low set-points are available for frequency response. As discussed in Section 3.2, this avoids the temperature of a load exceeding its pre-defined limits.

There are also constraints associated with the ON/OFF state of loads. In the case of refrigerators, a minimum ON/OFF time limited by the pressure in the refrigeration cycle is required. Bitumen tanks have limits of minimum ON/OFF time and maximum number of switches per hour. These are required to avoid frequent switching actions which may damage the heater.

5.3.2 Field investigations on demand availability at different time of day

Availability of refrigerators and of bitumen tanks at different time of day was measured through field investigations carried out by Open Energi.

a) Field investigations on refrigerators

The major factor that influences the ON/OFF cycle of refrigerators is the ambient temperature. In summer, refrigerators consume more electrical energy to cool down the stored food than during the winter. The period of an ON cycle in summer is longer than it is in winter. More refrigerators are available to be switched OFF in summer. Therefore, *LRA* of refrigerators (LRA_r) in summer is higher than it is in winter while *HRA* of refrigerators (HRA_r) in summer is lower than it is in winter.

Field investigations to measure LRA_r and HRA_r of refrigerators were undertaken from October 2011 to March 2012. The investigations were carried out on 1,000 refrigerators

in UK homes including different types of fridge-freezers covering almost 80% of the UK market. The average LRA_r and HRA_r at each hour over a day is shown in Fig. 5.2. LRA_r and HRA_r were nearly constant over a day and were estimated to be an average of 15.8% and 52% on a winter day. Refrigerator doors are opened more frequently at the time people cook an evening meal which causes a slightly increased number of refrigerators to start cooling. Therefore, LRA_r was slightly higher between 17:00 and 21:00.

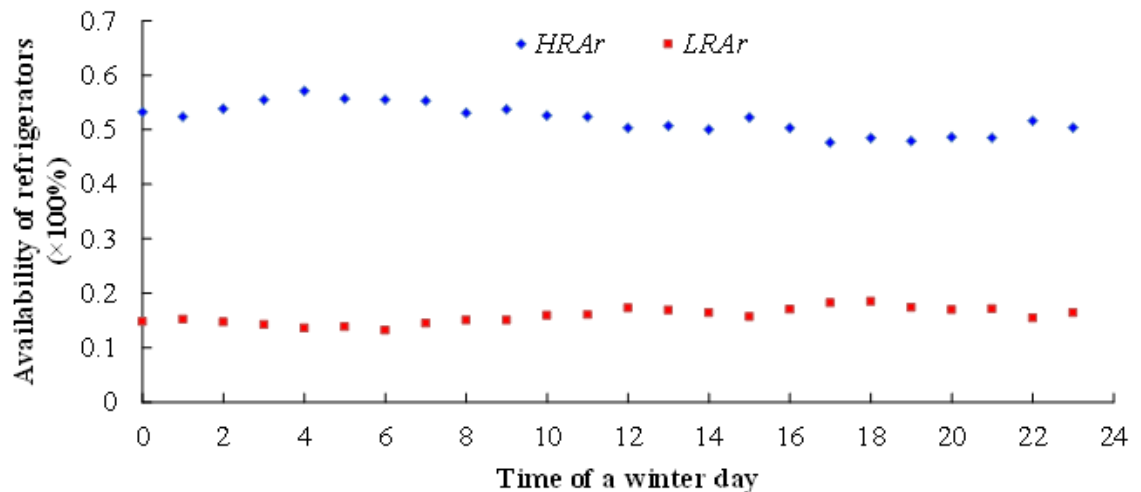


Fig. 5.2. HRA and LRA of refrigerators over a winter day

A seasonal effect on the ON/OFF cycle of refrigerators is noticeable. The seasonal effect on the energy consumption of cold appliances for a year was estimated by DECC [96]. The average consumption of a year was set to be 1. The average consumption of each week of the year was then used to calculate the seasonal factor as shown in Fig. 5.3. Seasonal factor for winter S_{winter} is 0.75 at week 1. Summer has a seasonal factor S_{summer} of 1.12 at week 29.

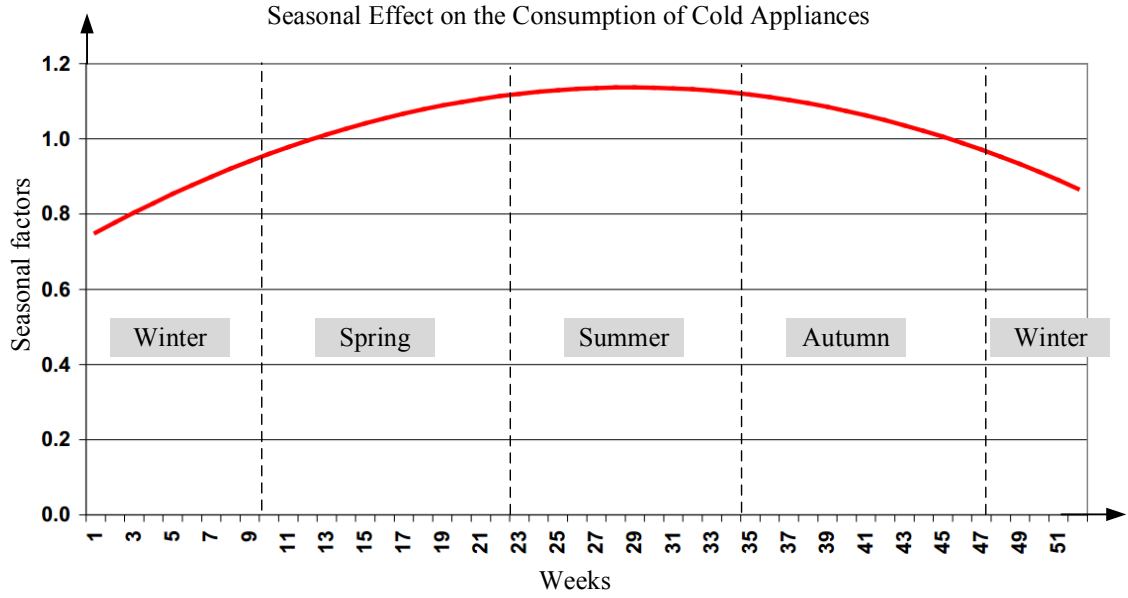


Fig. 5.3. Seasonal effect on the energy consumption of cold appliances obtained from DECC (modified figure based on [96])

Using LRA_r and HRA_r that were obtained from the field measurements in winter as shown in Fig. 5.2 (LRA_r^{winter} and HRA_r^{winter}) and the seasonal factors, LRA_r and HRA_r for a summer day (LRA_r^{summer} , HRA_r^{summer}) were calculated:

$$LRA_r^{summer} = LRA_r^{winter} \times \frac{S_{summer}}{S_{winter}} \tag{5.1}$$

$$HRA_r^{summer} = HRA_r^{winter} \times \frac{S_{winter}}{S_{summer}} \tag{5.2}$$

The estimated LRA_r and HRA_r for a summer day were obtained and are shown in Fig. 5.4. The averaged LRA_r was 23.6% and the averaged HRA_r was 34.8%.

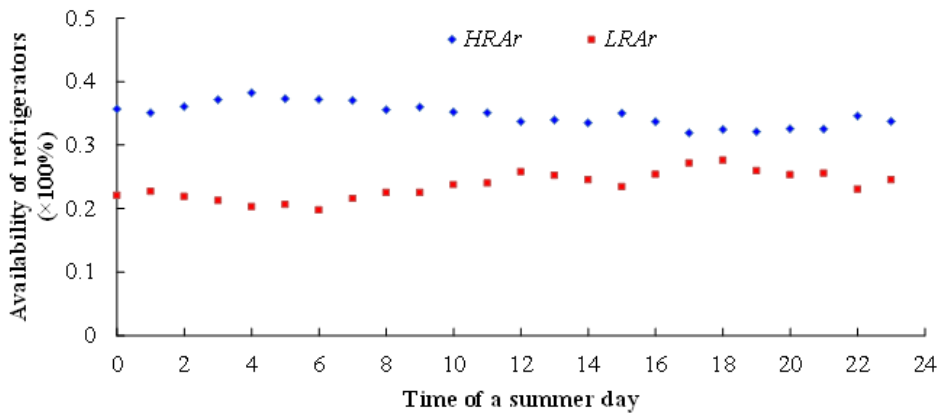


Fig. 5.4. LRA_r and HRA_r of refrigerators over a summer day

b) Field investigations on bitumen tanks

The major factor that influences the ON/OFF state of bitumen tanks is the price of electricity. Most bitumen tank owners switch ON their tanks when the price of electricity is low in early morning. Therefore, LRA of bitumen tanks (LRA_b) is higher when the electricity price is low. HRA of bitumen tanks (HRA_b) is higher when the electricity price is high during the day.

Field investigations to measure LRA_b and HRA_b of 76 bitumen tanks were undertaken over 1 month (14/09/2013-13/10/2013). The averaged records of LRA_b and HRA_b at half hourly intervals in a day are shown in Fig. 5.5. In the early morning, LRA_b was around 19.3% and HRA_b was around 51.8%. During the day, LRA_b fell to around 5% and HRA_b was around 68%.

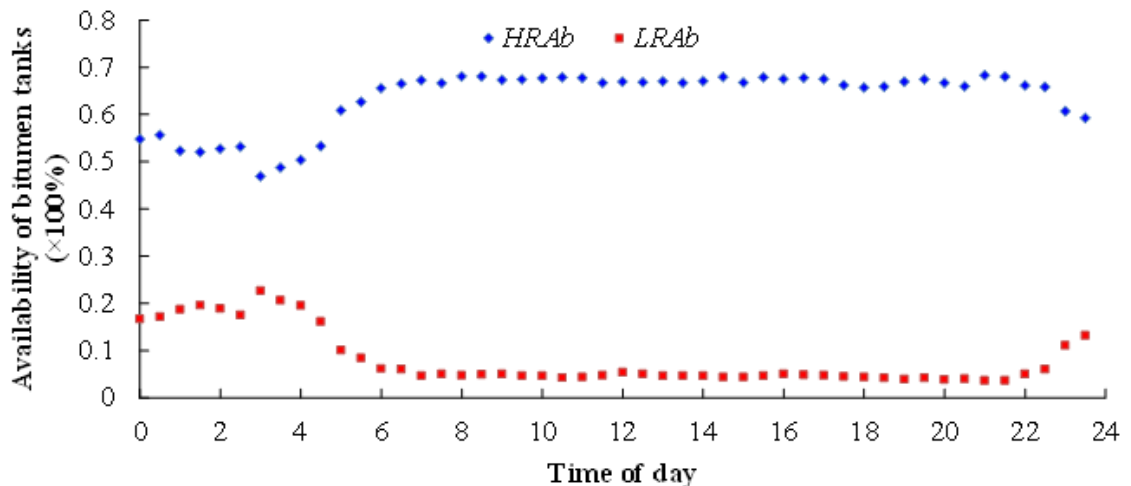


Fig. 5.5. HRA_b and LRA_b of bitumen tanks over a day

Data from field measurements of bitumen tanks in Fig. 5.5 shows that, at any particular time, there were a number of units (approximately 28.5%) that were unavailable to provide either high frequency response or low frequency response. These tanks were unavailable because of having exceeded the maximum number of switches per hour or of being outside the temperature limits.

5.3.3 Model of demand availability

a) Availability of refrigerators

Refrigerators that are available for low frequency response and high frequency response were modelled based on the thermodynamic model of refrigerators presented in Section

3.2. A refrigerator with cavity temperature T_{Ca} within the limits of its high set-point (T_{high}) and low set-point (T_{low}) is available for frequency response. The minimum ON/OFF time (t_{ON-s}^{min} and t_{OFF-s}^{min}) of the compressor is required. Therefore, refrigerators that are available for low frequency response R_{LRA} and for high frequency response R_{HRA} are determined by (5.3)-(5.4).

$$R_{LRA}(t) \in \{(s_c(t) = 1) \cap (T_{low} < T_{Ca}(t) < T_{high}) \cap (t_{ON-s}(t) > t_{ON-s}^{min})\} \quad (5.3)$$

$$R_{HRA}(t) \in \{(s_c(t) = 0) \cap (T_{low} < T_{Ca}(t) < T_{high}) \cap (t_{OFF-s}(t) > t_{OFF-s}^{min})\} \quad (5.4)$$

where s_c is compressor state, t_{ON-s} is ON time of a refrigerator and t_{OFF-s} is OFF time of a refrigerator.

Therefore, LRA_r and HRA_r of refrigerators are derived as:

$$LRA_r(t) = \frac{\text{number of refrigerators belong to } R_{LRA}(t)}{\text{total number of refrigerators}} \times 100\% \quad (5.5)$$

$$HRA_r(t) = \frac{\text{number of refrigerators belong to } R_{HRA}(t)}{\text{total number of refrigerators}} \times 100\% \quad (5.6)$$

b) Availability of bitumen tanks

Bitumen tanks that are available for low frequency response and high frequency response were modelled based on the curve-fit model presented in Section 4.3.3. Tank temperature (T) within the limits of its high set-point (T_{high}) and low set-point (T_{low}) is equivalent to its t_{ON} and t_{OFF} within their ranges of $0-P_{ON}$ and $0-P_{OFF}$. A tank also has constraints of minimum ON/OFF time (t_{ON-s}^{min} and t_{OFF-s}^{min}) and maximum number of switches per hour (N_s^{max}). Bitumen tanks available for low frequency response B_{LRA} and for high frequency response B_{HRA} are determined by:

$$B_{LRA}(t) \in \left\{ (s_h(t) = 1) \cap (0 < t_{ON}(t) < P_{ON}) \cap \dots \right. \\ \left. (t_{ON-s}(t) > t_{ON-s}^{min}) \cap (N_s(t) < N_s^{max}) \right\} \quad (5.7)$$

$$B_{HRA}(t) \in \left\{ (s_h(t) = 0) \cap (0 < t_{OFF}(t) < P_{OFF}) \cap \dots \right. \\ \left. (t_{OFF-s} > t_{OFF-s}^{min}) \cap (N_s(t) < N_s^{max}) \right\} \quad (5.8)$$

where s_h is heater state, t_{ON-s} is ON time of a tank, t_{OFF-s} is OFF time of a tank and N_s is the number of switches per hour.

Therefore, LRA_b and HRA_b of bitumen tanks are:

$$LRA_b(t) = \frac{\text{number of tanks belong to } B_{LRA}(t)}{\text{total number of tanks}} \times 100\% \quad (5.9)$$

$$HRA_b(t) = \frac{\text{number of tanks belong to } B_{HRA}(t)}{\text{total number of tanks}} \times 100\% \quad (5.10)$$

5.4 Demand aggregation for frequency response service

5.4.1 Potential response from all refrigerators and bitumen tanks

According to the investigation of Open Energi, there were approximately 40 million refrigerators connected to the GB power system in 2008. Approximately 500 bitumen tanks were connected to the GB power system in 2012. Each refrigerator has a typical power consumption of 0.1 kW and each bitumen tank has a typical power consumption of 40 kW. It was assumed that all the refrigerators and bitumen tanks are equipped with a type-specific frequency controller. Considering their availability over a day in Section 5.3.2, the total available load change at different time of day in response to frequency was estimated and is shown in Fig. 5.6.

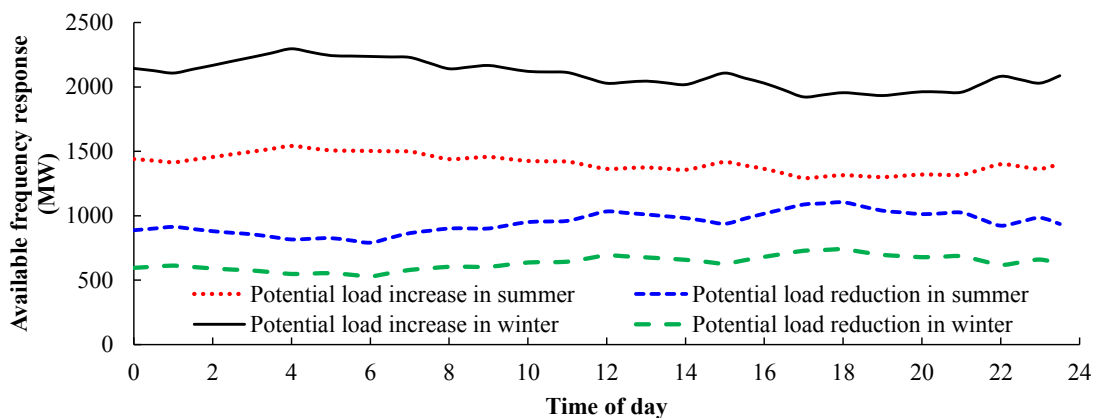


Fig. 5.6. Available frequency response from all refrigerators and bitumen tanks over a day

According to Fig. 5.6, the potential frequency response from refrigerators and tanks is considerable. On a winter day, these refrigerators and tanks were available to provide a minimum of 2,000 MW load increase and 500 MW load reduction. On a summer day, a minimum of 1,300 MW load increase and 800 MW load reduction were possible. It can be observed that the load increase is always greater than load reduction because both types of loads have a much longer OFF cycle than ON cycle.

5.4.2 Demand aggregation for Firm Frequency Response (FFR) service

In the GB power system, loads are able to provide frequency response services through Frequency Control by Demand Management (FCDM) and Firm Frequency Response (FFR) [18]. FCDM is the interruption of contracted demand when frequency transgresses the low frequency relay (typically at 49.7 Hz) [26]. This is regarded as a static response. However in this thesis, the frequency controller of either refrigerators or tanks aims to provide a dynamic response which varies their power consumption in proportion to frequency deviations. Therefore, refrigerators and tanks are able to provide frequency response service through FFR which includes both dynamic and non-dynamic response [25].

It is a technical requirement of FFR service that a minimum amount of 10 MW of frequency response is delivered. The power consumption of each refrigerator and of each tank is small. Therefore, a load aggregator will need access to a certain minimum number of refrigerators and tanks to aggregate so that more than 10 MW of frequency response is provided.

Demand availability at different time of day has to be considered by a load aggregator when planning the number of loads to be equipped with a frequency controller. Therefore, the number of each type of load to be aggregated for the provision of a 10 MW FFR service over a day was estimated using their measured demand availability shown in Fig. 5.2 and Fig. 5.5.

In Fig. 5.5, the demand availability over a day is separated into 4 periods: 00:00 – 04:00, 04:00 – 06:00, 06:00 – 22:00 and 22:00 – 00:00. For each of the four periods, the number of refrigerators (N_r) and bitumen tanks (N_b) that are required to be aggregated and to provide FFR was estimated using (5.11).

$$LRA_r \times N_r \times P_r + LRA_b \times N_b \times P_b \geq 10 \text{ (MW)} \quad (5.11)$$

P is the power consumption of each load with subscripts r indicating refrigerator and b indicating bitumen tank. P_b is 40 kW and P_r is 0.1 kW. The values of LRA_r and LRA_b are the averaged value of the four periods given in Fig. 5.2 and Fig. 5.5. They are listed in Table 5.1.

Equation (5.11) was used to estimate the required number of loads to provide low frequency response. Because LRA is always lower than HRA , if the estimated number of

loads is able to provide load reduction of greater than 10 MW, it will inevitably provide load increase of greater than 10 MW. The estimated combination of N_r and N_b for the provision of load reduction of more than 10 MW was calculated and is depicted in Fig. 5.8.

TABLE 5.1. LRA_r and LRA_b at Different Time of a Day

Period	Time of a day	LRA_r	LRA_b
1	00:00 – 04:00	0.145	0.193
2	04:00 – 06:00	0.138	0.101
3	06:00 – 22:00	0.163	0.046
4	22:00 – 00:00	0.164	0.111

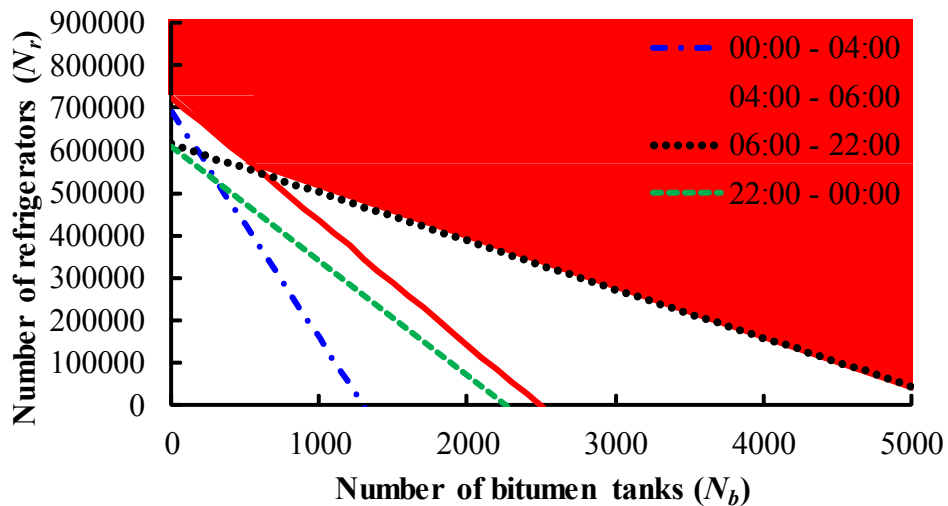


Fig. 5.7. Scheme of number of tanks and refrigerators to be combined for power reduction of more than 10 MW

The curves in Fig. 5.7 provide a scheme to estimate the minimum number of refrigerators required if a load aggregator has access to a certain number of bitumen tanks. The points in the shaded area show the possible combinations of numbers of refrigerators and numbers of bitumen tanks that are necessary to be aggregated in order to provide frequency response of greater than 10 MW over a day. For example, the intersection point of curve ‘04:00 – 06:00’ and curve ‘06:00 – 22:00’ indicates an aggregation of 600 bitumen tanks and 546,179 refrigerators (1.37% of domestic refrigerators in the GB power system). If a load aggregator has access to 600 bitumen tanks, it requires access to at least 546,179 refrigerators in order to participate in the Firm Frequency Response service over a day.

The payment structure of FFR service is shown in Table 5.2 [97]. FFR has a four-part payment structure. However, a participant does not have to tender for all four types of payments. A load aggregator of refrigerators and bitumen tanks in this thesis provides dynamic frequency response autonomously without receiving instructions from the system operator. Therefore, it can receive the availability fee.

TABLE 5.2. Payment Structure of Firm Frequency Response Service [97].

Type of payment		Description
Availability fee (£/hr)		the hours for which a provider has tendered to make the service available for
Utilisation fee	Window Initiation fee (£/window)	for each FFR window that National Grid instructs within the tendered frame
	Nomination fee (£/hr)	a holding fee for each hour utilised within FFR nominated windows
Tendered Window Revision fee (£/hr)		National Grid notifies providers of window nominations in advance and, if provider allows, this payment is payable if National Grid subsequently revises this nomination
Response Energy fee (£/MWh)		actual response energy provided in the nominated window

A load aggregator is also able to tender for the FFR service for several hours of a day. For example, if a load aggregator has access to 600 bitumen tanks and fewer than 546,179 refrigerators, it is still able to tender for the periods 22:00 – 00:00 and 00:00 – 04:00 as long as the number of refrigerators is at least the number stipulated by the correlating curves in Fig. 5.7.

5.4.3 Demand aggregation for FFR service: managing uncertainties

Table 5.1 shows the measured demand availability for frequency response at different time of day. However, in practice, there is expected to be a greater level of uncertainties in the demand availability. Considering the uncertainties, the number of each type of loads to be aggregated was determined for the provision of frequency response of

greater than 10 MW with a certain level of confidence. Chance-constrained programming [98] was used.

Chance-constrained programming describes constraints in the form of probable levels of attainment or confidence. If α is a pre-set confidence level determined by a decision maker, this indicates that a constraint is required to have a probability of satisfaction of α .

The chance constraint is generally formulated as [99]:

$$\vec{X} \in \{\vec{X} \in R^n | Probability(A\vec{X} \leq \vec{b}) \geq \vec{\alpha}, \vec{b} \in R^m\} \quad (5.12)$$

where \vec{X} is an n -directional vector of decision variables, A is an $(m \times n)$ coefficient matrix, \vec{b} is an m -directional vector and $\vec{\alpha}$ ($0 < \vec{\alpha} < 1$) represents the vector of confidence level which is the probability for the satisfaction of the defined constraints, i.e. $A\vec{X} \leq \vec{b}$.

For the four daily time periods shown in Table 5.1, the averaged values of LRA_r (μ_r) and LRA_b (μ_b) were obtained from field measurements. If it is assumed that both LRA_r and LRA_b follow the normal distribution, then the measured average LRA_r and LRA_b represent the expectations of the normal distributions. As the measurements of demand availability were carried out on a population of loads for a number of days, their standard deviations can be small. The standard deviation was assumed to be 10% of the averaged value as shown in (5.13) and (5.14):

$$\sigma_r = 0.1 \times \mu_r \quad (5.13)$$

$$\sigma_b = 0.1 \times \mu_b \quad (5.14)$$

where subscripts r indicating refrigerator and b indicating bitumen tank. LRA_r and LRA_b following the normal distribution are therefore represented by (5.15) and (5.16). n is 1, 2, 3 or 4 representing the four periods of a day in Table 5.1. Based on the data in Table 5.1, the expectations and standard deviations are listed in Table 5.3.

$$LRA_{rn} \sim N(\mu_{rn}, \sigma_{rn}^2) \quad (5.15)$$

$$LRA_{bn} \sim N(\mu_{bn}, \sigma_{bn}^2) \quad (5.16)$$

TABLE 5.3. Expectations and Standard Deviations of LRA_r and LRA_b at Different Time of Day

Period n	Time of a day	μ_{rn}	σ_{rn}	μ_{bn}	σ_{bn}
1	00:00 – 04:00	0.145	$0.1\mu_{r1}$	0.193	$0.1\mu_{b1}$
2	04:00 – 06:00	0.138	$0.1\mu_{r2}$	0.101	$0.1\mu_{b2}$
3	06:00 – 22:00	0.163	$0.1\mu_{r3}$	0.046	$0.1\mu_{b3}$
4	22:00 – 00:00	0.164	$0.1\mu_{r4}$	0.111	$0.1\mu_{b4}$

Use the following property of a normal distribution [100]:

- If $X \sim N(\mu, \sigma^2)$, $\forall a, b \in R$, then $aX + b \sim N(a\mu + b, (a\sigma)^2)$

For period n , aggregated low frequency response of a number of refrigerators (P_{rn}) each having a power rating P_r of 0.1 kW and aggregated low frequency response of a number of bitumen tanks (P_{bn}) each having a power rating P_b of 40 kW also follow the normal distributions:

$$P_{rtn}(kW) \sim N(\mu_{rn} \times P_r \times N_{rn}, (\sigma_{rn} \times P_r \times N_{rn})^2) \quad (5.17)$$

$$P_{bntn}(kW) \sim N(\mu_{bn} \times P_b \times N_{bn}, (\sigma_{bn} \times P_b \times N_{bn})^2) \quad (5.18)$$

where N_{rn} is the number of refrigerators required for period n and N_{bn} is the number of bitumen tanks required for period n .

FR_n is defined as the total available low frequency response from refrigerators and tanks for period n as shown in (5.19). To participate in the FFR service, the constraint, i.e. the total frequency response from refrigerators and tanks to be greater than 10 MW (10,000 kW), needs to be satisfied. A confidence level was used to describe the probability of meeting the constraint. Assuming that a 90% confidence level of the provision of 10 MW frequency response is acceptable, equation (5.20) is therefore obtained based on the chance-constrained programming illustrated in (5.12).

$$FR_n = P_{rtn} + P_{bntn} (kW) \quad (5.19)$$

$$Probability\{FR_n - 10,000 \text{ kW} \geq 0\} \geq 90\% \quad (5.20)$$

By combining equations (5.17)-(5.20), N_{rn} and N_{bn} is unknown and needs to be determined. Using the following property of a normal distribution [100]:

- If $X \sim N(\mu_X, \sigma_X^2)$, $Y \sim N(\mu_Y, \sigma_Y^2)$ are independent random variables,

then their sum : $X + Y \sim N(\mu_X + \mu_Y, \sigma_X^2 + \sigma_Y^2)$

Therefore, during each period n , $FR_n - 10,000$ (kW) also follows the normal distribution:

$$FR_n - 10,000 \sim N(\mu_{FRn}, \sigma_{FRn}^2) \quad (5.21)$$

$$\mu_{FRn} = \mu_{rn} \times P_r \times N_{rn} + \mu_{bn} \times P_b \times N_{bn} - 10000 \quad (5.22)$$

$$\sigma_{FRn}^2 = (\sigma_{rn} \times P_r \times N_{rn})^2 + (\sigma_{bn} \times P_b \times N_{bn})^2 \quad (5.23)$$

Equation (5.21) was standardized to the standard normal distribution using the following rule.

- Define a standardised random variable Z equivalent to [101]:

$$Z = \frac{X - \mu}{\sigma} \sim N(0,1)$$

where X is a random variable and $X \sim N(\mu, \sigma^2)$.

Therefore, random variable $FR_n - 10,000$ in (5.21) was standardized:

$$Z = \frac{FR_n - 10000 - \mu_{FRn}}{\sigma_{FRn}} \quad (5.24)$$

Equation (5.20) was then converted to standard normal distribution as shown in (5.25):

$$Probability \left\{ Z \geq \frac{0 - \mu_{FRn}}{\sigma_{FRn}} \right\} \geq 90\% \quad (5.25)$$

According to the table of standard normal distribution in Appendix IV, for a probability of 90% ($Z_{0.9}$), the value of Z in Fig. 5.8 [102] is -1.28 . Equation (5.26) is therefore obtained. By substituting (5.22) and (5.23) into (5.26), the relationship between N_{bn} and N_{rn} was estimated. Fig. 5.9 shows the relationship for the four periods over a day.

$$\frac{0 - \mu_{FRn}}{\sigma_{FRn}} \leq -1.28 \quad (5.26)$$

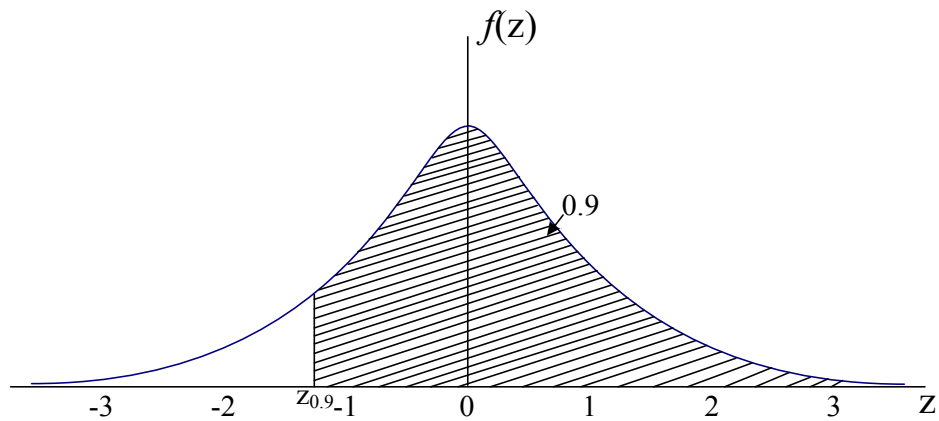


Fig. 5.8. Standard normal distribution curve

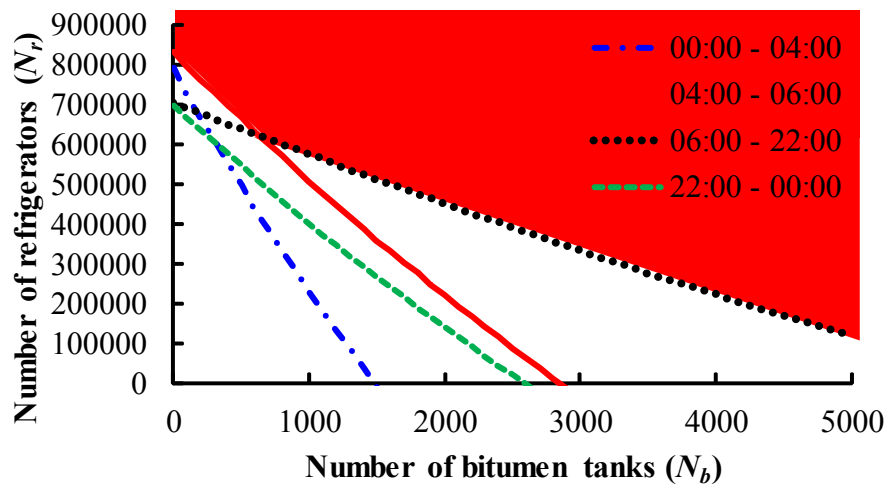


Fig. 5.9. Scheme of number of tanks and refrigerators to be combined for power reduction of more than 10 MW considering 90% confidence level

Therefore, if a load aggregator has access to a certain number of bitumen tanks, the number of refrigerators required to be aggregated is estimated taking into account uncertainties in the measurements of LRA_r and LRA_b . The points in the shaded area show the possible combinations of numbers of refrigerators and numbers of bitumen tanks that are necessary to be aggregated in order to provide frequency response of more than 10 MW over a day with a probability of greater than 90%. Compared with Fig. 5.7, with same number of tanks, the number of required refrigerators is greater in Fig. 5.9 as uncertainties in real conditions, i.e. the standard deviations of the measurements, are considered. This can be visualised in Fig. 5.10.

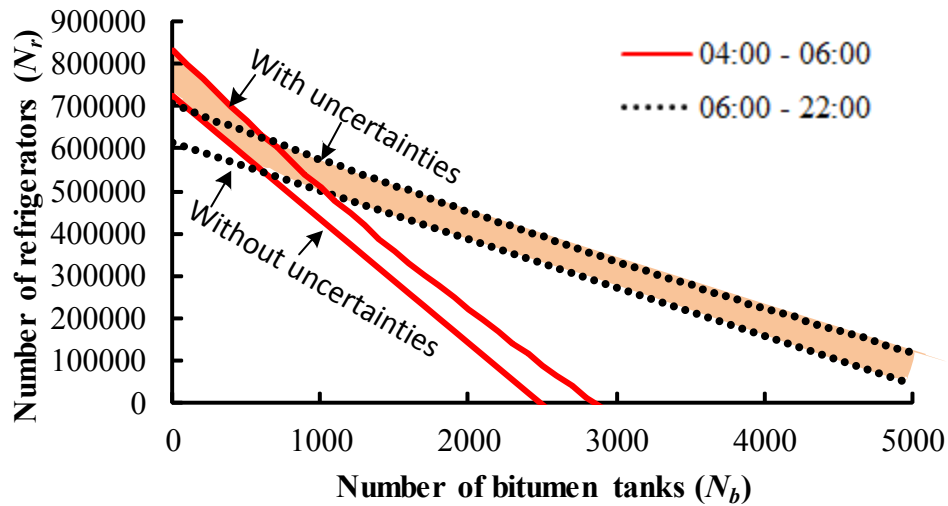


Fig. 5.10. Differences (shaded area) in the number of refrigerators and bitumen tanks with and without the consideration of uncertainties.

5.5 Case studies

5.5.1 Reduce the deviations of grid frequency

This case study was carried out to investigate the capability of the type-specific frequency controller of refrigerators and of tanks to reduce frequency deviations as discussed in Section 5.2.

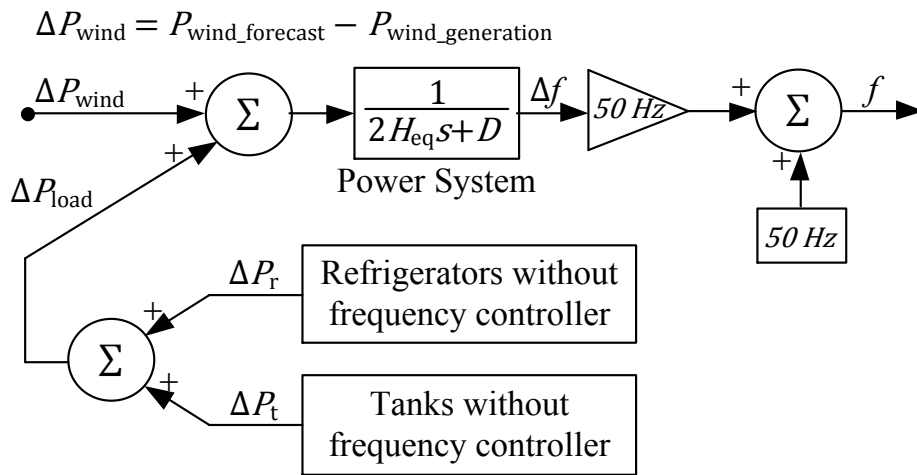
The power system model for this case study is shown in Fig. 5.11. The refrigerator model presented in Section 3.2 representing 40 million refrigerators with a power rating of 0.1 kW was connected to the power system model. The tank model presented in Section 4.3 representing 500 bitumen tanks each with a power rating of 40 kW was also connected.

System inertia H_{eq} was set to 3.1 s [37] in order to represent a future power system with significant generation connected through converters (i.e. 30% of generation capacity is wind generation). System demand was set to 20 GW. The effect of frequency sensitive loads was lumped into the damping constant D and was set to be 1 pu.

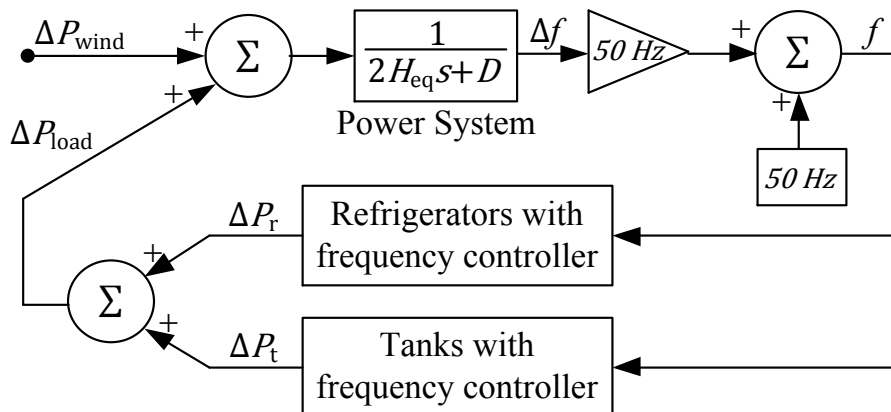
The droop control of generator governors was disabled in this case study assuming that generators were operating in a limited frequency-sensitive mode [38]. The system response to a generation or load change is therefore determined by H_{eq} , D and also the refrigerators and tanks if they are equipped with their frequency controller.

A wind generation profile including wind forecast (MW) and wind generation (MW) on 25 Aug 2014 was obtained from EIRGRID [103]. The difference between the forecasted wind generation and the measured wind generation (ΔP_{wind}), as shown in Fig. 5.12, was injected to the power system model representing unforeseen changes in power generation from wind.

In Fig. 5.11(a), refrigerators and bitumen tanks were not equipped with their frequency controllers. In Fig. 5.11(b), the type-specific frequency controllers of refrigerators and bitumen tanks were used. To show the capability of their frequency controllers to reduce the grid frequency deviations, simulation results of models in Fig. 5.11(a) and in Fig. 5.11(b) are compared in Figs. 5.13-5.16.



(a) Loads with frequency controller disabled



(b) Loads with frequency controller enabled

Fig. 5.11. Power system model with refrigerators and bitumen tanks connected

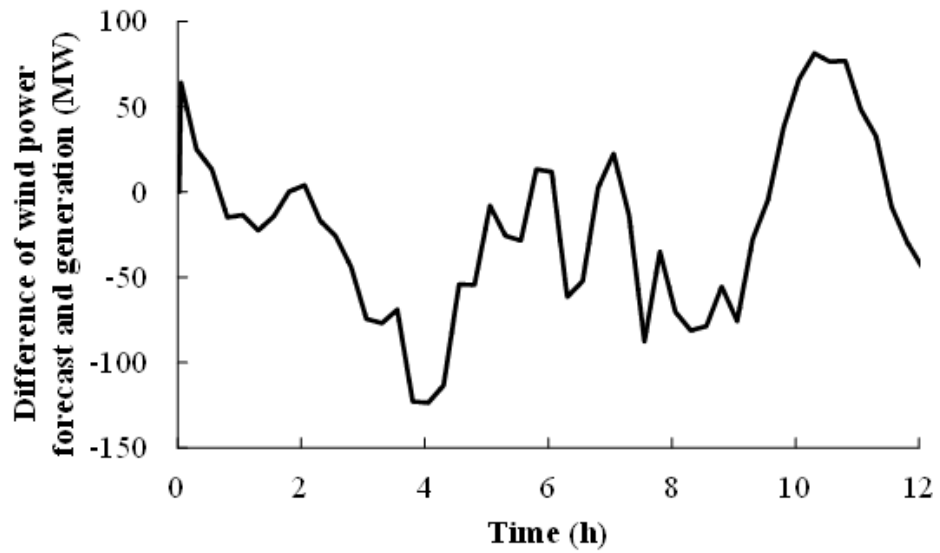


Fig. 5.12. Power change (ΔP_{wind}) injected to the power system

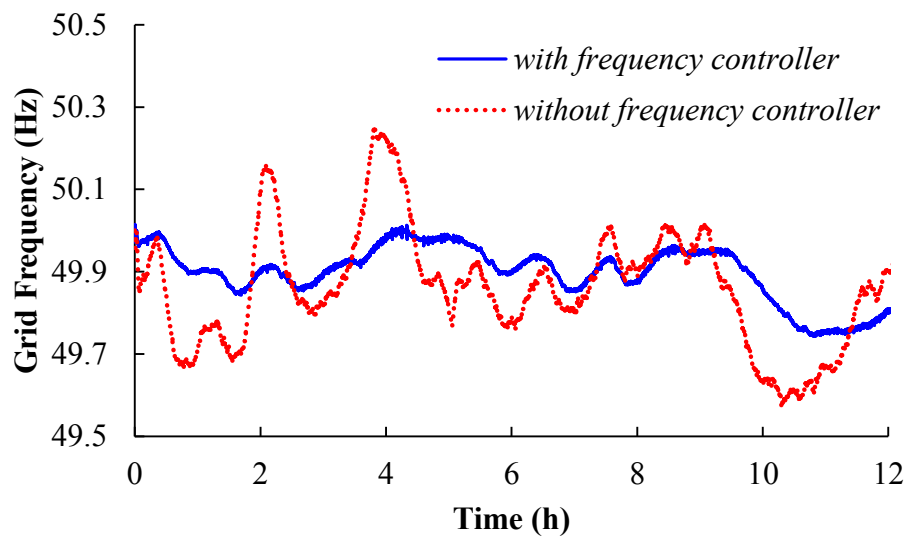


Fig. 5.13. Variation of grid frequency with and without frequency response from loads

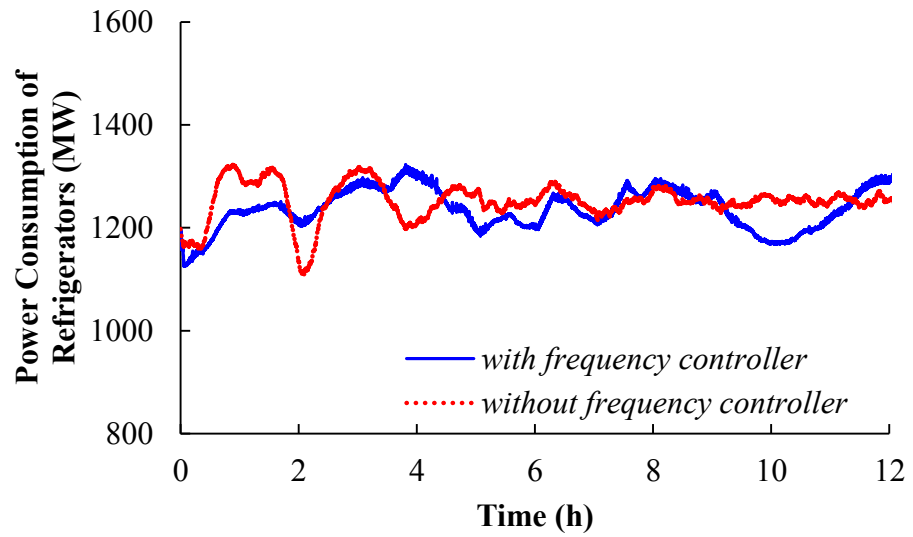


Fig. 5.14. Power consumption of refrigerators with and without the frequency controller

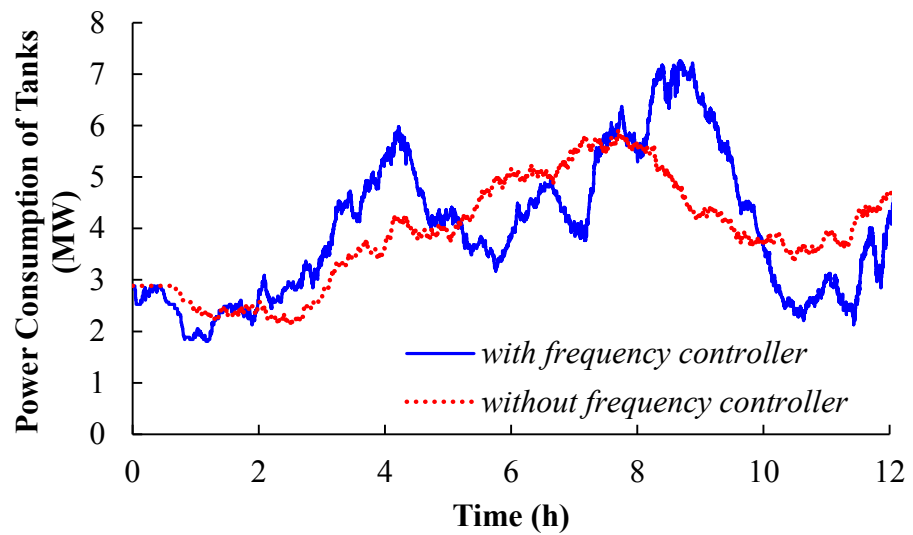


Fig. 5.15. Power consumption of tanks with and without the frequency controller

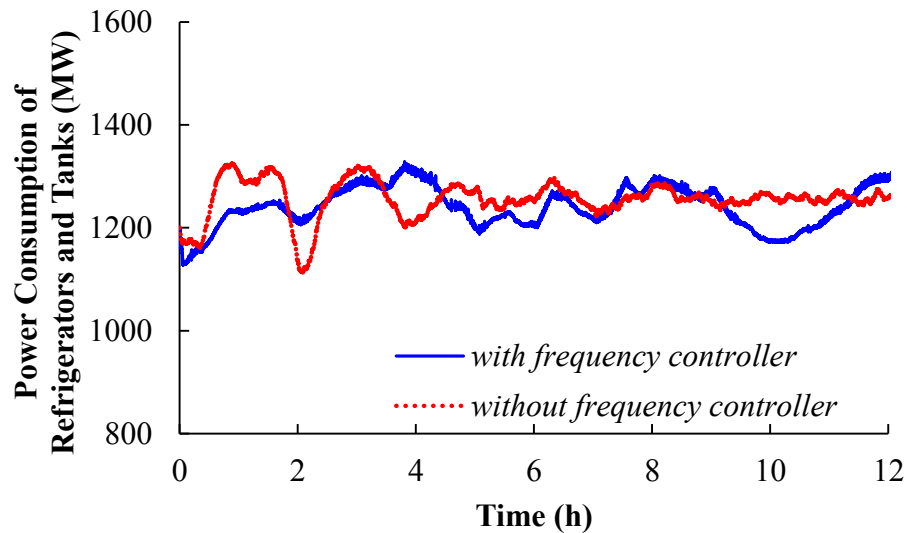


Fig. 5.16. Total power consumption of refrigerators and tanks with and without their type-specific frequency controller

Fig. 5.13 compares the deviations of grid frequency in the two simulations. With the frequency controllers of refrigerators and tanks equipped, frequency deviations reduced significantly compared to the case experienced without the frequency controllers.

Fig. 5.14 compares variations in power consumption of refrigerators. With the frequency controller, because the deviations of grid frequency were small (i.e. around 50 ± 0.2 Hz in Fig. 5.15 compared to the set-points in the frequency controller 50 ± 0.5 Hz), variations in the power consumption of refrigerators were not significant compared to the case ‘without frequency controller’. Furthermore, refrigerators inherently have load change during the day as indicated in the case ‘without frequency controller’. Therefore, the capability of the frequency controller of refrigerators is observed by relating Fig. 5.14 to Fig. 5.13:

- When grid frequency in the case of ‘with frequency controller’ is lower than that of ‘without frequency controller’, power consumption of refrigerators in the case of ‘with frequency controller’ is greater than in the case of ‘without frequency controller’. This indicates that with the frequency controller, refrigerators increase their power consumption and reduce the rise in frequency compared to the case ‘without frequency controller’.
- When frequency in the case of ‘with frequency controller’ is higher than that of ‘without frequency controller’, power consumption of refrigerators in the case of ‘with frequency controller’ is lower than in the case of ‘without frequency controller’.

controller'. This means that with the frequency controller, refrigerators reduce their power consumption and reduce the drop in frequency.

Hence, refrigerators that were equipped with their frequency controller contributed to the reduction of frequency deviations.

Fig. 5.15 compares variations in power consumption of tanks with and without their frequency controller. It can be seen that, with the frequency controller, power consumption of tanks tracks deviations of grid frequency in Fig. 5.13 '*with frequency controller*'. The load change of tanks dynamically contributed to the reduction of frequency deviations. Fig. 5.16 gives the total load change of refrigerators and tanks in response to grid frequency.

5.5.2 Demand aggregation for Firm Frequency Response service

A case study was carried out to investigate the aggregation of a certain number of refrigerators and bitumen tanks to provide more than 10 MW of frequency response for the FFR service as discussed in Section 5.4. The case included an aggregation of 622,980 refrigerators (0.1 kW/ refrigerator) and 591 bitumen tanks (40 kW/ tank) as according to the intersection point of curve 04:00 – 06:00 and curve 06:00 – 22:00 in Fig. 5.10.

The model of demand availability, i.e. LRA and HRA of refrigerators and bitumen tanks, was fitted to the field measurements that were depicted in Section 5.3.2. Initial values of LRA_r and HRA_r at 05:00 in Fig. 5.2 were used. Initial values of LRA_b and HRA_b of tanks at 05:00 in Fig. 5.5 were used. In addition, for the aggregated refrigerator models, a diversity factor div of 0.8 was chosen as discussed in Section 3.2.

Simulations were undertaken by injecting the frequency profile in Fig. 5.17 into the model at 05:00. The frequency profile is that of a severe low frequency incident which occurred in the GB power system on 28 May 2008 [22]. Frequency was assumed to be at 50 Hz before and after the frequency incident period. Simulation results are shown in Figs. 5.18-5.21. Zoomed figures in Fig. 5.19 and in Fig. 5.20 give the results of HRA and LRA of refrigerators and of tanks during the depression of grid frequency at 05:00–05:30.

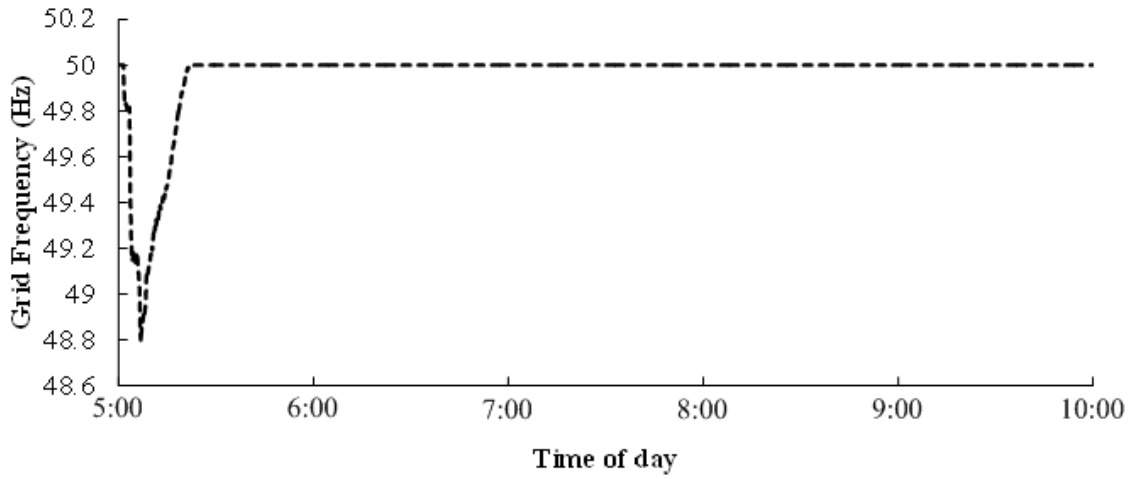


Fig. 5.17. Injected frequency input

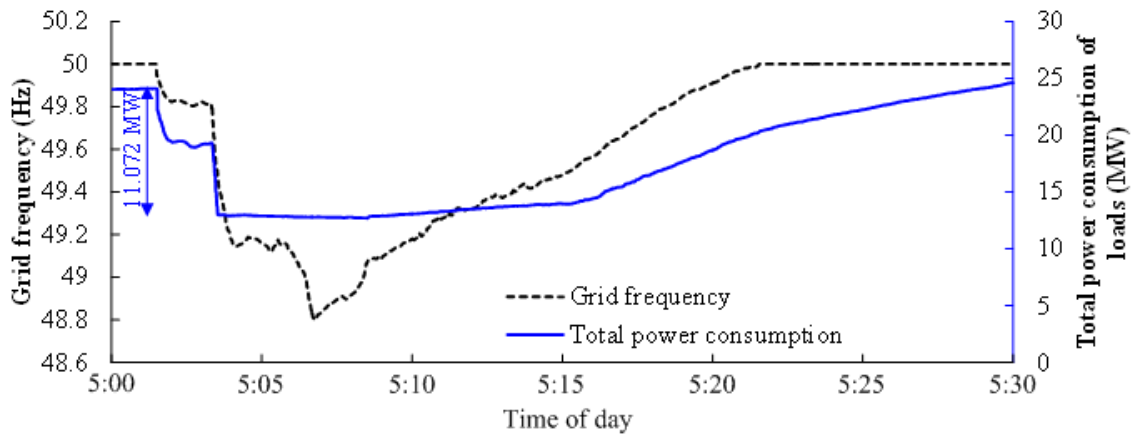


Fig. 5.18. Variation of aggregated power consumption of loads at 05:00 – 05:30 during the frequency incident

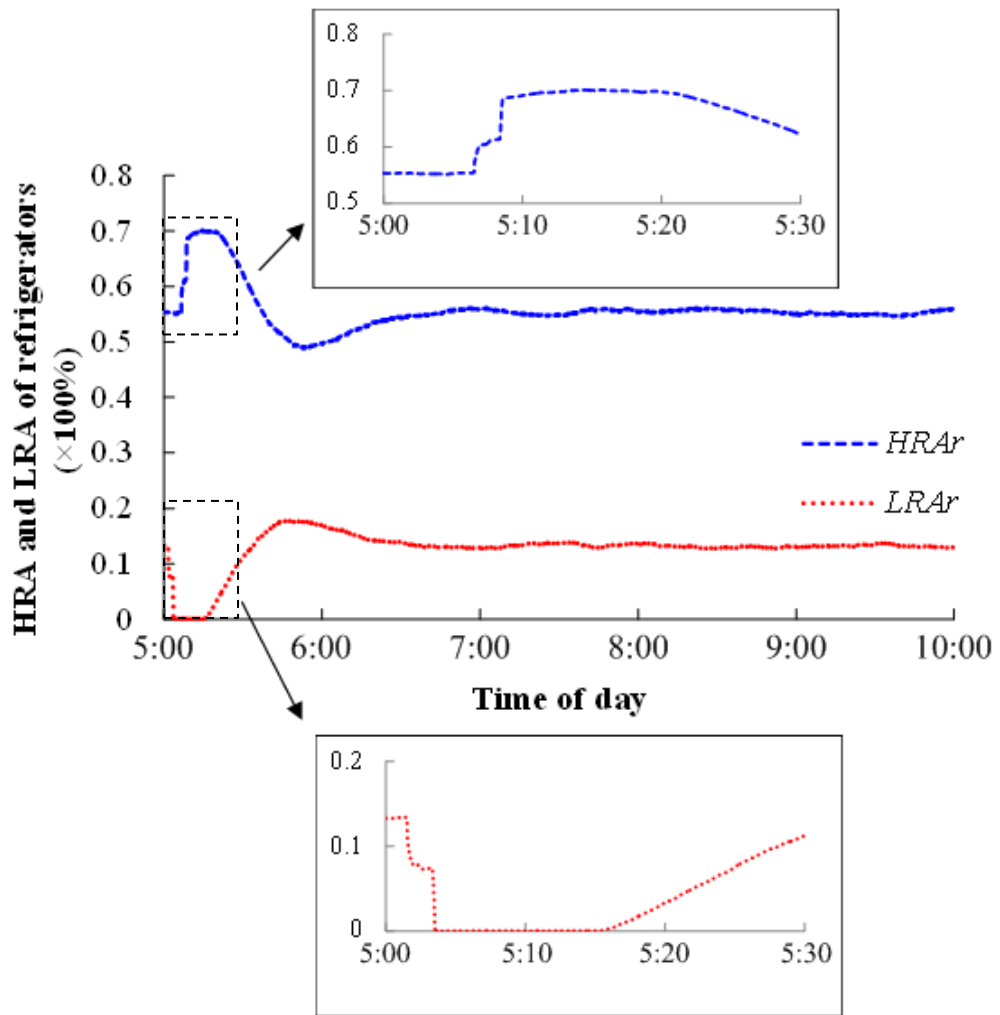


Fig. 5.19. Variations of HRA_r and LRA_r of refrigerators

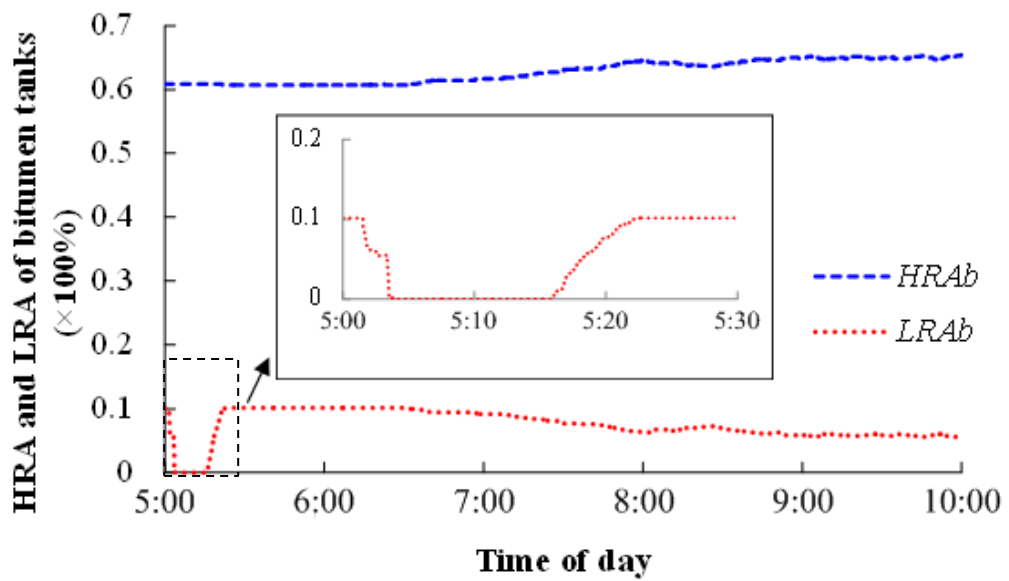


Fig. 5.20. Variations of HRA_b and LRA_b of bitumen tanks

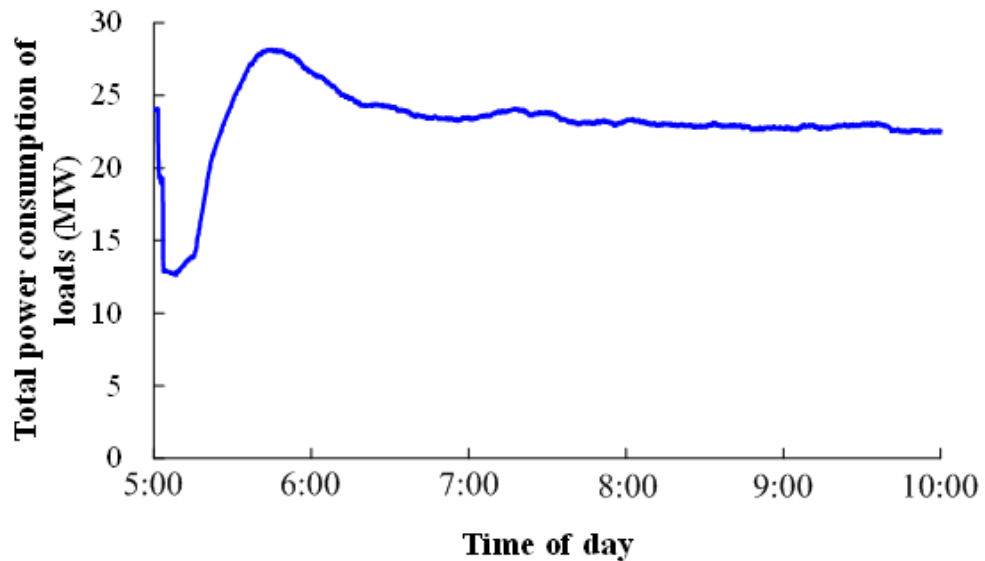


Fig. 5.21. Variations of aggregated power consumption of loads during and after the frequency incident

Fig. 5.18 shows variations of aggregated power consumption of refrigerators and tanks (see right axis) during the depressed frequency (see left axis). The aggregated power consumption reduced immediately in proportion to drops in frequency. When frequency dropped to below 49.5 Hz (pre-set minimum trigger frequency F_{OFF}), all available loads were switched OFF. The total power reduction of loads during the incident was 11.072 MW. Therefore, a combination of 591 bitumen tanks and 622,980 refrigerators was able to provide more than 10 MW of frequency response to the power system. The number of refrigerators was relatively large because power consumption of each unit was small (0.1 kW) and LRA_r was only 15% at 05:00, as shown in Fig. 5.11. Power consumption of loads started to recover when frequency recovered and reached 49.5 Hz at around 05:15, as shown in Fig. 5.18.

Fig. 5.19 shows variations in LRA and HRA of refrigerators. LRA_r varied dynamically with the deviations of frequency. When frequency became lower than 49.5 Hz, LRA_r reduced to zero which indicates that the response of refrigerators was exhausted. Refrigerators that are available for either high or low frequency response are required to be at a temperature within their high and low set-points. Therefore, following the drop of frequency, a number of refrigerators entered OFF-state if their temperature was within the high and low set-points. This led to increases in HRA_r with a decreasing LRA_r . The minimum OFF time of 5 min is shown in zoomed figures. Between the time when LRA_r became zero and the end of the 5-min minimum OFF time, HRA_r did not increase. LRA_r and HRA_r started to recover by switching ON early OFF-state refrigerators

following the frequency recovery as illustrated in Section 3.3. An increase in LRA_r up to 19% after the frequency incident is shown. This was caused by the reconnections of refrigerators which took place in order to complement their lost thermal energy during the period of depressed frequency (05:00 – 05:30) and also to ensure that they were ready to contribute to frequency control in the event of any future drops in frequency.

Fig. 5.20 shows variations in LRA and HRA of bitumen tanks. LRA_b varied with the deviations of grid frequency and reduced to zero when frequency dropped to below 49.5 Hz. The influence of frequency drop on HRA_b was slight because tanks were controlled to be OFF if frequency remains low. Following the recovery of frequency, tanks reverted back ON. LRA_b recovered while HRA_b did not increase as loads reverted back ON. The decrease in LRA_b and increase in HRA_b after the frequency incident was caused by the inherent variations of load availability with time.

Fig. 5.21 shows the total power consumption of loads after the frequency incident. The large fall in frequency caused refrigerators to be switched OFF almost simultaneously. This reduced the diversity of refrigerator loads. As frequency recovered, refrigerators were reconnected. This caused total power consumption to become greater than its pre-event level. However, as a diversity factor (div) of 0.8 was used, the increase in power consumption above its pre-event level was small, as illustrated previously in Fig. 3.29, Section 3.5.

5.5.3 Aggregated demand response in a future power system

A simulation was carried out on a scenario of 40 million refrigerators (0.1 kW/refrigerator) and 500 tanks (40 kW/tank) connected to a future power system.

The refrigerator model was that developed in Chapter 3 with an LRA_r of 14.3% and HRA_r of 55.8% at 04:00 in the morning. The tank model was the curve-fit model that developed in Chapter 4 with an LRA_b of 21.9% and HRA_b of 51.8% at 04:00 in the morning. The demand availability at 04:00 was chosen because, at around that time, system demand was estimated to be the lowest of a day in 2025 [104].

The power system model was illustrated in Section 3.4. The inertia of the power system was set to 3.1 s representing a future power system with more generation connected through converters. A low system demand of 20 GW was assumed.

The expected maximum loss of generation in the GB power system after April 2014 is 1,800 MW. A loss in generation of 1,800 MW ($\Delta P_{loss} = 0.09$ pu) was applied to the power system model at 90 s. Simulation results are shown in Figs. 5.22-5.26.

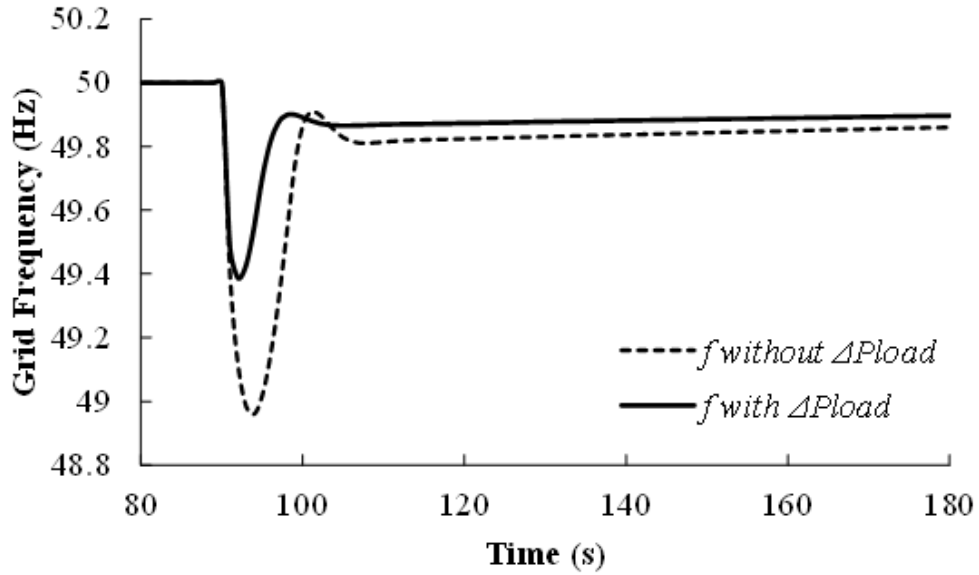


Fig. 5.22. Variations of grid frequency

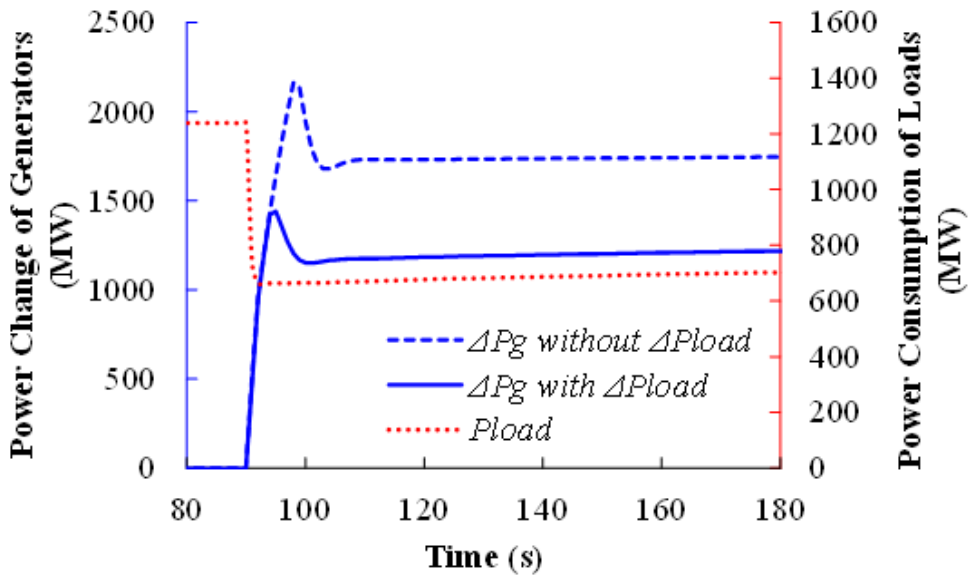


Fig. 5.23. Change of power output of generators and power consumption of loads

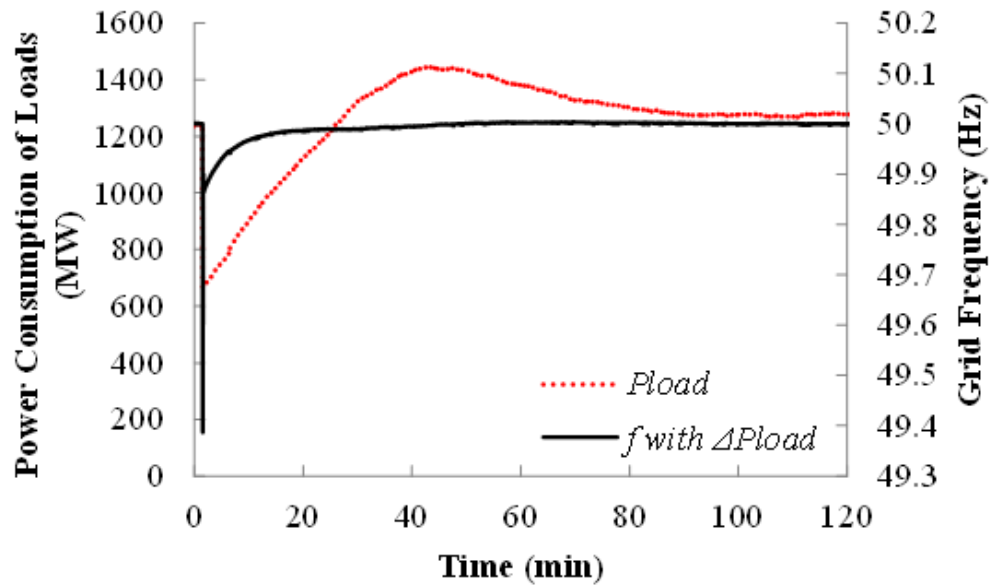


Fig. 5.24. Power consumption of loads after the frequency incident

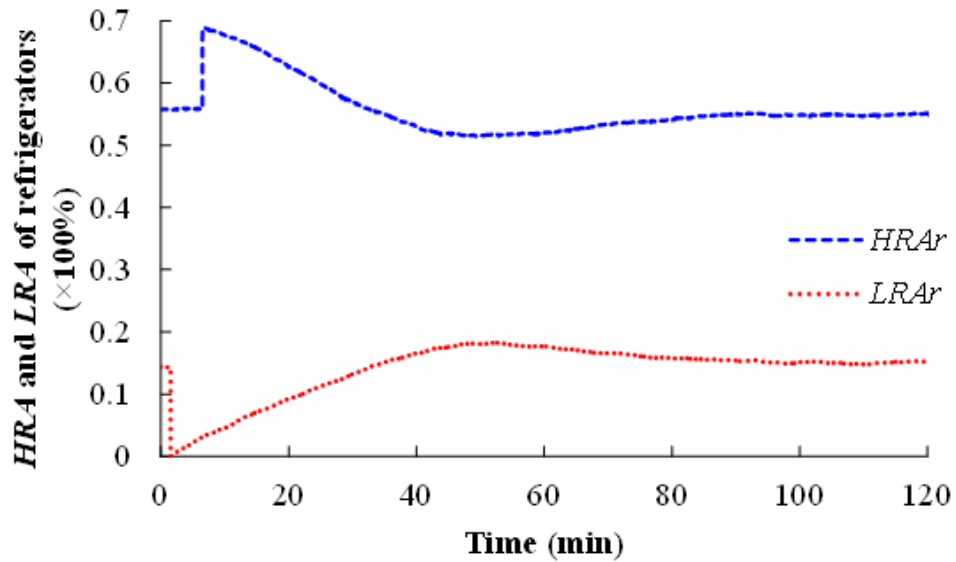


Fig. 5.25. Variations of *HRA* and *LRA* of refrigerators during and after the frequency incident

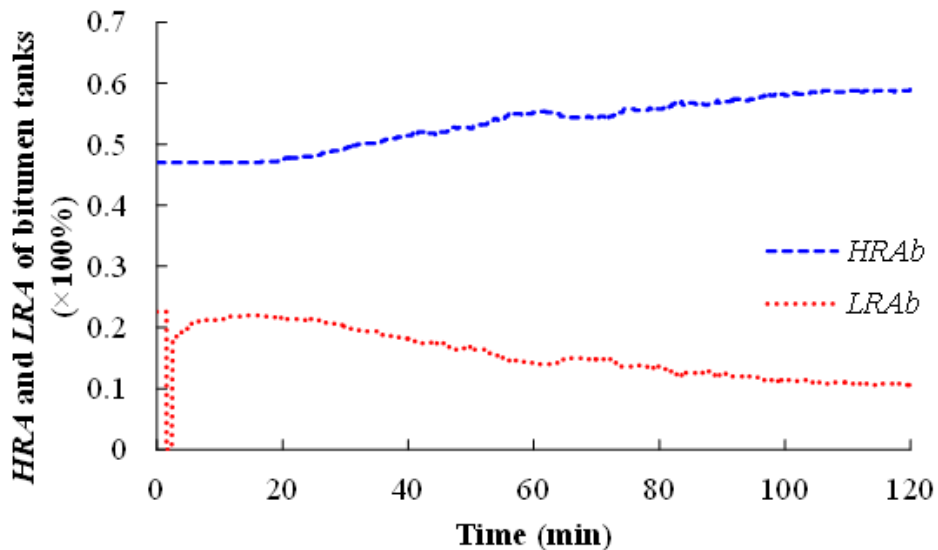


Fig. 5.26. Variations of *HRA* and *LRA* of bitumen tanks during and after the frequency incident

Fig. 5.22 shows variations of grid frequency after the generation loss of 1,800 MW. With the load change (ΔP_{load}) of both refrigerators and bitumen tanks, the drop of frequency was halted when frequency reached 49.39 Hz at 92 s. Without the load change, the frequency drop was not halted until frequency reached 48.96 Hz at 94 s. The steady-state limit of frequency in the GB power system is 50 ± 0.5 Hz. Simulation results show that immediate frequency response from refrigerators and tanks reduces the length of time that frequency is out of its steady-state limits.

Fig. 5.23 shows the change of power output of generators (see the left axis) and total power consumption of refrigerators and tanks (see the right axis). The 40 million refrigerators and 500 tanks gave an immediate load reduction of 576.38 MW following the frequency drop to 49.39 Hz. When output of generators reached the steady state at 30 s after the frequency drop, the power change of generators was reduced by around 542.79 MW compared with the case experienced without load reduction.

Fig. 5.24 shows the total power consumption of both types of loads (see the left axis) and variations of grid frequency (see the right axis) after the severe frequency incident. The interrupted loads started to be reconnected gradually following frequency recovery. Power consumption of loads increased to be higher than the pre-event level at around 30 min after the frequency incident. This was caused by the reconnections of refrigerators which took place in order to complement their lost thermal energy when frequency had returned to its normal range.

Fig. 5.25 and Fig. 5.26 show variations of demand availability (LRA_r , HRA_r , LRA_b and HRA_b) during and after the frequency drop. As illustrated in the previous case study (Section 5.5.2), following the frequency drop to below 49.5 Hz, LRA of both refrigerators and tanks reached zero indicating that all available loads were switched OFF. Following the recovery of frequency, demand availability also recovered in order to provide any possible future frequency response.

5.6 Conclusions

Comparison of the frequency controllers of refrigerators and bitumen tanks showed that, with type-specific frequency controllers, both types of loads will be capable of providing dynamic response to frequency deviations similar to the droop control of frequency-sensitive generators. Hence, the higher the number of refrigerators and tanks that are aggregated, the larger the spinning reserve capacity of frequency-sensitive generators they can replace. A case study was carried out to validate the capability of the frequency controllers.

Field investigations showed that the availability of both refrigerators and bitumen tanks to provide frequency response varies with time. Therefore, at different time of day, the possible amount of load change from the two types of loads can be predicted based on the measurements from field investigations. Considering the measured demand availability and using chance-constrained programming, the number of refrigerators and bitumen tanks to be aggregated in order to provide more than 10 MW of frequency response with a certain confidence level was estimated. A load aggregator is then able to provide FFR service to the GB power system operator by installing the frequency controllers for a minimum population of refrigerators and bitumen tanks.

The availability of refrigerators and bitumen tanks for frequency response were modelled. A case study showed that load changes reduced frequency deviations continuously and repetitively. The aggregated loads are technically feasible to participate in the FFR service. A load aggregator can receive availability fees through the tender for the FFR service.

A case study of a future GB power system with more generation connected through converters and frequency controller of refrigerators and bitumen tanks deployed at scale was carried out. Results showed that after a loss of generation, with the load change of

approximately 576 MW from 40 million refrigerators and 500 bitumen tanks in the GB power system, the drop in frequency was halted quickly and reduced significantly. The frequency response from loads was faster than that from frequency-sensitive generators. The change of power output of generators was also reduced. Hence, the fast frequency response from loads will yield benefits in the future power system in which there will be a reduction in system inertia due to the increasing use of converter connected generation.

Therefore, refrigerators and bitumen tanks equipped with frequency controllers are able to replace the spinning reserve capacity of frequency-sensitive generators. If certain numbers of refrigerators and bitumen tanks are aggregated, the aggregated frequency response is visible to the system operator. The aggregated loads are then able to participate in the FFR service of the GB power system.

Chapter 6

Conclusions

The conclusions drawn from the research work in previous chapters are summarised. Contributions of the thesis are outlined. Possible future work is suggested. Publications are listed.

6.1 Conclusions

Dynamic Demand Technology (DDT) avoids the use of expensive Information and Communication Technology and provides fully automatic and rapid control of grid frequency without any adverse impact on the normal use of loads. DDT was applied to domestic refrigerators and industrial bitumen tanks enabling them to reduce the deviations of grid frequency and reduce the spinning reserve capacity of frequency-sensitive generators. The feasibility of these loads to participate in frequency response services was analysed.

6.1.1 Domestic refrigerators for frequency control

A thermodynamic model of refrigerators was developed and verified against tests conducted by Open Energi on a number of refrigerators at the premises of the Indesit Company. A population of refrigerators was then modelled with randomised refrigerator mass and size. Their initial temperature and ON/OFF state were also randomised. An aggregated model of refrigerators representing all 40 million refrigerators connected to the present GB power system was then developed.

The aggregated model of refrigerators was connected to a simplified GB power system model. Case studies showed that following a sudden loss in generation, the maximum drop of grid frequency was limited by reducing the power consumption of refrigerators. The increase of power output of frequency-sensitive generators caused by the drop in frequency was reduced. Following a sudden loss in demand, the maximum rise of grid frequency was controlled by increasing the power consumption of refrigerators. The decrease of power output of frequency-sensitive generators caused by the rise in frequency was reduced.

Results from the simulations showed that the power consumption of domestic refrigerators was controlled by deviations of grid frequency proportionally without undermining their primary function of cold storage. Domestic refrigerators with the capability of grid frequency control were able to reduce frequency deviations in a manner similar to and faster than that of frequency-sensitive generators. If such capability of grid frequency control is deployed on refrigerators at scale, an effective means of grid frequency control will be provided. The requirements for the spinning reserve capacity of frequency-sensitive generators will be reduced.

6.1.2 Industrial bitumen tanks for frequency control

A thermodynamic model of bitumen tanks was developed and validated through field tests conducted by Open Energi. A simplified model of the duty cycles of bitumen tanks was also developed using the same field measurements. The accuracy and computational time of the two models were compared. The simplified model was used for subsequent studies because it was accurate enough and its computational time was shorter.

The simplified models of multiple bitumen tanks were aggregated to study the control of GB power system frequency. Power system frequency profiles including a frequency rise to 50.5 Hz and a frequency drop to 49.2 Hz were injected to the frequency controllers of tanks in the model. The same power system frequency profiles were also injected to the frequency controller of tanks in the field tests by Open Energi to validate their capability of frequency control. The behaviour of the aggregated tank models and that of the tanks in the field tests was similar.

Case studies were carried out by connecting the aggregated model of 5,000 tanks to a simplified GB power system model. Following a sudden loss in generation, the drop of grid frequency was limited by the reduction in the power consumption of bitumen tanks. The increase of the power output of frequency-sensitive generators was reduced. Following a sudden loss in demand, the rise of grid frequency was controlled by the increase in the power consumption of bitumen tanks. The decrease of power output of frequency-sensitive generators was reduced.

The load reduction obtained from 5,000 bitumen tanks was 72 MW. Even though this is small in the context of the GB power system, if frequency control can be employed on other industrial heating loads, their contributions to grid frequency control will be significant. The power consumption of bitumen tanks was controlled by deviations of grid frequency proportionally without undermining their storage of hot bitumen. These tanks provided the grid frequency control in a way similar to and faster than the frequency-sensitive generators. Therefore, a large scale deployment of such frequency responsive bitumen tanks will reduce reliance on the frequency-sensitive generators.

6.1.3 Demand aggregation for frequency response services

The models of domestic refrigerators each having a typical power consumption of 0.1 kW and bitumen tanks each having a power consumption of 40 kW were aggregated to participate in the Firm Frequency Response service. This service requires a participant to deliver a minimum frequency response of 10 MW.

The availability of refrigerators and bitumen tanks for grid frequency control was defined as the percentage of these loads that was available to be switched ON/OFF in response to frequency deviations. Their availability was measured through a different set of field tests carried out by Open Energi at different times of day. Uncertainties in the availability of these loads for frequency control were analysed. Based on the measured availability and the analysis of uncertainties, the number of refrigerators and bitumen tanks that should be aggregated to obtain more than 10 MW of response was calculated over a day with a pre-defined confidence level.

An aggregated model consisting of the calculated number of bitumen tank models and refrigerator models was developed. Their availability for grid frequency control was also modelled. The profile of a recorded severe frequency incident was used to investigate the response of the aggregated loads. Results verified that the aggregated loads delivered more than 10 MW of response.

A case study was also carried out for the future GB power system with reduced system inertia. Simulation results indicated that with the use of dynamic demand, the frequency drop after a sudden loss of generation was halted quickly and the magnitude of the drop was reduced significantly. Requirements for more frequency-sensitive generation will be reduced if such dynamic demand is deployed at scale.

The method of using domestic refrigerators for grid frequency control is able to be used by other loads with short ON/OFF cycles. Similarly other loads with long ON/OFF cycles are able to be used for grid frequency control with the technique demonstrated on bitumen tanks.

In conclusion, the capability of frequency control from these loads will reduce the need for costly generation reserve capacity from frequency-sensitive generators. Benefits such as the reduction of the system operating costs and reduction in Green House Gas emissions will be achieved.

The financial value that a load aggregator can achieve can be roughly estimated. According to the monthly report of National Grid, for the year 2012, National Grid paid £192.6 million for the total frequency response volume of 18533 GWh. It is assumed that the load aggregator has the capability of providing 10 MW of frequency response for the year (8,760 hours). Therefore, the benefits it earns can be calculated:

$$\text{Benefit}(\pounds) = \frac{\pounds 192.6\text{M} \cdot 10 \text{ MW} \cdot 8760 \text{ h}}{18533 \text{ GWh}} = \pounds 0.91\text{M}$$

It can be seen, the benefit for the demand aggregator to provide frequency response service is significant. If there are 622,980 refrigerators and 591 bitumen tanks to provide the 10 MW of frequency response, each of the units will be rewarded by approximately £21 assuming a lifetime of 15 years. Considering the £3 cost of installing the frequency controller, each of the units will earn £18.

This rough evaluation gives little consideration on the benefits of the service that may come from reduced carbon emissions. Future work can be carried out for detailed study on the benefits of dynamic demand.

Therefore, it is expected that policy makers will look closely at the use of dynamic demand to improve the efficiency of power supply and reduce the carbon emission of partly-loaded fossil fuel generators.

6.2 Contributions of the thesis

The contributions of the thesis are listed:

(a) Modelling and experimental validation

A thermodynamic model of domestic refrigerators was developed in *Matlab/Simulink*. The model was validated by Open Energi through tests on a number of refrigerators at the premises of the Indesit Company.

A thermodynamic model of bitumen tanks was developed in *Matlab/Simulink* and validated by Open Energi through field tests. A simplified model of the duty cycles of bitumen tanks was developed in *Matlab/Simulink* based on the same field measurements. The simplified model of bitumen tanks was verified to be accurate in comparison with the thermodynamic model.

A simplified GB power system model for the study of grid frequency control was developed in *DIgSILENT PowerFactory*.

A Dynamic Link Library (dll) interface between *DIgSILENT PowerFactory* and *Matlab/Simulink* was implemented. The interface platform enables the load models developed in *Matlab/Simulink* to be connected to the GB power system model for simulation studies.

(b) Capability of domestic refrigerators to provide grid frequency control

The capability of domestic refrigerators to provide grid frequency control was obtained by connecting an aggregated model of 40 million refrigerators to the simplified GB power system model. Simulation results showed that 40 million refrigerators provided around 500 MW of load reduction following a drop of grid frequency to 49.5 Hz. Refrigerators were able to provide grid frequency control in a manner similar and faster than that of frequency-sensitive generators. Reliance on spinning reserve from frequency-sensitive generators was reduced with the implementation of frequency control on refrigerators.

(c) Capability of industrial bitumen tanks to provide grid frequency control

The capability of bitumen tanks to provide grid frequency control was obtained by connecting an aggregated model of 5,000 tanks to the GB power system model. Simulation results showed that 5,000 tanks provided around 72 MW of load reduction following a drop of grid frequency to 49.4 Hz. The tanks were able to provide grid frequency control in a manner similar and faster than that of frequency-sensitive generators. Reliance on spinning reserve from frequency-sensitive generators was reduced with the capability of frequency control from such industrial heating loads.

(d) Demand aggregation for the participation of Firm Frequency Response service

The availability of refrigerators and bitumen tanks to provide frequency control at different time of day was obtained through field tests carried out by Open Energi. The number of refrigerators and bitumen tanks to be aggregated was then determined so that more than the required 10 MW of frequency response was delivered over a day with a pre-defined confidence level. An aggregation of loads was able to participate in the Firm Frequency Response service.

6.3 Publications

1. **M. Cheng**, J. Wu, J. Ekanayake, T. Coleman, W. Hung and N. Jenkins, ‘Primary frequency response in the Great Britain power system from dynamically controlled refrigerators’, 22nd *International Conference and Exhibition on Electricity Distribution (CIRED)*, Stockholm, June 2013.
2. **M. Cheng**, J. Wu, S. Galsworthy, U. L. Carlos, W. Hung and N. Jenkins, ‘Power system frequency response from the control of bitumen tanks’, *IEEE Transactions on Power Syst.* --Accepted
3. **M. Cheng**, J. Wu, S. Galsworthy, N. Jenkins and W. Hung, ‘Availability of load to provide frequency response in the Great Britain power system’, 18th *Power Systems Computation Conference (PSCC)*, Wroclaw, Aug 2014.

6.4 Future work

The following future work is proposed:

(a) Financial value of the dynamic demand services

This thesis mainly focuses on the technical feasibility of dynamic demand to provide frequency response service in the view of demand aggregator. In the future work, more detailed evaluation of the financial value of dynamic demand is interesting. In addition to a detailed evaluation of the benefits to the demand aggregator, the benefits to National Grid of replacing the spinning reserve capacity of conventional generators are necessary. This may also include the savings in the area of reducing carbon emissions. It would also be interesting and necessary to design some regulatory framework for the novel dynamic demand services.

(b) Investigate the possibility of demand to participate in different balancing services

Dynamic demand allows demand to provide dynamic response to the power system. However, there are also other balancing services such as the Frequency Control by Demand Management and Short Term Operating Reserve in the power system in

which demand is able to participate. It is proposed to investigate whether a load is able to participate in more than one service without conflicts.

(c) Virtual energy storage system for grid frequency control

In this study, two types of loads were studied. Other load types that may be possible for the provision of grid frequency control such as melting pots are candidates to be studied. In addition, energy storage units such as flywheels are also good options. The frequency controller developed in this thesis can be generalised so that it is able to be applied to different devices. As different devices have different physical characteristics, there will be coordination amongst different devices. This constructs a virtual energy storage system which can be used for frequency control and can also be easily changed to provide power smooth as a back-up of renewable energy generation. The frequency response from the virtual energy storage system will be more constant and reliable and it will reduce the capacity of the costly spinning reserve from the frequency-sensitive generators with greater confidence.

References

- [1] Department of Trade and Industry, 'Meeting the energy challenge – A white paper on energy', May 2007. [Online]. Available: http://webarchive.nationalarchives.gov.uk/20121205174605/http://www.decc.gov.uk/assets/decc/publications/white_paper_07/file39387.pdf
- [2] Markus Trilling, 'Decreasing dependency on fossil fuels', April 2013. [Online]. Available: <http://www.europarl.europa.eu/document/activities/cont/201304/20130425ATT65196/20130425ATT65196EN.pdf>
- [3] EDF Energy, 'What is security of fuel supply?', 2014. [Online]. Available: <http://www.edfenergy.com/energyfuture/the-energy-gap-security-of-supply>
- [4] European Commission, 'Climate Action – The 2020 climate and energy package', [Online]. Available: http://ec.europa.eu/clima/policies/package/index_en.htm
- [5] DECC, 'Reducing the UK's greenhouse gas emissions by 80% by 2050', [Online]. Available: <https://www.gov.uk/government/policies/reducing-the-uk-s-greenhouse-gas-emissions-by-80-by-2050>
- [6] Electricity North West Limited, 'Smart networks', [Online]. Available: <http://www.enwl.co.uk/docs/default-source/about-us/rriio-ed1-smart-networks.pdf?sfvrsn=0>
- [7] ENSG, 'Our Electricity Transmission Network: A Vision for 2020', pp. 8, Feb 2012, [Online]. Available: https://www.gov.uk/government/uploads/system/uploads/attachment_data/file/48274/4263-ensgFull.pdf
- [8] National Grid plc, 'Operating the Electricity Transmission Networks in 2020', pp. 10, [Online]. Available: http://www.nationalgrid.com/NR/rdonlyres/DF928C19-9210-4629-AB78-BBAA7AD8B89D/47178/Operatingin2020_finalversion0806_final.pdf
- [9] Chris Train, 'UK Energy Scenarios', National Grid, [Online]. Available: <http://www.one.ox.ac.uk/pdfs/10.%20National%20Grid%20Scenarios%20Chris%20Train.pdf>
- [10] Ofgem, 'National electricity transmission system security and quality of supply standard (NETS SQSS): Review of infeed losses', Jan 2011, [Online]. Available: <https://www.ofgem.gov.uk/ofgem-publications/52793/gsr007-decision-letter-final.pdf>
- [11] National Grid plc, '2013 Electricity Ten Year Statement', Nov 2013, [Online]. Available: <http://www2.nationalgrid.com/WorkArea/DownloadAsset.aspx?id=29430>
- [12] Electricity North West Limited, 'Impact of low carbon future', [Online]. Available: <http://www.enwl.co.uk/c2c/future-challenges>

- [13] Houses of Parliament, 'Electricity demand-side response', *POSTNOTE*, Number 452, Jan 2014, [Online]. Available: https://www.google.co.uk/url?sa=t&rct=j&q=&esrc=s&source=web&cd=3&cad=rja&uact=8&ved=0CDoQFjAC&url=http%3A%2F%2Fwww.parliament.uk%2Fbriefing-papers%2FPOST-PN-452.pdf&ei=rZQdVJT3N6LV7gbF5ICADA&usg=AFQjCNG2nFSDm5kTjUNw_ZSYzGYwBZG0HA&sig2=S9gx_y3jpTaAD8NrDy1z1A&bvm=bv.75775273,d.ZWU
- [14] DECC, 'Helping households to cut their energy bills', Sep 2014, [Online]. Available: <https://www.gov.uk/government/policies/helping-households-to-cut-their-energy-bills/supporting-pages/smart-meters>
- [15] CLNR, 'Time of Use Tariffs', [Online]. Available: <http://www.networkrevolution.co.uk/customers/domestic-customer-trials/%EF%BF%BCtime-of-use-tariffs/>
- [16] K. Samarakoon, J. Ekanayake and N. Jenkins, 'Investigation of domestic load control to provide primary frequency response using smart meters', *IEEE Trans on Smart Grid*, vol. 3, pp. 282-292, March 2012.
- [17] Engage Consulting Limited, 'ENA smart metering system requirements update', April 2010, [Online]. Available: http://www.energynetworks.org/modx/assets/files/electricity/futures/smart_meters/ENACR006-002-1-1_Requirements_100412.pdf
- [18] National Grid plc, 'Frequency Response Services', [Online]. Available: <http://www2.nationalgrid.com/UK/Services/Balancing-services/Frequency-response/>
- [19] dynamicDemand – promoting new technology to integrate green energy, 'How balance is the UK grid at the moment?', [Online]. Available: <http://www.dynamicdemand.co.uk/grid.htm>
- [20] National Grid, 'National electricity transmission system security and quality of supply standard issue 2.2', March 2012, [Online]. Available: <http://www2.nationalgrid.com/UK/Industry-information/Electricity-codes/SQSS/The-SQSS/>
- [21] I. A. Erinmez, D. O. Bickers, G. F. Wood and W. W. Hung, 'NGC experience with frequency control in England and Wales –provision of frequency response by generators', *Power Engineering Society 1999 Winter Meeting*, vol. 1, pp. 590-596, Feb. 1999.
- [22] National Grid plc, 'Report of the investigation into the automatic demand disconnection following multiple generation losses and the demand control response that occurred on the 27th May 2008', [Online]. Available: <http://www2.nationalgrid.com/assets/0/745/746/3464/3466/3488/3475/623fcdf6-31e3-416a-bfb7-c4edbfd763d2.pdf>
- [23] B. M. Weedy and B. J. Cory, 'Electric Power Systems', John Wiley & Sons Ltd, 1998.

- [24] National Grid plc, 'Mandatory Frequency Response', [Online]. Available: <http://www2.nationalgrid.com/UK/Services/Balancing-services/Frequency-response/Mandatory-Frequency-Response/>
- [25] National Grid plc, 'Firm Frequency Response (FFR)', [Online]. Available: <http://www2.nationalgrid.com/UK/Services/Balancing-services/Frequency-response/Firm-Frequency-Response/>
- [26] National Grid plc, 'Frequency Control by Demand Management', [Online]. Available: <http://www2.nationalgrid.com/uk/services/balancing-services/frequency-response/frequency-control-by-demand-management/>
- [27] KiWiPOWER demand management, 'A closer look at Frequency Response', [Online]. Available: <http://demandresponseblog.com/>
- [28] National Grid plc, 'Monthly Balancing Services Summary – January 2014', [Online]. Available: <http://www2.nationalgrid.com/WorkArea/DownloadAsset.aspx?id=35258>
- [29] National Grid plc, 'Monthly Balancing Services Summary – July 2014', [Online]. Available: <http://www2.nationalgrid.com/WorkArea/DownloadAsset.aspx?id=31962>
- [30] National Grid plc, 'What are Reserve Services?', [Online]. Available: <http://www2.nationalgrid.com/uk/services/balancing-services/reserve-services/>
- [31] National Grid plc, 'Fast Reserve Service Description 2013', April 2013, [Online]. Available: <http://www2.nationalgrid.com/WorkArea/DownloadAsset.aspx?id=11757>
- [32] National Grid plc, 'Short Term Operating Reserve – General Description of the Service', July 2014, [Online]. Available: <http://www2.nationalgrid.com/WorkArea/DownloadAsset.aspx?id=34525>
- [33] National Grid plc, 'Service Summary – Proposed BM Start-Up Service', Sep. 2006, [Online]. Available: <http://www2.nationalgrid.com/WorkArea/DownloadAsset.aspx?id=10980>
- [34] P. Kundur, N. J. Balu and M. G. Lauby, 'Power system stability and control', pp. 582, McGraw-Hill, 1994.
- [35] P. Kundur, N. J. Balu and M. G. Lauby, 'Power system stability and control', pp. 128, McGraw-Hill, 1994.
- [36] T. Bopp, 'Technical and commercial integration of distributed and renewable energy sources into existing electricity networks', *PhD Thesis*, The University of Manchester, 2006.
- [37] J. Ekanayake, N. Jenkins and G. Strbac, 'Frequency response from wind turbines', *Wind Engineering*, pp. 219-222, Multi-science publishing company, 2008.
- [38] National Grid plc, 'Guidance Notes – Synchronous Generating Units', Issue 12, September 2012, [Online]. Available: <http://www2.nationalgrid.com/assets/0/745/746/3464/3466/3488/3475/f400221d-60af-423e-ba3a-ad31dc19f592.pdf>
- [39] K. B. Samarakoon, 'Use of smart meters for frequency and voltage control', *PhD Thesis*, Cardiff University, 2012.

- [40] National Grid plc, ‘The Grid Code – Issue 5, Revision 9’, National Grid Electricity Transmission plc, pp. 188, July 2014, [Online]. Available: <http://www2.nationalgrid.com/uk/industry-information/electricity-codes/grid-code/the-grid-code/>
- [41] O. A. Lara, N. Jenkins and J. Ekanayake, P. Cartwright, M. Hughes, ‘Wind energy generation modelling and control’, *John Wiley & Sons Ltd*, 2009.
- [42] J. Licari, ‘Control of a variable-speed wind turbine’, *PhD Thesis*, Cardiff University, 2013.
- [43] C. Lalor, A. Mullane and M. O’Malley, ‘Frequency control and wind turbine technologies’, *IEEE Transactions on Power Syst*, vol. 20, No. 4, November 2005.
- [44] I. F. Moore, ‘Inertia response from wind turbines’, *PhD Thesis*, Cardiff University, 2012.
- [45] M. Kayikci and J. V. Milanovic, ‘Dynamic contribution of DFIG-based wind plants to system frequency disturbances’, *IEEE Transactions on Power Syst*, vol. 24, No.2, May 2009.
- [46] J. Ekanayake, K. Liyanage, J. Wu, A. Yokoyama and N. Jenkins, ‘Smart Grid technology and applications’, pp. 99-100, *John Wiley & Sons Ltd*, 2012.
- [47] Smart-A project, ‘Smart domestic appliances supporting the system integration of renewable energy’, [Online]. Available: http://www.smart-a.org/SmartA_Project_Final_Brochure_2009.pdf
- [48] uSwitch, ‘What is Economy 7 and how does it work?’, [Online]. Available: <http://www.uswitch.com/gas-electricity/guides/economy-7/#step2>
- [49] S. Nistor, J. Wu, M. Sooriyabandara and J. Ekanayake, ‘Cost optimisation of smart appliances’, *Innovative Smart Grid Technologies, IEEE PES International Conference*, Dec 2011.
- [50] E. McKenna, P. Grunewald, M. Thomson, ‘Going wind the wind: temporal characteristics of potential wind curtailment in Ireland in 2020 and opportunities for demand response’, *IET Renewable Power Generation*, Apr. 2014.
- [51] ENA and Energy UK, ‘Smart demand response: A discussion paper’, [Online]. Available: <http://www.energy-uk.org.uk/publication/finish/5/701.html>
- [52] Electricity North West Limited, ‘About C2C’, [Online]. Available: <http://www.enwl.co.uk/c2c>
- [53] Electricity North West Limited, ‘C2C customer seminar (slide show)’, [Online]. Available: [http://www.enwl.co.uk/docs/default-source/c2c-key-documents/c2c-customer-seminar-\(slideshow\)9CF443A0D83C.pptx?sfvrsn=8](http://www.enwl.co.uk/docs/default-source/c2c-key-documents/c2c-customer-seminar-(slideshow)9CF443A0D83C.pptx?sfvrsn=8)
- [54] Electricity North West Limited, ‘Review of Standards – Accommodating Responsive Demand in ER P2/6, Jan 2013. [Online]. Available: <http://www.enwl.co.uk/docs/default-source/c2c-key-documents/c2c-external-workshop-p2-6.pptx?sfvrsn=8>
- [55] N. O’Connell, P. Pinson, H. Madsen and M. O’Malley, ‘Benefits and challenges of electrical demand response: A critical review’, *Renewable and Sustainable Energy Reviews*, vol. 39, pp. 686-699, 2014.
- [56] Northern Powergrid, ‘Domestic and SME tariff development for the Customer-Led Network Revolution’, *frontier economics*, pp. 25, June 2012, [Online].

Available: <http://www.networkrevolution.co.uk/wp-content/uploads/2012/06/CLNR-L006-Domestic-and-SME-tariff-development-for-CLNR-June-2012.pdf>

- [57] T. Mount, L. Anderson, R. Zimmerman and J. Cardell, 'Coupling wind generation with controllable load and storage: A time-series application of the SuperOPF', *Final Project Report*, Power Systems Engineering Research Centre, November 2012.
- [58] DECC, 'Digest of United Kingdom Energy Statistics (DUKES) 2013', pp. 115, 2013. [Online]. Available: https://www.gov.uk/government/uploads/system/uploads/attachment_data/file/279546/DUKES_2013_Chapter_5.pdf
- [59] National Grid plc, 'Demand Side Developments Operational Forum', March 2003, [Online]. Available: <https://www.yumpu.com/en/document/view/3260790/fcdm-national-grid>
- [60] Leicester University, 'Demand side response in the non-domestic section, Final report for Ofgem', pp. 29, July 2012. [Online]. Available: <http://www.element-energy.co.uk/wordpress/wp-content/uploads/2012/07/Demand-Side-Response-in-the-non-domestic-sector.pdf>
- [61] J. Kondoh, 'A direct load management scheme to control appliances and EVs while considering end users comfort', *Proc. Of Grid-Interop 2009*, pp. 144-152, Deven, CO, USA, Nov 2009.
- [62] S. A. Pourmousavi and M. H. Nehrir, 'Real-time central demand response for primary frequency regulation in Microgrids', *IEEE Trans on Smart Grid*, vol. 3, pp. 1988-1996, Dec 2012.
- [63] A. Bieshoy, 'Operation of Energy MicroGrids', *PhD Thesis*, Cardiff University,, 2010.
- [64] F. C. Schweppe, R. D. Tabors, J. L. Kirtley, H. R. Outhred, F. H. Pickel and A. J. Cox, 'Homeostatic utility control', *IEEE Trans on Power Apparatus and Systems*, PAS-99(5/6), pp/ 1151-1163, 1980.
- [65] dynamicDemand, 'The technology', [Online]. Available: http://www.dynamicdemand.co.uk/the_technology.htm
- [66] J. Kondoh, N. Lu and D. J. Hammerstrom, 'An evaluation of the water heater load potential for providing regulation service', *IEEE Trans on Power Syst*, vol. 26, no. 8, pp. 1309-1316, 2011.
- [67] N. Lu, 'An evaluation of the HVAC load potential for providing load balancing service', *IEEE Trans on Smart Grid*, vol. 3, no. 9, pp. 1263-1270, 2012.
- [68] S. Koch, M. Zima, G. Andersson, 'Active coordination of thermal household appliances for load management purpose', *IFAC Symposium on Power Plants and Power Systems Control*, Finland, July 2009.
- [69] B. Biegel, L. H. Hansen, P. Andersen, J. Stoustrup, 'Primary control by ON/OFF demand-side devices', *IEEE Trans on Smart Grid*, vol. 4, pp. 2061-2071, Dec 2013.
- [70] M. Kintner-Meyer, R. Guttromson, D. Oedingen and S. Lang, 'Final report for the energy efficient and affordable small commercial and residential buildings

- research program, Project 3.3 – Smart load control and grid friendly appliances’, Pacific Northwest National Laboratory, 2003.
- [71] A. M. Garcia, F. Bouffard, and D. S. Kirschen, ‘Decentralised demand-side contribution to primary frequency control’, *IEEE Trans on Power Syst*, vol. 26, pp. 411-419, Feb 2011.
- [72] A. Abiri-Jahromi and F. Bouffard, ‘Characterising statistical bounds on aggregated demand-based primary frequency control’, *Power and Energy Society General Meeting (PES)*, July 2013.
- [73] J. A. Short, D. G. Infield and L. L. Freris, ‘Stabilisation of grid frequency through dynamic demand control’, *IEEE Trans on Power Syst*, vol. 22, pp. 1284-1293, Aug 2007.
- [74] D. G. Infield, J. A. Short, C. Home and L.L. Freros, ‘Potential for domestic dynamic demand-side management in the UK’, *Power Engineering Society General Meeting*, June 2007.
- [75] Z. Xu, J. Ostergaard, M. Togeby and C. Marcus-Moller, ‘Design and modelling of thermostatically controlled loads as frequency controlled reserve’, *Power Engineering Society General Meeting*, June 2007.
- [76] P. Nyeng, J. Stergaard, M. Togeby and J. Hethey, ‘Design and implementation of frequency-responsive thermostat control’, *Universities Power Engineering Conference (UPEC)*, 45th International, Aug 2010.
- [77] X. Zhao, J. Ostergaard and M. Togeby, ‘Demand as frequency controlled reserve’, *IEEE Trans on Power Syst*, vol. 26, pp. 1062-1071, Aug 2011.
- [78] H. J. Jia, Y. Qi and Y. F. Mu, ‘Frequency response of autonomous microgrid based on family-friendly controllable loads’, *Science China Press and Springer-Verlag Berlin Heidelberg*, vol. 56, pp. 693-702, March 2013.
- [79] T. A. Marshall, ‘Using dishwashers to provide frequency regulation through dynamic demand’, Science Symposium, 2011, [Online]. Available: https://www.google.co.uk/webhp?sourceid=chrome-instant&ion=1&espv=2&es_th=1&ie=UTF-8#q=Using%20dish%20washer%20for%20frequency%20regulation
- [80] DECC, ‘The potential for dynamic demand’, 2008, [Online]. Available: <http://www.supergen-networks.org.uk/filebyid/50/file.pdf>
- [81] Open Energi, ‘Demand response and dynamic demand market overview’, 2013, [Online]. Available: <http://www.openenergi.com/big-picture/demand-response/>
- [82] DECC, ‘Digest of United Kingdom Energy Statistics (DUKES) 2013’, Table 5.2 Electricity supply and consumption, A National Statistics publication, 2013, [Online]. Available: https://www.gov.uk/government/uploads/system/uploads/attachment_data/file/279546/DUKES_2013_Chapter_5.pdf
- [83] DECC (2013), ‘Energy Consumption in the UK, Chapter 1: Overall data tables’, Table 3.12 Number of appliances owned by households in the UK 1970 to 2012, 2013, [Online]. Available: <https://www.gov.uk/government/statistics/energy-consumption-in-the-uk>

- [84] B. Drysdale, J Wu and N. Jenkins, 'Flexible demand in the GB domestic electricity sector in 2030', *The 5th International Conference on Applied Energy (ICAE 2013)*, Pretoria, South Africa, July 2013.
- [85] Charchitecture, 'Independent Study: Refrigeration', a systematic approach towards architecture, Nov 2011, [Online]. Available: <http://charchitecture.wordpress.com/2011/11/08/independent-study-refrigeration/>
- [86] H. Jonsson and P. Bohdanowicz, 'Sustainable Energy Utilisation', *KTH Energy Technology*, Royal Institute of Technology, Stockholm, Sweden 2010. pp. 56
- [87] H. Jonsson and P. Bohdanowicz, 'Sustainable Energy Utilisation', *KTH Energy Technology*, Royal Institute of Technology, Stockholm, Sweden 2010. pp. 51-52
- [88] Gorenje, 'Dual compressor operation for improved power efficiency' [Online]. Available: <http://www.gorenje.com/ngfridge/340>
- [89] P. Kundur, 'Power system stability and control', McGraw-Hill 1994, pp. 581-627.
- [90] W. Hung, G. Ray, G. Stein, 'Frequency changes during large disturbances WG', National Grid plc. <http://www.nationalgrid.com/NR/rdonlyres/D07952E0-2B58-426F-B61F-C77A239D3964/5720/Meeting1Presentation.pdf>
- [91] BM Reports, 'Historic Initial Demand Out-turn for 2012-09-30 (INDO, ITSDO)', http://www.bmreports.com/bwh_Indo.htm
- [92] G. Strbac, 'Demand side management: benefits and challenges', *Energy Policy* 2008, vol. 36, pp. 4419-4426.
- [93] Eurobitume, 'What is bitumen?' [Online]. Available: <http://www.eurobitume.eu/bitumen/what-bitumen>
- [94] M. M. Aziz, 'System Response', Control Engineering, 2013. [online]. Available: http://people.exeter.ac.uk/mmaziz/ecm2105/ecm2105_n4.pdf
- [95] W. Bolton, 'Control Engineering', *Longman Group UK Limited*, 1992. pp. 84.
- [96] M. Cheng, J. Wu, S. Galsworthy and et al, 'Power System Frequency Response from the Control of Bitumen Tanks', *IEEE Transactions on Power Syst*, accepted.
- [95] Y. Mu, J. Wu, J. Ekanayake and N. Jenkins, 'Primary frequency response from electric vehicles in the Great Britain power system', *IEEE Transactions on Smart Grid*, vol. 4, pp. 1142-1150, June 2013.
- [96] Intertek, 'Household Electricity Survey', pp. 246, May 2012. [Online]. Available: https://www.gov.uk/government/uploads/system/uploads/attachment_data/file/208097/10043_R66141HouseholdElectricitySurveyFinalReportissue4.pdf
- [97] KiWiPOWER demand management, 'A closer look at Frequency Response', [Online]. Available: <http://demandresponseblog.com/>
- [98] David L. Olson and Scott R. Swenseth, 'A linear approximation for Chance-Constrained Programming', *Journal of the Operational Research Society*, vol. 38, Mar. 1987, pp. 261-267.
- [99] Bijay Baran Pal and Somsubhra Gupta, 'A genetic algorithm approach for fuzzy goal programming formulation of chance constrained problems using stochastic simulation', *Fourth International Conference on Industrial and Information Systems*, December 2009.
- [100] Murray R. Spiegel, John Schiller and R. Alu Srinivasan, 'Probability and Statistics', pp. 80, Second Edition, McGraw-Hill, 1976.

- [101] Murray R. Spiegel, John Schiller and R. Alu Srinivasan, 'Probability and Statistics', pp. 81, Second Edition, McGraw-Hill, 1976.
- [102] 'Standard normal distribution: Table values represent area to the left of the Z score', [Online]. Available:
<https://www.stat.tamu.edu/~lzhou/stat302/standardnormaltable.pdf>
- [103] EIRGRID, 'System Performance Data - Wind Generation', [Online]. Available:
<http://www.eirgrid.com/operations/systemperformancedata/windgeneration/>
- [104] Serena Hesmondhalgh, 'GB Electricity Demand - 2010 and 2025. Initial Brattle Electricity Demand-Side Model – Scope for Demand Reduction and Flexible Response.', The Brattle Group and Sustainability First, February 2012, pp. 72-75, [Online]. Available:
<http://www.sustainabilityfirst.org.uk/docs/2011/Sustainability%20First%20-%20GB%20Electricity%20Demand%20Project%20-%20Paper%202%20-%20GB%20Electricity%20Demand%202010%20and%202025%20-%20Initial%20Brattle%20Electricity%20Demand-Side%20Model%20-%20February%202012.pdf>

Appendix I

This appendix analyses the influence of ambient temperature on the thermodynamics of refrigerators.

The refrigerator model developed in Chapter 3 was used for simulation. Four set of simulation were carried out with ambient temperature to be 22 °C, 20 °C, 18 °C and 16 °C. The cavity temperature, evaporator temperature and ON/OFF state of the refrigerator are given by Fig. I1- Fig. I3.

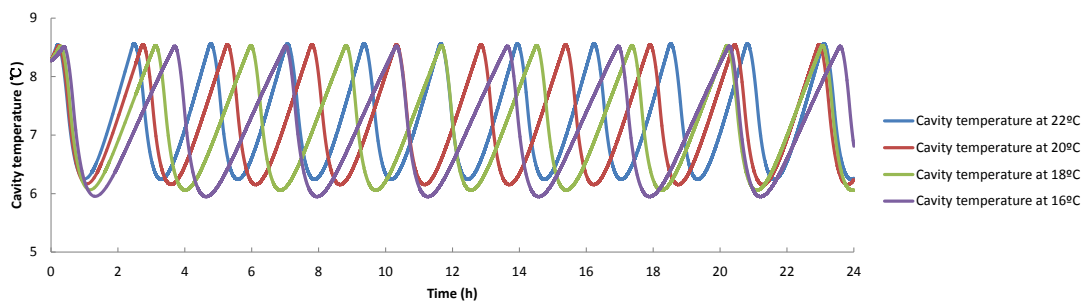


Fig. I1. Cavity temperature of a refrigerator at different ambient temperature

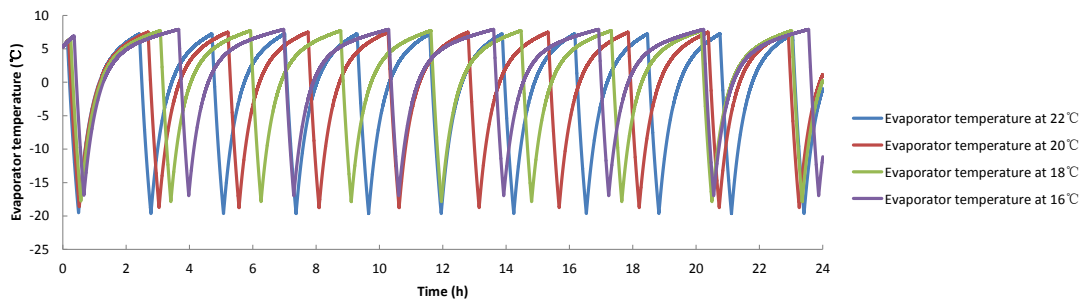


Fig. I2. Evaporator temperature of a refrigerator at different ambient temperature

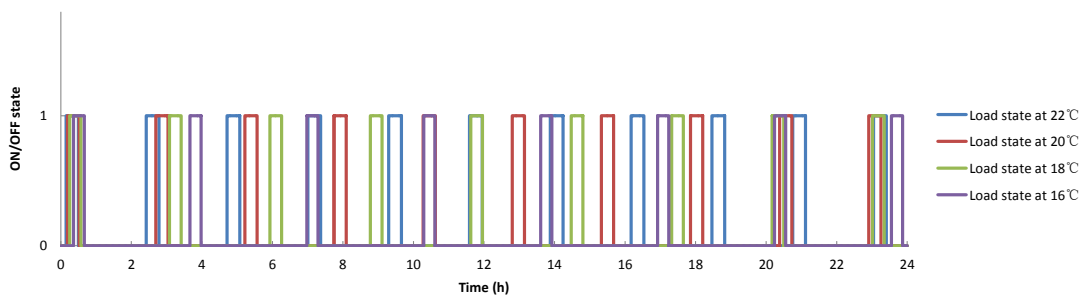


Fig. I3. ON/OFF of a refrigerator at different ambient temperature

It can be seen, the ambient temperature leads to significant impacts on the thermal behaviour of a refrigerator. Hence, this explains the differences between the real measurements and simulation in Fig. 3.2.

Appendix II

This appendix analyses the influence of temperature set-points on the behaviour of refrigerators for grid frequency control.

1. Different temperature set-points

Temperature set-points (T_{high} and T_{low}) are set as shown in Table III. The ambient temperature was 22 °C in all the cases. A frequency drop from 50 Hz to 49.5 Hz was injected to 1,000 refrigerator models at 10 s. The simulation results are given in Fig. III.

Table III. Temperature set-points for each simulation

	1	2	3	4
T_{high} (°C)	8.5	7.5	6.5	5.5
T_{low} (°C)	7.5	6.5	5.5	4.5

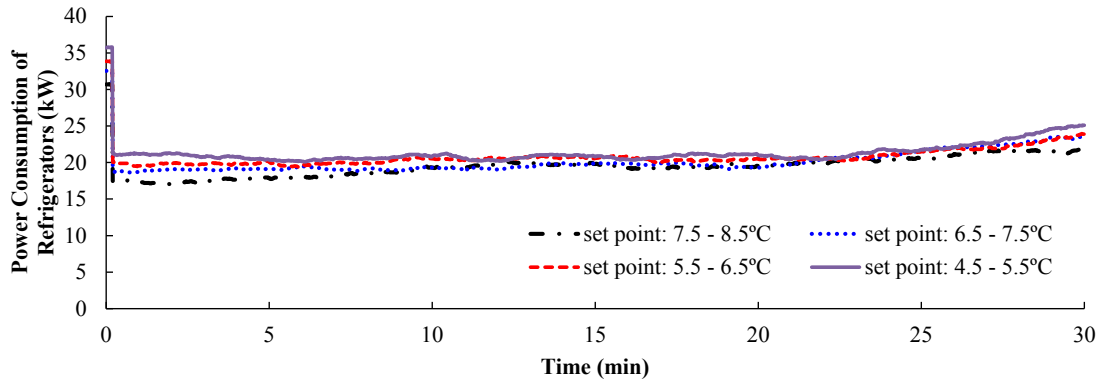


Fig. III. Power consumption of refrigerators with different temperature set-points

As can be seen, temperature set-point of refrigerators has an impact of the initial power consumption of refrigerators. Because the ambient temperature was same at 22 °C in all cases, refrigerators with lower temperature set-point require more power to cool down in order to reach the set-point. In addition, the temperature set-points show little impact on the power change following the frequency drop. Hence, the temperature set-points has little impact on the amount of frequency response of refrigerators.

2. Increase the difference between T_{high} and T_{low}

The difference between T_{high} and T_{low} was set to 1 °C in this thesis. This represents the worst scenario that the frequency response from refrigerators will be the smallest caused by the limitation of its temperature set-points. Hence, it is expected that the frequency response provided by refrigerators in reality will be more.

Simulations were carried out with the temperature difference between T_{high} and T_{low} . Temperature set-points (T_{high} and T_{low}) are set as shown in Table II2. The ambient temperature was 22 °C in all the cases. A frequency drop from 50 Hz to 49.5 Hz was injected to 1,000 refrigerator models at 10 s. The simulation results are given in Fig. II2.

Table II2. Differences between T_{high} and T_{low} for each simulation

Differences between T_{high} and T_{low} (°C)	1	2	3
T_{high} (°C)	8.5	9	9.5
T_{low} (°C)	7.5	7	6.5

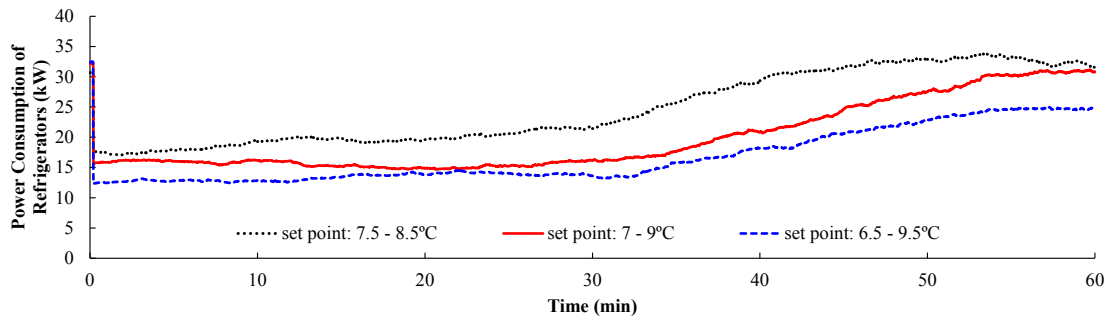


Fig. II2. Power consumption of refrigerators with different differences between T_{high} and T_{low}

As shown in Fig. II2, the greater the differences between the temperature set-points, the more reduction in the power consumption of refrigerators following the frequency drop. Therefore, the wider the temperature control band of refrigerators, the more frequency response is expected.

Appendix III

This appendix evaluated the general ON/OFF period of refrigerators and bitumen tanks. Thermodynamics of both loads can be simply represented by first order differential equations. When switch ON a refrigerator, it is a cooling process that leads to temperature decay. When switch ON a bitumen tank, it is a heating process that leads to temperature increase. The physical parameters of refrigerators and bitumen tanks that are used for the evaluation are given in Table III.1.

Table III.1. Parameters for a refrigerator and a bitumen tank

Parameters	Physical Parameters					Calculations	
	U (Wm ⁻² K ⁻¹)	A (m ²)	c _v (Jkg ⁻¹ K ⁻¹)	m (kg)	P (W)	On period	Off period
Refrigerator	0.61	3.5	4000	10	100	18.5 min	48.1 min
Bitumen Tanks	0.57	110.27	920	10,000	50,000	1.9 h	8.4 h

A. Refrigerator

Based on the analysis of thermodynamics in Chapter 3, a first order equation (III.1) is obtained:

$$\frac{dT}{dt} = \frac{UA(T_{\text{amb}} - T)}{c_v m} - \frac{Ps}{c_v m} \quad (\text{III.1})$$

where T (K) represents the inside temperature of a refrigerator. P (W) is the power consumption. s is the ON/OFF state. c_v (Jkg⁻¹K⁻¹) represents specific heat capacity. U (Wm⁻²K⁻¹) is the overall heat coefficient. A (m²) is the area. m (kg) is thermal mass. T_{amb} is the ambient temperature. These physical parameters are given in Table III.1 for this evaluation.

For the ON-period, s is 1 and temperature starts to decay. To calculate the ON-period, it is equivalent to calculate the time for the temperature to decrease from T_{high} to T_{low} . It is assumed T_{low} to be 6 °C (279.15 K), T_{high} to be 8 °C (281.15 K) and T_{amb} to be 20 °C (293.15 K).

The integration of (III.1) can be obtained as shown in (III.2):

$$\Delta t = -\frac{c_v m}{UA} \int_{T_{high}}^{T_{low}} \frac{1}{T - T_{amb} + P/UA} dT \quad (III. 2)$$

Taking the parameters in Table III.1 into (III.2), it can be calculated that the ON period Δt is 18.5 min.

For the OFF-period, s is 0 and temperature starts to increase. To calculate the OFF-period, it is equivalent to calculate the time for the temperature to increase from T_{low} to T_{high} .

The integration of (III.1) (with $s=0$) can be obtained as shown in (III.3):

$$\Delta t = -\frac{c_v m}{UA} \int_{T_{low}}^{T_{high}} \frac{1}{T - T_{amb}} dT \quad (III. 3)$$

Taking the parameters in Table III.1 into (III.3), it can be calculated that the OFF period Δt is 48.1 min.

B. Bitumen Tank

Based on the analysis of thermodynamics in Chapter 4, a first order equation (III.4) is obtained:

$$\frac{dT}{dt} = \frac{Ps}{c_v m} - \frac{UA(T - T_{amb})}{c_v m} \quad (III. 4)$$

where T (K) represents the inside temperature of a tank. P (W) is the power consumption. s is the ON/OFF state. c_v ($\text{Jkg}^{-1}\text{K}^{-1}$) represents specific heat capacity. U ($\text{Wm}^{-2}\text{K}^{-1}$) is the overall heat coefficient. A (m^2) is the area. m (kg) is thermal mass. T_{amb} is the ambient temperature. These physical parameters are given in Table III.1 for this evaluation.

For the ON-period, s is 1 and temperature starts to increase. To calculate the ON-period, it is equivalent to calculate the time for the temperature to increase from T_{low} to T_{high} . It is assumed T_{low} to be 150 °C (423.15 K), T_{high} to be 180 °C (453.15 K) and T_{amb} to be 20 °C (293.15 K).

The integration of (III.4) can be obtained as shown in (III.5):

$$\Delta t = -\frac{c_v m}{UA} \int_{T_{low}}^{T_{high}} \frac{1}{T - T_{amb} - P/UA} dT \quad (III. 5)$$

Taking the parameters in Table III.1 into (III.5), it can be calculated that the ON period Δt is 1.9 h.

For the OFF-period, s is 0 and temperature starts to decay. To calculate the OFF-period, it is equivalent to calculate the time for the temperature to decrease from T_{high} to T_{low} .

The integration of (III.4) (with $s=0$) can be obtained as shown in (III.6):

$$\Delta t = -\frac{c_v m}{UA} \int_{T_{high}}^{T_{low}} \frac{1}{T - T_{amb}} dT \quad (III. 6)$$

Taking the parameters in Table III.1 into (III.6), it can be calculated that the ON period Δt is 8.4 h.

Appendix IV

This appendix presents the table for the values of standard normal distribution.

STANDARD NORMAL DISTRIBUTION: Table Values Represent AREA to the LEFT of the Z score.

Z	.00	.01	.02	.03	.04	.05	.06	.07	.08	.09
-3.9	.00005	.00005	.00004	.00004	.00004	.00004	.00004	.00004	.00003	.00003
-3.8	.00007	.00007	.00007	.00006	.00006	.00006	.00006	.00005	.00005	.00005
-3.7	.00011	.00010	.00010	.00010	.00009	.00009	.00008	.00008	.00008	.00008
-3.6	.00016	.00015	.00015	.00014	.00014	.00013	.00013	.00012	.00012	.00011
-3.5	.00023	.00022	.00022	.00021	.00020	.00019	.00019	.00018	.00017	.00017
-3.4	.00034	.00032	.00031	.00030	.00029	.00028	.00027	.00026	.00025	.00024
-3.3	.00048	.00047	.00045	.00043	.00042	.00040	.00039	.00038	.00036	.00035
-3.2	.00069	.00066	.00064	.00062	.00060	.00058	.00056	.00054	.00052	.00050
-3.1	.00097	.00094	.00090	.00087	.00084	.00082	.00079	.00076	.00074	.00071
-3.0	.00135	.00131	.00126	.00122	.00118	.00114	.00111	.00107	.00104	.00100
-2.9	.00187	.00181	.00175	.00169	.00164	.00159	.00154	.00149	.00144	.00139
-2.8	.00256	.00248	.00240	.00233	.00226	.00219	.00212	.00205	.00199	.00193
-2.7	.00347	.00336	.00326	.00317	.00307	.00298	.00289	.00280	.00272	.00264
-2.6	.00466	.00453	.00440	.00427	.00415	.00402	.00391	.00379	.00368	.00357
-2.5	.00621	.00604	.00587	.00570	.00554	.00539	.00523	.00508	.00494	.00480
-2.4	.00820	.00798	.00776	.00755	.00734	.00714	.00695	.00676	.00657	.00639
-2.3	.01072	.01044	.01017	.00990	.00964	.00939	.00914	.00889	.00866	.00842
-2.2	.01390	.01355	.01321	.01287	.01255	.01222	.01191	.01160	.01130	.01101
-2.1	.01786	.01743	.01700	.01659	.01618	.01578	.01539	.01500	.01463	.01426
-2.0	.02275	.02222	.02169	.02118	.02068	.02018	.01970	.01923	.01876	.01831
-1.9	.02872	.02807	.02743	.02680	.02619	.02559	.02500	.02442	.02385	.02330
-1.8	.03593	.03515	.03438	.03362	.03288	.03216	.03144	.03074	.03005	.02938
-1.7	.04457	.04363	.04272	.04182	.04093	.04006	.03920	.03836	.03754	.03673
-1.6	.05480	.05370	.05262	.05155	.05050	.04947	.04846	.04746	.04648	.04551
-1.5	.06681	.06552	.06426	.06301	.06178	.06057	.05938	.05821	.05705	.05592
-1.4	.08076	.07927	.07780	.07636	.07493	.07353	.07215	.07078	.06944	.06811
-1.3	.09680	.09510	.09342	.09176	.09012	.08851	.08691	.08534	.08379	.08226
-1.2	.11507	.11314	.11123	.10935	.10749	.10565	.10383	.10204	.10027	.09853
-1.1	.13567	.13350	.13136	.12924	.12714	.12507	.12302	.12100	.11900	.11702
-1.0	.15866	.15625	.15386	.15151	.14917	.14686	.14457	.14231	.14007	.13786
-0.9	.18406	.18141	.17879	.17619	.17361	.17106	.16853	.16602	.16354	.16109
-0.8	.21186	.20897	.20611	.20327	.20045	.19766	.19489	.19215	.18943	.18673
-0.7	.24196	.23885	.23576	.23270	.22965	.22663	.22363	.22065	.21770	.21476
-0.6	.27425	.27093	.26763	.26435	.26109	.25785	.25463	.25143	.24825	.24510
-0.5	.30854	.30503	.30153	.29806	.29460	.29116	.28774	.28434	.28096	.27760
-0.4	.34458	.34090	.33724	.33360	.32997	.32636	.32276	.31918	.31561	.31207
-0.3	.38209	.37828	.37448	.37070	.36693	.36317	.35942	.35569	.35197	.34827
-0.2	.42074	.41683	.41294	.40905	.40517	.40129	.39743	.39358	.38974	.38591
-0.1	.46017	.45620	.45224	.44828	.44433	.44038	.43644	.43251	.42858	.42465
-0.0	.50000	.49601	.49202	.48803	.48405	.48006	.47608	.47210	.46812	.46414

STANDARD NORMAL DISTRIBUTION: Table Values Represent AREA to the LEFT of the Z score.

Z	.00	.01	.02	.03	.04	.05	.06	.07	.08	.09
0.0	.50000	.50399	.50798	.51197	.51595	.51994	.52392	.52790	.53188	.53586
0.1	.53983	.54380	.54776	.55172	.55567	.55962	.56356	.56749	.57142	.57535
0.2	.57926	.58317	.58706	.59095	.59483	.59871	.60257	.60642	.61026	.61409
0.3	.61791	.62172	.62552	.62930	.63307	.63683	.64058	.64431	.64803	.65173
0.4	.65542	.65910	.66276	.66640	.67003	.67364	.67724	.68082	.68439	.68793
0.5	.69146	.69497	.69847	.70194	.70540	.70884	.71226	.71566	.71904	.72240
0.6	.72575	.72907	.73237	.73565	.73891	.74215	.74537	.74857	.75175	.75490
0.7	.75804	.76115	.76424	.76730	.77035	.77337	.77637	.77935	.78230	.78524
0.8	.78814	.79103	.79389	.79673	.79955	.80234	.80511	.80785	.81057	.81327
0.9	.81594	.81859	.82121	.82381	.82639	.82894	.83147	.83398	.83646	.83891
1.0	.84134	.84375	.84614	.84849	.85083	.85314	.85543	.85769	.85993	.86214
1.1	.86433	.86650	.86864	.87076	.87286	.87493	.87698	.87900	.88100	.88298
1.2	.88493	.88686	.88877	.89065	.89251	.89435	.89617	.89796	.89973	.90147
1.3	.90320	.90490	.90658	.90824	.90988	.91149	.91309	.91466	.91621	.91774
1.4	.91924	.92073	.92220	.92364	.92507	.92647	.92785	.92922	.93056	.93189
1.5	.93319	.93448	.93574	.93699	.93822	.93943	.94062	.94179	.94295	.94408
1.6	.94520	.94630	.94738	.94845	.94950	.95053	.95154	.95254	.95352	.95449
1.7	.95543	.95637	.95728	.95818	.95907	.95994	.96080	.96164	.96246	.96327
1.8	.96407	.96485	.96562	.96638	.96712	.96784	.96856	.96926	.96995	.97062
1.9	.97128	.97193	.97257	.97320	.97381	.97441	.97500	.97558	.97615	.97670
2.0	.97725	.97778	.97831	.97882	.97932	.97982	.98030	.98077	.98124	.98169
2.1	.98214	.98257	.98300	.98341	.98382	.98422	.98461	.98500	.98537	.98574
2.2	.98610	.98645	.98679	.98713	.98745	.98778	.98809	.98840	.98870	.98899
2.3	.98928	.98956	.98983	.99010	.99036	.99061	.99086	.99111	.99134	.99158
2.4	.99180	.99202	.99224	.99245	.99266	.99286	.99305	.99324	.99343	.99361
2.5	.99379	.99396	.99413	.99430	.99446	.99461	.99477	.99492	.99506	.99520
2.6	.99534	.99547	.99560	.99573	.99585	.99598	.99609	.99621	.99632	.99643
2.7	.99653	.99664	.99674	.99683	.99693	.99702	.99711	.99720	.99728	.99736
2.8	.99744	.99752	.99760	.99767	.99774	.99781	.99788	.99795	.99801	.99807
2.9	.99813	.99819	.99825	.99831	.99836	.99841	.99846	.99851	.99856	.99861
3.0	.99865	.99869	.99874	.99878	.99882	.99886	.99889	.99893	.99896	.99900
3.1	.99903	.99906	.99910	.99913	.99916	.99918	.99921	.99924	.99926	.99929
3.2	.99931	.99934	.99936	.99938	.99940	.99942	.99944	.99946	.99948	.99950
3.3	.99952	.99953	.99955	.99957	.99958	.99960	.99961	.99962	.99964	.99965
3.4	.99966	.99968	.99969	.99970	.99971	.99972	.99973	.99974	.99975	.99976
3.5	.99977	.99978	.99978	.99979	.99980	.99981	.99981	.99982	.99983	.99983
3.6	.99984	.99985	.99985	.99986	.99986	.99987	.99987	.99988	.99988	.99989
3.7	.99989	.99990	.99990	.99990	.99991	.99991	.99992	.99992	.99992	.99992
3.8	.99993	.99993	.99993	.99994	.99994	.99994	.99994	.99995	.99995	.99995
3.9	.99995	.99995	.99996	.99996	.99996	.99996	.99996	.99996	.99997	.99997